Boron-bridged constrained geometry complexes and related compounds

A Thesis presented by

Frank Michael Breitling

In partial fulfilment of the requirements

for the award of

Doctor of Philosophy of

University of London

and Diploma of Imperial College London

August 2005

Department of Chemistry

Imperial College London

For Spyridoula

Acknowledgements

I would like to thank my supervisor, Prof. Dr Holger Braunschweig, for giving me the opportunity to work in his group, for providing me with a very interesting project, for his encouragement and for giving me freedom in the way I carried out my research. My thanks also go to my second supervisor, Prof. Dr Tom Welton, for giving me all the support I needed after the move of my initial group, and to his group for 'adopting' me.

Dr Christian Burschka, Dr Krzysztof Radacki, Dr David Scheschkewitz, Fabian Seeler, Dr Andrew J. P. White and Prof. Dr David J. Williams are thanked for performing *X*-ray diffraction experiments of my compounds. Dr Rüdiger Bertermann, Dr Carsten Kollann, Marie-Luise Schäfer, Dick Sheppard and Peter Haycock are acknowledged for performing countless NMR experiments on my behalf. I also have to thank John Barton, Dr Stephan Wagner and Dr Justin Wolf for conduct various MS and GC-MS analyses. In addition, I want to thank Richhilde Schedl for carrying out thermogravimetric measurements and Dr Steve Holding of RAPRA Technology for performing numerous GPC polymer analyses.

The Fonds der Chemischen Industrie (FCI) is thanked for financial support of my PhD studies by means of a Kekulé scholarship.

I am particularly grateful to Dr Mario Kraft who generously paved my way both before my arrival in London and Würzburg, for sharing the good and bad times of a PhD studentship and his friendship. I also want to specially acknowledge Sascha Stellwag for his relentless help in lab 204 and Carina Grimmer and Viktor Weber for performing polymerisation experiments. Many thanks go to Dr Melanie Homberger, for lots of helpful discussions particularly during the early stages of my project. Dr Guy Clentsmith and Dr George Whittell are also gratefully acknowledged for their very thorough and patient proof-reading of this manuscript.

Furthermore, I wish to thank all my past and present colleagues in the group, André, Carina, Carsten, Daniela, David, Emanuel, Fabian, George, Giovanni, Guy, Justin B., Justin W., Katharina, Krzysztof, Mario, Martina, Matthias, Melanie H.,

Melanie L., Natalia, Nele, Stefan, Thomas and Viktor, for their help and assistance when needed and just a great time.

Finally, I want to thank my parents and family for their continued support during my education. And a special thanks goes to Spyridoula Ntella for her loving support and care throughout my PhD studies, especially during the writing up of my thesis that was testing her patience much more than I ever envisaged.

The work described in this Thesis was carried out in part at Imperial College, Department of Chemistry, University of London, from September 2001 to September 2003, under the supervision of Prof. Holger Braunschweig and Prof. Tom Welton, and in part at the Institut für Anorganische Chemie, Bayerische Julius-Maximilians-Universität Würzburg, Germany, from October 2003 to February 2005, under the supervision of Prof. Holger Braunschweig. The research described in this Thesis is original, unless otherwise stated and to my knowledge it has not been submitted previously for a degree at this or any other University.

Frank Michael Breitling

August 2005

Abstract

Boron-bridged constrained geometry complexes and related compounds

Group 3 and 4 complexes bearing linked cyclopentadienyl amido ligands, often referred to as constrained geometry complexes (CGCs), have experienced considerable interest due to their superior ability to copolymerise ethylene and higher α-olefins when activated with suitable co-catalyst.

The work presented in this thesis aimed to replace the most commonly applied bridge in CGCs, which is silicon based, by one containing boron. The potential of the bridging element to have Lewis acidic character was expected to positively alter the catalytic activity of the activated species and possibly allowing for self-activation.

Synthetic approaches to ligand precursors based on aminoboranes, diaminodiboranes(4) and ferrocenylboranes are described. Starting from the dihalo derivatives of these boranes, sequential substitution of the halides by one equivalent each of a cyclopentadienide derivative and an amide allowed the synthesis and isolation of a broad range of new CGC ligand precursors.

Complexation of these ligand precursors to Group 4 metals was studied by utilising various protocols. The reaction with Group 4 tetraamides *via* amine elimination was the most successful yielding numerous new boron-bridged CGCs and related complexes in which the boron-bridged ligand binds in a non-chelating fashion.

The newly synthesised compounds were fully characterised by multinuclear NMR spectroscopy, supplemented by *X*-ray diffraction studies where applicable.

Studies on the reactivity of boron-bridged CGCs in the presence of alkylating agents indicated susceptibility of the boron atom to nucleophilic attack resulting in a decomposition of the linking moiety between the cyclopentadienyl and amido

fragments. This is as well reflected in the data gathered from polymerisation experiments, in which methylaluminoxane activated boron-bridged CGCs displayed a low activity towards ethylene polymerisation, but a high activity towards styrene polymerisation. Such characteristics are comparable to unbridged compounds, *e.g.* [(η^5-C_5H_5)$TiCl_3$], rather than silicon-bridged CGCs, thus suggesting degradation of the boron-bridged CGCs to unbridged complexes under polymerisation conditions.

Table of contents

List of abbreviations used

a	allylic	DEPT	distortionless enhancement by polarisation transfer
Å	angstrom unit	$\Delta G^{\ddagger}$	free activation enthalpy
α^{*}	dip angle	DSC	differential scanning calorimetry
APT	attached proton test	E	chemical element
br	broad	ee	enantiomeric excess
Bz	benzyl	EI	electronic ionisation
cat.	catalytic amounts of	Eq.	equation
CGC	constrained geometry complex	Et	ethyl
CI	chemical ionisation	Fc	ferrocenyl
COSY	correlation spectroscopy	Flu	fluorenyl
Cp	cyclopentadienyl	GC	gas chromatography
Cp^{*}	pentamethylcyclopentadienyl	GPC	gel permeation chromatography
Cy	cyclohexyl	h	homoallylic
d	doublet	HMQC	heteronuclear multiple quantum coherence
δ	chemical shift in ppm	*i*Bu	*iso*butyl
D	deuterium	Ind	indenyl
Δ	difference	*i*Pr	*iso*propyl
Δ	thermal energy	IR	infrared
DBU	1,8-diazabicyclo[5.4.0]undecene-7	*J*	coupling constant

L	ligand	pd	pseudo-doublet
m	multiplet	PE	polyethylene
m	mass	Ph	phenyl
m	*meta*	PMMA	poly(methyl methacrylate)
M	metal	PP	polypropylene
M	molar	ppm	parts per million
M	molecule	PS	polystyrene
MAO	methylaluminoxane	pt	pseudo-triplet
Me	methyl	R	molecule fragment
Mes	mesityl	r.m.s.	root mean square
M_n	number-average molecular weight	s	singlet
MS	mass spectrometry	*t*Bu	*tertiary*-butyl
M_w	weight-average molecular weight	TGA	thermogravimetric analysis
n	*normal*	thf	tetrahydrofuran
ν	stretching vibration frequency	v	vinylic
*n*Bu	*normal* butyl	v	volume
NMR	nuclear magnetic resonance	vol	volume
o	*ortho*	w	weak
$\omega_{1/2}$	peak width at half maximum	X	molecule fragment
p	*para*	*z*	ion charge
P	polymer chain	□	vacant coordination site

List of figures

List of schemes

List of tables

Chapter 1. Introduction

The amount of the classic polyolefins {polyethylene (PE), polypropylene (PP) and polystyrene (PS)} currently produced world wide is well above 130×10^6 tons per year, thus making up some 60% of the entire production of plastics.[1] Polyolefins (besides low-density polyethylene from the ICI high pressure radical process) are afforded by transition metal catalysts that are going back to the discovery of Ziegler[2, 3] and Natta[4, 5, 6] that ethylene and propylene polymerise in the presence of $TiCl_4$ and Et_2AlCl even at low pressure or the discovery of the catalytic activity for olefin polymerisation of chromium oxides (Phillips-type catalysts) by Hogan and Banks.[7, 8] A major shortcoming of these early systems was the heterogeneous nature of the catalysts, which prevented a thorough characterisation of the active sites and left many questions open concerning the mechanisms involved in polymer growth. [9, 10]

Stimulated by related developments in other fields of catalysis, homogeneous organometallic compounds were introduced as suitable model systems for a deeper investigation of the polymerisation process at transition metal centres. Metallocenes were particularly attractive for mechanistic studies, since they exhibit simple coordination geometries, only one type of active site and easily polymerise ethylene when activated by alkylaluminiums.[9, 11, 12, 13, 14, 15] With the discovery by Kaminsky *et al.* of methylaluminoxane (MAO) as a highly effective activator,[16, 17] polymerisation rates and yields have been increased to an industrially useful level. These developments combined with the attractive product properties, *e.g.* well defined structure, little branching and very narrow molar mass distribution, initiated extensive efforts in industry and academia to expand further the capabilities of the system. Besides attempts to alter polymerisation characteristics and product properties by simple variation of the substituents on the cyclopentadienyl ring, more sophisticated alterations were introduced.[18] Since the 1980´s, work by Ewen, Brintzinger *et al.* in particular showed how the controlled, stereoselective polymerisation of propylene and other α-olefins may be achieved by employing catalysts of suitable symmetry and geometry.[9, 19, 20, 21, 22]

More recently, a new family of active polymerisation catalysts was developed by formally exchanging one cyclopentadienyl ring by an amido moiety; these are often referred to as constrained geometry complexes (CGCs), given the chelate bite angle

imposed by the cyclopentadienyl and amido donors. Dianionic, bifunctional chelating ligands of this type have been first employed by Bercaw *et al.* for the preparation of Sc(III) complexes such as **1** (Figure 1).[23, 24] Only a short time later, reports appeared on the preparation of related Group 4 complexes such as **2** (Figure 1)[25] and their exceptional characteristics in ethylene polymerisation and co-polymerisation of ethylene and higher α-olefins.[26, 27]

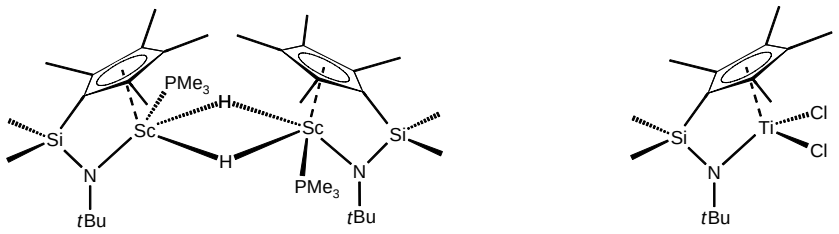

1 **2**

Figure 1. First reported scandium and titanium CGCs.

The superiority of the CGCs for co-polymerisation of ethylene and α-olefins when compared to metallocenes and metallocenophanes is generally ascribed to (i) a less crowded coordination sphere, (ii) a smaller $Cp_{centroid}$–M–N bite angle (by 25-30° compared to $\angle Cp_{centroid}$–M–$Cp_{centroid}$ in metallocenes and metallocenophanes) and (iii) a decreased tendency of the bulk polymer chain to undergo chain transfer reactions. The latter, as well as the high activity of such CGCs, most probably result from a more Lewis-acidic transition metal centre (according to the "neutral ligand formalism", an amido moiety can donate, at most, three electrons to the transition metal and thereby two electrons less than a cyclopentadienyl group).[23, 24, 28] Another advantage is the higher thermal stability of alkyl and dialkyl CGCs when compared to related metallocenes[29, 30] that allows higher polymerisation temperatures.

Since the early 1990's, the chemistry of CGCs experienced a rapid advancement, particularly because catalytic systems based on such compounds gave access to a wide array of copolymers with unique material properties and considerable commercial value.[31] Certain aspects of this development were covered by several reviews, however, the most general surveys are dating back to the late 1990's.[32, 33, 34, 35] Therefore, the following sections aim to give a broad survey about the development in the field since its early beginnings. Synthetic methods for the preparation of CGCs as well as the numerous alterations of the ligand framework will be summarised. Characteristics of

CGC catalysed polymerisation reactions will be thoroughly discussed, since they provide a good insight into the versatility and special qualities of this class of compounds that make it so unique. Furthermore, the application of CGCs in the catalysis of transformations other than polymerisations will be examined. The discussion of the catalytic potential of CGCs will highlight the sensitivity of the system to changes in the ligand framework; alterations in the ligand framework also mandate changes in the transition metal or co-catalyst.

1.1. Definition of Constrained Geometry Complex

The term constrained geometry complex (CGC) was originally coined by Stevens *et al.* for complexes in which a π-bonded moiety (*e.g.* cyclopentadienyl or a derivative) is linked to one of the other ligands on the same metal centre in such a way that the angle at this metal between the centroid of the π-system and the additional ligand is smaller than in comparable unbridged complexes. Stevens *et al.* claimed in their patent, that such a strain inducing link would improve catalyst performance. Their thesis was supported by a comparison of the polymerisation performance of a series of silanediyl- and disilanediyl-bridged cyclopentadienyl amido complexes.

Obviously, the scope of the definition by Stevens *et al.* goes far beyond *ansa*-bridged cyclopentadienyl amido complexes and was accordingly used in connection with other more or less related ligand systems, including (i) other *ansa*-complexes with $\eta^5:\eta^1$ coordination, where at least one of the coordinating fragments of bridged cyclopentadienyl-amido complexes is replaced by an isolobal fragment, (ii) other *ansa*-complexes with $\eta^5:\eta^1$ coordination, where at least one of the coordinating fragments is not isolobal to the formally replaced fragments of bridged cyclopentadienyl-amido complexes and (iii) other *ansa*-complexes with a coordination mode different from $\eta^5:\eta^1$ coordination.

Furthermore, the term is frequently used in connection with cyclopentadienyl amido complexes with long *ansa*-bridges such as $-(CH_2)_n-$ ($n > 2$). However, due to the length and flexibility of the bridge in such compounds there is virtually no strain induced.[36]

The work presented here spotlights certain aspects of bridged cyclopentadienyl amido complexes. Hence, this introduction will aim to give a thorough overview about

this specific class of CGCs. A few very closely related ligand systems (very similar coordination modes and charge distributions) will be briefly mentioned, but chemically less related systems, *e.g.* bridged cyclopentadienyl amino ligands will not be considered.

1.2. Synthesis of CGCs

Over the years, various routes for the synthesis of CGCs have been developed. In the following paragraphs, synthetic methods that were reported in the literature for the synthesis of Group 4 CGCs will be described. However, many of these methods have been applied as well to the synthesis of CGCs of other transition metals. Two general approaches can be distinguished: (i) the synthesis of the *ansa*-ligand precursor and subsequent complexation to a transition metal and (ii) the introduction of the *ansa*-bridge by reaction in the ligand sphere of a transition metal complex.

1.2.1. Synthesis of CGCs by complexation of the pre-assembled *ansa*-ligand precursor

The former approach is by far more extensively studied and a number of variants has been developed. The most successful routes comprise the dimetalation of the ligand precursor (ligand precursor will usually refer to the protonated, neutral species throughout the text) followed by a salt elimination reaction and the direct reaction of the ligand precursor with transition metal amides under amine elimination (*i.e.* σ-bond metathesis), respectively. In addition, there are several other routes including toluene elimination, amine assisted HCl elimination and trimethylsilylchloride elimination.

1.2.1.1. Dimetalation/salt elimination sequence

Dimetalation of the ligand precursor can be usually achieved using two equivalents of alkyl lithium reagents such as *n*BuLi, *t*BuLi and MeLi. Other lithium reagents, *e.g.* $LiNR_2$ (R = *i*Pr, $SiMe_3$), and Grignard reagents, *e.g.* *i*PrMgCl,[37] have also been successfully applied for the deprotonation of the ligand precursors. The dimetalated species can then be reacted with suitable Group 4 metal chlorides, *e.g.* $[TiCl_4(thf)_2]$, $ZrCl_4$,[38] $[ZrCl_4(thf)_2]$,[39] $[ZrCl_2(NEt_2)_2(thf)_2]$[40] or $HfCl_4$, *via* salt elimination to give the corresponding CGCs (Eqs. 1 – 3).

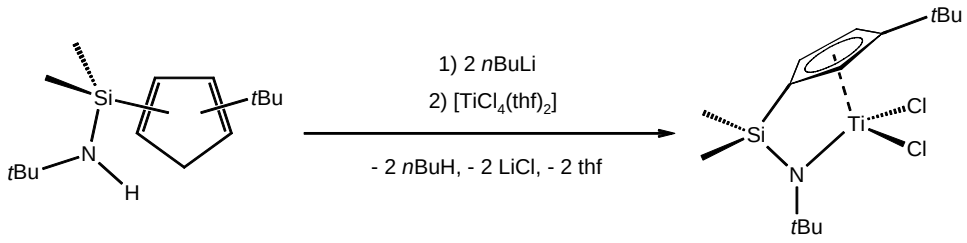

(Eq. 1)

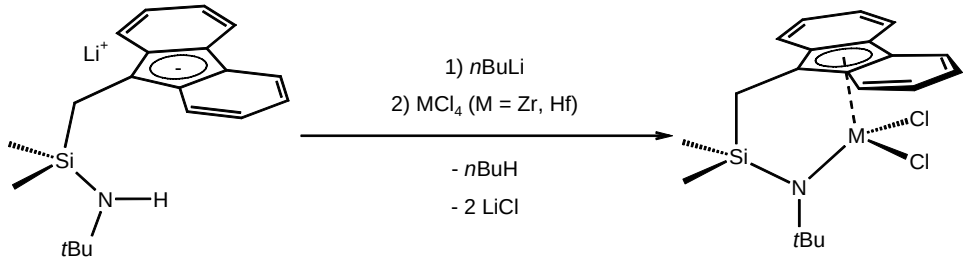

(Eq. 2)

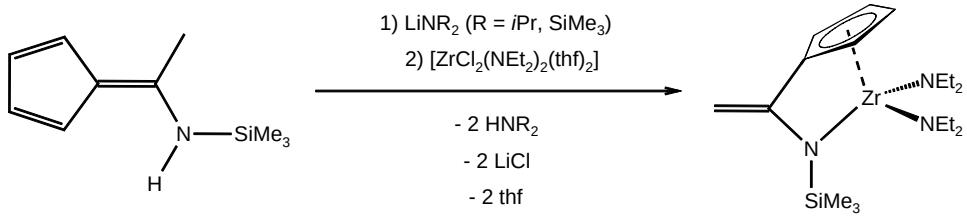

(Eq. 3)

While this route is quite effective for synthesis of the zirconium and hafnium species, the synthesis of the titanium congeners is often hampered by reduction of the titanium(IV) precursor in the course of the reaction. This obstacle can often be overcome by using $[TiCl_3(thf)_3]$ as the metal source and subsequent oxidation of the resultant titanium(III) complexes with $PbCl_2$ (Eq. 4).[41]

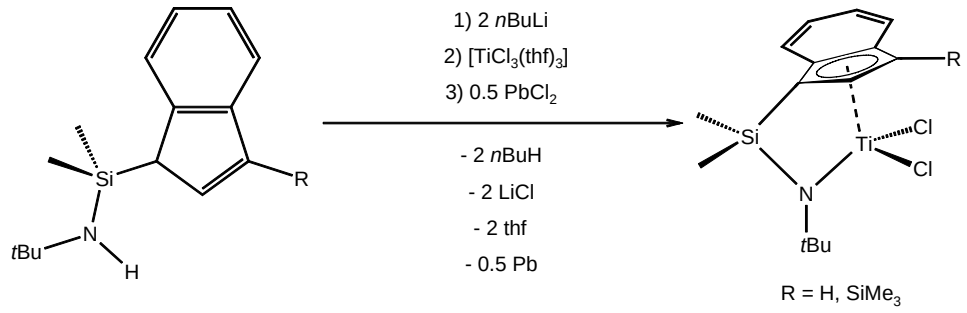

(Eq. 4)

More recently, it was also reported that reaction of the dilithiated ligand precursor with MCl_4 (M = Ti, Zr) in the presence of 2 equivalents of MeLi leads to the corresponding dimethylated CGCs in high yields, *i.e.* without competitive reduction reactions (Eq. 5).[42]

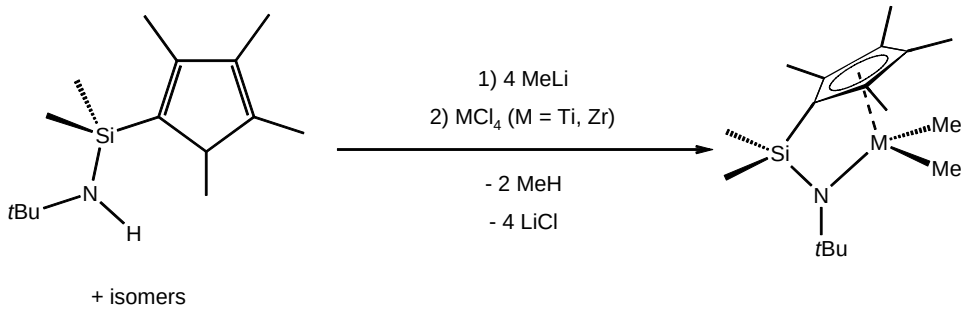

(Eq. 5)

+ isomers

In a variation of the reaction sequence, the dilithiated ligand precursor $[Li_2\{(C_5H_4)(CH_2)_3NMe\}]$ reacts with $[Cp_2ZrCl_2]$ under elimination of one equivalent of both lithium chloride and lithium cyclopentadienide to give $[\{\eta^5:\eta^1\text{-}(C_5H_4)(CH_2)_3NMe\}Zr(Cl)Cp]$.[43]

The reaction sequence of dimetalation and salt elimination is widely applicable to a range of differently substituted ligand precursors and different lengths of the *ansa*-bridge. However, substitution of all four chlorides on the metal precursor to give the bis-ligand metallocene (**3**) is frequently observed (Figure 2).

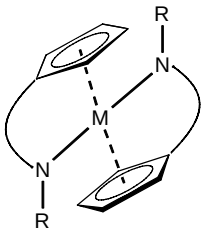

3

Figure 2. Metallocene complex with two CGC ligands.

Examples have been described for $[TiCl_4(thf)_2]$, $ZrCl_4$,[44] $[ZrCl_4(thf)_2]$[40, 45, 46, 47, 48] and $[HfCl_4(thf)_2]$ as Group 4 metal precursors. In most of these cases, the metallocene complexes are formed independent of the molar ratio of the starting materials. There is some evidence that the nature of the amido moiety as well as the solvent have some influence on the preference for CGC *vs*. metallocene formation.

1.2.1.2. Amine elimination

Reaction of CGC ligand precursors with Group 4 metal amides $[M(NR_2)_4]$ (M = Ti, Zr, Hf; R = Me, Et) under amine elimination developed into another versatile route to Group 4 CGCs. The first examples were reported for cyclopentadienyl ligands with long C_3H_6 *ansa*-bridges (Eq. 6) and shortly thereafter for cyclopentadienyl and indenyl ligands with short $SiMe_2$ *ansa*-bridges (Eq. 7).[49]

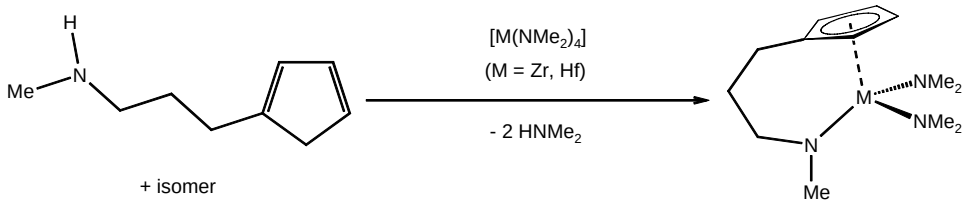

(Eq. 6)

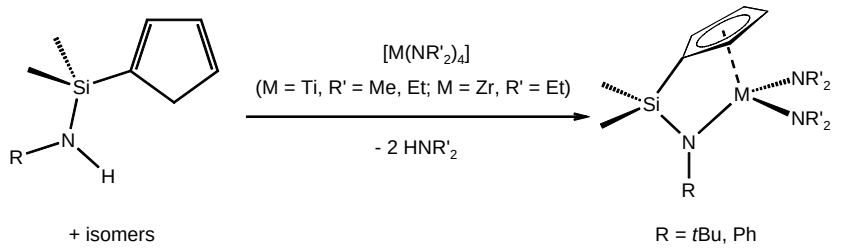

(Eq. 7)

Examples for substituted tetramethylcyclopentadienyl ligands appeared a few years later, while examples for substituted fluorenyl ligands seem to be still absent from the literature. In this context, Alt *et al.* reported the reaction of ligand precursor $(C_{13}H_9)(SiMe_2)N(H)tBu$ with $[Zr(NEt_2)_4]$ to give the unbridged complex $[(C_{13}H_9)(SiMe_2)N(tBu)Zr(NEt_2)_3]$. This observation was attributed to the comparably low acidity of the proton on the fluorenyl five-membered ring and the steric demand of the fluorenyl moiety. $[ZrCl_2(NMe_2)_2(thf)_2]$ may as well serve as a suitable precursor for such amine elimination reactions as was demonstrated for a few CGC ligand precursors (Eq. 8).[50]

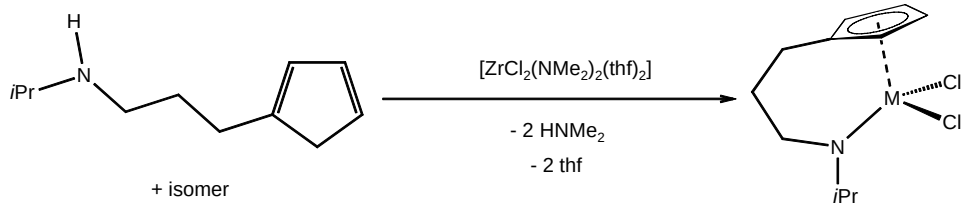

(Eq. 8)

The amine elimination route usually proceeds very cleanly and gives the desired products in high yields. In contrast to the dimetalation/salt elimination sequence, formation of metallocene type complexes (**3**) is not observed as a side reaction if the starting materials are applied in an equimolar ratio. However, such metallocenes may be obtained if the ligand precursors and the Group 4 metal *per*-amides are combined in a 2:1 molar ratio.[51]

1.2.1.3. Toluene elimination

Similar to the amine elimination route, Group 4 tetrabenzyl compounds may be used as precursors for the synthesis of CGCs. This has the added advantage that the

acidity of toluene is much lower than of any amine and therefore σ-bond metathesis should be more thermodynamically favoured. While the reaction of $(C_5Me_4H)(SiMe_2)N(H)tBu$ with $[TiBz_4]$ was reported to give the desired CGC in high yields, the reaction with the zirconium analogue resulted in low conversions and significant amounts of side products (Eq. 9).[52]

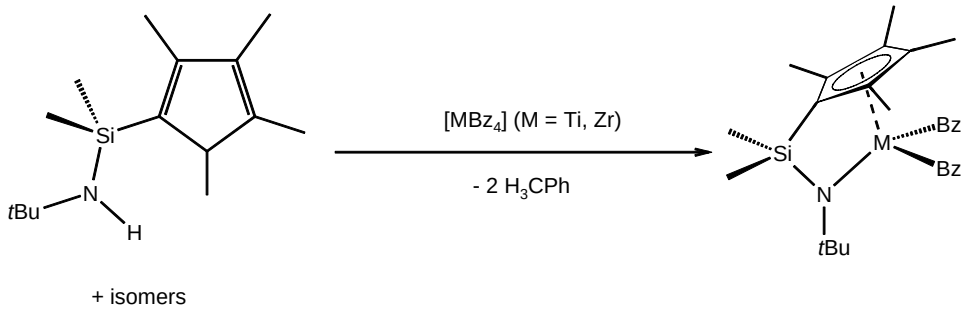

(Eq. 9)

1.2.1.4. Amine assisted HCl elimination

Direct reaction of the neutral ligand precursors with $TiCl_4$ in the presence of triethylamine gave the corresponding dichloro CGCs in moderate yields (Eq. 10). However, published examples for this HCl elimination reaction include only ligand systems with relatively long C_2H_4 and C_3H_6 *ansa*-bridges and consequently little strain in the *ansa*-ligand.

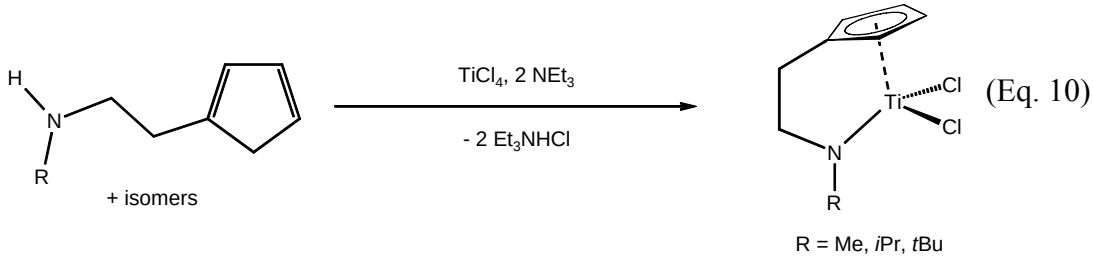

(Eq. 10)

1.2.1.5. Me_3SiCl elimination

Alternatively, ligand precursors may be utilised where the acidic protons are replaced by trimethylsilyl moieties. Such ligand precursors may react with suitable Group 4 metal halides under Me_3SiCl elimination conditions to give the corresponding CGCs (Eq. 11). Reported examples are limited to the reaction of $(C_5H_4SiMe_3)(CH_2)_3N(SiMe_3)_2$ with $TiCl_4$, $ZrCl_4$ and $[ZrCl_4(SMe_2)_2]$, *i.e.* unstrained systems.[53, 54]

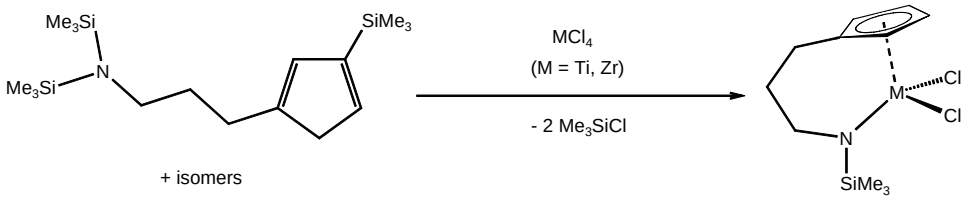

(Eq. 11)

1.2.1.6. Combined LiCl and Me_3SiCl elimination

One example has been described that combines the previously described approaches of salt elimination and Me_3SiCl elimination (Eq. 12). The yield of this synthesis, however, is relatively low. It gives rise to a relatively long C_3H_6 *ansa*-bridge, *i.e.* a ligand system without strain.[55]

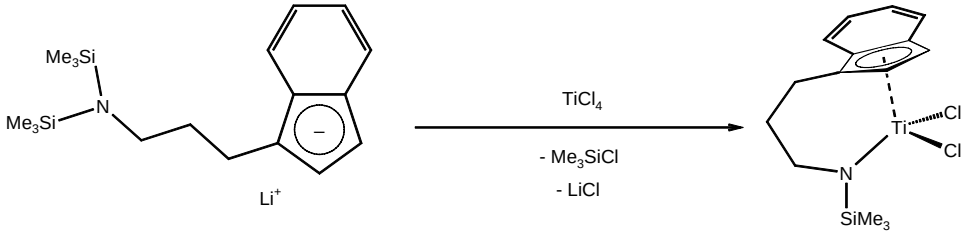

(Eq. 12)

1.2.2. Synthesis of CGCs by reaction in the ligand sphere of a transition metal

The approach of introducing an *ansa*-bridge by a reaction in the ligand sphere of a suitable half-sandwich complex to create CGCs is much less developed and gives access only to limited variety in terms of ligand design. When [{(η^5-C_5H_4)($SiMe_2Cl$)}$TiCl_3$] is treated with either NH_2R and NEt_3 in a 1:1:2 ratio,[56] with 1 equivalent of Li[NHR] in the presence of 1 equivalent of NEt_3 (Eq. 13)[56,57] or with excess Li[NHR][58] the corresponding CGCs [{η^5:η^1-(C_5H_4)($SiMe_2$)NR}$TiCl_2$] (R = alkyl) are isolated. Similarly, reaction of [{(η^5-C_5H_4)($SiMe_2Cl$)}M(η^5-1,3-*t*BuC_5H_3)Cl_2] (M = Ti, Zr, Hf) with 2 equivalents of Li[NH*t*Bu] yields the corresponding CGCs [{η^5:η^1-(C_5H_4)($SiMe_2$)N*t*Bu}M(η^5-1,3-*t*BuC_5H_3)Cl].[59] Neither the synthesis of indenyl nor fluorenyl analogues has been reported using this route, probably due to difficulties in the preparation of suitable precursors.[41]

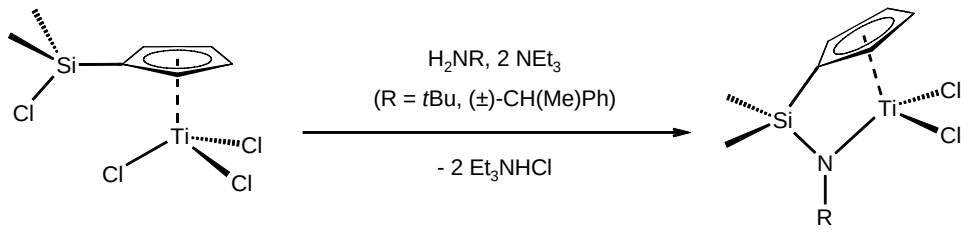

(Eq. 13)

Only recently, the synthesis of tetramethylcyclopentadienyl analogues by reaction of [{(η^5-C_5Me_4)(SiMeClX)}$TiCl_3$] (X = H, Cl) with 2 equivalents of LiNH*t*Bu has appeared. It was demonstrated that this reaction proceeds *via* intermediate formation of [{(η^5-C_5Me_4)(SiMeX)N(H)*t*Bu}$Ti(Cl)_2$N(H)*t*Bu] and subsequent ring closure under amine elimination.[60] While this route is of interest for facile variation of the amido fragment in silicon-bridged CGCs, expansion of this approach to CGCs with other *ansa*-bridges is restricted by the availability of suitable precursors.

Another very specific route is the reaction of fulvene complexes such as [{(C_5H_4)=C(H)*t*Bu}$Ti(Cp^*)Cl$] with nitriles or *iso*-nitriles. However, these reactions give only access to certain C_2-bridged CGCs and are therefore of limited practical value.[61]

1.3. Derivatisation of Group 4 CGCs

Most of the previously described synthetic routes yield the desired CGCs as the dichloro or diamido derivatives. Both may be activated by methylaluminoxane (MAO) to polymerise olefins. However, further derivatisation of these complexes is often required to obtain CGCs with a certain chemical reactivity, *e.g.* the dialkyl derivatives that may be activated by $B(C_6F_5)_3$ or $[Ph_3C^+][B(C_6F_5)_4^-]$ to give olefin polymerisation catalysts (*vide infra*). Most of these derivatisation reactions seem to be of quite general applicability. The dichloro derivatives can be easily converted to the corresponding diamido derivatives by reaction with 2 equivalents of $LiNMe_2$.[62] On the other hand, the diamido derivatives can be converted to the corresponding dichloro complexes using Me_3SiCl,[28, 63] PCl_5, HCl or $Me_2NH{\cdot}HCl$.[28, 36] In some cases, the dichloro complexes are obtained in the form of their Me_2NH adducts.[28, 36]

The dichloro complexes and their Me_2NH adducts can be easily converted to the corresponding dialkyl complexes by reaction with 2 equivalents of lithium alkyls,[36, 64] potassium alkyls or Grignard reagents.[36, 41, 65] Selective mono-alkylation of the dichloro complexes could as well be achieved by means of one equivalent of nBu_2Mg[30] or

$AlMe_3$. Similarly, reaction of the dichloro complexes with one equivalent of NaCp[66] or lithium aryls[67, 68, 65] resulted in selective substitution of one chloride per metal centre. It is noteworthy that CGCs with such substitution patterns are chiral at the metal centre, although resolution of any such system has yet to be accomplished.

The dichloro derivatives can be converted to the corresponding butadiene complexes by reaction with 2 equivalents of *n*BuLi in the presence of butadienes,[69] with magnesium butadiene $[Mg(C_4H_6)]_n$[70] or with 1,4-diphenylbutadiene magnesium $[Mg(C_4H_4Ph_2)(thf)_3]_n$.[71] Structural and spectroscopic studies of the resultant complexes revealed that the bonding mode of the butadiene ligand in CGCs is sensitive to the ligand framework and the nature of the transition metal. While the zirconium compounds displayed exclusively a metallacyclic σ^2, π coordination of the butadiene ligand (corresponding to zirconium in the oxidation state +IV),[70, 71] the titanium analogues showed both metallacyclic σ^2, π (oxidation state +IV) and conventional π^2 (oxidation state +II) coordination modes dependent on the specific nature of the co-ligands.[69, 70] In a similar reaction, $[\{\eta^5:\eta^1\text{-}(C_5Me_4)(SiMe_2)N\textit{t}Bu\}TiCl_2]$ was found to undergo reaction with disubstituted 1,3-butadiynes in the presence of magnesium to give the corresponding five-membered titanacyclocumulenes.[72]

1.4. Modification of the ligand system with constrained geometry

To date, a multitude of Group 4 CGCs and closely related compounds have been prepared by the synthetic methods described above. Obviously, the nature of the ligand system may be adjusted either by variation of the cyclopentadienyl moiety, the amido group, the *ansa*-bridge or a combination thereof (Figure 3).

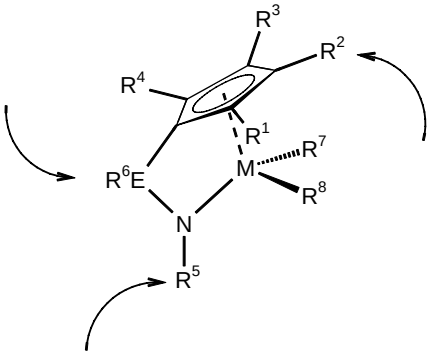

Figure 3. Sites of modification in ligands with constrained geometry.

The following sections aim to give a broad overview of the variations as they are found in the open literature, giving representative examples for each category. Influences of the structure of the CGCs on their polymerisation characteristics will be discussed in an individual section together with other aspects of CGC catalysed polymerisation reactions.

1.4.1. Variation of the cyclopentadienyl fragment

Modification of the η^5-coordinated cyclopentadienyl moiety may have significant impact on the chemistry of CGCs through steric and electronic effects. Besides the ubiquitous C_5H_4 (cyclopentadienyl), C_5Me_4 (tetramethylcyclopentadienyl), C_9H_6 (indenyl) and $C_{13}H_8$ (fluorenyl) fragments, a variety of other moieties have been studied (Figure 4). It should be noted that non-symmetric substitution patterns of the cyclopentadienyl system result in chiral CGCs.

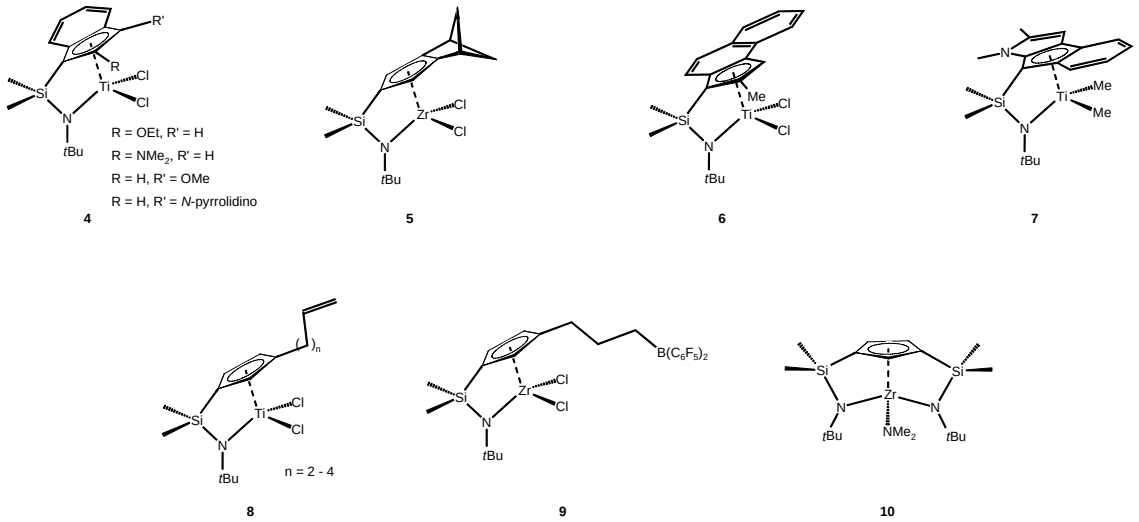

Figure 4. Variation of the cyclopentadienyl moiety of the CGC ligand.

Several studies were investigating alkyl and aryl substituted cyclopentadienyl moieties such as C_5H_3R (R = H, Me, *t*Bu, Bz)[73], C_5H_2(2-Me)(4-Ph)[74] and $CpMe_3R$ (R = H, Me, *n*Bu, 1-methylallyl, 1-methylprop-1-en-1-yl, Ph, 4-fluorophenyl, CMe_2Ph)[75, 76, 77]. Similarly, alkyl, aryl (R = Me, *t*Bu, Ph or a combination thereof, in various positions of the ring system) and heteroatom (3-OMe, 2-OEt, 2-NMe_2, 3-*N*-pyrrolidino)[78] substituted indenyl derivatives (**4**) and alkyl substituted fluorenyl (3,6-di-*t*Bu-fluorenyl)[79] derivatives were studied. Isodicyclopentadienyl based CGCs (**5**) were as well reported.[80] Beside indenyl and fluorenyl, other fused ring systems have been

incorporated as the η^5-coordinated moiety in CGCs, such as benz[*e*]indenyl (**6**)[42, 81, 82, 83] and heterocycle fused indenyl derivatives (**7**).[84]

Furthermore, a series of CGCs with ω-alkenyl substituted cyclopentadienyl and indenyl moieties (**8**) have been prepared and their self-immobilisation during polymerisation by incorporation of the pendent olefinic group into the polymer chain has been explored.[85, 86] Specifically an allyl substituted cyclopentadienyl moiety was further modified by hydroboration to give a derivative with a pendent $B(C_6F_5)_2$ moiety (**9**).

The η^5-coordinated moiety has also been substituted with additional $(SiMe_2)N$*t*Bu amido functionalities (**10**), resulting in a tridentate ligand and consequently a substantial change of the coordination characteristics.[87, 88, 89, 90]

Bimetallic systems are more than just a curiosity. Here, the CGC fragment is connected *via* a carbon linker that is attached at its η^5-coordinated moiety to an *ansa*-metallocene[91] (**11**) or a second CGC[92, 93, 94, 95] moiety (**12**) (Figure 5).

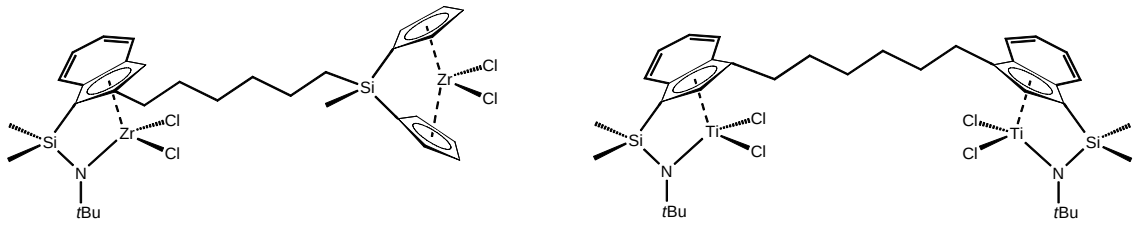

11 **12**

Figure 5. Bimetallic CGCs with a carbon linker attached to the indenyl moiety.

Besides cyclopentadienyl derivatives of all sorts, a few examples of CGCs incorporating other monoanionic 6-electron donor fragments have appeared in the literature (Figure 6). These examples comprise phospholyl- (**13**),[96] boratabenzene (**14**),[97] and cyclohexadienyl (**15**)[98] analogues of *ansa*-cyclopentadienyl amido complexes.

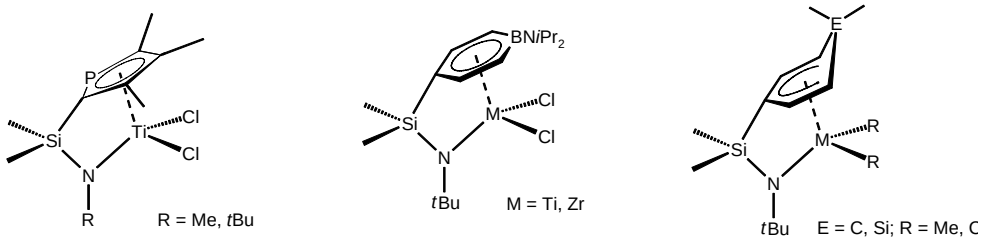

13 **14** **15**

Figure 6. CGCs containing 6-electron donor fragments other than cyclopentadienyl derivatives.

1.4.2. Variation of the amido fragment

Variation of the amido fragment in CGC ligands may have a marked effect on both the steric and particularly the electronic environment of the ligated transition metal. Simple alkyl and aryl amido fragments in the CGC ligand framework are omnipresent in the literature. Chiral varieties (**16**) of these have been introduced early on, particularly as they allow facile preparation of enantiomerically pure CGCs if suitable enantiomerically pure amines are used in the preparation (Figure 7).[37, 56, 57, 63, 99]

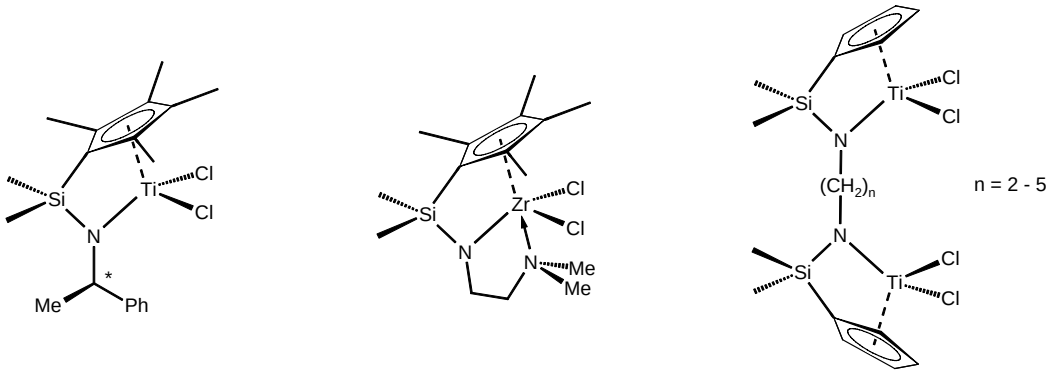

16 **17** **18**

Figure 7. Variation of the amido moiety of the CGC ligand.

CGCs containing potentially tridentate ligands with additional neutral donor sites attached to the amido moiety NR (**17**) have been reported as well (Figure 7). Substituents with relatively hard donors (R = CH_2OMe, CH_2NMe_2, CH_2CH_2NHMe, $CH_2CH_2NMe_2$, CH_2CH_2OMe)[46, 58, 65, 67, 100, 101, 102, 103, 104] as well as softer donor groups (R = *o*-$PhPPh_2$, CH_2CH_2SMe)[105] have been described. Chiral versions of such tridentate CGC ligands have also been published.[106] Furthermore, bimetallic CGCs with carbon spacers between the amido groups of the two CGC moieties (**18**) have been reported (Figure 7). A number of CGCs have been reported in the literature, in which the alkyl or aryl amido fragment of *ansa*-cyclopentadienyl amido complexes was formally replaced by a different monoanionic η^1-coordinating moiety.

Besides alkyl and aryl amido moieties, three other nitrogen based groups, *i.e.* sulfonamido, hydrazido and imino groups, have been introduced in such compounds (Figure 8). Due to the electron-withdrawing characteristics of the sulfonamido moiety, CGCs incorporating this group (**19**) display a significantly elongated Ti–N bond distance when compared to their alkyl or aryl amido counterparts. The monoanionic hydrazido moiety may adopt a η^1 (**20**) or η^2 (**21**) coordination mode, depending on the co-ligands at the metal centre.[107, 108] Bridged cyclopentadienyl imino complex **22** resembles to some extent the bridged cyclopentadienyl amido complexes. However, the electronic situation in the former is quite different, as the formally sp^2-hybridised nitrogen atom acts as a pure σ-donor to the metal since the remaining *p*-orbital on nitrogen participates in the double bond to the adjacent carbon atom.

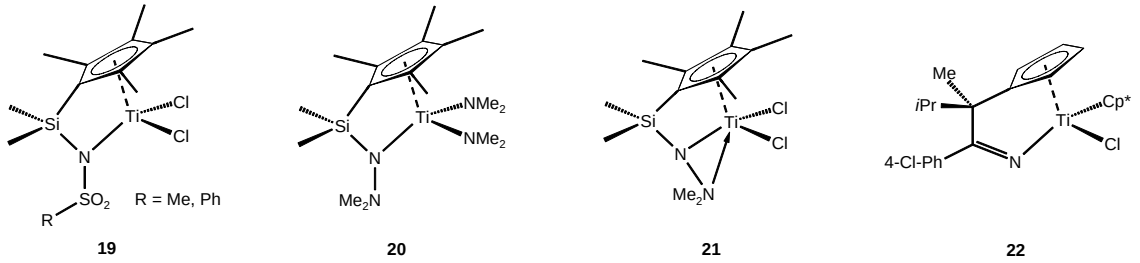

19 **20** **21** **22**

Figure 8. CGCs containing nitrogen based anionic fragments other than alkyl or aryl amido moieties.

Examples of complexes in which the amido moiety is replaced by a carbanionic fragment appear in **23**,[109] **24**[110] and **25**[111] (Figure 9) amongst others.[112, 113, 114, 115, 116, 117, 118] While the carbanion equivalent is formally isoelectronic to the amido moiety, the former is a pure σ-donor as no suitable lone pair for π-donation to the metal centre is available.

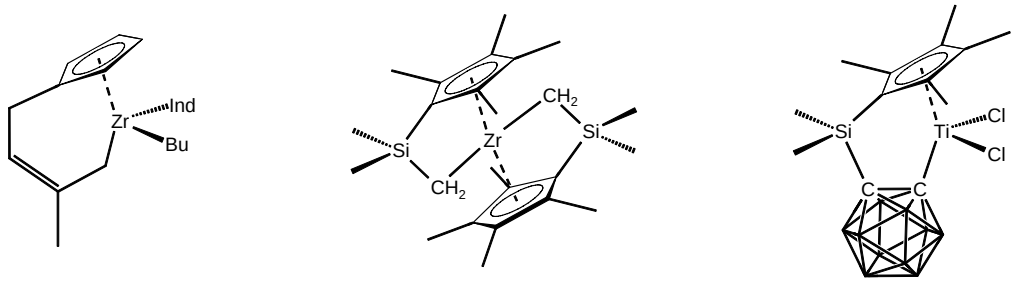

23 **24** **25**

Figure 9. CGCs in which the amido moiety is formally replaced by carbon based anionic fragments.

By formal substitution of the nitrogen atom in *ansa*-cyclopentadienyl amido ligands with its higher homologue phosphorus, linked cyclopentadienyl phosphido

complexes such as **26**,[119, 120] **27**[121] and **28**[122] have been synthesised (Figure 10).[123, 124, 125, 126] Despite some synthetic difficulties, this group of CGCs was studied intensively and a close resemblance to their amido analogues could be demonstrated, *e.g.* in their (co)polymerisation characteristics.

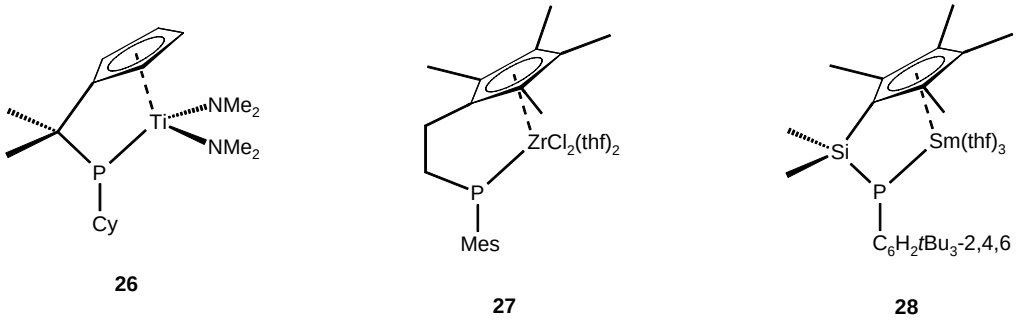

26 **27** **28**

Figure 10. CGCs in which the amido moiety is formally replaced by phosphido fragments.

Formal replacement of the R_2N^- fragment by isoelectronic RO^- or RS^- fragments is of course also conceivable. Indeed a number of such *ansa*-cyclopentadienyl oxy-complexes, *e.g.* **29**,[127] **30** and **31**[128] have been reported (Figure 11). Of this class of compounds,[129] particularly bridged cyclopentadienyl phenoxy complexes[128, 130, 131, 132, 133, 134, 135] amongst others[51, 136, 137, 138, 139, 140, 141, 142] have received a considerable amount of attention due to their structural features that are very similar to their amido counterparts and reasonable catalytic performance. To date, there has been only one report on related sulfur based *ansa*-complexes **32** (Figure 11).[143]

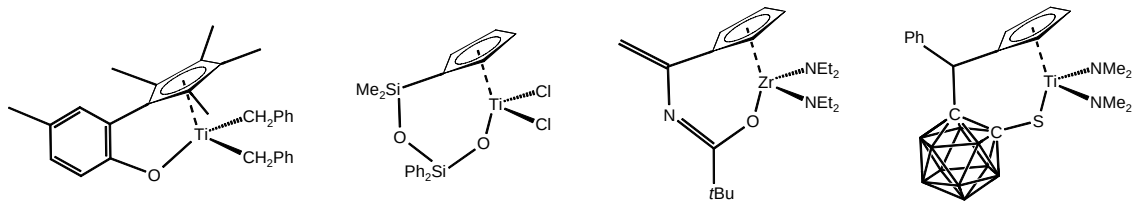

29 **30** **31** **32**

Figure 11. CGCs in which the amido moiety is formally replaced by Group 16 based anionic fragments.

1.4.3. Variation of the *ansa*-bridge

In the original patent by the Dow Chemical Company describing the use of Group 4 CGCs in the polymerisation of olefins, their exceptional characteristics in this reaction was attributed to the strain induced by an *ansa*-bridge between a π-bonded moiety and a second ligand of the same transition metal centre. In the closely related field of metallocene chemistry, the marked effect of an *ansa*-bridge between two

cyclopentadienyl moieties on stability and reactivity of these complexes is well documented.[144, 145] Owing to the similarity between *ansa*-metallocenes and CGCs, reasonable effort was undertaken to tune the latter by modification of the *ansa*-bridge. However, it should be noted that a recent report critically discussed whether the *ansa*-bridge in CGCs is a true prerequisite for their unique polymerisation characteristics.[146] Notwithstanding the former consideration, the modifications in the *ansa*-bridge as they are found in the literature will be summarised.

The first CGC (**1**) introduced by Bercaw *et al.* contained a ligand with a $SiMe_2$ moiety between a C_5Me_4 and an amido fragment (Figure 1). This bridging moiety was previously successfully applied in *ansa*-metallocene chemistry, particularly for Group 4 metallocenes. To date, it is still the most commonly applied bridging moiety in CGC chemistry, probably due to the facile synthetic accessibility and high thermal and chemical stability.

The commonly used $SiMe_2$ *ansa*-bridge has been further modified by replacement of one of the methyl substituents, resulting in a chiral silicon atom (Figure 12). Replacement by alkyl, alkenyl or phenyl substituents combined with asymmetrically substituted cyclopentadienyl derivatives gives rise to diastereomeric complexes (**33**). Substitution of one methyl group for hydrogen (**34**) or chlorine (**35**) introduced a reactive site in the *ansa*-bridge that may be used for linking the CGCs to heterogeneous supports.[60, 147] In addition, suitable linkers attached to a mono-silicon bridge have been used to connect CGC fragments to *ansa*-metallocene fragments in bimetallic complexes (**36**).[91]

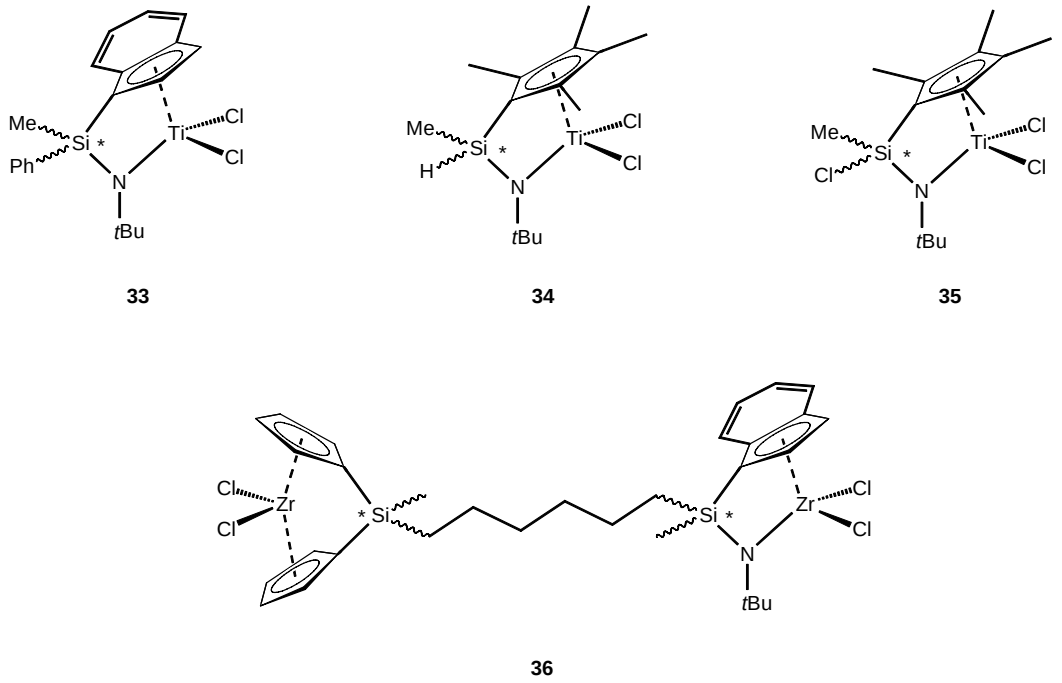

Figure 12. CGCs with mono-silicon bridges other than $SiMe_2$.

Besides silicon, only a few other elements have been reportedly used to connect the respective ligand fragments in *ansa*-cyclopentadienyl amido complexes by a short, single atom bridge (Figure 13). These comprise boron (*i*Pr_2NB) (**37**),[148] carbon in both the sp^2 (H_2C=C) (**38**)[40, 149] or sp^3 (RHC, R = alkyl, aryl) (**39**)[119, 150] hybridised forms and phosphorous (*t*BuP) (**40**).[151]

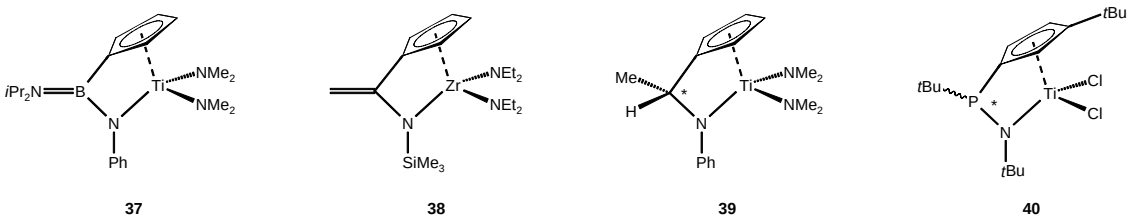

Figure 13. CGCs with mono-element bridges other than silicon based.

Longer bridges containing 2 or 3 atoms in the backbone were also described (Figure 14). Thus, $(SiMe_2)_2$-bridged CGCs (**41**) were used in the patent by the Dow Chemical Company as examples for *ansa*-bridged cyclopentadienyl amido complexes without substantial strain in the ligand framework and subsequently lower polymerisation activity. On the other hand, the CH_2SiMe_2 bridging moiety, first devised by Dias *et al.* (**42**), was found to be superior over the short $SiMe_2$ bridge in Group 3 CGC catalysed hydrosilylation (*vide infra*).[152] Furthermore, numerous CGCs bearing $(CH_2)_n$ (n = 2,[29, 153, 154] 3[29, 155]) bridges (**43**, **44**) have been reported.

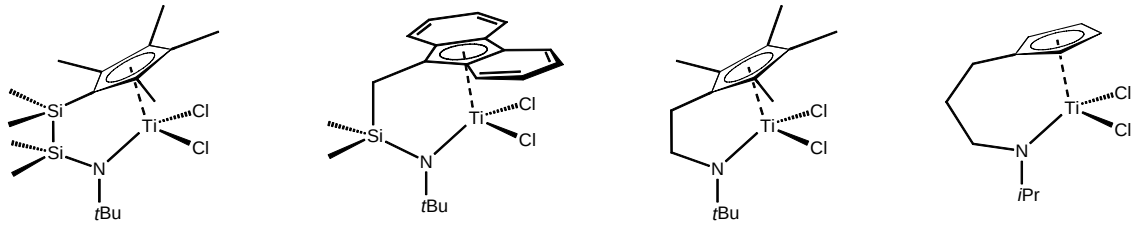

41 **42** **43** **44**

Figure 14. CGCs with bridges longer than one atom.

1.4.4. Variation of the metal centre

Linked cyclopentadienyl amido ligands have first been utilised by Bercaw *et al.* for the synthesis of Sc(III) complexes. Shortly thereafter, Okuda reported the first titanium compounds with such ligands and the Dow Chemical Company and Exxon Chemical Company issued fundamental patents that claimed unique polymerisation characteristics of the Group 4 congeners. Since then, the vast majority of the open literature focused on the tuning and understanding of properties of Group 4 CGCs. However, linked cyclopentadienyl amido ligands have been extensively applied to Group 3 transition metals and also to the lanthanides and actinides. Furthermore, the same ligand design has been successfully used in the coordination chemistry of other transition metals and even main group elements. The following sections intend to demonstrate the versatility of linked cyclopentadienyl amido ligands (without additional pendent donor functionalities) outside Group 4 chemistry.

Besides the first Group 3 CGCs published by Bercaw *et al.*,[23, 24, 156] various monomeric amido CGCs of Y(III) (**45**),[157] as well as monomeric alkyl[104, 158, 159, 160, 161] and dimeric hydrido[158, 159, 160] CGCs of Y(III), Lu(III), Yb(III), Er(III) and Tb(III) have been reported. Also described are a number of Y(III), La(III) and Nd(III) complexes that bear one or two $[(3,6\text{-}t\text{Bu}_2\text{C}_{13}\text{H}_6)(\text{SiMe}_2)\text{N}t\text{Bu}]^{2-}$ ligands and which display interesting bonding modes (η^5-, symmetric or non-symmetric η^3-coordination of the substituted fluorenyl moiety depending on the nature of the metal and the co-ligands).[162] Moreover, monomeric and dimeric CGCs of Yb(II) (**46**) and Sm(II)[163] as well as monomeric, dimeric and tetrameric CGCs of thorium Th(IV)[164, 165] and U(IV) such as **47** have been reported (Figure 15).

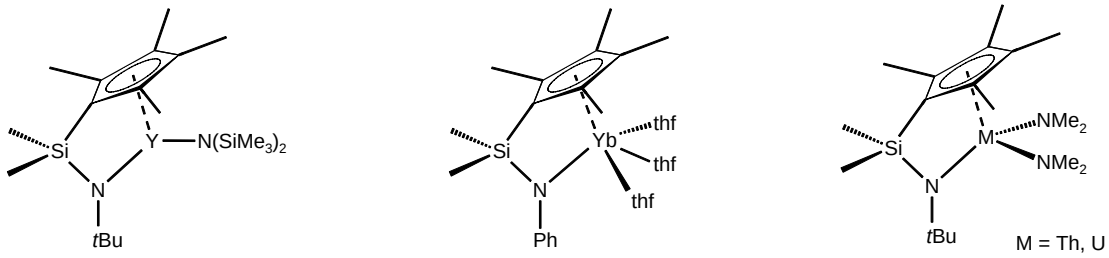

45 **46** **47**

Figure 15. Group 3 CGCs.

Beyond Groups 3 and 4 of the periodic table, numerous examples have been reported for CGCs of other elements, particularly of the earlier groups. For example, vanadium complexes bearing bridged cyclopentadienyl amido ligands were synthesised incorporating vanadium in the oxidation states +II (**48**), [166] +III (**49**),[166] +IV (**50**, **51**),[166, 167] +V (**52**).[168] For the higher Group 5 homologues niobium and tantalum CGCs are only known for the oxidation state +V (**53**) (Figure 16).[169, 170, 171, 172]

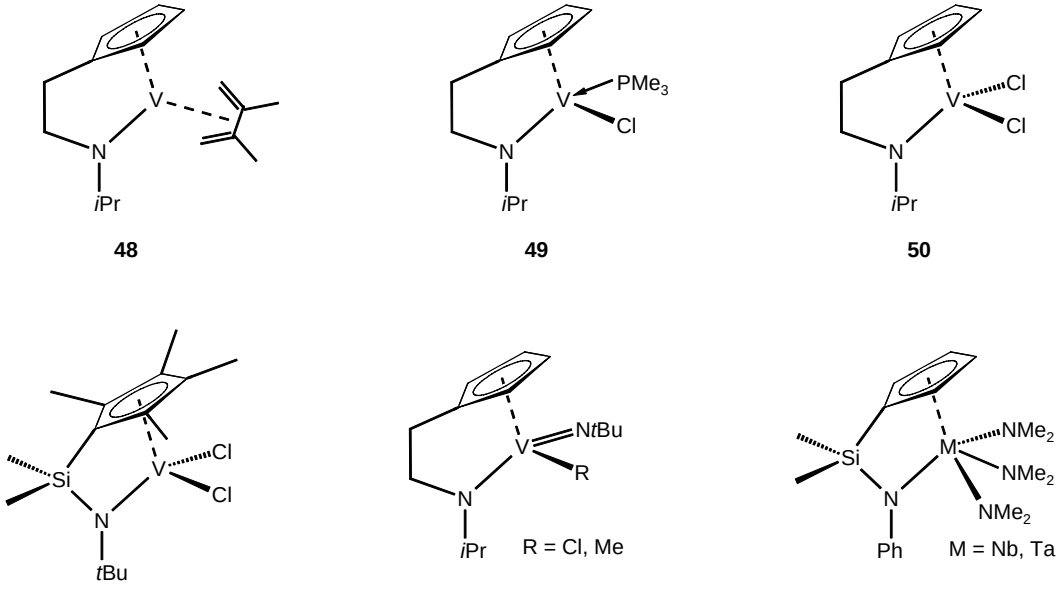

48 **49** **50**

51 **52** **53**

Figure 16. Group 5 CGCs.

CGCs are also known for all the Group 6 metals containing chromium(III) (**54**),[173] molybdenum(IV) (**55**),[174] molybdenum(V) (**56**),[53, 54] molybdenum(VI) and tungsten(VI) (**57**), respectively, reflecting the preferred oxidation states for the elements in this group (Figure 17).

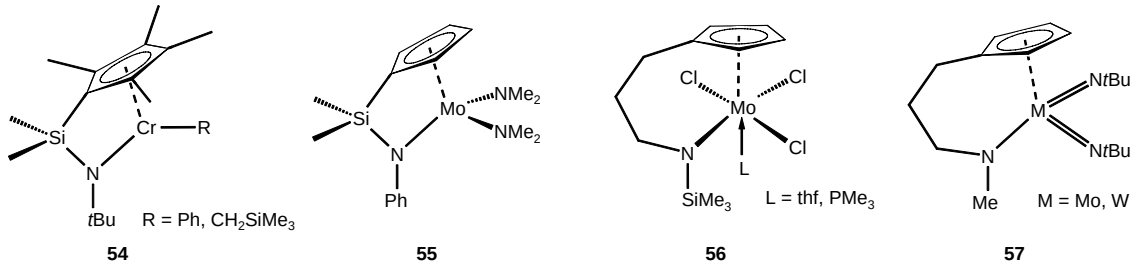

54 **55** **56** **57**

Figure 17. Group 6 CGCs.

The only reported Group 7 complexes bearing a linked cyclopentadienyl amido ligand contain rhenium in the oxidation state +III (**58**).[175, 176] For Group 8, only the Fe(II) complex **59**, albeit only with rudimentary spectroscopic characterisation, has been described (Figure 18).

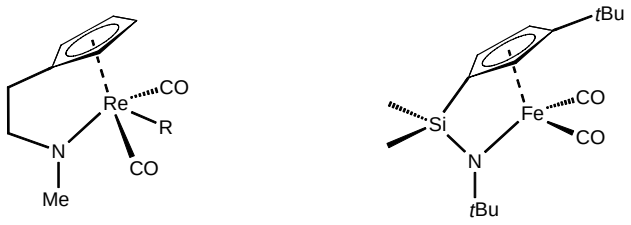

58 **59**

Figure 18. Group 7 and 8 CGCs.

Cowley *et al*. reported a number of Group 13 (Al, Ga, In)[177, 178] and Group 15 (P, As, Sb)[179] complexes utilising CGC ligands. However, the coordination modes in these compounds are completely different from those found in the previously discussed transition metal complexes, as the main group elements lack suitable orbitals for η^5-coordination of the Cp fragment.

1.5. Polymerisation with constrained geometry complexes

The first claims of exceptional catalytic activity of Group 4 CGCs for ethylene homopolymerisation, copolymerisation of ethylene with α-olefins such as 4-methyl-1-pentene, 1-hexene, 1-octene and 4-vinylcyclohexene (as an example of a hindered vinylic monomer) and copolymerisation of ethylene and styrene can be found in the patent literature.[26, 27] Such performance triggered intensive research activity to (i) understand, (ii) further improve and (iii) exploit the full catalytic potential of these compounds. Since then, ongoing industrial research into the field is documented in numerous patents.[180] However, the following summary focuses on aspects of CGC catalysed polymerisations as they appear in the open literature.

1.5.1. Mechanism of the polymerisation reaction

It is generally agreed that the CGC catalysed polymerisation of α-olefins proceeds according to the Cossee-Arlman mechanism.[181, 182] This mechanism (Scheme 1) assumes that the catalytically active centre incorporates both an alkyl group and a vacant coordination site that allows π-coordination of the incoming monomer. In a concerted rearrangement *via* a four-centred transition state, a new bond between the alkyl group and the α olefinic carbon atom is established, while at the same time a new bond between the β olefinic carbon atom and the transition metal centre is formed. In this way, both a new alkyl group and a vacant site are generated, providing the conditions for the next propagation step.

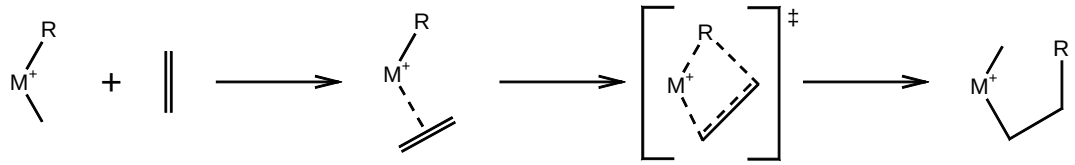

Scheme 1. Cossee-Arlman mechanism for olefin polymerisation on transition metal centres; ancillary ligands and counter-ion omitted for clarity.

Various computational studies specifically on CGC catalysed olefin polymerisation support these assumptions.[183, 184, 185, 186, 187, 188, 189, 190, 191, 192] Experimental studies showed a strong influence of the solvent on polymerisation rate.[193] Related computational studies rationalised this observation by demonstrating competition of the counter-ion, monomer and solvent molecules for the vacant coordination sites at the cationic active centre[187, 188] and the influence of the solvent on ion-pair separation.[187, 190, 191, 192] Besides the characteristics of the solvent, the steric demand and ability of the ancillary ligands to stabilise the positive charge on the active centre were found to affect the equilibrium between the contact-ion pair and the solvated, fully separated ion-pair.[194]

Early in the development of CGCs, the occurrence of long-chain branches in CGC derived polyolefins was observed. It was reasoned that these long-chain branches may stem from incorporation of vinyl-terminated macromonomers formed in the course of the reaction.[195] Indeed, exclusively vinyl terminated polyethylene was obtained with [{η^5:η^1-(C_5Me_4)($SiMe_2$)N*t*Bu}$TiCl_2$]/MAO systems.[196] An alternative long chain branching mechanism *via* σ-bond metathesis involving transfer of a proton in the

growing polymer chain to the α-carbon of the transition metal alkyl cation was excluded based on results from computations.[197]

Computational and experimental studies on the potential mechanisms for generation of vinyl-terminated macromonomers established that β-hydrogen transfer to the monomer was the energetically most favourable (Scheme 2). Other conceivable mechanisms such as β-hydride elimination (β-hydrogen transfer to the metal) and σ-bond metathesis involving one equivalent of monomer were found to be highly disfavoured energetically.[184, 197, 198] Experimental data also suggest that the probability of incorporation of the vinyl terminated macromonomers is enhanced by a low diffusion rate, probably due to entanglement effects.[199]

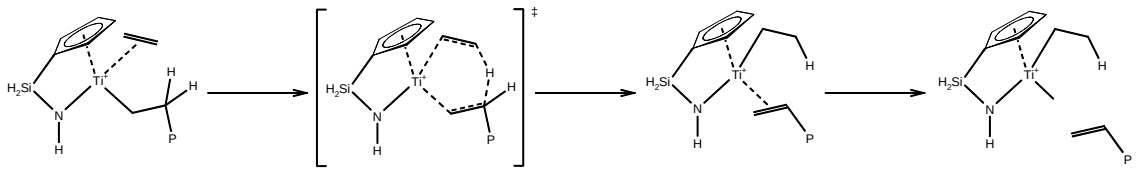

Scheme 2. Chain termination with generation of vinyl terminated macromonomer by β-hydrogen transfer to the monomer.

1.5.2. Activation of CGC for the polymerisation of α-olefins

Common, neutral Group 4 CGCs have to be converted to the cationic species that are active olefin polymerisation catalysts by reaction with suitable co-catalysts. The formation of these active species usually involves abstraction of a hydrocarbyl group (*e.g.* methyl or benzyl) from the metal centre. A suitable co-catalyst should combine both advantageous features in the activation process itself (abstraction) and in the coordination characteristics of the generated anion, which acts as a counter-ion to the cationic active centre. A vast number of different co-catalysts have been reported in the literature.[200]

Methylaluminoxane (MAO), which can be prepared by controlled hydrolysis of $AlMe_3$, and related activators are currently the commercially most successful co-catalysts, though they exhibit some quite disadvantageous features. Firstly, to obtain optimal polymerisation activities and an acceptable kinetic stability of the polymerisation reactions, high MAO:catalyst precursor ratios of about 10^2–10^4:1 are necessary, making MAO the major cost factor in the process. Secondly, despite prolonged and extensive research in the area, the exact composition and structure of

MAO remains unclear,[201, 202] mainly due to multiple equilibria between different MAO oligomers and residual trimethylaluminium. Both the use of MAO in superstoichiometric quantities and its structural fluxionality and instability prevent a full characterisation of the active species in the polymerisation reaction,[203] and consequently make further improvement of the process highly dependent of empirical studies. It should be noted that MAO facilitates the use of dichloro or diamido CGCs as catalyst precursors since MAO (or the $AlMe_3$ residue therein) is a strong methylating agent capable of converting these species to their dimethyl derivatives that are in turn activated by methyl abstraction.[204]

Another class of compounds that was successfully applied as co-catalysts in the CGC catalysed olefin polymerisation are highly Lewis-acidic perfluoroarylboranes, particularly $B(C_6F_5)_3$ and a number of other perfluoroarylboranes.[205] Despite lower polymerisation activities of the resulting catalyst systems, they have the great advantage of allowing isolation and thorough characterisation of the ion pairs comprising the catalytically active cationic complexes and their respective counter anions.[206, 207] A major drawback of the perfluoroarylboranes in their application as co-catalysts is the considerable interaction of the abstracted methyl group (that is incorporated in the generated $MeBR_3^-$ counter-ion) with the cationic centre. A way to circumvent this problem is the use of the triphenylcarbenium (trityl) salts of the corresponding perfluorotetraarylborates, *e.g.* $[Ph_3C^+][B(C_6F_5)_4^-]$, as co-catalysts. In these systems, the trityl cation reacts as a strong methyl abstractor generating a neutral hydrocarbon, while the perfluorotetraarylborate moiety acts as a largely non-coordinating anion.[205, 208] Surprisingly, a beneficial effect of superstoichiometric amounts of $[Ph_3C^+][B(C_6F_5)_4^-]$ was observed in CGC catalysed olefin polymerisation. For example, the $[\{\eta^5:\eta^1\text{-}(C_5Me_4)(SiMe_2)N\textit{t}Bu\}TiCl_2]/Al\textit{i}Bu_3/[Ph_3C^+][B(C_6F_5)_4^-]$ system showed a tenfold increased productivity in propylene polymerisation when pre-catalyst/alkylating agent/co-catalyst were employed in a 1:10:10 ratio compared to a 1:10:1 ratio.[209]

Naturally, every co-catalyst displays its specific characteristics in hydrocarbyl abstraction reactivity and interaction of the resulting ion pairs.[210] Therefore, it is not surprising that a strong effect of the combination of catalyst precursor and co-catalyst on polymerisation characteristics is observed. The following sections give an overview about reports that specifically address such dependencies.

The influence of the chosen co-catalyst with respect to the tacticity of the obtained polymer was observed in the polymerisation of propylene with [{η^5:η^1-($C_{13}H_8$)($SiMe_2$)N*t*Bu}$ZrCl_2$]. The MAO activated system resulted in mainly syndiotactic polymer, whereas the [Ph_3C^+][$B(C_6F_5)^-$]/Al*i*Bu_3 activated system yielded mainly isotactic polymer. A change from solvent-separated ion pair in the former to contact ion pair in the latter was suggested as a plausible explanation for this observation.[211] In a consecutive study, [{η^5:η^1-($C_{13}H_8$)($SiMe_2$)N*t*Bu}ZrX_2] (X = Cl, NMe_2) was demonstrated to act as single site catalyst when activated with MAO, while generating a number of catalytically active species in the presence of [Ph_3C^+][$B(C_6F_5)_4^-$]/AlR_3. At the same time, it was shown that the catalytic performance of such systems is independent of the substituent X; X = Cl or NMe_2 gave identical results. In addition, use of the dimethylated derivative [{η^5:η^1-($C_{13}H_8$)($SiMe_2$)N*t*Bu}$TiMe_2$] had a tremendous effect on the observed polymerisation characteristics when the co-catalyst was varied. Systems involving $B(C_6F_5)_3$ as a co-catalyst were capable of polymerising propylene and 1-hexene, respectively, at low temperatures (–50 °C) in a living manner to give syndiotactic-rich homopolymer, but were quickly deactivated at 0 °C.[212] MAO activated systems, in which the added MAO had been freed of all traces of $AlMe_3$, formed polypropylene with high activities and displayed all the characteristics of a living polymerisation system even at 0 °C.[213] Similar catalytic behaviour, albeit producing atactic polypropylene, was demonstrated for the related pre-catalyst [{η^5:η^1-(C_5Me_4)($SiMe_2$)N*t*Bu}$TiMe_2$].[214, 215] Living copolymerisation of ethylene and norbornene was also reported for CGCs activated with dried MAO.[216]

Excess $Al(C_6F_5)_3$, in contrast to its boron analogue $B(C_6F_5)_3$, was found to facilitate abstraction of both titanium-bonded methyl groups from [{η^5:η^1-(C_5Me_4)($SiMe_2$)N*t*Bu}$TiMe_2$] under formation of the corresponding dicationic complex. This complex produced a copolymer from ethylene and 1-octene with higher efficiency and higher molecular weight than the corresponding cationic catalyst.[217]

A marked temperature dependency was observed for the catalyst system [{η^5:η^1-(C_5Me_4)($SiMe_2$)N*t*Bu}$ZrMe_2$]/[Ph_3C^+][$(C_{12}F_9)_3AlF^-$] ($C_{12}F_9$ = 2-nonafluorobiphenyl). This system was found to be inactive towards the polymerisation of ethylene at 25 °C, but at higher temperatures (60 °C, 110 °C) a significant polymerisation activity was

observed. This change in reactivity may be ascribed to an alteration of the nature of the ion pairing at different temperatures.[218]

1.5.3. Zwitterionic CGCs as single component olefin polymerisation catalysts

Devore, Marks *et al.* reported the activation of titanium(II) CGC diene complexes with common activators such as MAO and $B(C_6F_5)_3$ for the copolymerisation of ethylene and 1-octene. Later, the products of the 1:1 reaction of related diene complexes with $B(C_6F_5)_3$ were found to be well defined, zwitterionic complexes (Eq. 14). In these complexes, the charge of the cationic transition metal centre is matched by the anionic borate moiety on the original diene ligand.[219, 220, 221] Since the zwitterionic complexes contain a cationic transition metal centre with only weak stabilisation by the counter-ion, they can act as single component olefin polymerisation catalysts and no additional co-catalyst is required.[222]

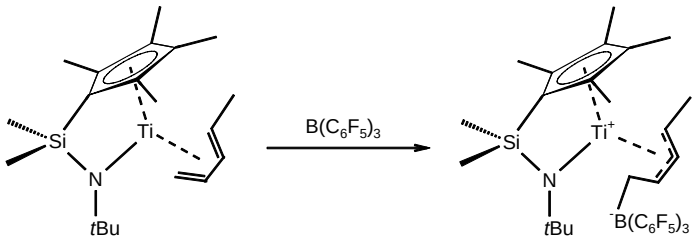

(Eq. 14)

Piers *et al.* attempted the incorporation of the co-catalyst into the ligand framework of CGCs by hydroboration of a pendent allyl group on the cyclopentadienyl ring with $[HB(C_6F_5)_2]_n$. The resulting pendent borane moiety was conceived to be sufficiently Lewis acidic to yield a zwitterionic single component catalyst. However, synthetic difficulties prevented a successful realisation of this idea. On one hand, the dichloro derivative with a pendent $B(C_6F_5)_2$ group could be easily prepared, but alkylation failed under various conditions (Eq. 15). On the other hand, starting from the dimethyl, dibenzyl or bis(trimethylsilylmethyl) derivatives with a pendent allyl group, reaction with the hydroboration reagent was usually not selective and always resulted in undesired products (Eq. 16).[64]

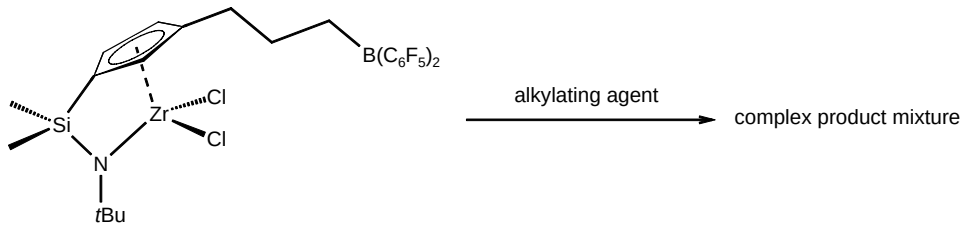

(Eq. 15)

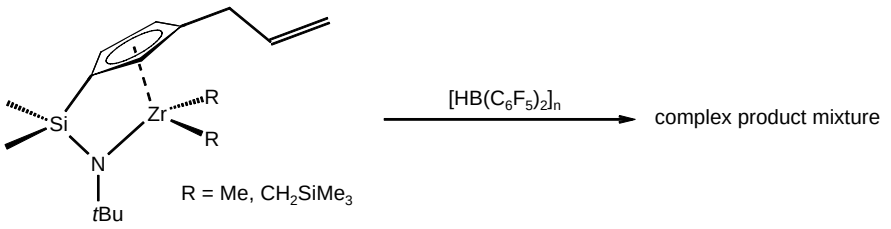

(Eq. 16)

1.5.4. Structure-activity relationship for constrained geometry complexes

Since the first publication of CGCs, a wide range of modified and related compounds has been published. Nonetheless, one of the most systematic investigations into the CGC structure-activity relationship for olefin polymerisation is Stevens' report dating back to 1991[223] that essentially summed up the claims in the initial patent of the Dow Chemical Company.[26] Stevens demonstrated that high catalyst efficiencies and comonomer incorporation are correlated with increased electron density at the metal centre for a series of catalyst precursors. An electron increase at the metal centre can be both induced by variation of the substituted cyclopentadienyl moiety (indenyl < C_5H_4 < C_5Me_4) or the substituent on the nitrogen of the chelating ligand (4-F-Ph < Ph < *t*Bu). Furthermore, it was shown that the nature of the bridge has a strong effect on both catalyst efficiency and comonomer incorporation, with more acute $Cp_{centroid}$–M–N angles giving the better results.[224] Comparison of $SiMe_2$-and $(CH_2)_2$-bridged complexes, which both exhibit $Cp_{centroid}$–M–N angles of about 108°, revealed some electronic influence of the bridge on the polymerisation results: for the dimethyl silyl bridge, comonomer intake is lower, but catalyst activity is higher. A strong influence of the Group 4 metal was also demonstrated, with titanium compounds being generally more efficient and giving polymers with distinctly higher comonomer incorporation than their zirconium analogues. This is in stark contrast to related bis(cyclopentadienyl) Group 4 complexes, where the zirconium derivatives are usually far more active than their titanium counterparts.[225]

Compared to metallocenes and *ansa*-metallocenes, CGCs incorporate longer α-olefins to a much higher extent in copolymerisation experiments and without sacrifice of the high molecular mass of the produced polymer.[226] The mechanical properties of such long-chain branched polyolefins resemble in some instances those of crosslinked polymers.[227] A further improvement of comonomer incorporation for a variety of α-olefins was observed for catalyst systems derived from complexes in that two CGC type moieties are connected *via* a short linker.[92, 228]

Improved catalyst performance in terms of higher activity, stability, 1-octene incorporation and polymer molecular weight was obtained by replacing the commonly applied C_5Me_4 fragment by either a particular benzannelated cyclopentadienyl derivative, namely a 2-methylbenz[*e*]indenyl moiety, or a specific amino functionalised indenyl derivative, namely the 3-pyrrolidino-indenyl group. Copolymerisation of ethylene and 1-octene resulted in poly{ethylene-*co*-(1-octene)} with a high content of 1-octene and oligoethylene side-chains. Virtually ideal copolymerisation of ethylene and propylene was observed with [{η^5:η^1-(C_5Me_4)($SiMe_2$)N*t*Bu}$TiCl_2$]/MAO as a catalyst, a characteristic that could not yet be achieved with any metallocene system.[229]

Homopolymerisation of propylene with CGC based systems usually results in atactic products.[37, 42] However, introduction of suitable amido moieties into the *ansa*-$SiMe_2$-bridged ligand, such as $^-$N(CHRR') (R = alkyl, R' = aryl), resulted in formation of isotactically enriched polypropylene. Furthermore, it was shown that fluorenyl based CGCs can produce polypropylenes with a high content of syndiotactic or isotactic sequences, depending on the utilised co-catalysts[211, 213] and solvents.[230, 231] If heterocycle-fused titanium indenyl silylamido complexes are employed as pre-catalysts, predominantly syndiotactic polypropylene is accessible.[84, 232] Due to its semicrystalline nature, this new type of polypropylene showed unique mechanical properties combining some characteristics of both crystalline syndiotactic PP and amorphous atactic PP, making it an interesting thermoplastic elastomeric material.[233]

A strong influence of the nature of the amido group on the molecular weight of obtained PP was reported. While for [{η^5:η^1-(C_5Me_4)($SiMe_2$)NR}$TiCl_2$]/MAO, polymer molecular weights increased with increasing bulk of the substituent R, a reversed tendency was observed for [{η^5:η^1-(C_5H_4)$(CH_2)_2$NR}$TiCl_2$]/MAO and [{η^5:η^1-(C_5H_4)$(CH_2)_2$NR}$TiBz_2$]/$B(C_6F_5)_3$. Differences in cation-anion interactions in the respective catalyst systems were suggested to be a probable explanation for these trends.[234]

For ethylene-bridged ligand systems, a pronounced effect of the nature of the amido moiety (NR) on the activity towards propylene polymerisation was reported. Only for R = Me was the catalytic formation of PP observed, while for R = *i*Pr and *t*Bu the systems were rendered inactive for the polymerisation of propylene. These observations are rather surprising considering that the $(CH_2)_2$-bridged system showed

higher activities for the polymerisation of ethylene than the analogous $SiMe_2$-bridged systems, while the latter readily polymerises propylene even for R = *t*Bu.

A number of CGCs have also been tested as catalysts for the homopolymerisation of 4-methyl-1-pentene and copolymerisation of this monomer with ethylene. A certain degree of isotacticity (up to 39%) and some irregularities derived from 2,1-insertion were observed in the homopolymerisation experiments, both parameters being distinctly sensitive to variations in the ligand framework. The trends observed in the copolymerisation of 4-methyl-1-pentene with ethylene were similar to those observed in comparable copolymerisation experiments of ethylene with other α-olefins.[235]

CGCs with electron-withdrawing groups on the *ansa*-bridged amido moiety (**19**) were studied as catalysts in the homopolymerisation of propylene and styrene and the copolymerisation of ethylene and styrene. Activity for homopolymerisation of propylene and ethylene/styrene copolymerisation was diminished by the electron-withdrawing groups compared to the previously described alkyl amido substituted catalysts. On the other hand, productivity in styrene homopolymerisation was increased, resulting in mainly syndiotactic polystyrene. Overall, the CGCs carrying electron-withdrawing groups on the amido moiety showed a behaviour more similar to non-bridged complexes such as Cp^*TiCl_3 than to alkyl amido substituted CGCs. This observation was attributed to a cleavage of the titanium amido linkage under polymerisation conditions in the former systems. Hence, it was concluded, that high ethylene polymerisation activity of most CGCs is not solely a result of the constraints induced by a short bridge, but as well a consequence of the donor characteristics of alkyl amido ligands.[236]

1.5.5. Further aspects of (co)polymerisation of ethylene and α-olefins

5,7-Dimethylocta-1,6-diene and 3,7-dimethylocta-1,6-diene, readily available non-conjugated linear dienes from terpene feedstocks (Eq. 17), are incorporated exclusively *via* their less hindered double bond into polyethylene copolymers using the $[\{\eta^5:\eta^1\text{-}(C_5Me_4)(SiMe_2)N\textit{t}Bu\}TiCl_2]$/MAO system.[237, 238]

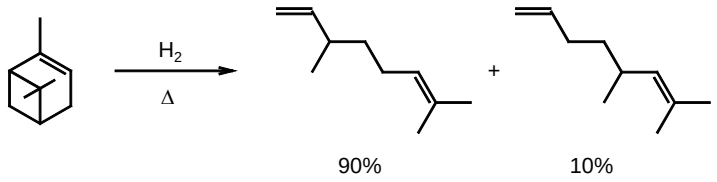

(Eq. 17)

The capability of CGC based system to incorporate long-chain vinylic monomers has been utilised in the copolymerisation of ethylene and a decenyl-functionalised silsesquioxane **60** (Figure 19).

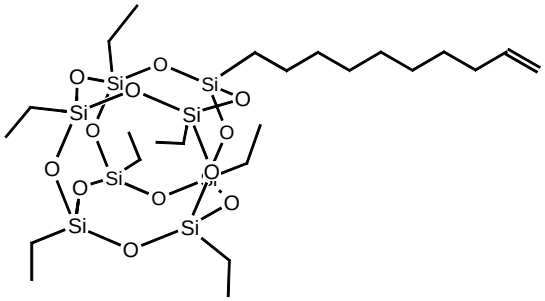

60

Figure 19. Decenyl-functionalised silsesquioxane.

The incorporation of silicon-oxygen cages into the polymer resulted in improved thermal stability of the material and may have further influence on the material properties.[239] The capability to incorporate long-chain vinylic monomers was further established by the homopolymerisation of ω-undecenyl PS macromonomers, giving access to unique polyethylene-*graft*-(nonyl-*block*-polystyrene).[240]

[{η^5:η^1-(C_5Me_4)($SiMe_2$)N*t*Bu}$TiCl_2$]/MAO has also been used for the copolymerisation of ethylene and 3-(penten-1-yl)thiophene. The presence of the soft Lewis-base had no detrimental effect on the copolymerisation performance. Subsequent grafting with conjugated poly(3-hexylthiophene) by $FeCl_3$-mediated copolymerisation of the copolymer with 3-hexylthiophene yielded a new material with interesting physical properties, *e.g.* fluorescence (Scheme 3).[241]

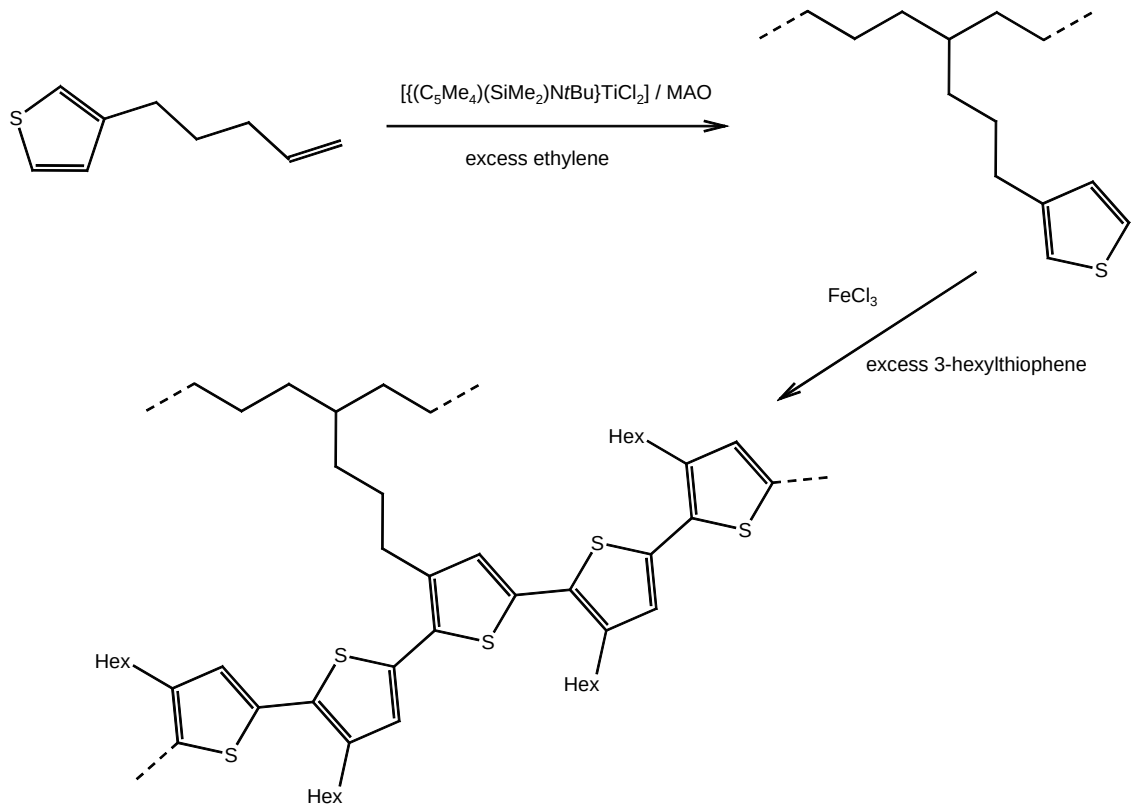

Scheme 3. Synthesis of a novel ethylene-thiophene copolymer involving CGC catalysis.

1.5.6. Polymerisation of monomers other than α-olefins

1.5.6.1. Styrene and derivatives

CGCs were found to be superior catalysts for the production of ethylene/styrene copolymers. On the one hand, commonly used catalysts for the homopolymerisation of styrene such as [$CpTiCl_3$] and related half-sandwich complexes produce predominantly syndiotactic polystyrene in styrene/ethylene mixtures besides traces of copolymer.[242] On the other hand, highly active catalyst systems for the homopolymerisation of ethylene such as *ansa*-zirconocene dichlorides and related compounds fail to incorporate larger quantities of styrene comonomer due to their crowded coordination sphere.[243] CGCs are bridging this gap by allowing high styrene content in the copolymer, high activity and virtually no contamination by polystyrene. Ethylene and styrene were copolymerised in the presence of [{η^5:η^1-(C_5Me_4)($SiMe_2$)N*t*Bu}$TiCl_2$]/MAO. A linear relationship between concentration and styrene incorporation was found only for low styrene concentrations.[244]

Mülhaupt *et al.* demonstrated that CGC derived systems incorporate styrene units in the copolymer either in an isolated fashion or with tail-to-tail coupling (Figure

20). The strict absence of head-to-tail coupling in the polymerisation process limits the maximum number of neighbouring styrene units to two and results in a *pseudo*-random poly(ethylene-*co*-styrene).[245]

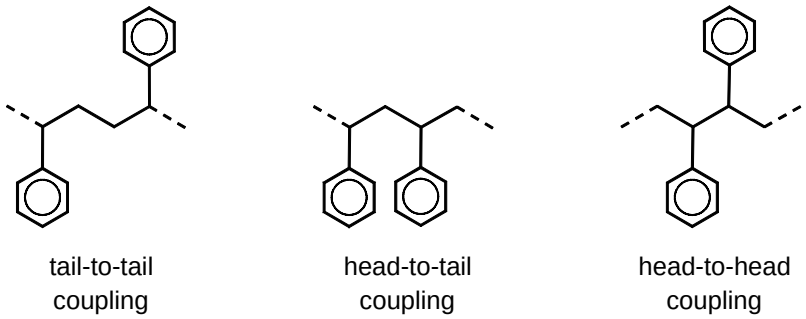

Figure 20. Possible coupling modes of neighbouring styrene units in styrene polymers.

Comparison of poly-(ethylene-*co*-styrene) derived from [{η^5:η^1-(C_5Me_4)($SiMe_2$)NR}$TiCl_2$]/MAO (R = *t*Bu, Cy) provided evidence for a significant influence of the amido ligand. While the *t*Bu substituted system displayed some tail-to-tail coupling, the products of the Cy substituted system showed only isolated styrene units despite a higher styrene incorporation.[246] Selectivity of styrene incorporation is as well highly sensitive to variations in the cyclopentadienyl derivative, as was demonstrated by a comparative study on [{η^5:η^1-(C_5Me_3R)($SiMe_2$)N*t*Bu}$TiCl_2$]/MAO (R = H, Me, Bu, Ph, 4-F-Ph, but-2-en-2-yl).[247] Xu applied a tailored catalyst system, [{η^5:η^1-($C_{13}H_8$)($SiMe_2$)N*t*Bu}$TiMe^+$][$B(C_6F_5)_4^-$], to obtain perfectly alternating poly(ethylene-*co*-styrene) with isotactic arrangement of the styrene units.[248]

The preference for isolated incorporation of styrene units in the polymer chain usually limits the styrene content to 50 mol-%. However, Marks *et al.* could obtain up to 92 mol-% styrene incorporation utilising a bimetallic CGC, [{η^5:η^1-(C_9H_5)($SiMe_2$)N*t*Bu}$TiCl_2$}$_2$(μ-C_2H_4)], with close proximity of the two active sites. This system apparently facilitates to some extent head-to-tail coupling and tail-to-tail-coupling of styrene units.[249] If the linker between the two CGC units is elongated (6, 9, or 12 carbon atoms), the bimetallic systems behave rather like singular CGCs and styrene incorporation into the copolymer is below 50 mol-%.[250, 251]

A study on ethylene/(methyl)styrene copolymerisation using the [{η^5:η^1-(C_5Me_4)($SiMe_2$)N*t*Bu}$TiCl_2$]/MAO catalytic system showed an increase in comonomer intake in the order *m*-methylstyrene < *o*-methylstyrene < styrene < *p*-methylstyrene that

was attributed both to steric and electronic effects. The good copolymerisation characteristic of *p*-methylstyrene was particularly promising, as the reactivity of the benzylic protons of the methylstyrene moieties allow further functionalisation of the obtained polymers.[252] Contrary to the occurrence of tail-to-tail coupling in ethylene/styrene copolymers derived from CGC catalysis, only isolated *p*-methylstyrene units were observed in the obtained poly(ethylene-*co*-*p*-methylstyrene).[253]

[{η^5:η^1-(C_5Me_4)($SiMe_2$)N*t*Bu}$TiCl_2$]/MAO was also found to facilitate the terpolymerisation of ethylene and styrene or *p*-methylstyrene, respectively, with a variety of termonomers such as propylene, 1-octene, norbornene and 1,5-hexadiene with high efficiency.[254, 255] 1,5-hexadiene cyclopolymerised under the applied conditions resulting in terpolymers incorporating randomly distributed 1,3-*cis*- and 1,3-*trans*-cyclopentane rings (Figure 21).[254, 256]

cis *trans*

Figure 21. Possible microstructures of 1,3-cyclopentane units.

Waymouth *et al.* found that CGCs bearing electron-withdrawing amido functions behaved in a distinctively different manner compared to that of the previously described systems and closely resembled the characteristics of non-bridged systems such as Cp^*TiCl_3, producing predominantly syndiotactic styrene homopolymer even in the presence of ethylene (*vide supra*).

1.5.6.2. Cyclic monomers

Ethylene-norbornene copolymers are thermoplastic materials with interesting properties, *e.g.* they are amorphous, highly transparent and chemically resistant.[257] Ethylene-norbornene copolymerisation using metallocenes and CGCs has been extensively studied by Ruchatz and Fink.[258, 259, 260, 261] In most aspects, CGCs were found to behave similarly to the *ansa*-metallocenes investigated in the same studies. All catalytic systems under investigation incorporated norbornene solely in *cis*-2,3-*exo* fashion (Figure 22) and titanium CGCs were found to incorporate virtually exclusively isolated norbornene units.[259, 262, 263]

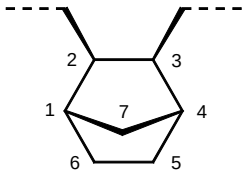

cis-2,3-*exo*

Figure 22. Preferred microstructure of norbornene units in CGC derived norbornene polymers.

On the other hand, the investigated zirconium CGC allowed even homopolymerisation of norbornene. In the case of a bulky amido moiety in the *ansa*-bridged ligand, homopolymerisation can be surpressed and almost perfectly alternating ethylene-norbornene copolymers can be obtained.[264] In these alternating copolymers, subsequent norbornene units arrange largely in an atactic fashion.[265] Copolymerisation activities of CGC based systems were moderate, but frequently lower than those of *ansa*-metallocenes. While *ansa*-metallocenes yielded increased polymer molecular weights with increasing norbornene concentration, [{η^5:η^1-(C_5Me_4)($SiMe_2$)N*t*Bu}$TiCl_2$] gave lower polymer molecular weights with increasing comonomer concentration. At the same time, higher comonomer concentrations correlated with lower numbers of long chain branches along the polymer chain.[266] These experimental results could be largely rationalised through computational studies.[267]

In terpolymerisation experiments, ethylene and norbornene were terpolymerised with 5-vinyl-2-norbornene, demonstrating the exclusive incorporation of 5-vinyl-2-norbornene by reaction of its cyclic double bond. The presence of 5-vinyl-2-norbornene increased the polymer molecular mass of the produced polymers for CGC catalysts, whereas the opposite effect was observed for *ansa*-metallocenes.[268]

Sundararajan *et al.* claimed that [{η^5:η^1-(C_5Me_4)($SiMe_2$)N*t*Bu}$TiCl_2$]/MAO can be converted by reaction with phenylacetylene to give a catalytic system that facilitates ring-opening metathesis polymerisation (ROMP) of cyclic olefins such as norbornene.[269, 270] In the copolymerisation of ethylene and cyclopentene, alternating copolymers with 1,2-enchainment of the resulting cyclopentane units were obtained. While catalyst systems based on achiral CGCs [{η^5:η^1-(C_5Me_4)($SiMe_2$)N*t*Bu}TiR_2] (R = Cl, Me) produced alternating atactic poly-(ethylene-*co*-cyclopentene), chiral versions of the pre-catalyst incorporating substituted indenyl-moieties produced alternating

isotactic copolymer (Figure 23).[83, 271] Analogous observations were reported for copolymerisation of ethylene with cycloheptene and cyclooctene, respectively.[83]

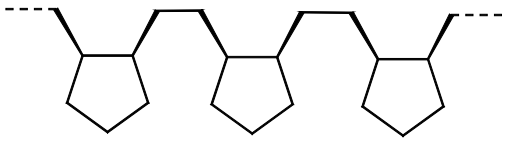

Figure 23. Section of isotactic poly(*cis*-1,2-cyclopentene-*alt*-ethylene).

In the copolymerisation of ethylene with 7-methylenebicyclo[4.1.0]heptane, $[\{\eta^5:\eta^1\text{-}(C_5Me_4)(SiMe_2)N\textit{t}Bu\}MMe^+][B(C_6F_5)_4^-]$ (M = Ti, Zr) catalysed the incorporation of the cyclic monomer *via* a ring-opening Ziegler polymerisation (ROZP) mechanism (Eq. 18), involving sequential double-bond insertion and β-alkyl shift ring-opening. The copolymers obtained are of particular interest as they carry *exo*-methylene functionalities that facilitate further derivatisation.[272]

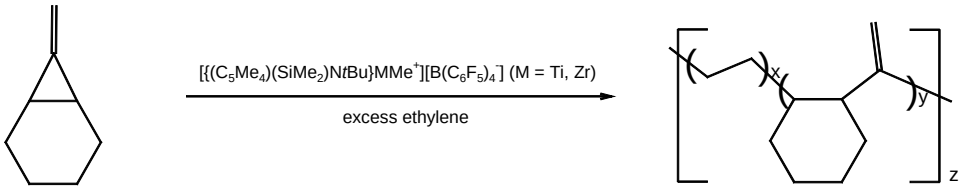

(Eq. 18)

1.5.6.3. Conjugated dienes

It was demonstrated that CGCs, such as $[\{\eta^5:\eta^1\text{-}(C_5Me_4)(SiMe_2)N\textit{t}Bu\}TiCl_2]$, activated with MAO catalyse polymerisation of 1,3-butadiene[273, 274] and 1,3-pentadiene with similar activity and produce polymers with comparable microstructure as it is observed for non-bridged systems, *i.e.* Cp^*TiX_3/MAO. Poly-(ethylene-*co*-1,3-butadiene) could be as well produced with these systems.[275] While activities of Group 4 CGC catalysts were found to be rather poor for the polymerisation of 1,3-pentadiene due to the steric hindrance imposed by the methyl group, the vanadium CGC based system $[\{\eta^5:\eta^1\text{-}(C_5Me_4)(SiMe_2)N\textit{t}Bu\}VCl_2]$/MAO showed four times higher productivity than its Group 4 analogues under standardised conditions.

1.5.6.4. Polar monomers

The copolymerisation of polar monomers with olefins using transition-metal complexes is still a great challenge. Correspondingly functionalised copolymers are

expected to exhibit desirable material properties of potentially great commercial value.[276] CGCs provided some advancement in this field.

[{η^5:η^1-(C_5Me_4)($SiMe_2$)N*t*Bu}$TiCl_2$] was found to facilitate copolymerisation of ethylene and $AlMe_3$ protected polar vinyl comonomers, *e.g.* $AlMe_3$ protected 5-hexen-1-ol and 10-undecen-1-ol, albeit with low activity. Attempts to incorporate $AlMe_3$ protected vinylic carboxy comonomers, *e.g.* 10-undecen-1-oic acid, failed.[277]

The cationic zirconium enolate complex [{η^5:η^1-(C_5Me_4)($SiMe_2$)N*t*Bu}Zr{OC(OR)=CMe_2}(L)]$^+$ is capable of producing highly isotactic poly(methyl methacrylate) (PMMA) (Eq. 19),[278] while its titanium analogue was reported to produced predominantly syndiotactic PMMA.[279] Isoelectronic [{η^5:η^1-(C_5Me_4)($SiMe_2$)N*t*Bu}Y(thf)(μ-H)]$_2$ and [{η^5:η^1-(C_5Me_4)($SiMe_2$)N*t*Bu}Y(CH_2SiMe_3)(thf)] were shown to catalyse the polymerisation of *tert*-butyl acrylate in a predominantly atactic fashion without addition of a co-catalyst. [{η^5:η^1-(C_5Me_4)($SiMe_2$)N*t*Bu}Y(thf)(μ-H)]$_2$ also showed activity towards polymerisation of acrylonitrile. A group-transfer mechanism was suggested for these reactions.

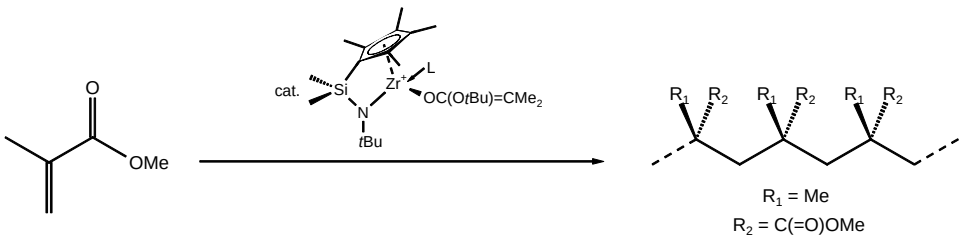

(Eq. 19)

[{η^5:η^1-(C_5Me_4)($SiMe_2$)N*t*Bu}$TiMe_2$] was found to be active for methyl methacrylate and *n*-butyl methacrylate homo- and copolymerisation when activated by $B(C_6F_5)_3$ or $Al(C_6F_5)_3$.[66, 279]

$Al(C_6F_5)_3$ activated [{η^5:η^1-(C_5Me_4)($SiMe_2$)N*t*Bu}Ti(Cp)Me] was demonstrated to be an efficient catalyst for the production of PMMA. The lack of a similar reactivity in the analogous borane activated system gave rise to the assumption that the reaction involves enolaluminates as key-intermediates.

Stepwise copolymerisation of propylene and methyl methacrylate with $B(C_6F_5)_3$ activated [{η^5:η^1-(C_5Me_4)($SiMe_2$)N*t*Bu}$TiMe_2$] afforded unique *block*-(atactic-PP)-

block-(syndiotactic-PMMA) beside some homopolymeric material. The diblock structure of the obtained polymers indicates the capability of the catalytic system for mechanism-crossover, specifically the transition from a coordination insertion type polymerisation of propylene to group-transfer type polymerisation of methyl methacrylate.[280]

1.6. Other transformations catalysed by CGCs

Beyond their application in polymerisation reactions, CGCs experience increasing relevance in the catalysis of various other transformations. This section gives an overview about this development.

In a comparative study, Teuben *et al.* demonstrated the catalytic activity of some Group 4 CGCs, namely [{η^5:η^1-(C_5H_4)(CH_2)$_3$NMe}MR_2] {MR_2 = $TiMe_2$, $Zr(BH_4)_2$, $ZrBz_2$}, for the hydroboration of 1-hexene with catecholborane (Eq. 20). These CGCs showed a much lower catalytic activity than the benchmark catalyst [$Cp^*_2LaCH(SiMe_3)_2$], but a better stability under the reaction conditions applied.[281]

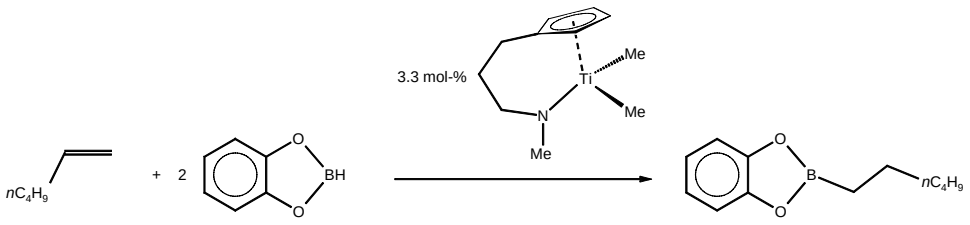

(Eq. 20)

Okuda *et al.* showed that [{η^5:η^1-(C_5Me_4)($SiMe_2$)NR^*}$TiCl_2$] (R^* = optically pure chiral alkyl group) can efficiently catalyse the hydrogenation of imines, *e.g.* acetophenone *N*-benzylimine, upon activation with 2 equivalents of *n*BuLi (Eq. 21). While conversions were generally high, enantioselectivity was low with a maximum of 24% enantiomeric excess observed in the hydrogenation product.[57, 99] Related complexes bearing an additional donor site in the amido moiety {R = -Cy(OCH_2Ph)-2} were also tested under the same conditions, but activities were lower while enantioselectivity was not improved.

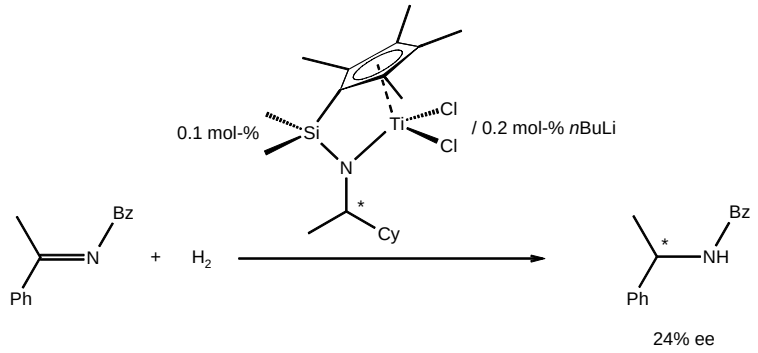

(Eq. 21)

Waymouth *et al.* applied catalytic amounts of titanium CGC [{η^5:η^1-(C_5Me_4)($SiMe_2$)N*t*Bu}$TiMe_2$]/[Ph_3C^+][$B(C_6F_5)_4^-$] in the presence of $AlMe_3$ and $AlEt_3$, respectively, for the carboalumination of a variety of α-olefins. Strong evidence that supports a mechanism involving olefin insertion into a Ti–C bond followed by transmetalation was given in the report. Catalytic amounts of titanium CGCs [{η^5:η^1-(C_5Me_4)($SiMe_2$)N*t*Bu}$TiCl_2$] and [{η^5:η^1-(C_9H_6)($SiMe_2$)N(CH{Me}Ph)}$TiCl_2$] were also reacted with α-olefins in the presence of $AlEt_3$. Analysis of the carboalumination products after work-up strongly suggested a mechanism *via* a metallacyclic intermediate for this combination of catalyst and alkyl reagent. Enantioselectivity of the chiral catalyst [{η^5:η^1-(C_9H_6)($SiMe_2$)N(CH{Me}Ph)}$TiCl_2$] was moderate with a maximum 28% enantiomeric excess for a specific substrate (allylbenzene) (Eq. 22).

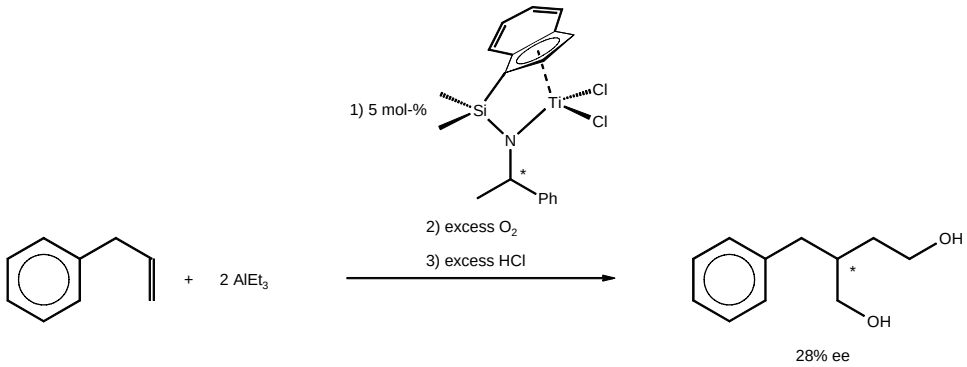

(Eq. 22)

The same titanium dichloride CGCs were also utilised in ring-opening reactions of 4,5-bis(methoxymethyl)-7-oxabicyclo-2-heptene in the presence of $AlEt_3$. This type of ring-opening of oxabicyclic alkene compounds is of great interest in synthetic organic chemistry. Depending on the amount of $AlEt_3$, either ethyl (2 equivalents of $AlEt_3$) or hydride (5 equivalents of $AlEt_3$) were transferred to the cyclic substrate upon ring opening. The chiral CGC [{η^5:η^1-(C_9H_6)($SiMe_2$)N(CH{Me}Ph)}$TiCl_2$] catalysed

the reaction with up to 34% (ethyl transfer) (Eq. 23) and 17% (hydride transfer) enantiomeric excess, respectively.[282]

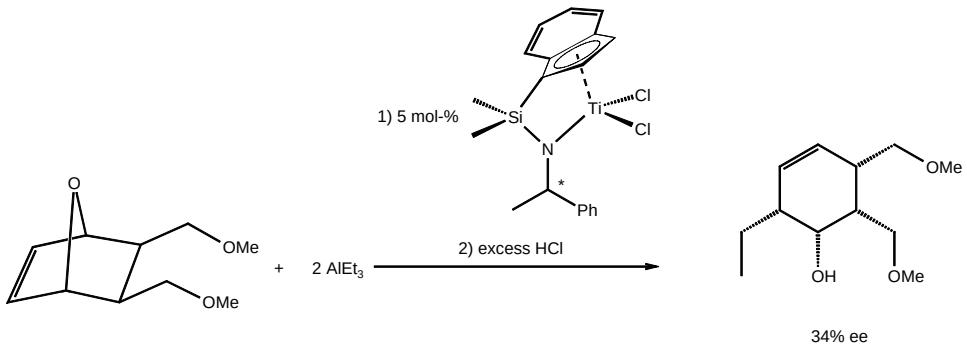

(Eq. 23)

Polymerisation of the abundant polar monomer vinyl chloride with activated CGCs has not yet been achieved. Instead, only 1.0 equivalent of vinyl chloride undergoes insertion into the M–Me^+ bond of the catalyst, followed by rapid β-chloride elimination.[283] Marks *et al.* reported a detailed study on the reaction of α-chloronorbornene, a vinyl chloride analogue that is conformationally locked and prevents rapid β-chloride elimination, with M–Me^+ in aromatic solvents (Eq. 24). Rather surprisingly, it was found that M–Me^+ (*e.g.* activated CGCs) catalyse formation of *exo*-1-chloro-2-arylnorbornanes. The catalytic reaction proceeds *via* a sequence of olefin addition to the cationic metal moiety, skeletal rearrangement of the bicyclic norbornene system and subsequent electrophilic attack on an aromatic solvent molecule.[284]

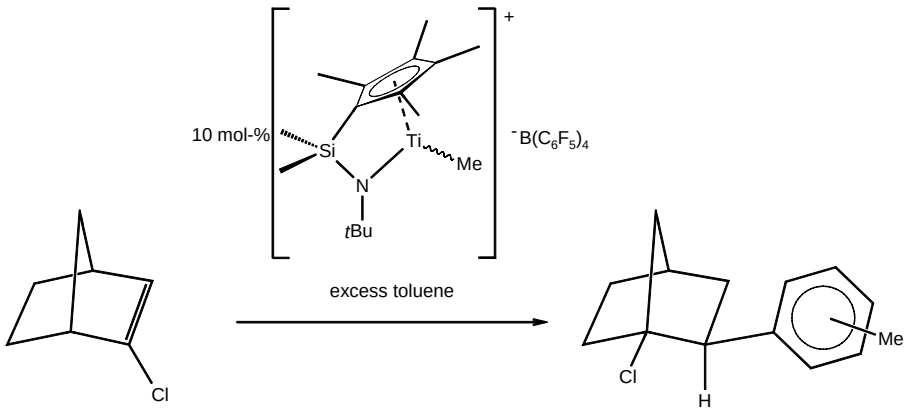

(Eq. 24)

CGCs of the Group 3 transition metals have also been successfully applied to a number of catalytic organic transformations. Okuda *et al.* applied [{η^5:η^1-(C_5Me_4)(CH_2SiMe_2)N*t*Bu}Y(thf)(μ-H)]$_2$ and [{η^5:η^1-(C_5Me_4)($SiMe_2$)N*t*Bu}Y(thf)(μ-H)]$_2$ in the hydrosilylation of olefins with good results. Thus, the former catalyst

quantitatively converted 1-decene in the presence of $PhSiH_3$ to the *anti*-Markovnikov product *n*-$C_{10}H_{21}SiH_2Ph$ (Eq. 25). Related dimeric CGCs bearing linked cyclopentadienyl phosphido ligands were also found to be highly active and selective catalysts for the hydrosilylation of a range of substrates.

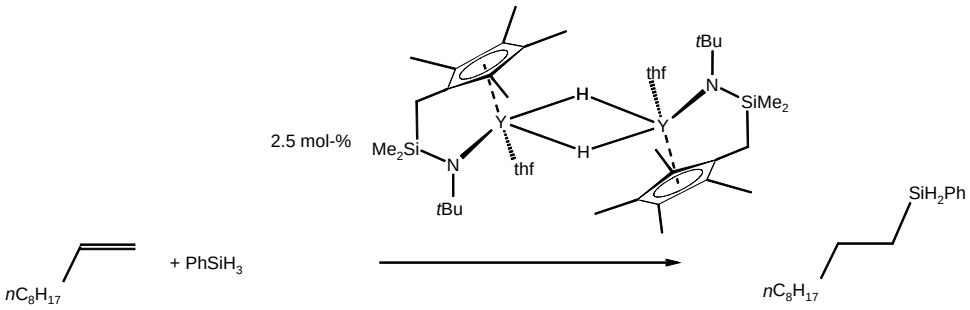

(Eq. 25)

Marks *et al.* reported the high efficiency of [{η^5:η^1-$(C_5Me_4)(SiMe_2)NtBu$}$MN(SiMe_3)_2$](M = Sm, Nd), [{η^5:η^1-$(C_5Me_4)(SiMe_2)NtBu$}$MCH(SiMe_3)_2$] (M = Yb, Lu)[285, 286] and [{η^5:η^1-$(C_5Me_4)(SiMe_2)NtBu$}$M(NRR')_2$] (M = Th, U; R, R' = Me, Et) for the intramolecular hydroamination/cyclisation reaction of various substrates (Eq. 26). Turnover frequencies were similar or exceeded those of related lanthanocene systems. This reactivity was as well exploited in a key step of the natural product synthesis of (+)-xenovenine, *i.e.* a catalytic stereoselective tandem bicyclisation of an intermediate (Eq. 27). In comparison, conventional hydroamination/cyclisation catalysts yield only a monocyclic product for this substrate.[285, 286]

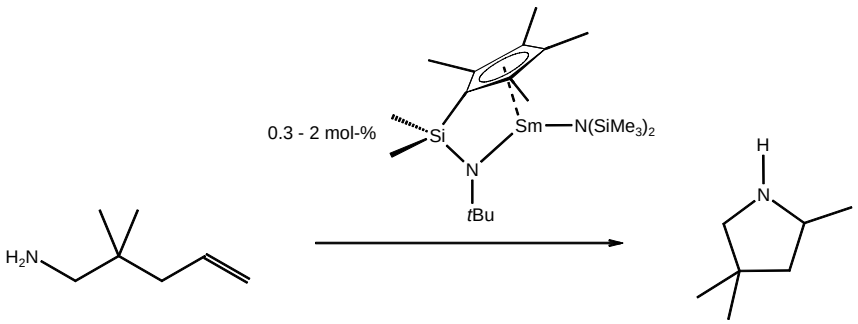

(Eq. 26)

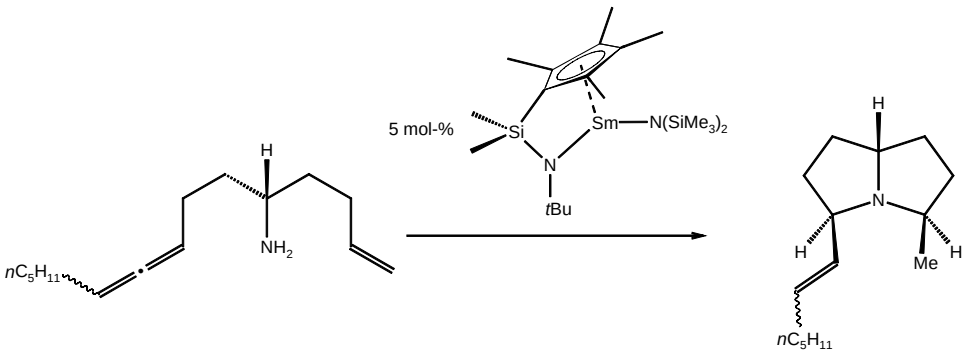

(Eq. 27)

Furthermore, [{η^5:η^1-(C_5Me_4)($SiMe_2$)NR}M(CH_2SiMe_3)(thf)$_n$] (M = Y, Yb, Lu; R = *t*Bu, Ph, $C_6H_2Me_3$-2,4,6; n = 1, 2) were found to catalyse dimerisation of various terminal alkynes with high activity; almost exclusively head-to-head-(*Z*)-dimerisation products were formed, exhibiting a high degree of regio- and stereoselectivity (Eq. 28). In fact, this reaction presents the first example of such selectivity for aromatic alkynes.[287] The reaction proceeds cleanly even in the presence of carbon-halide bonds that are known to be highly susceptible to reductive cleavage by transition metals.

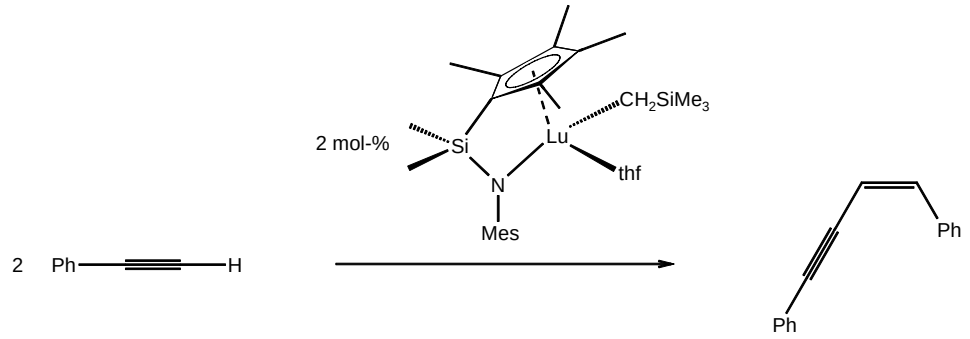

(Eq. 28)

1.7. Boron-bridged metallocenophanes and related compounds

As previously mentioned, the presence of the bridging moiety in *ansa*-metallocenes and related *ansa*-cyclopentadienyl amido complexes, *i.e.* CGCs, may significantly alter their reactivity when compared to their non-bridged congeners. Variation of the nature of the bridging group may allow for the fine tuning of this reactivity.

In the extensively studied field of metallocene chemistry, introduction of a boron bridge between the respective cyclopentadienyl type fragments[288] was associated with several beneficial characteristics: (i) the small size of the boron atom and the resulting short *ansa*-bridge should reduce the flexibility of the two η^5-coordinated ligand fragments, thus enhancing, in principle, the stereospecifity of the catalyst, especially if

higher polymerisation temperatures are required,[289] (ii) the Lewis acidic character of a three coordinate boron moiety in the vicinity of the transition metal centre may positively affect the catalytic activity of the latter[290, 291] and (iii) the Lewis acidic character of a three coordinate boron moiety may allow the activation of the transition metal centre in a way comparable to commonly used external Lewis acid co-catalysts.

The first structurally authentic [1]borametallocenophanes **60**[292, 293] and **61**[294], however, incorporated phenylboranediyl bridges with additional donor ligands, *i.e.* tetra coordinate boron centres with no significant Lewis acidity (Figure 24). The isolation of a base free analogue was subsequently reported,[295] although this report was called in question as only rudimentary spectroscopic evidence was provided and the results could not be reproduced independently. In 1999, Braunschweig *et al.* reported on the titanium complex **62** as the first base-free [1]borametallocenophane incorporating a three coordinate boron atom that is stabilised by π-donation from the attached amino moiety (Figure 24).[296] In due course, reports on the synthesis of a number of related Group 4 [1]borametallocenophanes appeared in the literature.[289, 297, 298, 299, 300, 301] Studies on the ethylene polymerisation of [1]borametallocenophanes activated with MAO demonstrated activities and product characteristics comparable of those observed for analogous silicon-bridged systems.[289, 300] In propylene polymerisation experiments, [{(η^5-$C_{13}H_8$)(η^5-C_5H_4)BN*i*Pr$_2$}$ZrCl_2$]/MAO exhibited high activity and modest stereoselectivity with syndiotactic preference. More recently, the syntheses of [2]borametallocenophanes **63** (Figure 24) were published and their application in ethylene polymerisation to produce very high molecular weight PE demonstrated.[302]

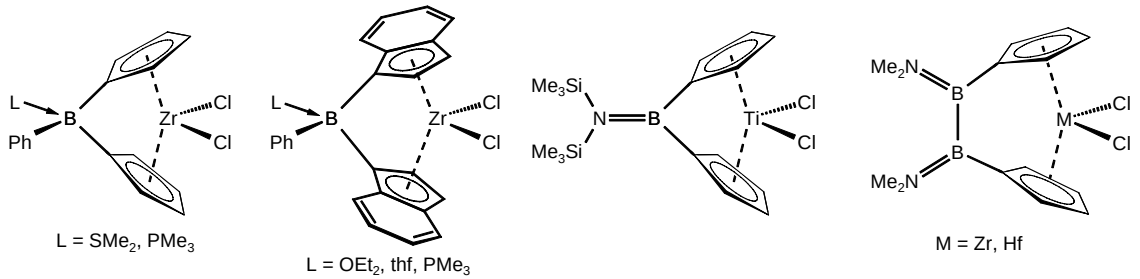

60 **61** **62** **63**

Figure 24. [n]Borametallocenophanes (n = 1, 2).

In principle, similar advantages of a short, Lewis acidic boron bridge as anticipated for metallocenophanes can be expected for corresponding CGCs. Particularly the high rigidity of the ligand backbone may be beneficial for the selectivity

of transformations catalysed by derived CGCs. Consequently, Braunschweig *et al.* extended their approach to the synthesis of CGC ligand precursors and related complexes. The ligand precursors are usually prepared from aminodichloroboranes R_2NBCl_2 by stepwise substitution of the two chlorides using a cyclopentadienide and a primary amide derivative (Scheme 4). Reported examples of boron-bridged CGC ligand precursors comprise (η^1-C_5H_5)B(N*i*Pr$_2$)N(H)R {R = *t*Bu (**64**),[303, 304] Ph (**65**)[304, 305]}, (1-C_9H_7)B(N*i*Pr$_2$)N(H)Ph (**66**),[48, 304] (3-C_9H_7)B(N*i*Pr$_2$)N(H)Ph (**67**)[48, 304] and (η^1-C_5Me_4H)B{N(SiMe$_3$)$_2$}N(H)R {R = *t*Bu (**68**), Ph (**69**)}.[305, 306]

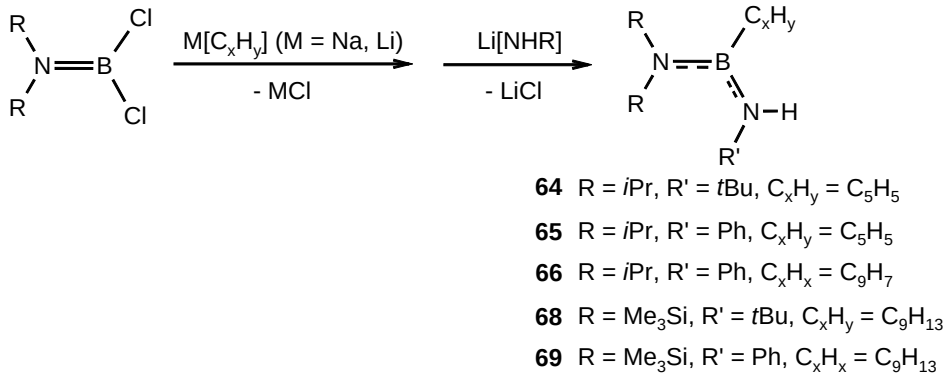

Scheme 4. Synthesis of boron-bridged CGC ligand precursors.

Reaction of **65** with [Ti(NMe$_2$)$_4$] yielded the corresponding CGC [Ti{η^5:η^1-(C_5H_4)B(N*i*Pr$_2$)NPh}(NMe$_2$)$_2$] (**37**) that could be further converted by reaction with excess Me$_3$SiCl to its dichloro analogue [Ti{η^5:η^1-(C_5H_4)B(N*i*Pr$_2$)NPh}Cl$_2$] (**70**) (Scheme 5). Upon activation with MAO, an active catalyst for the polymerisation of ethylene was obtained. The syntheses of analogues complexes [Ti{η^5:η^1-(C_5H_4)B(N*i*Pr$_2$)N*t*Bu}R$_2$] {R = NMe$_2$ (**71**), Cl (**72**)} following the same route were briefly reported; however, the preliminary spectroscopic data remained inconclusive.[304]

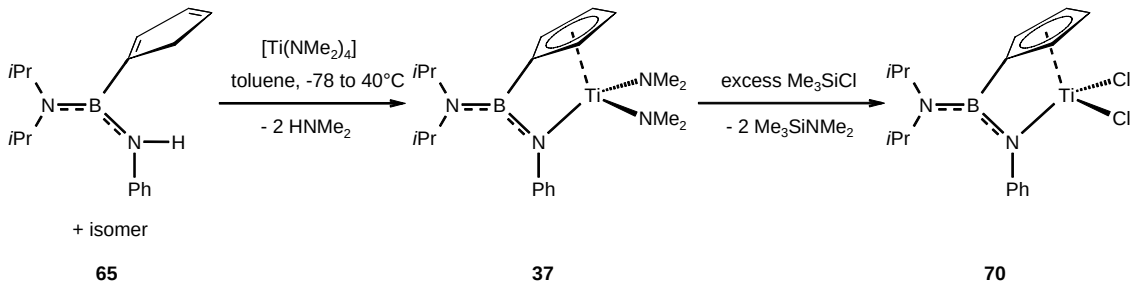

Scheme 5. Synthesis of the first boron-bridged CGCs.

Double deprotonation of **66** with *n*BuLi and subsequent treatment with $ZrCl_4$ yielded inevitably the metallocene $[Zr\{\eta^5:\eta^1\text{-}(C_9H_6)B(NiPr_2)NPh\}_2]$ (**73**), regardless of the applied ratio of dilithiated ligand to metal halide (Eq. 29).[48, 304]

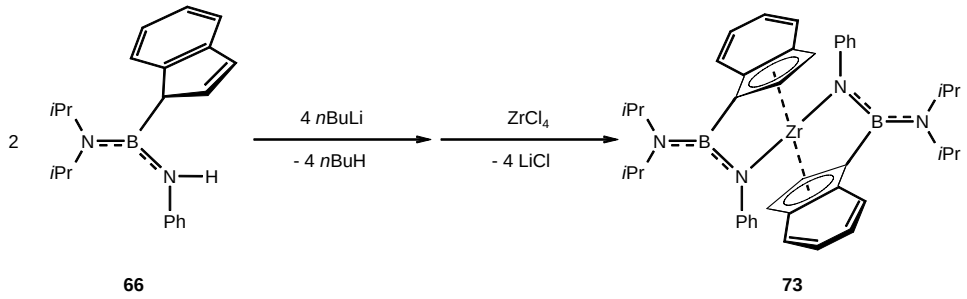

66 **73** (Eq. 29)

When **64** was treated with $K[N(SiMe_3)_2]$ and $YbCl_3$ in the presence of thf, the unbridged metallocene $[Yb\{\eta^5:\eta^1\text{-}(C_5H_4)B(NiPr_2)N(H)tBu\}_2\{N(SiMe_3)_2\}]$ (**74**) was obtained following a somewhat unclear reaction pathway (Eq. 30).[303, 306]

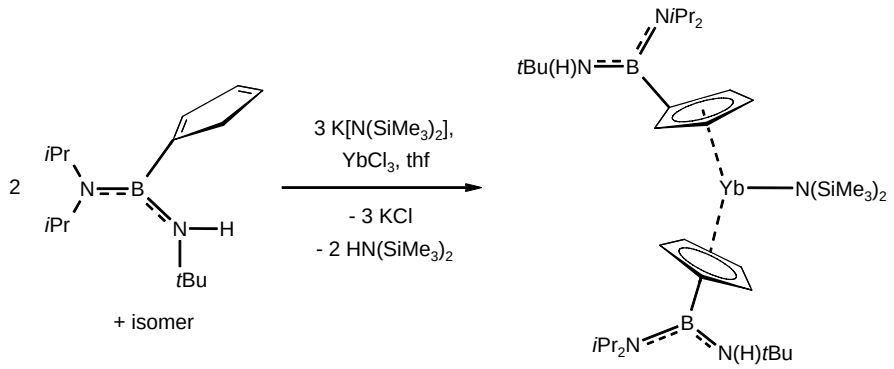

64 **74** (Eq. 30)

1.8. Aims of this research

The prospective benefits of a short, latently Lewis-acidic boron bridge in CGCs have been previously described. The number of CGCs bearing the structural motif of a boron bridge as well as data on their catalytic activity were, however, very limited.

The research project presented here aims to generate a more general understanding of the chemistry of boron-bridged CGCs. To achieve this challenging target, the previously employed approach for the synthesis of boron-bridged CGC ligand precursors is exploited and extended to new bridging moieties, *i.e.* ferrocenylboranediyl and diaminodiborane(4)diyl (Chapter 2.1). Although the newly synthesised ligand precursors may serve as ligands to a wide variety of transition metals, their ligation to Group 4 metals, especially titanium, is particularly interesting

due to the very advantageous chemical characteristics of related silicon-bridged congeners. Consequently, various synthetic strategies to prepare corresponding CGCs of Group 4 metals are assessed (Chapter 2.2). The catalytic potential of selected boron-bridged CGCs is then studied in ethylene and styrene polymerisation experiments, representing the commercially most important reactions involving CGCs (Chapter 2.3).

Chapter 2. Results and Discussion

2.1. Ligand precursors

One of the aims of this research project was the further development of the previously described procedure for the synthesis of boron-bridged CGC ligand precursors.[48, 303, 305] Variations in the ligand precursor may be introduced in three positions (Figure 25).

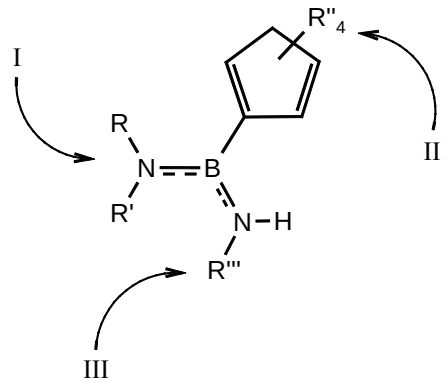

Figure 25. Sites for modification of boron-bridged CGC ligand precursors.

Modification of the dialkylamino substituent on the borane precursor should allow the π-donation of the amino function towards the boron atom to be tuned, thereby influencing the Lewis acidity of the latter. By extending the synthetic procedure to borane precursors other than aminodihaloboranes, *e.g.* diaminodichlorodiborane(4) or ferrocenyldibromoborane, [$FcBBr_2$], novel boron-bridged CGC ligand precursors with altered electronic and steric features should be available. Applying various cyclopentadienyl derivatives, such as indenyl and fluorenyl, should give rise to ligands with different steric demand and electronic characteristics, hence modifying two of the crucial factors influencing the catalytic activity and copolymerisation characteristics in derived CGCs. Finally, changes in the alkyl- or arylamino fragment, which is to be deprotonated to afford an amido donor function, should influence both the electron density at the neighbouring boron centre and the transition metal centre.

When synthesising and characterising the ligand precursors, it should be borne in mind that η^1-coordinated main group element cyclopentadienyl compounds show dynamic behaviour in solution. This arises from two different rearrangements: a

degenerate 1,2-sigmatropic shift of the ER_x group and a non-degenerate 1,2-sigmatropic shift of a proton, resulting in three different regioisomers (Scheme 6).[307]

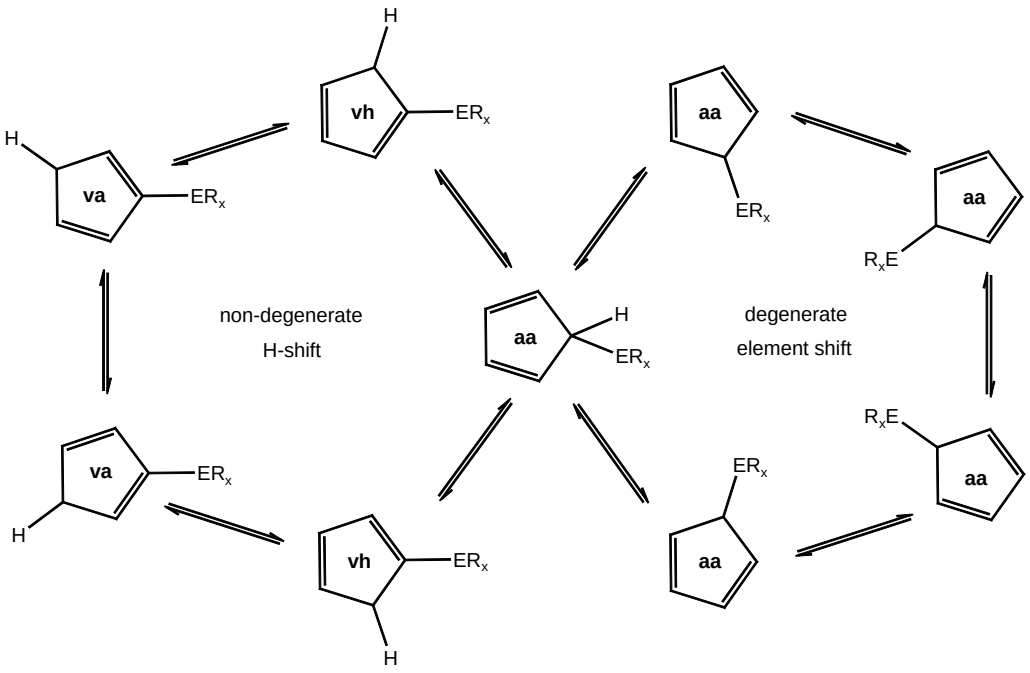

Scheme 6. Sigmatropic processes in (η^1-C_5H_5)ER_x compounds.

These isomers can be distinguished by the position of the ER_x group with respect to the double bonds as allyl/allyl (**aa**), vinyl/allyl (**va**) and vinyl/homoallyl (**vh**) isomers. Thorough investigations into the properties of cyclopentadienyl diorganyl boranes (η^1-C_5H_5)BR_2 revealed that under normal conditions only those isomers where the BR_2 group is bonded to an unsaturated carbon atom are observed, *i.e.* the **va** and **vh** isomers, making interaction of the conjugated π-system of the cyclopentadienyl ring with the empty *p*-orbital of the boron centre possible.[308, 309, 310, 311, 312, 313] Generally the **aa** isomers are only spectroscopically detectable below –15 °C and irreversibly rearrange into the thermodynamically more stable **va** and **vh** isomers at higher temperatures. Due to these characteristics, the synthesised cyclopentadienyl diamino boranes are usually obtained as mixtures of **va** and **vh** isomers, resulting in two sets of signals in the NMR spectra and, frequently, poor crystallisation behaviour.

Likewise, for (tetramethylcyclopentadienyl)boranes (η^1-C_5Me_4H)BR_2 mixtures of isomers have to be expected. Again, the position of the BR_2 moiety relative to the double bonds in the ring system may be denoted **aa**, **va** and **vh**. It is known that activation energies for carbon migration on the cyclopentadienyl system are high.

Hence, no additional isomers derived from migration of the methyl groups should be anticipated. As for the cyclopentadienyl derivatives, the **va** and **vh** isomers are expected to be more stable due to π-donation from the vinylic double bonds of the respective ring systems into the empty *p*-orbital at boron. Indeed, the **vh** isomer of (η^1-C_5Me_4H)B{$N(SiMe_3)_2$}Cl was obtained as the single product from the salt elimination reaction of $(Me_3Si)_2NBCl_2$ with Li[C_5Me_4H]. However, reaction of this intermediate with Li[NHR] (R = *t*Bu, Ph) resulted in a product mixture of at least three isomers. The unexpectedly large number of signals was subsequently attributed to the presence of several rotamers resulting from hindered rotation about the B–C and B–N bonds in the exclusively formed **vh** isomer (Scheme 7). Such a high number of species may result in poor crystallisation behaviour and very complex ^{1}H and ^{13}C NMR spectra. Therefore, ^{11}B NMR spectroscopy and MS characterisation are the only practical analytical techniques for such (tetramethylcyclopentadienyl)borane based CGC ligand precursors. However, subsequent deprotonation of these compounds should reduce the number of isomers and simplify the ^{1}H and ^{13}C NMR spectra significantly.

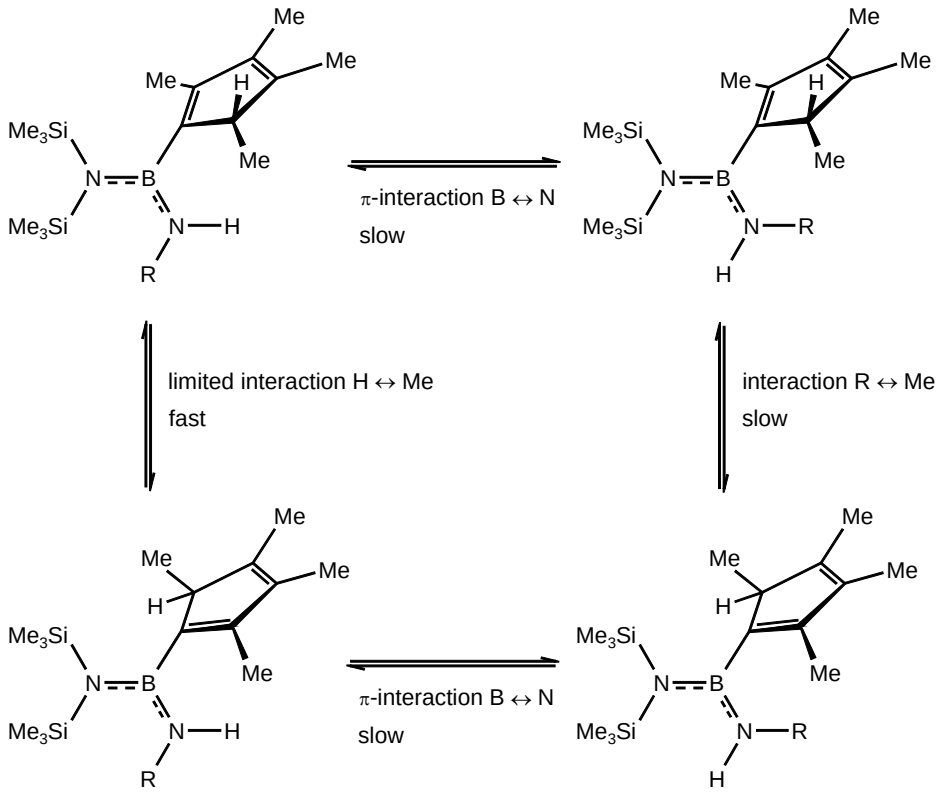

Scheme 7. Rotational isomers of (η^1-C_5Me_4H)B{$N(SiMe_3)_2$}N(H)R (R = *t*Bu, Ph).

For indenyl boranes (η^1-C_9H_7)BR_2, similar rearrangements have to be considered. Starting from lithium indenide and boron halides, the boron can, in

principle, become attached to either the 1- (allyl), 2- (vinyl) or 3-position (vinyl) of the indenyl system (Figure 26). In most cases, only 1-indenyl and 3-indenyl products are observed,[314] with the former being the kinetically favoured and the latter the thermodynamically favoured product.[48, 297, 310, 311, 313, 315, 316, 317] Isomerisation of the kinetic product by prototropic rearrangement (1,3-shift) can generally be achieved at elevated temperatures or in the presence of bases. The allyl (**a**) and vinyl (**v**) isomers of the indenyl boranes can be easily distinguished by ^{1}H NMR spectroscopy due to the characteristic integration and chemical shift of the protons attached to the sp^3-hybridised carbon atoms.

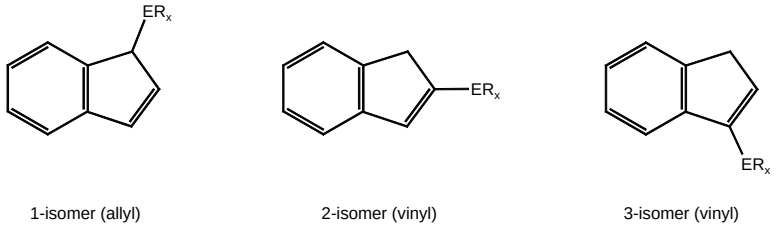

Figure 26. Constitutional isomers of (η^1-C_9H_7)BR_2

2.1.1. Amino monoborane based ligand precursors

2.1.1.1. Cyclopentadienyl substituted ligand precursors

The synthesis of new boron-bridged ligand precursors (η^1-C_5H_5)B(N*i*Pr$_2$)N(H)*i*Pr (**77**), (η^1-C_5H_5)B(N*i*Pr$_2$)N(H)Cy (**78**), (η^1-C_5H_5)B(N*i*Pr$_2$)N(H)(*p*-F-Ph) (**79**) and (η^1-C_5H_5)B{N(SiMe$_3$)$_2$}N(H)Ph (**80**) has been accomplished by an adaptation of the previously reported procedure for the preparation of cyclopentadienyl(diamino)boranes (Scheme 8).

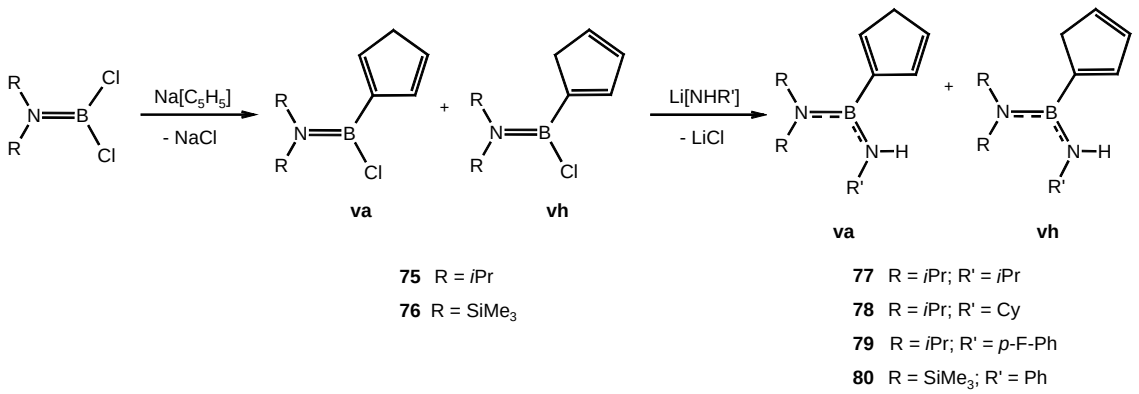

Scheme 8. Preparation of cyclopentadienyl(diamino)boranes.

The syntheses can be performed as two-step, one-pot reactions from the dichloroborane by subsequent addition of NaCp and the appropriate lithium amide. However, the intermediates (η^1-C_5H_5)B(N*i*Pr$_2$)Cl (**75**) and (η^1-C_5H_5)B{N(SiMe$_3$)$_2$}Cl (**76**) were isolated for full characterisation.

Although formation of two distinct isomers, arising from the relative position of the boron atom on the cyclopentadienyl ring (**va** and **vh**, *vide supra*), can be anticipated, only one isomer was formed in the preparation of the di*iso*propyl substituted amino(cyclopentadienyl)borane (**75**). The trimethylsilyl substituted analogue **76** exhibits an approximate 7:1 predominance of one isomer, as was demonstrated by ^{1}H and ^{13}C NMR spectra. This distribution stands in contrast to the syntheses of a series of aminobis(cyclopentadienyl)boranes and amino(cyclopentadienyl)(indenyl)boranes, where the respective isomers were observed as approximate 1:1 mixtures. Due to the structural similarity of the two isomers, assignment of the predominant configuration as **va** or **vh** was not feasible. **75** and **76** gave signals at δ = 33.9 and 43.5, respectively, in the ^{11}B NMR spectrum, values that are significantly down-field shifted compared to the corresponding dichloroboranes.

The di*iso*propylamino substituted ligand precursors **77** – **79** were obtained as mixtures of **va** and **vh** isomers after work-up and careful sublimation *in vacuo*. ^{1}H NMR spectra of **77** – **79** display all the expected signals except for, in the case of **77** and **78**, the signals corresponding to the NH resonances. The absence of the NH resonances in these spectra can be attributed to extensive line broadening due to proton exchange and/or the neighbouring quadrupolar ^{14}N nucleus, both well established phenomena.[318] In the ^{13}C NMR spectra, all expected signals except for carbon atoms attached to boron are observed. This can likewise be ascribed to coupling of the ^{13}C nucleus to quadrupolar ^{10}B or ^{11}B nucleii and resulting line broadening.[319]

^{1}H and ^{13}C NMR spectroscopic data of **77** – **79** show coalescence of the two diastereotopic *iso*propyl groups in the respective compounds already at ambient temperature, indicating fast rotation about the B–N*i*Pr$_2$ bond on the NMR time scale. This observation suggests a delocalisation of π-electron density over the whole N–B–N fragment. ^{11}B NMR spectroscopic signals at δ = 29.6, 29.3 and 29.9 respectively are in the expected range for (alkyldiamino)boranes[320] and shifted to high-field by approximately 4 ppm in comparison to the chlorinated intermediate **75**.

IR spectra were recorded for **77**, **78** and previously published (η^1-C_5H_5)B(N*i*Pr$_2$)N(H)*t*Bu (**64**). Characteristic NH stretching bands were observed at 3439, 3435 and 3454 cm^{-1}, respectively.

Compound **80** was obtained as an approximate 3:1 mixture of **va** and **vh** isomers. Although ^{1}H and ^{13}C NMR spectroscopy indicated that the isolated material was pure, its yellow colour indicated the presence of some trace impurities. Attempts to purify the compound by recrystallisation failed and distillation *in vacuo* at temperatures of up to 105 °C only resulted in decomposition, as was evidenced by darkening of the substance. The ^{1}H NMR spectrum showed all expected signals apart from the NH resonance, while the ^{13}C NMR spectrum showed all anticipated signals except for the BC resonance. The ^{11}B NMR spectroscopic signal for **80** at $\delta = 34.3$ is only moderately down-field shifted when compared to the analogous (di*iso*propylamino)borane **65**, due to the deshielding effect of the trimethylsilyl substituents. This effect, however, is somewhat cancelled out by the presence of the second amino group at the boron atom {*cf.* $\Delta\delta$(**75**, **76**) = 9; $\Delta\delta$(**65**, **80**) = 4}. Such indication of electron distributions through ^{11}B NMR spectroscopy is of interest because it can give an indirect measure of the Lewis-acidity of the boron centre.

2.1.1.2. Indenyl substituted ligand precursors

The synthetic method employed above has been further extended to the synthesis of diamino(indenyl)boranes incorporating an NHR group where R is alkyl instead of the previously reported phenyl. Sequential reaction of the aminodichloroboranes with LiInd and the respective lithium amide yielded (1-C_9H_7)B(N*i*Pr$_2$)N(H)*i*Pr (**83**), (1-C_9H_7)B(N*i*Pr$_2$)N(H)Cy (**84**) and (1-C_9H_7)B{N(SiMe$_3$)$_2$}N(H)Cy (**85**) exclusively as the allylic isomers (Scheme 9).

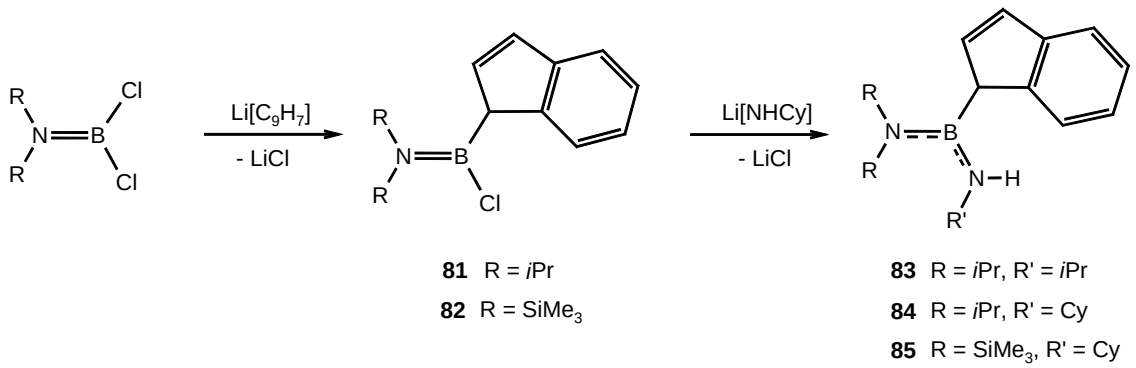

Scheme 9. Preparation of indenyl(diamino)boranes.

Compounds **83** and **84** were purified by recrystallisation affording colourless crystals. In the case of **83**, the crystals were analysed by means of *X*-ray diffraction (*vide infra*). Attempts to free **85** from trace impurities by recrystallisation or sublimation *in vacuo* have failed so far. The indenyl(diamino)boranes as well as the intermediate **82** were characterised by multinuclear NMR spectroscopy. Spectroscopic data of intermediate **81** have been previously reported. The ^{1}H NMR spectra of all four compounds displayed broad signals characteristic of a BCH moiety, thus establishing the attachment of boron in the allylic position. No CH_2 resonances indicating formation of the 3-indenyl isomer were observed.

Ambient temperature ^{1}H and ^{13}C NMR spectra of **83** showed very broad signals for the methyl groups of the *iso*propyl moieties. Another set of spectra was recorded at low temperature. At –50 °C, the ^{1}H and ^{13}C NMR spectra display all the expected signals and the signals of the methyl groups are well resolved. Apparently, rotation about the *i*Pr_2N–B bond in **83** at –50 °C is slow on the NMR time scale, giving rise to distinct signals for all six chemically inequivalent methyl groups in the ^{1}H and ^{13}C NMR spectra.

The ^{1}H and ^{13}C NMR spectra of **84** that were recorded at ambient temperature show all anticipated signals except for the NH and BC resonances. Two sets of signals for the methyl groups of the *iso*propyl moieties are observed in both spectra, indicating fast rotation about the *i*Pr_2N–B bond on the NMR time scale.

Ambient temperature ^{1}H and ^{13}C NMR spectra of intermediate **82** show all expected signals. Only one signal for the $SiMe_3$ moieties is observed in both spectra, indicating fast rotation about the $(Me_3Si)_2$N–B bond on the NMR time scale. This is in contrast to the spectral features of **85**, for which resonances of two chemically inequivalent $SiMe_3$ groups are observed in both the ^{1}H and ^{13}C NMR spectra at ambient temperature. This finding is somewhat unexpected since the presence of two amino groups on boron in **85**, compared to one amino group in **82**, would be expected to lower the π-contribution to the B–N bond and hence the rotational barrier. Hindered rotation about the $(Me_3Si)_2$N–B bond in **85**, therefore, probably results from a steric interaction with the other quite bulky substituents on boron. In addition, ^{1}H and ^{13}C NMR spectra of **85** exhibit all the expected signals apart from the NH and BC resonances.

The ^{11}B NMR chemical shifts of **83** and **84** are δ = 30.0 and 29.2, respectively, and thus, in close proximity to the corresponding signal for the related compound (1-C_9H_7)B(N*i*Pr$_2$)N(H)Ph (**66**). For **85** the corresponding chemical shift is δ = 32.9, which is slightly down-field shifted due to the deshielding effect of the pendent bis(trimethylsilyl)amino moiety. This effect is only very moderate in comparison to that in **82** (δ = 47.2) and for the related compound (1-C_9H_7)$_2$B{N(SiMe$_3$)$_2$} (δ = 57.6).

2.1.1.3. Fluorenyl substituted ligand precursors

Applying the previously described procedure, the first boron-bridged CGC ligand precursors incorporating a fluorenyl moiety, (9-$C_{13}H_9$)B(N*i*Pr$_2$)N(H)*t*Bu (**87**) and (9-$C_{13}H_9$)B(N*i*Pr$_2$)N(H)Ph (**88**) have been prepared in a two step procedure avoiding isolation of the intermediate **86** (Scheme 10).

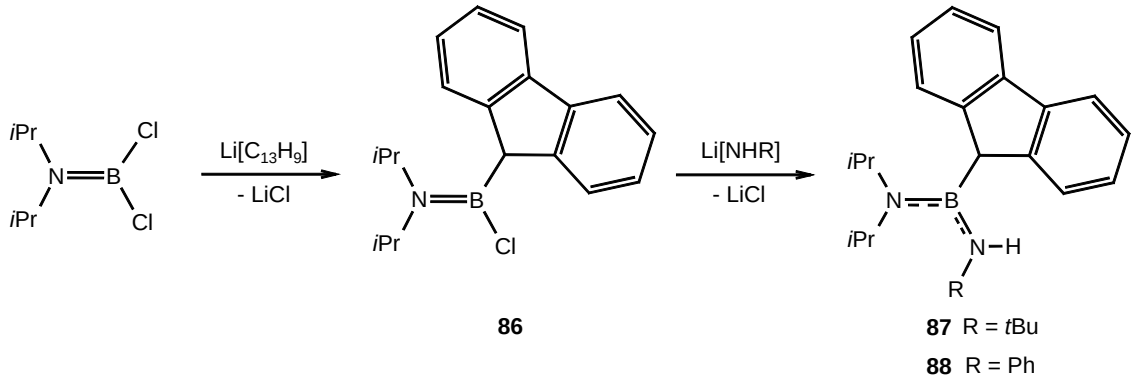

Scheme 10. Preparation of fluorenyl(diamino)boranes.

From ^{1}H and ^{11}B NMR spectra it is apparent that the reaction sequence yields significant amounts of by-products beside the target compounds **87** and **88**. GC-MS of the crude product of the reaction of **86** with Li[NH*t*Bu] revealed formation of the target compound **87** (*m*/*z* = 348) in only *ca.* 20% yield. Identified additional products comprise (*i*Pr$_2$N)B(NH*t*Bu)$_2$ (*m*/*z* = 255), (*i*Pr$_2$N)B($C_{13}H_8$) (*m*/*z* = 275) and fluorene (*m*/*z* = 166). Similarly, GC-MS analysis of the product mixture of the reaction of **86** with Li[NHPh] showed formation of **88** (*m*/*z* = 368), (*i*Pr$_2$N)B(NHPh)$_2$ (*m*/*z* = 295), B(NHPh)$_3$ (*m*/*z* = 287) and fluorene. However, in this case, the ratio of target product to additional products was more favourable. The nature of the additional products indicates the susceptibility of particularly the B–C bond, but as well the B–N bond, in **86** (and/or intermediates formed in the course of the reaction) to cleavage in the presence of strong nucleophiles such as Li[NHR] (R = *t*Bu, Ph) under the applied conditions. Despite the complexity of the product mixture, **87** and **88** could be obtained

as pure materials after recrystallisation and were subsequently analysed by means of *X*-ray diffraction (*vide infra*).

Compounds **87** and **88** have been further characterised by multinuclear NMR spectroscopy. ^{1}H and ^{13}C NMR spectra showed all the expected signals except for the respective BC resonances. The number of observed signals in the ^{1}H and ^{13}C NMR spectra is consistent with approximate C_s symmetry of **87** and **88** in solution. The ^{1}H NMR signals for the *iso*propyl groups were too broad at ambient temperature to determine their multiplicity, which may be attributed to rotation about the *i*Pr$_2$N–B bond on the NMR time scale. This rotation can be sufficiently slowed down at low temperature as was demonstrated by the ^{1}H NMR spectrum of **87** at –30 °C. This clearly showed the expected multiplicity (two sets of doublets and heptets) of the signals for the *iso*propyl groups. The chemical shifts of the ^{11}B NMR spectroscopic signals with δ = 30.2 and δ = 30.8 for **87** and **88** are in the expected range for (alkyldiamino)boranes.

2.1.1.4. Tetramethylcyclopentadienyl substituted ligand precursors

Following the same synthetic approach as previously described, (η^1-C$_5$Me$_4$H)B(N*i*Pr$_2$)Cl (**89**) and the new CGC ligand precursor (η^1-C$_5$Me$_4$H)B(N*i*Pr$_2$)N(H)Ph (**90**) have been synthesised (Scheme 11). Tetramethylcyclopentadienyl substituted CGCs are of particular interest as their specific combination of steric and electron features gives rise to some of the most active CGC type polymerisation catalysts.

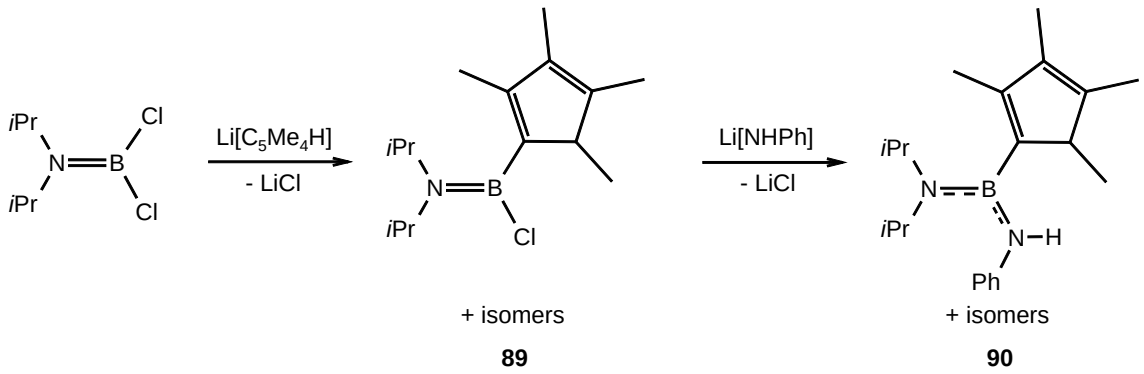

Scheme 11. Preparation of (tetramethylcyclopentadienyl)(diamino)borane **90**.

The formation of **89** from *i*Pr_2NBCl_2 and Li[C_5Me_4H] was monitored by ^{11}B NMR spectroscopy. The substitution reaction was found to be quite slow and needed 7 d to go to completion. The crude reaction product was subsequently analysed by multinuclear NMR spectroscopy. Although the ^{11}B NMR spectrum showed a single signal at δ = 37.6, the ^{1}H and ^{13}C NMR spectra were found to be complex and thus suggested formation of a mixture of the **va** and **vh** isomers. This is in contrast to the corresponding synthesis of (η^1-C_5Me_4H)B{$N(SiMe_3)_2$}Cl where the **vh** isomer is formed exclusively. Unfortunately, the complete assignment of all signals to the respective isomers of **89** through $^{1}H,^{1}H$-COSY and $^{13}C,^{1}H$-HMQC-COSY NMR spectroscopy could not be accomplished. GC-MS analysis performed on the mixture could not separate the isomers, but demonstrated the high purity of the mixture by showing only one main peak (peak area > 99%). The MS analysis of this peak was consistent with the formulation of **89** (*m*/*z* = 267).

Substitution of the chlorine in **89** by reaction with Li[NHPh] was found to proceed to completion within 16 h. The ^{11}B NMR spectrum of the crude product displayed a single signal at δ = 30.4 that is in the expected range for the target compound **90**. Again, the ^{1}H and ^{13}C NMR spectra were found to be very complex and full assignment of the signals to the proposed product could not be achieved. This may be attributed to the presence of a large number of isomers of **90** that may result from the variation in the relative position of the boryl group and the double bonds in the ring system and rotation of the substituents on boron (*vide supra*). Furthermore, GC-MS analysis supports the formulation of **90** as the predominant product of the reaction. MS analysis of the main peak in the chromatograph (peak area *ca.* 85%) displayed a molecular peak at *m*/*z* = 324 and a fragmentation pattern that are consistent with the proposed compound. MS analysis of the second largest peak in the chromatograph (peak area *ca.* 15%) suggests (η^1-C_5Me_4H)B{$N(H)Ph\}_2$ to be the main impurity. This compound may be formed by reaction of the target product with superstoichiometric amounts of Li[NHPh].

2.1.1.5. *X*-ray crystallographic analysis of amino mono borane based ligand precursors 83, 87 and 88

The structures of the indenyl substituted ligand precursor **83** (Figure 27) and the fluorenyl substituted ligand precursors **87** and **88** (Figures 28 and 29, respectively) in

the solid state largely resemble that of the related indenyl compound (1-C_9H_7)B(N*i*Pr$_2$)N(H)Ph (**66**).

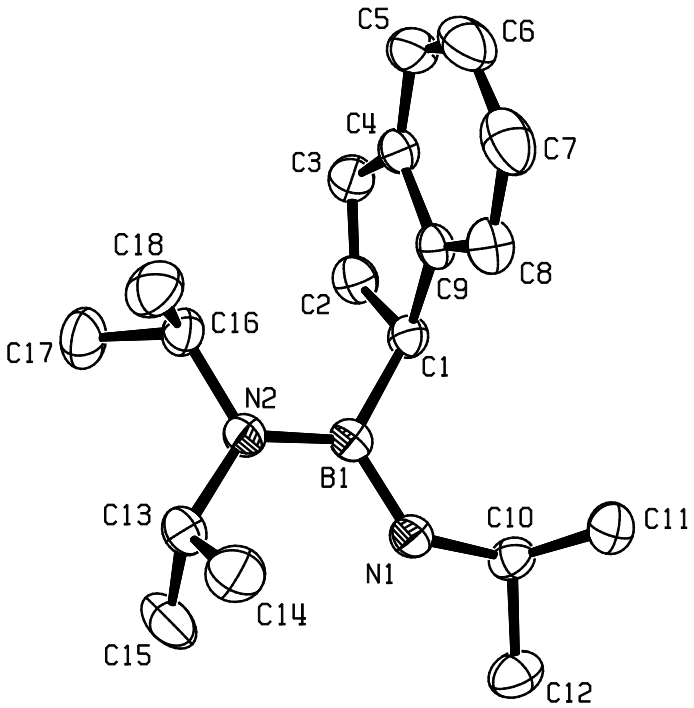

Figure 27. ORTEP representation of (1-C_9H_7)B(N*i*Pr$_2$)N(H)*i*Pr (**83**) in the solid state; thermal ellipsoids are drawn at the 50% probability level; hydrogen atoms are omitted for clarity.

Compound **83** crystallises in the monoclinic space group $P2_1/n$ and adopts C_1 symmetry in the crystal. The crystal structure confirms the assumed constitution with the boron atom attached to the sp^3-hybridised carbon atom of the indenyl system. Both the boron and N(2) centres adopt trigonal planar geometries with the central atoms lying only 0.015 Å [B] and 0.025 Å [N(2)] out of the planes defined by their respective substituents. These two trigonal planes are virtually coplanar with the torsional twist about the B–N(2) bond being less than 2°. The B–N(1) and B–N(2) bond lengths of 1.4153(19) and 1.4187(18) Å are almost identical, indicating equal contributions to π-bonding from both amino groups. The N(2)-bound *iso*propyl group *syn* to the indenyl moiety is oriented such that the methine proton is directed towards the middle of the C_5 ring (a conformation also seen in the corresponding compound **66**) with H$\cdots\pi$ distances to the centres of the C(12)–C(13) olefinic and C(14)–C(19) aromatic bonds of 2.446 and 2.509 Å, respectively. There are no noteworthy intermolecular interactions in the crystals of **83**.

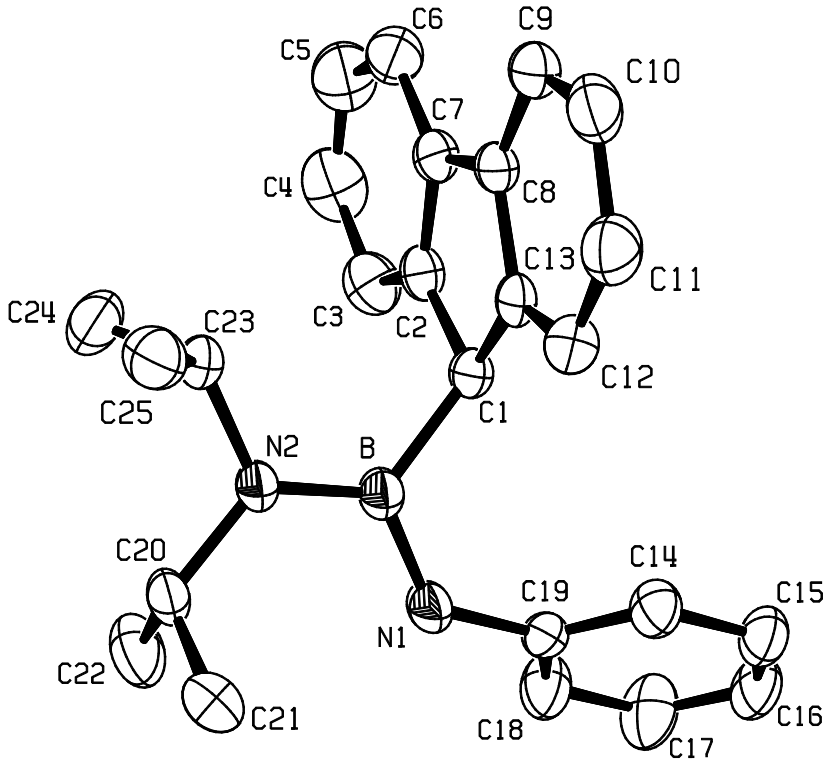

Figure 28. ORTEP representation of (9-$C_{13}H_9$)B(N*i*Pr_2)N(H)Ph (**88**) in the solid state; thermal ellipsoids are drawn at the 30% probability level; hydrogen atoms are omitted for clarity.

Compound **88** crystallises in the triclinic space group $P\bar{1}$ and adopts C_1 symmetry in the crystal. Both the boron and N(2) centres adopt trigonal planar geometries with the central atoms lying only 0.019 Å [B] and 0.012 Å [N(2)] out of the planes defined by their respective substituents. These two trigonal planes are virtually coplanar, the torsional twist about the B–N(2) bond being less than 2°. The B–N(1) and B–N(2) bond lengths of 1.431(4) and 1.407(4) Å, respectively, indicate a degree of delocalisation of π-electron density across the N(1)-B-(N2) linkages with a significantly higher π-contribution from the dialkylamino group compared to the anilido moiety. The N(2)-bound *iso*propyl group *syn* to the fluorenyl moiety is oriented such that the methine proton is directed towards the middle of the C_5 ring, as previously described for the indenyl substituted ligand precursor **83** (*vide supra*), such that the H$\cdots\pi$ distances to the centres of the C(2)–C(7) and C(8)–C(13) aromatic bonds are 2.502 and 2.567 Å, respectively. There are no intermolecular packing interactions of note.

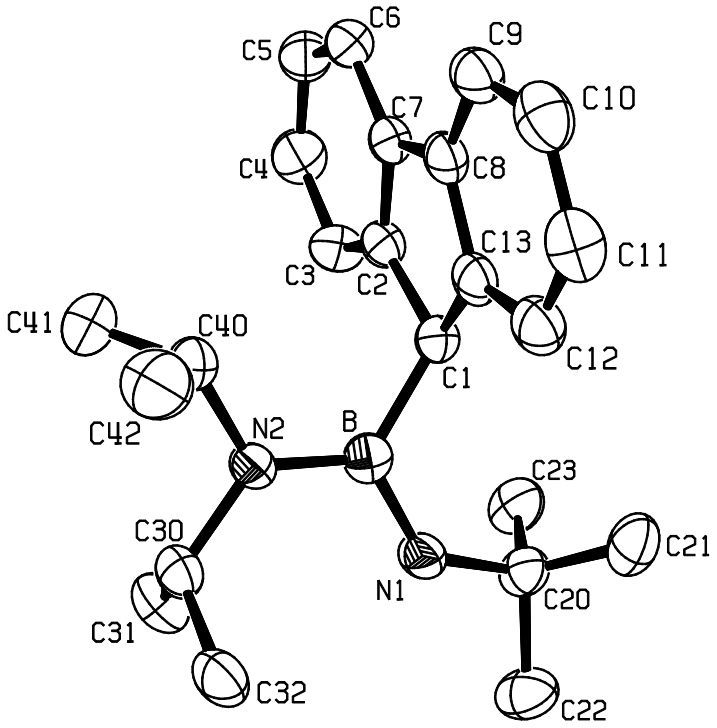

Figure 29. ORTEP representation of (9-$C_{13}H_9$)B(N*i*Pr_2)N(H)*t*Bu (**87**) in the solid state; thermal ellipsoids are drawn at the 50% probability level; hydrogen atoms are omitted for clarity.

Compound **87** crystallises in the monoclinic space group $P2_1/n$ and adopts approximate C_S symmetry in the crystal. Again, both the boron and N(2) centres adopt trigonal planar geometries with the central atoms lying only 0.002 Å [B] and 0.001 Å [N(2)] out of the planes defined by their respective substituents. These two trigonal planes are almost coplanar, the torsional twist about the B–N(2) bond being *ca*. 5°. The B–N(1) and B–N(2) bond lengths of 1.419(2) and 1.414(2) Å are equivalent to within experimental error, indicating equal amounts of π-contribution from both amino groups. The N(2)-bound *iso*propyl group *syn* to the fluorenyl moiety is again oriented such that the methine proton is directed towards the middle of the C_5 ring with H$\cdots\pi$ distances to the centres of the C(2)–C(7) and C(8)–C(13) aromatic bonds of 2.561 and 2.558Å, respectively. No short intermolecular contacts were detected.

2.1.2. Diborane(4) based ligand precursors

Only very recently have the syntheses of [2]borametallocenophanes [{η^5:η^5-$(C_5H_4)_2(BNMe_2)_2$}MCl_2] (M = Zr, Hf) been reported. Preliminary polymerisation experiments demonstrated a high catalytic activity of these compounds in the presence of MAO towards polymerisation of ethylene. The resulting polymers were found to be of much higher molecular weight than polyethylenes obtained with

[1]borametallocenophane catalysts. Corresponding CGC ligand precursors and CGCs bearing a [2]bora-*ansa*-bridge have not yet been described in the literature, despite the knowledge that the catalytic properties of CGCs are sensitive to changes in the *ansa*-bridge (see section 1.4.3). Consequently, the extension of the previously applied synthetic procedure to the selective substitution of diaminodiborane(4) compounds was attempted with the aim of synthesising the first CGC ligand precursors featuring [2]bora-*ansa*-bridges as well as corresponding complexes (*vide infra*). Subsequent substitution of the two chlorine atoms in $B_2(NMe_2)_2Cl_2$ with suitable reagents should in principle lead to the desired CGC ligand precursors. The critical issue in this approach is to find reaction conditions that facilitate sequential chlorine atom substitution.

2.1.2.1. Cyclopentadienyl substituted ligand precursors

Nöth *et al.* described their attempts to react $B_2(NMe_2)_2Cl_2$ with TlCp or NaCp in toluene or thf with the aim of synthesising $B_2(NMe_2)_2(\eta^1\text{-}C_5H_5)_2$. Their target product was not obtained and the other products formed in the course of the reaction were scarcely characterised. The reaction of $B_2(NMe_2)_2Cl_2$ with NaCp was therefore reassessed (Scheme 12). The 1:1.1 reaction of the reactants in toluene was monitored by ^{11}B NMR spectroscopy. Reaction progress could be easily followed by the slow disappearance of the signal at δ = 38.4 corresponding to $B_2(NMe_2)_2Cl_2$ and simultaneous growth of a new signal at $\delta \approx 42$. After the complete disappearance of the signal corresponding to the starting material, the reaction was worked up by removal of the precipitated NaCl and excess NaCp by centrifugation before evaporation of the solvent *in vacuo*.

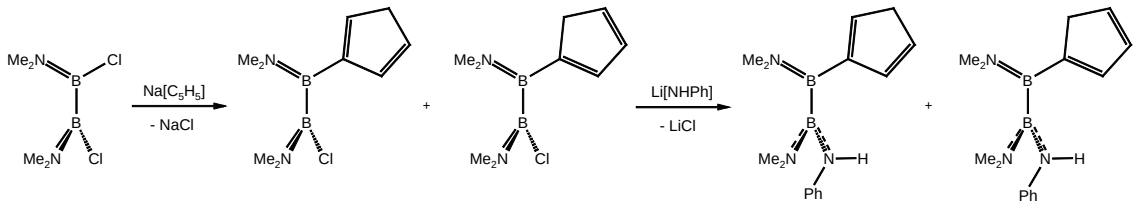

Scheme 12. Preparation of a cyclopentadienyl substituted diborane(4) based CGC ligand precursor.

The crude product obtained was analysed by multinuclear 1D and 2D NMR spectroscopy and MS. The obtained spectra were found to be consistent with the formulation of the target product $(\eta^1\text{-}C_5H_5)(BNMe_2)_2Cl$ (**91**) and demonstrated the

absence of any significant amounts of by-products. The ^{1}H and ^{13}C NMR spectra both display two sets of signals in an approximate ratio of 5:2, corresponding to the **va** and **vh** isomers of **91**. The four chemically non-equivalent methyl groups of each isomer give rise to four distinct signals in both the ^{1}H and ^{13}C NMR spectra, indicative of hindered rotation about the Me_2N–B bonds. All other expected resonances, except for the BC resonance, are observed in these spectra. The resonances for the two distinct boron atoms in the molecule are not resolved in the ^{11}B NMR spectrum, but produce a very broad signal ($\omega_{1/2}$ = 245 Hz) at δ = 41.5.

Compound **91** was further reacted with one equivalent of Li[NHPh] (Scheme 12). The crude product that was obtained after removal of the precipitate and solvents could be further purified by distillation over a short path. The product was analysed by multinuclear 1D and 2D NMR spectroscopy, MS and IR spectroscopy. ^{1}H and ^{13}C NMR spectra showed two sets of signals in integration ratios of approximately 3:1 that are consistent with the formulation of the target compound **92** as a mixture of **va** and **vh** isomers. All expected resonances for the proposed structures were observed apart from the BC resonances. The four methyl groups of each isomer gave rise to four distinct signals in both spectra, indicating hindered rotation about the Me_2N–B bonds. In the ^{11}B NMR spectrum, two signals are present at δ = 34.0 and 46.0, reflecting the two distinctly different environments of the boron atoms in **92**. The signal at higher field corresponds to diamino-substituted boron atoms, whereas the resonance at lower field corresponds to boron atoms carrying one amino and one cyclopentadienyl substituent. The molecular peak at m/z = 266 and the fragmentation pattern that were observed in the mass spectrum support as well the formulation of the product. In the IR spectrum, a weak stretching band at 3399 cm^{-1} for the NH group in **92** was detected.

2.1.2.2. Indenyl substituted ligand precursors

Selective substitution of one chlorine atom in $B_2(NMe_2)_2Cl_2$ by an indenyl moiety using LiInd was previously described in the literature. $(1\text{-}C_9H_7)(BNMe_2)_2Cl$ is formed as the kinetically favoured product in the reaction and can be converted to the thermodynamically favoured isomer $(3\text{-}C_9H_7)(BNMe_2)_2Cl$ by heating. Both these indenyl substituted diborane(4) derivatives may be suitable intermediates for the synthesis of CGC ligand precursors.

In initial experiments, (1-C_9H_7)($BNMe_2$)$_2$Cl was reacted with Li[NHPh]. Reaction progress was then monitored by ^{11}B NMR spectroscopy. The signals corresponding to the starting material at δ = 39.9 and 43.4 were found to shift gradually apart to δ = 33.0 and 46.9 during the course of the reaction. The resulting chemical shifts are consistent with the distinctly different environments of the boron atoms in the desired CGC precursor, (C_9H_7)($BNMe_2$)$_2${N(H)Ph}. However, the ^{1}H and ^{13}C NMR spectra were found to be complex, suggesting formation of a mixture of 1-indenyl and 3-indenyl isomers. Full assignment of all signals could not be achieved. The isomerisation reaction that leads to the 3-indenyl derivative may be promoted by the formed CGC ligand precursor, that is presumably a more basic amine derivative than the starting material (1-C_9H_7)($BNMe_2$)$_2$Cl. It is well established that the rearrangement of (1-indenyl)boranes to the thermodynamically more stable (3-indenyl)boranes can be promoted not only by heat, but as well by bases such as NEt_3.[48, 297, 310, 316, 317] Indeed, reassessment of the conversion of (1-C_9H_7)($BNMe_2$)$_2$Cl to (3-C_9H_7)($BNMe_2$)$_2$Cl (**93**) showed that the former may be distilled *in vacuo* without isomerisation, but can be converted to the latter by addition of catalytic amounts of NEt_3 (Scheme 13).

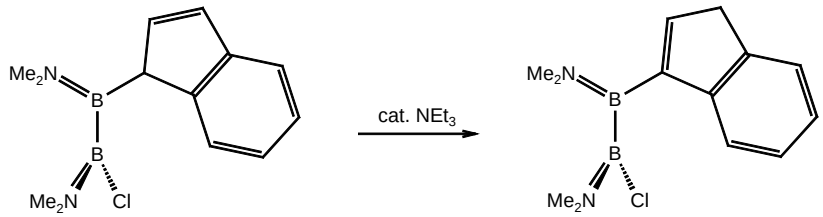

93

Scheme 13. Isomerisation of (1-C_9H_7)($BNMe_2$)$_2$Cl to (3-C_9H_7)($BNMe_2$)$_2$Cl (**93**).

Since reaction of (1-C_9H_7)($BNMe_2$)$_2$Cl with Li[NHPh] resulted in an isomeric mixture, it appeared promising to use the thermodynamically more stable derivative (3-C_9H_7)($BNMe_2$)$_2$Cl (**93**) for the substitution reaction. Only one well defined product would be anticipated from this reaction as the rearrangement of (1-indenyl)boranes to the corresponding (3-indenyl)boranes is usually irreversible. Consequently, **93** was reacted with Li[NHPh] (Scheme 14). The crude product was obtained as a brown oil after removal of precipitated LiCl and solvents. The product could be purified further by precipitation from a concentrated toluene solution by addition of hexane.

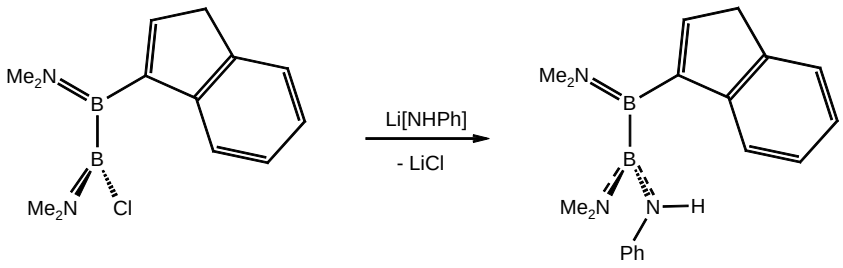

93 **94**

Scheme 14. Preparation of an indenyl substituted diborane(4) based CGC ligand precursor.

The purified product was analysed by means of multinuclear 1D and 2D NMR spectroscopy, MS and IR spectroscopy. The ^{1}H and ^{13}C NMR spectra showed all the expected signals for the target compound (3-C_9H_7)($BNMe_2$)$_2${N(H)Ph} (**94**) apart from the BC resonance. The four methyl groups in the product give rise to four distinct signals in both spectra at $\delta(^{1}H)/\delta(^{13}C)$ = 2.31 / 35.6, 2.70 / 41.7, 2.73 / 42.4 and 2.87 / 44.4. The two signals at δ = 2.31 and 2.73 in the ^{1}H NMR spectrum are significantly broader than the two other methyl resonances. These, presumably, correspond to the NMe_2 group in the Me_2NB{N(H)Ph} fragment as the additional amino group should lower the π-contribution in the Me_2N–B linkage and thus facilitate rotation about this bond. To further assess the barrier to rotation about the Me_2N–B bonds in **94**, high temperature ^{1}H NMR studies were performed (*vide infra*). Compound **94** gives rise to two resonances in the ^{11}B NMR spectrum at δ = 34.3 and 48.0 that reflect the distinctively different environments of the two boron atoms in the molecule. By comparison to the related cyclopentadienyl derivative **92**, the signal at lower field is likely to correspond to the carbon substituted boron atom, whereas the signal at higher field may be attributed to the diamino substituted boron atom. The mass spectrum obtained for the product displays a molecular peak at m/z = 317 and a fragmentation pattern that support the proposed formulation. In the IR spectrum, a weak stretching band for the NH moiety of **94** at 3398 cm^{-1} was observed.

(3-C_9H_7)($BNMe_2$)$_2${N(H)Ph} (**94**) was chosen as a model compound to study the energy barriers for rotation about the Me_2N–B bonds in CGC ligand precursors bearing a $(Me_2NB)_2$ bridging moiety. Compound **94** appeared to be a suitable candidate for such a study, as it can be obtained as a single isomer, in contrast to the related cyclopentadienyl derivative **92**, and because the signals for the four methyl groups are well separated at ambient temperature. A good understanding of the rotational barriers

for the different Me_2N moieties in such molecules is of interest, because it will aid interpretation of the NMR spectra of such compounds and corresponding CGCs. Figure 30 shows the crucial section of the ^1H NMR spectra of **94** recorded at various temperatures.

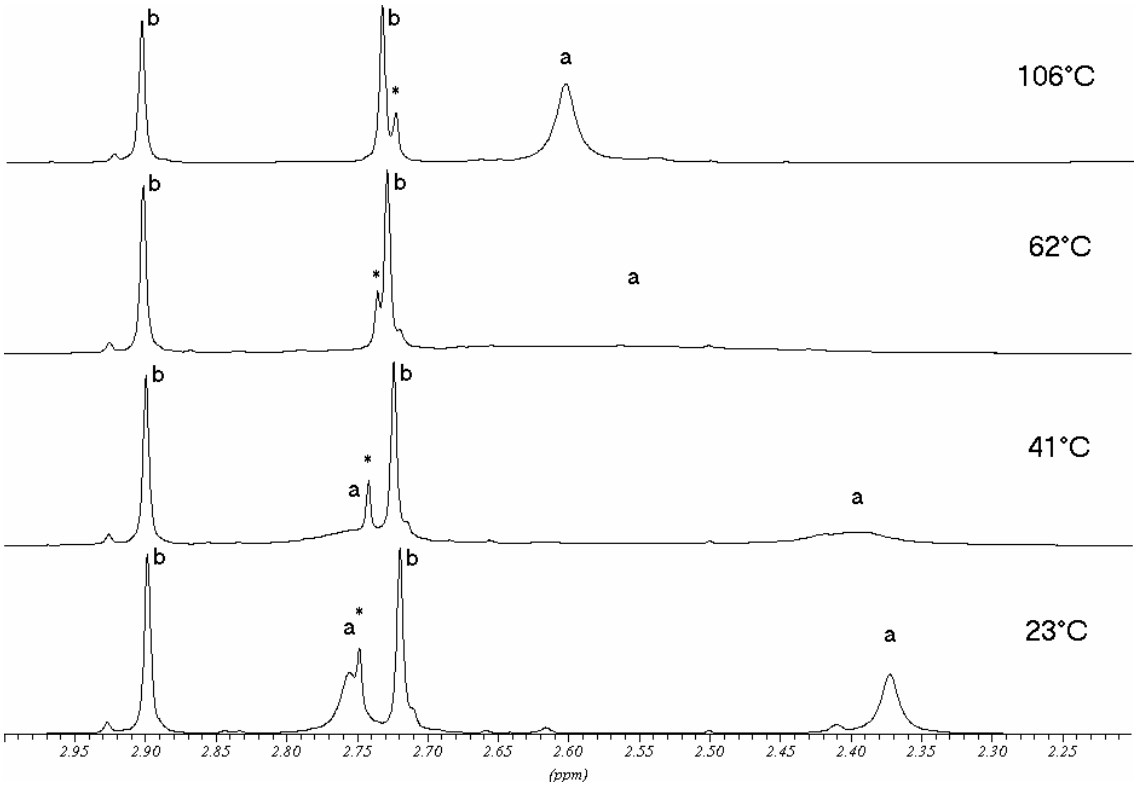

Figure 30. Section showing the NMe_2 resonances (a, b) in the ^1H NMR spectra of (3-C_9H_7)$(BNMe_2)_2${N(H)Ph} (**94**) at various temperatures; * denotes a resonance corresponding to an unidentified impurity.

The two signals that are already somewhat broadened at ambient temperature further widen on increasing temperature and eventually coalesce in the temperature interval between 57°C and 62°C. The observed coalescence temperature corresponds to a free activation enthalpy $\Delta G^{\ddagger}$ of *ca.* 67 kJ/mol[321] for the rotation of one of the Me_2N groups. For the other two signals, only negligible line broadening is observed up to 111°C, the maximum temperature as was defined by the boiling point of the solvent (toluene). This indicates the free activation enthalpy $\Delta G^{\ddagger}$ for the rotation of the other Me_2N moiety to be distinctly higher than 81 kJ/mol. Assignment of the lower rotational barrier to the Me_2N–B{N(H)Ph} bond seems reasonable as the second amino group in this fragment should donate π-electron density towards the boron atom and therefore lower the π-contribution in the Me_2N–B linkage. To the contrary, in the (Me_2N)B(3-indenyl) fragment, the electron deficiency of the boron atom should be mainly

compensated by π-donation from the Me_2N group, resulting in a stronger π-character of the respective Me_2N–B bond and consequently a higher rotational barrier. The determined $\Delta G^{\ddagger}$ values for the barrier to rotation about the N–B bonds in **94** are well within the range of previously reported values for such bonds.[322]

2.1.3. Ferrocenyl borane based ligand precursors

One of the long-term aims of this research is the synthesis of CGCs bearing a Lewis acidic boron linker that, at best, allows for self-activation (*vide supra*). The Lewis acidity of the boron atom in the previously described CGC ligand precursors is, however, cancelled by the attached dialkyl (or bistrimethylsilyl) amino groups. Obviously, in all CGC ligand precursors discussed here, a second amino group NHR (R = alkyl, aryl) is present that can donate π-electron density to the neighbouring boron atom and reduce its Lewis acidic character. In the corresponding CGCs derived from these precursors, however, this effect may be moderated by competition for π-electron density by the ligated transition metal centre.

Ferrocenyldibromoborane, [$FcBBr_2$], appeared to be a suitable starting material for the synthesis of boron-bridged CGC ligand precursors without stabilising, Lewis basic, dialkyl (or bistrimethylsilyl) amino groups on the boron centre. [$FcBBr_2$] can be easily synthesised and purified by recrystallisation.[323] It is a solid a room temperature and is therefore easy to handle compared to many aminodihaloboranes that are corrosive liquids. Furthermore, redox chemistry involving the pendent ferrocenyl moiety in derived CGCs might allow for completely new ways of tuning the catalytic activity of such complexes.[324] Metallocenophane ligand precursors, *e.g.* **95**[325]**,** and tris(1-pyrazolyl)borate complexes, *e.g.* **96**[326]**,** derived from [$FcBBr_2$] have been previously reported (Figure 31).

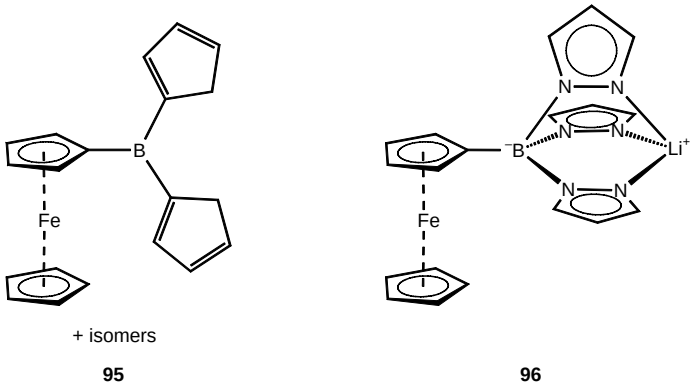

Figure 31. Examples of previously reported ferrocenyl borane based ligand precursors and complexes.

2.1.3.1. Attempted synthesis of [FcB(R)Br] (R = η^1-C_5H_5, 1-C_9H_7, 3-C_9H_7)

In analogy to the synthetic route previously employed for the synthesis of aminoborane based CGC ligand precursors (*vide supra*), sequential reaction of [$FcBBr_2$] with a salt of cyclopentadiene or a derivative and a suitable lithium amide was envisioned to lead to the corresponding ferrocenyl borane based CGC ligand precursors. Consequently, [$FcBBr_2$] was reacted with a substoichiometric amount of NaCp at 0 °C (Scheme 15). After slow warming to ambient temperature and subsequent stirring for several hours, the mixture was worked-up to yield a red oil. Multinuclear NMR spectra indicated the formation of [FcB(η^1-C_5H_5)$_2$] (**95**) and the presence of unreacted [$FcBBr_2$]. In the ^{13}C NMR spectrum, an additional set of signals could be identified that may be attributed to one (presumably the **vh**) isomer of the target compound [FcB(η^1-C_5H_5)Br] (**97**). However, the intensities of these resonances are low compared to those corresponding to **95**, indicating only a low concentration of **97** in the product mixture. Formation of **95** as the predominant product in the reaction suggests that substitution of bromide in [FcB(η^1-C_5H_5)Br] (**97**) proceeds significantly faster than in [$FcBBr_2$].

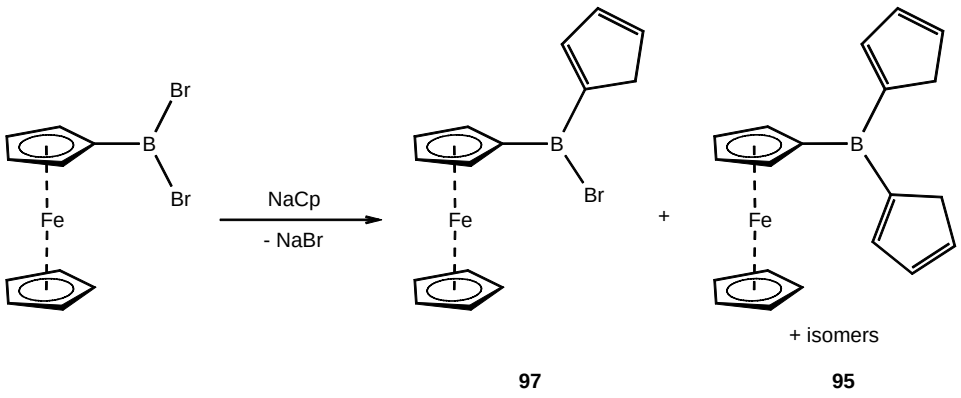

Scheme 15. Reaction of [$FcBBr_2$] with NaCp.

Under similar conditions, the synthesis of [FcB(1-C_9H_7)Br] from [$FcBBr_2$] and LiInd was attempted. An ^{11}B NMR spectrum recorded after a reaction time of 45 min at –80 °C showed a signal at $\delta = 60.7$ that could indicate formation of the target product (high field relative to the chemical shift for [FcB(1-C_9H_7)$_2$] ($\delta = 68.4$) and low field compared to the chemical shift for [$FcBBr_2$]) and a signal at $\delta = 45.2$ corresponding to the starting material [$FcBBr_2$]. After prolonged reaction times, an additional signal in the ^{11}B NMR spectrum at $\delta = 38.3$ revealed formation of another boron containing product that could not be identified.

Apparently, the selective 1:1 reaction of [$FcBBr_2$] with salts of cyclopentadienide or derivatives is hampered by the reactivity of the target product and further unidentified reaction pathways under the applied conditions. Therefore, alternative approaches for the synthesis of FcB(R)Br (R = η^1-C_5H_5, 1-C_9H_7, 3-C_9H_7) were sought after. The reaction of trialkylboranes BR_3 with two equivalents of BCl_3 in the presence of catalytic amounts of boron hydrides is known to yield the corresponding redistribution products $RBCl_2$ (Scheme 16).[327, 328, 329] Hence, the possibility for similar substituent redistribution was envisioned for the reaction of [$FcBBr_2$] and [$FcBR_2$] (R = η^1-C_5H_5, 1-C_9H_7, 3-C_9H_7) in the presence of boron hydrides, although the presence of three different substituents (Br, Fc, R) in the mixture might impair selectivity dramatically.

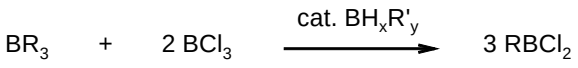

Scheme 16. Boron hydride catalysed substituent redistribution between BR_3 and BCl_3.

In an initial control experiment, the reactivity of [$FcBBr_2$] with the selected boron hydride reagent, [BH_3·SMe_2], was assessed (Scheme 17). Immediately after mixing of the two reagents, the ^1H and ^{11}B NMR spectra displayed signals corresponding to the bromide-hydride exchange products [$BBrH_2$·SMe_2] and [BBr_2H·SMe_2]. Furthermore, an additional boron containing species giving rise to a signal at $\delta = 42.3$ (singlet) in the ^{11}B NMR spectrum was observed. Additional signals in the ^1H NMR spectrum that might correspond to the same species did not allow the constitution of that compound to be clarified. No signals corresponding to the starting material [$FcBBr_2$] were detected in the spectrum. After 16 h, the ^1H and ^{11}B NMR

spectra were re-recorded. Signals corresponding to diborane(6), [$BBrH_2{\cdot}SMe_2$], [$BBr_2H{\cdot}SMe_2$] and surprisingly [$FcBBr_2$] could be unambiguously assigned. The latter must re-form during the complex reaction, since it is absent in the reaction mixture after a short reaction time (*vide supra*). Furthermore, in the ^{1}H NMR spectrum another set of signals showing the characteristic multiplicities and integral ratios for substituted ferrocenyl boranes (one singlet for the unsubstituted cyclopentadienyl moiety, two pseudo-triplets for the boron substituted cyclopentadienyl moiety; integral ratios 5:2:2) was detected as well as a corresponding signal at δ = 54.5 (singlet) in the boron spectrum. As the components of the reaction mixture could not be separated, unambiguous determination of the structure of this compound was not feasible.

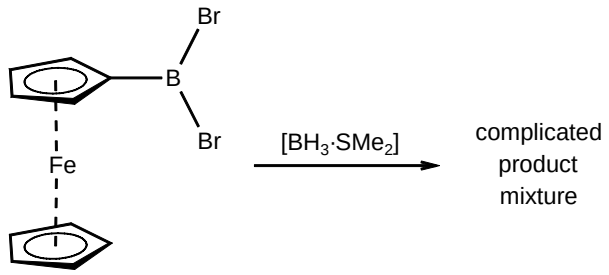

Scheme 17. Reaction of [$FcBBr_2$] with [$BH_3{\cdot}SMe_2$].

Given the already complex reaction pathways involved in the reaction of [$FcBBr_2$] with [$BH_3{\cdot}SMe_2$], a selective substituent redistribution between [$FcBBr_2$] and [$FcBR_2$] in the presence of [$BH_3{\cdot}SMe_2$] as envisaged seemed to be highly unlikely. Nonetheless, such substituent redistribution reactions were attempted by combining solutions of [$FcBBr_2$] and [$FcBR_2$] (R = η^1-C_5H_5, 1-C_9H_7, 3-C_9H_7) and subsequently adding small quantities of [$BH_3{\cdot}SMe_2$] (Scheme 18). In all cases, ^{1}H and ^{11}B NMR spectra indicated complex reaction pathways resulting in a large number of products. Since the resulting product mixtures could not be separated, identification of all the products was not possible.

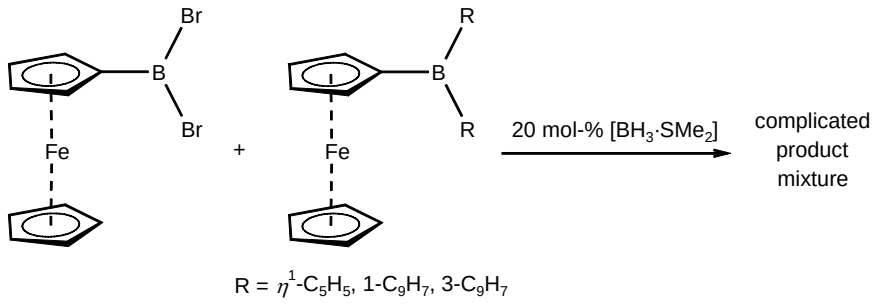

R = η^1-C_5H_5, 1-C_9H_7, 3-C_9H_7

Scheme 18. Reaction of [$FcBBr_2$] and [$FcBR_2$] (R = η^1-C_5H_5, 1-C_9H_7, 3-C_9H_7) in the presence of [BH_3·SMe_2].

2.1.3.2. Synthesis of [FcB(Br)N(H)R] (R = *t*Bu, Ph)

In the previous section, unsuccessful attempts to first introduce the cyclopentadienyl fragment into ferrocenyl borane based CGC ligand precursors were described. The obvious alternative approach is to first introduce the amino moiety, NHR, and then the cyclopentadienyl fragment into the ligand precursors.

[$FcBBr_2$] was reacted with Li[NHR] (R = *t*Bu, Ph) to give [FcB(Br)N(H)R] {R = *t*Bu (**98**), Ph (**99**)} *via* salt elimination (Scheme 19). The ^{11}B NMR spectra of **98** and **99** displayed singular resonances at δ = 35.3 and 36.7 respectively that are in the expected range for boron atoms with such substitution pattern and significantly high-field shifted relative to [$FcBBr_2$]. The ^{1}H and ^{13}C NMR spectra of **98** at ambient temperature showed two sets of signals in an integral ratio of *ca.* 10:1, corresponding to two rotamers. Resonances of **99** in the ^{1}H and ^{13}C NMR spectra at ambient temperature were very broad. However, at low temperature (–30 °C) resonances were well resolved. Again, two sets of signals were observed in an integral ratio of *ca.* 5:2, indicating the presence of two rotamers.

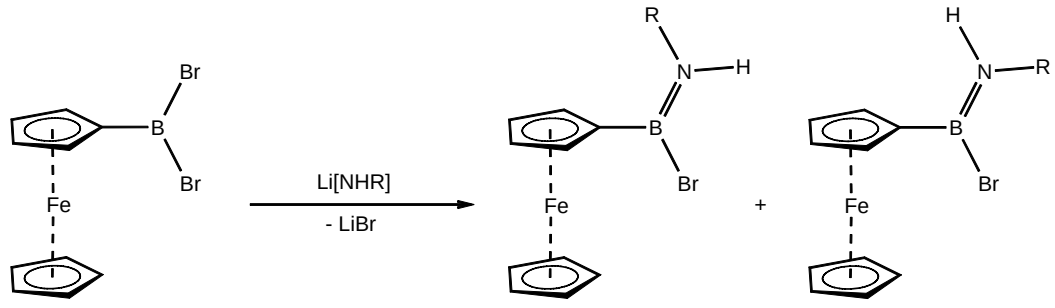

98 R = *t*Bu
99 R = Ph

Scheme 19. Synthesis of [FcB(Br)N(H)R] {R = *t*Bu (**98**), Ph (**99**)}.

The observation of two isomers of **98** and **99** is most certainly the result of π-donation from the nitrogen lone pair into the empty *p*-orbital on boron and, hence, strong double bond character in the B–N bond. Given four different substituents on the B=N linkage and hindered rotation about this bond, both *E* and *Z* isomers would be expected. Whether the *E* or *Z* isomers predominate in solution could not be determined. The *Z* isomers (where the Fc and R groups are positioned in *trans* position relative to each other), however, are less sterically congested, thus would be expected to be lower in energy. The lower barrier for rotation about the B–N bond in **99** compared to **98**, as indicated by the resolution of the signals for the two isomers in the former only at low temperature, can be explained by the modest electron withdrawing effect of the phenyl group moderating the π-donation from nitrogen to boron.

2.1.3.3. Synthesis of [FcB(R)N(H)Ph] (R = η^1-C_5H_5, 1-C_9H_7, 3-C_9H_7)

The compound [FcB(Br)N(H)Ph] (**99**) was sequentially reacted with NaCp and LiInd respectively to generate the desired CGC ligand precursors. The reaction of **99** with NaCp (Scheme 20) was performed either heterogeneously in toluene or homogeneously in a toluene/thf mixture. In both cases, an orange coloured oil was obtained after work-up. The products from both reactions were analysed by ^{1}H and ^{11}B NMR spectroscopy and showed virtually identical spectroscopic features. The ^{11}B NMR spectra displayed single resonances at $\delta = 40$, slightly low-field shifted compared to **99** {$\delta(^{11}B) = 36.7$} as would be expected from the substitution of a B–Br for a B–C moiety. However, ^{1}H NMR spectra were very poorly resolved, probably due to the presence of several isomers of the target compound [FcB(η^1-C_5H_5)N(H)Ph] (**100**) (**va** and **vh** isomers with respect to the position of boron relative to the double bonds in the η^1-C_5H_5 moiety and *E* and *Z* isomers arising from hindered rotation about the B–N bond), that may be partially interconverting (resulting in line broadening/coalescence of signals for corresponding *E* and *Z* isomers due to rotation about the B–N bond). An unambiguous characterisation of the obtained product was therefore not feasible.

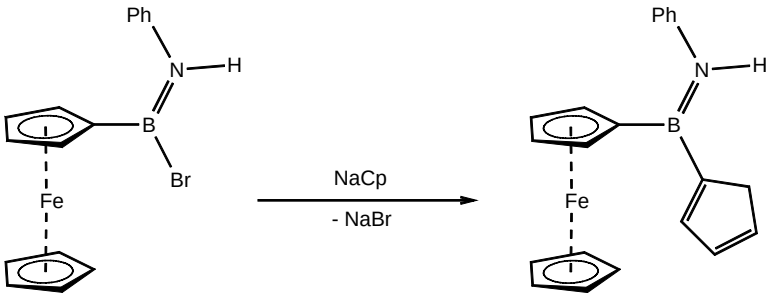

+ isomer
99

+ isomers
100

Scheme 20. Reaction of [FcB(Br)N(H)Ph] with NaCp.

Similarly, the reaction of **99** with LiInd (Scheme 21) afforded a red oil after work-up that solidified on standing at ambient temperature. Recrystallisation from toluene at –30 °C yielded the pure target compound [FcB(1-C_9H_7)N(H)Ph] (**101**). Although the crystalline solid was identified as the *Z* isomer (where the Fc and Ph groups are positioned in *cis* position relative to each other) by *X*-ray diffraction methods (*vide infra*), ^{1}H and ^{13}C NMR spectra displayed two sets of signals in an integral ratio of *ca*. 5:2, indicating the presence of two isomers in solution. As in **99**, this observation may be likewise attributed to the presence of *E* and *Z* isomers with respect to the substituents on the B–N linkage in **101**. The ^{11}B NMR spectrum of **101** displayed a single resonance at δ = 42.9 that falls in the expected range for the substitution pattern at boron.

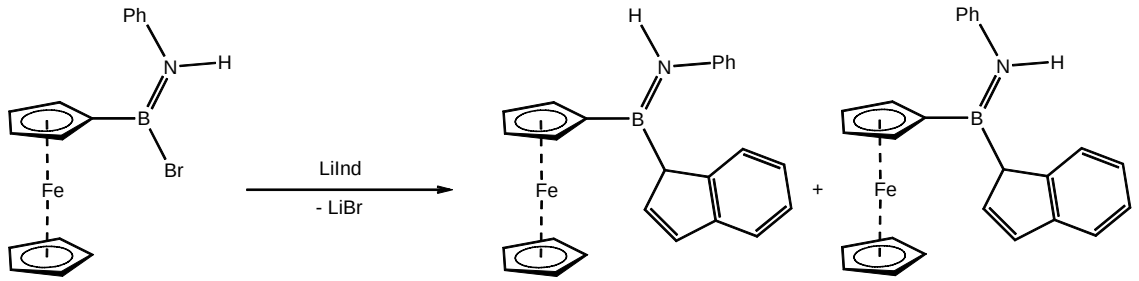

+ isomer
99

(*E* isomer)

(*Z* isomer)
101

Scheme 21. Synthesis of [FcB(1-C_9H_7)N(H)Ph] (**101**).

Rearrangement of (1-indenyl)borane derivatives to their thermodynamically more stable 3-indenyl congeners in the presence of heat or Lewis bases is well established in the literature.[48, 297, 310, 311, 313, 315 316, 317] Such isomerisation of **101** to the more stable isomer [FcB(3-C_9H_7)N(H)Ph] (**102**) was achieved in the presence of NEt_3

(Scheme 22). Rather surprisingly, ^{1}H and ^{13}C NMR spectra of **102** displayed only one set of signals. Presumably, π-donation from the indenyl fragment to the boron atom results in a reduced double character of the B–N linkage and in turn facilitates fast interconversion of the *E* and *Z* isomers on the NMR timescale. The ^{11}B NMR resonance observed for the 3-indenyl isomer **102** at δ = 41.5 is slightly high-field shifted compared to the corresponding resonance in the 1-indenyl isomer **101** at δ = 42.9, in agreement with the relative chemical shifts for other pairs of closely related (1-indenyl)- and (3-indenyl)borane derivatives.[297, 315]

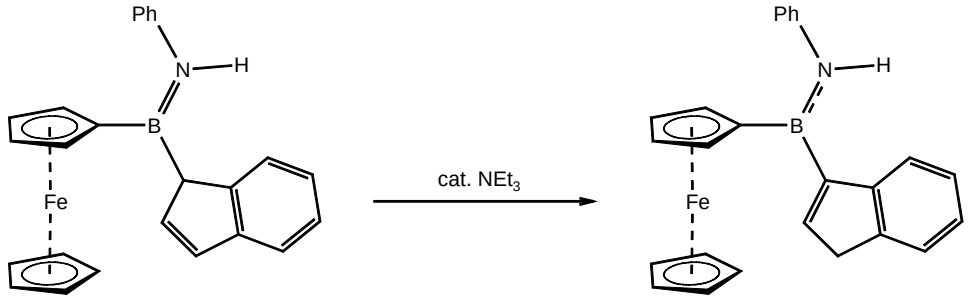

+ isomer

101 **102**

Scheme 22. Synthesis of [FcB(3-C_9H_7)N(H)Ph] (**102**).

2.1.3.4. Synthesis of [FcB{N(H)R}$_2$] (R = *t*Bu, Ph)

To obtain a broader understanding of the reactivity of [FcBBr$_2$] in salt elimination reactions, substitution of both bromine atoms with amine functionalities was attempted. The products so obtained may enable the synthesis of new transition metal complexes with a pendent redox-active ferrocenyl moiety. Related ligand precursors of the general formula PhB{N(H)R}$_2$ {R = Me, *t*Bu, Si(Me)$_2$*t*Bu} have been previously employed for the synthesis of Group 4,[330, 331, 332, 333] 5 and 6[334] transition metal complexes.

[FcBBr$_2$] was reacted with two equivalents of Li[NHR] (R = *t*Bu, Ph) to give the symmetrically substituted diamino compounds [FcB{N(H)R}$_2$] {R = *t*Bu (**103**), Ph (**104**)} (Scheme 23). Ambient temperature ^{1}H and ^{13}C NMR spectra of **103** and **104** exhibit only one set of signals corresponding to the respective target compounds, consistent with facile rotation about the B–N bonds for which bond orders are expected to be 1.5 at most. The ^{11}B NMR chemical shift of δ = 29.3 and 31.5 for **103** and **104**, respectively, are, as expected, high-field shifted by *ca.* 6 ppm compared to the chemical

shifts of δ = 35.3 and 36.7 for the corresponding monoamino ferrocenyl boranes **98** and **99**. They are also consistent with the assumed substitution pattern at the boron centres.

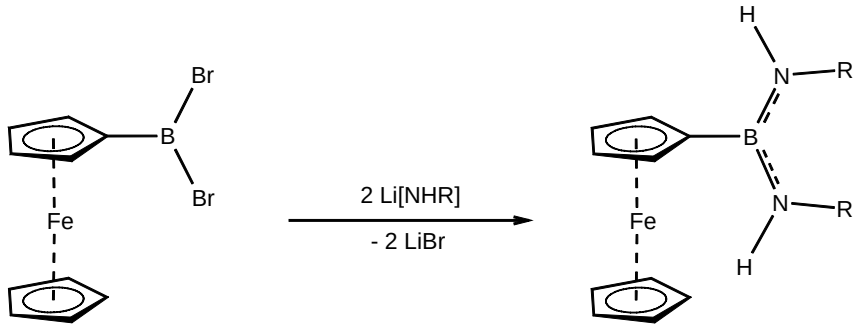

103 R = *t*Bu
104 R = Ph

Scheme 23. Synthesis of [FcB{N(H)R}$_2$] {R = *t*Bu (**103**), Ph (**104**)}.

The ^{1}H and ^{13}C NMR spectra revealed contamination of **103** by a second product in significant amounts (*ca.* 25%). Chemical shifts and integral ratios of the corresponding signals in the ^{1}H NMR spectrum are consistent with the tentative formulation of this product as [{–(Fc)B–N(*t*Bu)–}$_3$]. It can be envisaged that such a compound may be formed *via* base induced HBr abstraction from the intermediate [FcB(Br)N(H)*t*Bu] (**98**). Similar cyclic compounds of the general formula [{–(Fc)B–N(R)–}$_3$] (R = H, *p*-MeO-Ph) have been previously described in the literature.[335] In the ^{11}B NMR spectrum a corresponding resonance at δ = 42.6 was detected that would also be consistent with the proposed substitution pattern.

2.1.3.5. *X*-ray crystallographic analysis of ferrocenyl borane based ligand precursor 101

Single crystals of **101** suitable for *X*-ray crystallographic analysis were grown from a concentrated toluene solution at –30 °C. Compound **101** crystallises in the triclinic space group *P*1 and adopts C_1 symmetry in the crystal (Figure 32).

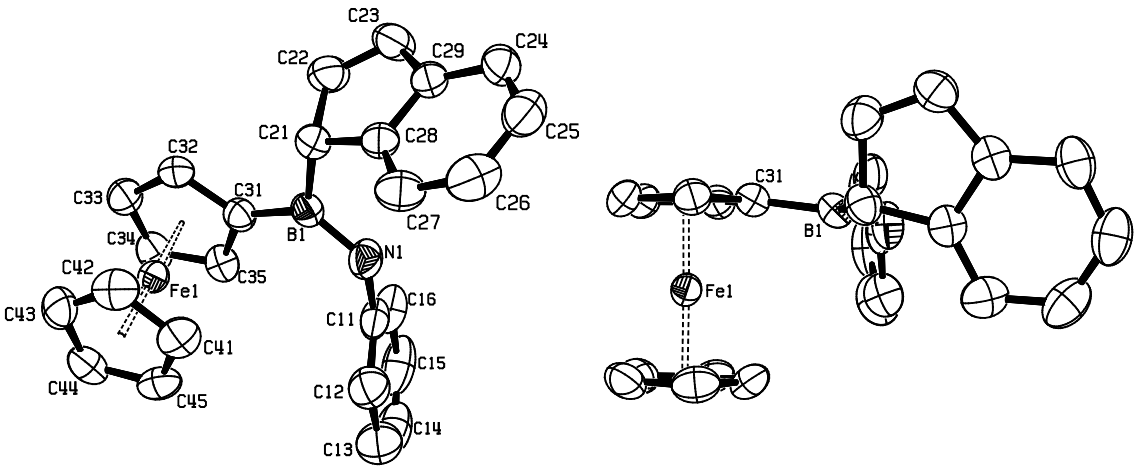

Figure 32. Two perspective views of the ORTEP representation of FcB(1-C_9H_7)N(H)Ph (**101**) in the solid state; thermal ellipsoids are drawn at the 50% probability level; hydrogen atoms are omitted for clarity.

The crystal structure confirms the assumed constitution with boron being attached to the sp^3-hybridised carbon atom of the indenyl system, *i.e.* the 1-indenyl position. The cyclopentadienyl rings of the ferrocenyl unit are oriented in an eclipsed fashion with a minor tilt of 1.1° between the two virtually planar ring systems (r.m.s. deviation of 0.0030 Å for C_5H_4 and 0.0004 Å for C_5H_5, respectively). The boron centre is situated in an trigonal planar environment (sum of angles between respective substituents is 360.0°). The B-N distance of 1.406(3) Å is in the expected range of B-N double bonds and the phenyl and indenyl moiety are *trans* disposed. The B-C(21) and B-C(31) bond lengths of 1.609(3) and 1.549(3) Å differ significantly and reflect the difference in hybridisation of the two carbon atoms. The short B-C(31) distance, together with the almost coplanar arrangement of the [C_5]–B–N–C11 linkage {reflected by the torsion angles C(35)–C(31)–B–N and C(31)–B–N–C(11) of –0.8(4) and 0.9(4)°, respectively}, may indicate some π-delocalisation *via* the B-C(31) bond. The most interesting feature of the *X*-ray structure is the positioning of the boryl moiety relative to the ferrocenyl fragment. The boryl substituent is moderately bent out of the cyclopentadienyl plane towards the iron centre, a disposition that is frequently observed in ferrocenylboranes with Lewis-acidic boron centres. As the boron atom is significantly displaced from the mirror plane dissecting the ferrocenyl unit in C(31) {indicated by angles C(32)–C(31)–B and C(35)–C(31)–B of 123.32(19) and 130.76(19)° respectively}, the usually applied method for the calculation of the dip angle α^* ($\alpha^* = 180° - \alpha$, with α being the angle $Cp_{centroid}$-C_{ipso}-B) as a measure for the bending is invalid. Therefore, the angle between the r.m.s. plane of the substituted

cyclopentadienyl ring and the r.m.s. plane calculated for boron and its three substituents is determined to be 9.8°. This value is slightly smaller than α^* found in FcB(OH)Me (10.3°, 10.8° and 12.9°, respectively, for three crystallographically independent molecules), which represents another example for a ferrocenylborane in which the Lewis-acidity of the boron centre is partially cancelled by a neighbouring π-donor.[336] The bending of the boryl group towards the iron centre in such compound was initially attributed to direct B–Fe interactions.[337, 338] Recent studies, however, excluded such a direct interaction between the two atoms and proposed instead a strongly delocalised, multicentred bonding model involving Fe, C_{ipso} and B to explain the observed bending.

2.2. Complex synthesis

2.2.1. Amino monoborane based complexes

The synthesis of titanium CGCs [Ti{η^5:η^1-(C_5H_4)B(N*i*Pr_2)N*t*Bu}(NMe_2)$_2$] (**71**) and [Ti{η^5:η^1-(C_5H_4)B(N*i*Pr_2)NPh}(NMe_2)$_2$] (**37**) by reaction of the respective ligand precursors with [Ti(NMe_2)$_4$] has been previously reported. Conversion of these diamino titanium complexes to their dichloro derivatives was allegedly achieved by reaction with excess Me_3SiCl.[148, 304] A re-assessment of these reactions as part of the work presented here, however, concluded that only the preparation of [Ti{η^5:η^1-(C_5H_4)B(N*i*Pr_2)NPh}R_2] (R = NMe_2, Cl) was reproducible. (η^1-C_5H_5)B(N*i*Pr_2)N(H)*t*Bu, on the other hand, was found to react with [Ti(NMe_2)$_4$] under elimination of only one equivalent of $HNMe_2$ to give the non-chelating complex [Ti{(η^5-C_5H_4)B(N*i*Pr_2)N(H)*t*Bu}(NMe_2)$_3$] (*vide infra*).

Starting from these preliminary results, a number of non-chelating as well as bridged titanium complexes have been synthesised and characterised as described in the following sections. Consequently, alternatives to the amine elimination reaction for the synthesis of amino monoborane based titanium CGCs have been investigated. Moreover, extension of the successful amine elimination approach for the synthesis of amino monoborane based titanium CGCs to the synthesis of corresponding CGCs of the higher Group 4 homologues zirconium and hafnium have been examined.

2.2.1.1. Non-chelating titanium complexes

The reaction of the ligand precursors (η^1-C_5H_5)B(N*i*Pr$_2$)N(H)R {R = *i*Pr (**77**), Cy (**78**), *t*Bu (**64**)} with [Ti(NMe$_2$)$_4$] in refluxing toluene yielded after 3 h the corresponding non-chelating, half-sandwich complexes [Ti{(η^5-C_5H_4)B(N*i*Pr$_2$)N(H)R}(NMe$_2$)$_3$] {R = *i*Pr (**105**), Cy (**106**), *t*Bu (**107**)} (Scheme 24). The related ligand precursor (η^1-C_5H_5)B(N*i*Pr$_2$)N(H)Ph is known to react with [Ti(NMe$_2$)$_4$] at lower temperatures and in short time to give the corresponding CGC under elimination of two equivalents of HNMe$_2$. Evidently, the pendent NHR groups with R = alkyl are significantly less acidic than their NHPh counterpart and thus, the second amine elimination step is impaired. Steric effects might contribute as well to the outcome of the reaction, however probably only to a minor extent given the huge difference in reaction rates between the two sterically relatively non-demanding substituents *i*Pr and Ph.

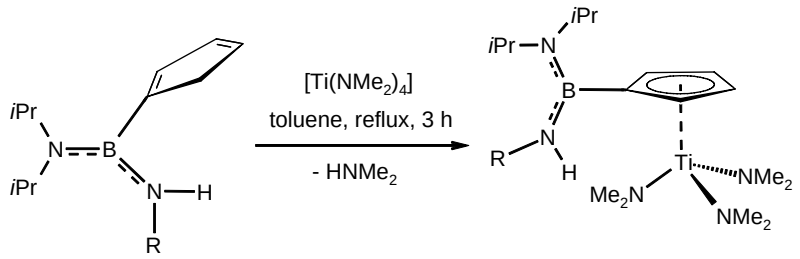

+ isomer

77 R = *i*Pr
78 R = Cy
64 R = *t*Bu

105 R = *i*Pr
106 R = Cy
107 R = *t*Bu

Scheme 24. Synthesis of non-chelating, half-sandwich complexes [Ti{(η^5-C_5H_4)B(N*i*Pr$_2$)N(H)R}(NMe$_2$)$_3$] {R = *i*Pr (**105**), Cy (**106**), *t*Bu (**107**)}.

The complexes **105** – **107** were characterised by multinuclear 1D and 2D NMR, IR spectroscopy and MS. ^{1}H NMR spectra of all three compounds display the characteristic pair of pseudo-triplets corresponding to the titanium coordinated mono-substituted cyclopentadienyl moiety as well as typical resonances for the N*i*Pr$_2$ moiety. Furthermore, resonances corresponding to the alkyl part of the NHR fragment were observed, but the NH resonances were not visible in the spectra, probably due to quadrupolar coupling to the neighbouring ^{14}N nuclei. However, the integration of the sharp resonances corresponding to the NMe$_2$ groups at the respective titanium centres in relation to that of the other signals strongly support the non-chelating formulation of the compounds. Further evidence is provided by the IR spectra of **105** – **107** that show characteristic NH stretching bands at 3441, 3441 and 3456 cm^{-1}, respectively. The ^{11}B

NMR spectra of **105** – **107** are unremarkable and the observed chemical shifts closely resemble those determined for the respective ligand precursors **77**, **78** and **64**. In addition, the ^{13}C NMR spectra of **105** – **107** are also unremarkable showing all the expected signals apart from the BC resonances. MS data for **105** – **107** are not very informative as mass spectra of these compounds frequently lack the molecular ion peak and are dominated by low molecular weight fragments resulting from the ligand framework.

Substitution of the NMe_2 groups on titanium in **105** and **107** was attempted by reaction with excess Me_3SiCl with the aim of preparing the corresponding half-sandwich complexes $[Ti\{(\eta^5\text{-}C_5H_4)B(N\textit{i}Pr_2)N(H)R\}Cl_3]$ (R = *i*Pr, *t*Bu). These compounds appeared to be interesting synthetic targets as they may further react to the corresponding CGCs under elimination of HCl. However, Me_3SiCl, even in large excess, was found to substitute only two of the three NMe_2 groups in the respective starting materials **105** and **107**, affording $[Ti\{(\eta^5\text{-}C_5H_4)B(N\textit{i}Pr_2)N(H)R\}Cl_2(NMe_2)]$ {R = *i*Pr (**110**), *t*Bu (**111**)} (Scheme 25). In the case of the reaction of **105** with excess Me_3SiCl, the almost pure mono-chlorinated intermediate $[Ti\{(\eta^5\text{-}C_5H_4)B(N\textit{i}Pr_2)N(H)\textit{i}Pr\}Cl_2(NMe_2)]$ (**108**) could be isolated and characterised after 16 h, while conversion to the dichlorinated species **110** needed a significantly longer reaction time (64 h). Apparently, the substitution of one NMe_2 group by a chloride significantly reduces the reaction rate of further substitution. Subsequent disubstitution then reduces the reaction rate further, so that the third substitution step is practically not observed.

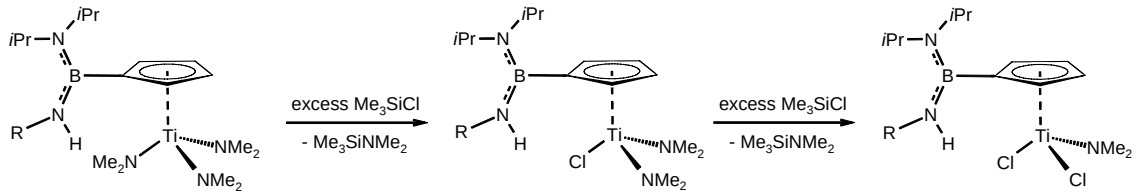

105 R = *i*Pr
107 R = *t*Bu

108 R = *i*Pr
109 R = *t*Bu

110 R = *i*Pr
111 R = *t*Bu

Scheme 25. Stepwise substitution of NMe_2 by Cl in $[Ti\{(\eta^5\text{-}C_5H_4)B(N\textit{i}Pr_2)N(H)R\}(NMe_2)_3]$ {R = *i*Pr (**110**), *t*Bu (**111**)}.

Compounds **108**, **110** and **111** were analysed by multinuclear 1D and 2D NMR spectroscopy and the latter two additionally by IR spectroscopy. Furthermore, an *X*-ray structure determination of **111** was obtained confirming the assumed constitution (*vide infra*). ^1H, ^{11}B, ^{13}C NMR and IR spectra were unremarkable and closely resembled the

spectra of the respective starting materials **105** and **107**. The NMe_2 groups in **108**, **110** and **111** give rise to only one signal in the respective ^{1}H and ^{13}C NMR spectra at ambient temperature.

2.2.1.2. *X*-ray crystallographic analysis of [Ti{(η^5-C_5H_4)B(N*i*Pr$_2$)N(H)*t*Bu}Cl$_2$(NMe$_2$)] (111)

Compound **111** crystallises in the monoclinic space group *C*2/c and adopts C_1 symmetry in the crystal (Figure 33).

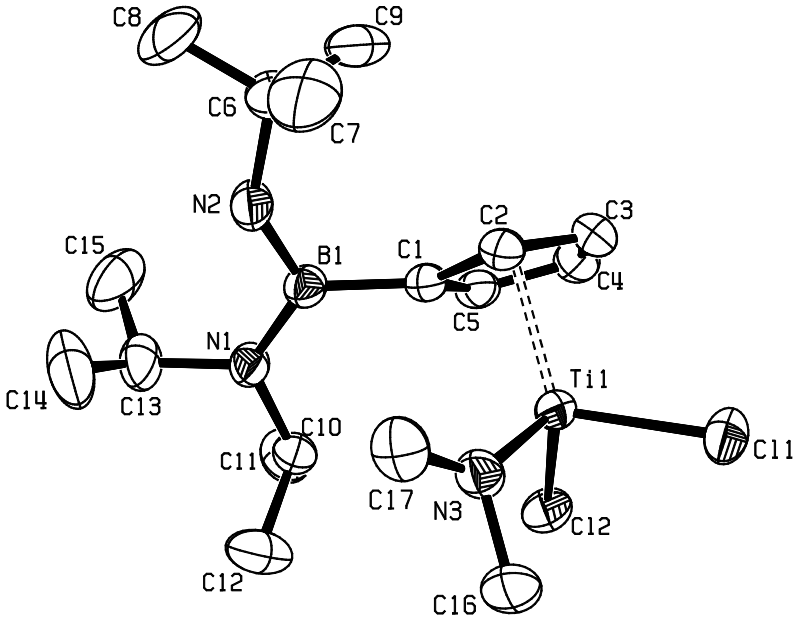

Figure 33. ORTEP representation of [Ti{(η^5-C_5H_4)B(N*i*Pr$_2$)N(H)*t*Bu}Cl$_2$(NMe$_2$)] (**111**) in the solid state; thermal ellipsoids are drawn at the 50% probability level; hydrogen atoms are omitted for clarity.

As expected for a compound of the general formula [(η^5-C_5H_4R)TiCl$_2$X], the titanium centre is placed in a pseudo-tetrahedral environment that is defined by the $Cp_{centroid}$, two chloride ions and the N-donor of the dimethylamido ligand. Overall, the structure very much resembles those of previously reported related compounds [(η^5-C_5R_4R')TiCl$_2$(NH*t*Bu)] (R, R' = H, Me),[339, 340] [(η^5-C_5R_5)TiCl$_2$(N*i*Pr$_2$)] (R = H, Me),[341] and [(η^5-C_5H_5)TiCl$_2${N(SiMe$_3$)$_2$}].[342]

The refinement was complicated by the presence of positional disorder in the N(2)-bound *tert*-butyl group. The boryl substituent is bent out of the C_5 ring plane away from the titanium centre as indicated by a dip angle α^* ($\alpha^* = 180° - \alpha$, with α being the angle $Cp_{centroid}$–C_{ipso}–B) of 10.5°. Both the B and N(1) atoms adopt trigonal planar geometries and the B–N(1) and B–N(2) bond lengths of 1.432(3) and 1.427(3) Å,

respectively, indicate some degree of π-delocalisation along these linkages. The C–C bond lengths in the C_5 ring range from 1.395 to 1.433 Å. This asymmetry is as well reflected in the disposition of the titanium centre such that the distance to the boryl substituted carbon atom C(1) of 2.400(2) Å is distinctly longer than the distances to C(2) – C(5) which range from 2.339 – 2.362 Å. The Ti–$Cp_{centroid}$ distance of 2.033 Å is comparable to the corresponding distances in boron-bridged constrained geometry titanium dichloride complexes **70** (1.989 and 1.995 Å, respectively, for two crystallographically independent molecules) and **116** (1.992 Å) (*vide infra*) and in the half-sandwich complexes [(η^5-C_5H_5)$TiCl_2$(NH*t*Bu)] (2.032 Å) and [(η^5-C_5H_5)$TiCl_2$(N*i*Pr_2)] (2.035 Å). The relative disposition of the bulky boryl substituent on the C_5 ring to the NMe_2 group, the sterically most demanding η^1-substituent on titanium, can be described by the N(3)–Ti–$Cp_{centroid}$–B torsion angle of 38.0°. This most likely results from crystal packing forces. The trigonal planar geometry of the N(3) atom on titanium (sum of angles = 359.9°) and the short N(3)–Ti distance of 1.867(2) Å indicate a significant π-interaction despite the observation of only one resonance in the ^{1}H NMR spectrum at ambient temperature for the NMe_2 group (*vide supra*). However, variable temperature NMR investigations on the related complexes [(η^5-C_5H_5)$TiCl_2$(NMe_2)] and [(η^5-C_5H_5)$TiCl_2$(NH*t*Bu)] indicated virtually free rotation about the Ti–N vector that is facilitated by two orthogonal sets of π-acceptor orbitals on titanium. The NMe_2 moiety adopts a virtually orthogonal position with respect to the C_5 ring plane (torsion angle between respective planes: 86.8°) and is bent away from the C_5 ring as is illustrated by the angles Ti–N(3)–C(17) and Ti–N(3)–C(16) of 140.64(18)° and 108.66(19)°, respectively. A similar arrangement was observed in [(η^5-C_5H_5)$TiCl_2$(N*i*Pr_2)] where it was accompanied by a β-agostic interaction involving the methine C–H bond of an *iso*propyl group and the metal centre with a Ti···H distance of *ca*. 2.25 Å. However, in the present case, the minimum Ti···H distance is *ca*. 2.55 Å, so that the somewhat peculiar geometry of the NMe_2 substituent appears to be an outcome of steric repulsion rather than of agostic interaction.

2.2.1.3. Hydrolysis of [Ti{(η^5-C_5H_4)B(N*i*Pr$_2$)N(H)R}Cl$_2$(NMe$_2$)] {R = *i*Pr (110), *t*Bu (111)}

Solutions of [Ti{(η^5-C_5H_4)B(N*i*Pr$_2$)N(H)R}Cl$_2$(NMe$_2$)] {R = *i*Pr (**110**), *t*Bu (**111**)} in dichloromethane were left open to the atmosphere. In both cases, small yellow crystals formed within weeks and were subsequently identified by *X*-ray diffraction methods as [{TiCl$_2$(μ-{OB(NHMe$_2$)-η^5-C_5H_4})}$_2$-μ-O] (**112**) (*vide infra*). Presumably, this product is formed by partial hydrolysis of the respective starting materials (Scheme 26).

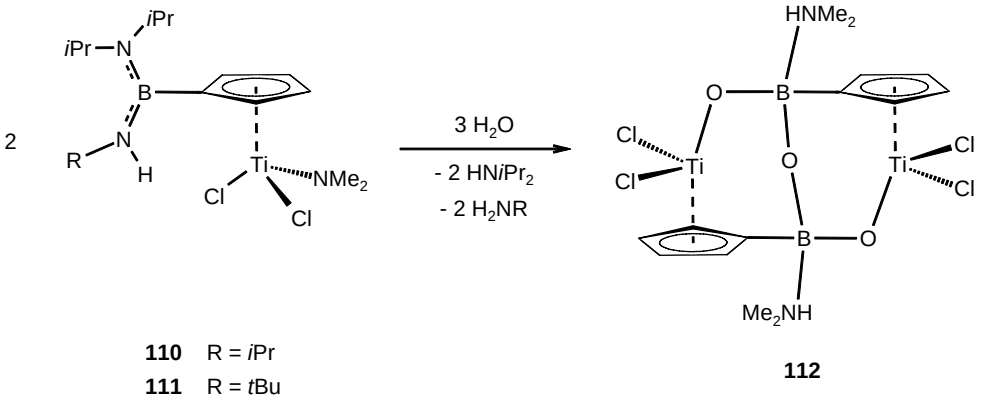

Scheme 26. Formation of [{TiCl$_2$(μ-{OB(NHMe$_2$)-η^5-C_5H_4})}$_2$-μ-O] (**112**).

The course of the hydrolysis reaction, however, remains unclear. Noteworthy are the stability of the Ti–Cl bonds under the applied conditions and the formal migration of the protonated NMe$_2$ fragments from the titanium centres to boron, while two other B–N bonds per boron centre are cleaved in the course of the reaction. Characterisation of **112** by means of solution NMR spectroscopy failed due to its poor solubility in common NMR solvents. This may be ascribed to the zwitterionic nature of the compound (formally, each boron centre carries a negative charge and each nitrogen centres carries a positive charge).

2.2.1.4. *X*-ray crystallographic analysis of [{TiCl$_2$(μ-{OB(NHMe$_2$)-η^5-C_5H_4})}$_2$-μ-O] (112)

Single crystals of **112** were obtained by precipitation from the reaction mixture in dichloromethane at ambient temperature. Compound **112** crystallises in the monoclinic space group *C*2/c and adopts C_2 symmetry in the crystal with the C_2 axis piercing O(1) (Figure 34).

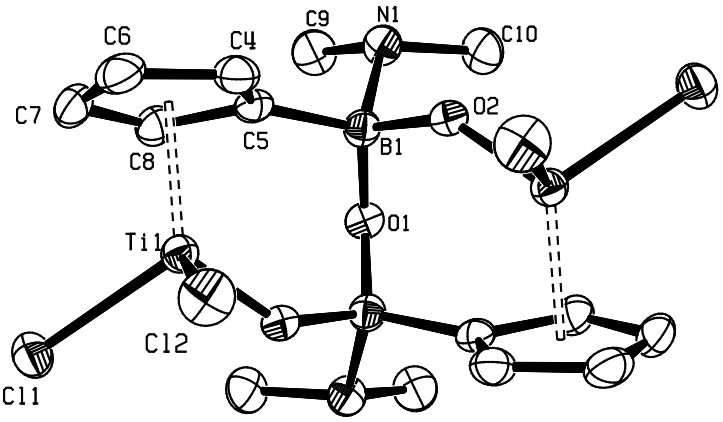

Figure 34. ORTEP representation of [{$TiCl_2$(μ-{OB($NHMe_2$)-η^5-C_5H_4})}$_2$-μ-O] (**112**) in the solid state; thermal ellipsoids are drawn at the 50% probability level; hydrogen atoms are omitted for clarity.

The coordination around each independent titanium centre is that of a pseudo-three-legged piano-stool as is commonly found in titanium half-sandwich complexes of the type [$CpTiCl_2X$]. Two of these half-sandwich titanium fragments are bridged by –B–O– units in such a way that the cyclopentadienyl ring of one fragment is substituted by a boron atom that is connected *via* an oxygen atom to the other titanium centre. The respective boron atoms of the two linkages are in turn connected *via* another oxygen bridge. The boron centres are both tetra-coordinated, carrying NMe_2H groups as the fourth substituent. The molecule is overall neutral, with the boron centres being formally negatively charged, while the nitrogen atoms carry positive charges.

The molecular structure of **112** in some way resembles that of the dimeric silicon-oxo-bridged complex [$TiCl_2$(μ-$OSiMe_2$-η^5-C_5H_4)]$_2$,[343, 344] however, the latter exhibits C_i symmetry due to a different relative disposition of the silyl moieties compared to the borate groups. This difference is the outcome of a higher degree of freedom in the silicon-oxo-bridged compound, resulting from the absence of an *endo*-cyclic bridge, where the silyl groups are positioned to ensures minimum interaction, *i.e.* with the methyl substituents *exo* to the cyclic core (–Cp–Si–O–Ti–Cp'–Si'–O'–Ti'–) of the molecule. To the contrary, in the boron-oxo-bridged complex, one of the substituents on boron, *i.e.* O(2) of the central B(1)–O(2)–B(1') linkage, is positioned *endo* to the cyclic core (–Cp–B–O(1)–Ti–Cp'–B'–O(1')–Ti'–), thus constraining the molecule to the observed conformation.

The Ti–$Cp_{centroid}$ distance of 2.009 Å is comparable to the corresponding distances in boron-bridged titanium dichloride CGCs **70** (1.989 and 1.995 Å for two crystallographically independent molecules, respectively) and **116** (1.992 Å), the

unbridged half-sandwich complex **111** (2.033 Å) and the aforementioned related complex $[TiCl_2(\mu\text{-}OSiMe_2\text{-}\eta^5\text{-}C_5H_4)]_2$ (2.026 Å). The titanium centres are slightly displaced from a position directly beneath the respective C_5 ring centroids such that the Ti–C_5 ring centroid vectors subtend angles of 1.9° to the normals to the ring planes. The boron atoms are at 6.1° slightly bent out of the C_5 ring plane towards the titanium centre. The C_{ipso}-B distance of 1.618(3) Å are longer than those in boron-bridged CGCs **70** (1.602(6) and 1.605(6) Å for two crystallographically independent molecules, respectively) and **116** (1.595(5) Å) and the unbridged boryl substituted half-sandwich complex **111** (1.605(3) Å) and reflect the different degree of hybridisation of the boron centres involved. The B(1)–O(2)–B(1') linkage is at 116.76(19)° substantially more bent than the B(1)–O(1)–Ti(1) moiety {145.22(11)°}, indicating some degree of π-interaction between O(1) and Ti(1) (maximum π-interaction in a Ti–O bond corresponds to angles of 180° with regard to the two substituents on oxygen). This assumption is further supported by the relative short Ti(1)–O(1) distance of 1.7472(12) Å and an elongation of the B–O bond length in the B–O–Ti unit relative to the B–O–B' unit {1.487(2) Å and 1.427(2) Å, respectively}. Both the Ti(1)–O(1) distance and B(1)–O(1)–Ti(1) angle very much resemble the corresponding values found in the C_3-bridged cyclopentadienyl alkoxy complex $[Ti\{\eta^5\text{:}\eta^1\text{-}(C_5Me_4)(CH_2)_3O\}Cl_2]$.[345]

2.2.1.5. Constrained geometry complexes of titanium

The reaction of the ligand precursors $(\eta^1\text{-}C_5H_5)B(N\textit{i}Pr_2)N(H)(\textit{p}\text{-F-Ph})$ (**79**) and $(\eta^1\text{-}C_5H_5)B\{N(SiMe_3)_2\}N(H)Ph$ (**80**) with $[Ti(NMe_2)_4]$ in refluxing toluene resulted in the formation of the corresponding CGCs $[Ti\{\eta^5\text{:}\eta^1\text{-}(C_5H_4)B(N\textit{i}Pr_2)N(\textit{p}\text{-F-Ph})\}(NMe_2)_2]$ (**113**) and $[Ti\{\eta^5\text{:}\eta^1\text{-}(C_5H_4)B(N\{SiMe_3\}_2)NPh\}(NMe_2)_2]$ (**114**). Subsequent reaction with excess Me_3SiCl gave the corresponding dichloro-complexes $[Ti\{\eta^5\text{:}\eta^1\text{-}(C_5H_4)B(N\textit{i}Pr_2)N(\textit{p}\text{-F-Ph})\}Cl_2]$ (**115**) and $[Ti\{\eta^5\text{:}\eta^1\text{-}(C_5H_4)B(N\{SiMe_3\}_2)NPh\}Cl_2]$ (**116**) in virtually quantitative yields (Scheme 27). Compounds **113**, **115** and **116** were obtained as orange or red crystals, whereas **114** was obtained in the form of a red oil. The compounds proved to be air- and moisture-sensitive, very soluble in dichloromethane and moderately soluble in toluene and hexane.

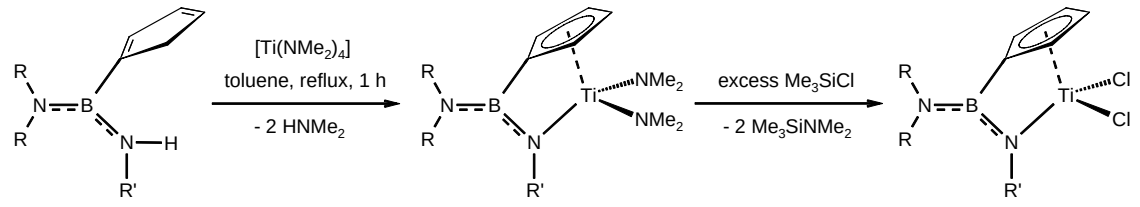

79 R = *i*Pr, R' = *p*-F-Ph
80 R = $SiMe_3$, R' = Ph

113 R = *i*Pr, R' = *p*-F-Ph
114 R = $SiMe_3$, R' = Ph

115 R = *i*Pr, R' = *p*-F-Ph
116 R = $SiMe_3$, R' = Ph

Scheme 27. Synthesis of $[Ti\{\eta^5:\eta^1\text{-}(C_5H_4)B(NR_2)NR'\}R''_2]$ (R = *i*Pr, $SiMe_3$; R' = *p*-F-Ph, Ph; R'' = NMe_2, Cl) (**113** – **116**).

Cyclopentadienyl complexes **113** – **116** were characterised by multinuclear 1D and 2D NMR spectroscopy. In the case of compound **116**, the solid-state structure was determined by *X*-ray diffraction. ^{1}H and ^{13}C NMR spectra of **113** – **116** exhibit all of the signals expected for the proposed constitutions apart from the BC resonances in the latter. ^{1}H and ^{13}C NMR spectra of **113** – **115** each display two signals corresponding to the methine groups of the cyclopentadienyl moiety, indicating approximate C_s symmetry in solution. In contrast, the ^{1}H and ^{13}C NMR spectra of **116** show four sets of signals corresponding to the cyclopentadienyl methine groups and the ^{29}Si NMR spectrum displays two resonances indicating C_1 symmetry. Such a structure would appear to arise from a torsion of the $(Me_3Si)_2N$ fragment and hindered rotation about the $(Me_3Si)_2N$–B bond, as observed in the solid state (*vide infra*). Also noteworthy are the line shapes of the ^{1}H NMR resonances corresponding to the *i*Pr moieties in **113** and **115**. The ^{1}H NMR spectrum of **113** displays two broad resonances at δ = 0.91 and 1.56 corresponding to the Me_{iPr} groups and two equally broad signals at δ = 3.20 and 3.54 corresponding to the CH_{iPr} groups, indicating a rate of rotation about the iPr_2N–B linkage that is approaching the NMR time scale. The ^{1}H NMR spectrum of **115**, however, exhibits two well resolved doublets at δ = 0.91 and 1.54 and two well resolved septets at δ = 3.14 and 3.42 corresponding to the *i*Pr groups, consistent with a rigid conformation of the iPr_2N–B fragment on the NMR time scale. Similar NMR characteristics were observed for the Ph substituted analogues **37** and **70**. Apparently, the substituents on the titanium centre significantly alter the electron density in the N–B–N–Ti linkages and consequently the barrier for rotation about the iPr_2N–B bond. Thus, the relatively poor π-donor substituent Cl in **115** and **70** (compared to the good π-donor substituent NMe_2 in **113** and **37**) may result in increased π-character in the Ti–N bond, weaker π-donation from the titanium bonded nitrogen atom towards the boron

centre and consequently a stronger π-interaction across the iPr$_2$N–B bond. The latter would explain the higher rotational barrier observed for the dichloro derivatives. Further evidence for such an electron density distribution can be obtained by comparison of bond lengths in **37** and **70** as determined by *X*-ray diffraction experiments (*vide infra*).

The ^{11}B NMR chemical shifts of δ = 28.0 and 28.1 for the iPr$_2$N substituted complexes **113** and **115**, and δ = 33.0 and 33.1 for the (Me$_3$Si)$_2$N substituted complexes **114** and **116**, closely resemble those of the respective ligand precursors. As in the ligand precursors, the relative down field shift of the ^{11}B NMR resonances of the (Me$_3$Si)$_2$N substituted compounds **114** and **116**, with respect to their iPr$_2$N substituted analogues **37** and **70** (δ = 27.8 and 28.4), can be attributed to the comparatively poor π-donor characteristics of the (Me$_3$Si)$_2$N substituent[346, 347] resulting in a deshielding effect.

The same synthetic route as outlined above was extended to the preparation of the indenyl substituted CGCs [Ti{η^5:η^1-(C$_9$H$_6$)B(NiPr$_2$)NPh}R$_2$] {R = NMe$_2$ (**117**), Cl (**118**)} (Scheme 28). In the first reaction step, extended reaction times had to be applied to obtain full conversion. After two subsequent recrystallisation steps, the analytically pure target compound **117** could be obtained in the form of orange crystals. Deamination-chlorination of **117** with Me$_3$SiCl gave the corresponding dichloro-complex **118** in high yield as a red microcrystalline material.

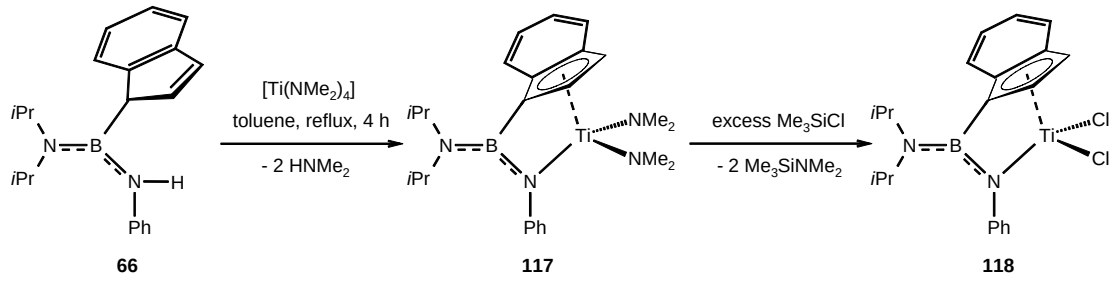

Scheme 28. Synthesis of [Ti{η^5:η^1-(C$_9$H$_6$)B(NiPr$_2$)NPh}R$_2$] {R = NMe$_2$ (**117**), Cl (**118**)}

Compounds **117** and **118** were characterised by multinuclear 1D and 2D NMR spectroscopy, the former was structurally characterised by *X*-ray diffraction methods (*vide infra*). The ^{1}H and ^{13}C NMR spectra of **117** and **118** are unremarkable and show all of the expected signals except for the BC resonance in the latter. As observed for the corresponding cyclopentadienyl derivatives **37** and **70**, the ^{1}H NMR resonances

corresponding to the *i*Pr moieties in the NMe_2 derivative **117** were significantly broadened, suggesting a lower barrier to rotation about the iPr_2N–B bond as compared to the dichloro derivative **118**. The ^{11}B NMR chemical shifts of **117** and **118** at $\delta = 27.7$ and 28.0, again, resemble the value observed for the ligand precursor.

Starting from the open half-sandwich complex **105**, the corresponding CGC [Ti{η^5:η^1-(C_5H_4)B(N*i*Pr_2)N*i*Pr)}(NMe_2)$_2$] (**119**) could be prepared after prolonged heating (68 h reflux in toluene) (Scheme 29). Exposing the analogous *t*Bu substituted non-chelating complex **107** to the same conditions did not result in the formation of the corresponding CGC, but in uncontrolled decomposition of the starting material. Compound **119** is the first boron-bridged CGC incorporating an alkylamido moiety in the chelating ligand. Such substitution is of particular interest since for the analogous silicon-bridged systems better catalytic performance in olefin polymerisation was reported for alkylamido derivatives when compared to their arylamido congeners.

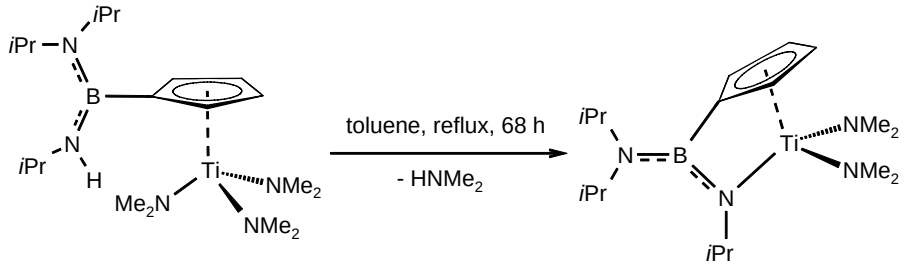

105 **119**

Scheme 29. Synthesis of [Ti{η^5:η^1-(C_5H_4)B(N*i*Pr_2)N*i*Pr)}(NMe_2)$_2$] (**119**).

Compound **119** was characterised by multinuclear 1D and 2D NMR spectroscopy. The ^1H and ^{13}C NMR spectra display all of the expected signals with the exception of the BC resonance in the latter. The proposed formulation of **119** is supported by the integral ratio of the NMe_2 resonance to the other signals in the ^1H NMR spectrum that indicates the presence of two NMe_2 groups per boron-bridged CGC type ligand in the molecule. The ^{11}B NMR chemical shift of $\delta = 29.1$, again, resembles the values observed for the corresponding ligand precursor **77**, as well as for the starting material **105**.

2.2.1.6. *X*-ray crystallographic analysis of amino monoborane based titanium CGCs

As part of this study, previously reported **70** as well as the new boron-bridged titanium CGCs **116** and **117** have been structurally characterised. The molecular structures of **70**, **116** and **117** as determined by single crystal *X*-ray analysis are depicted in Figures 35 – 37, respectively. Complex **70** crystallised with two independent molecules (**A** and **B**) per asymmetric unit, each having essentially identical geometries — the r.m.s. deviation of the best fit between the two molecules being only 0.058 Å. The gross structures of complexes **70**, **116** and **117** are very similar to that of the previously structurally characterised species **37**, each exhibiting a characteristic angling of the B–C(1) bond to the [C_5] ring plane (Table 1). There are, however, a few notable differences between the four structures.

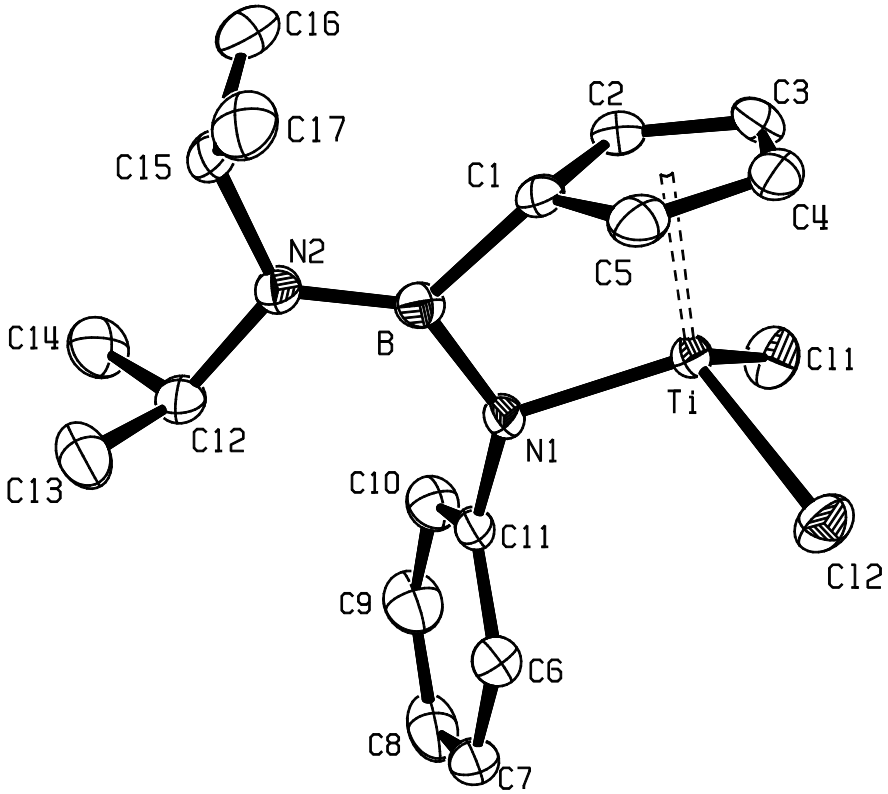

Figure 35. ORTEP representation of [Ti{η^5:η^1-(C_5H_4)B(N*i*Pr$_2$)NPh}Cl_2] (**70**) in the solid state; thermal ellipsoids are drawn at the 50% probability level; hydrogen atoms are omitted for clarity.

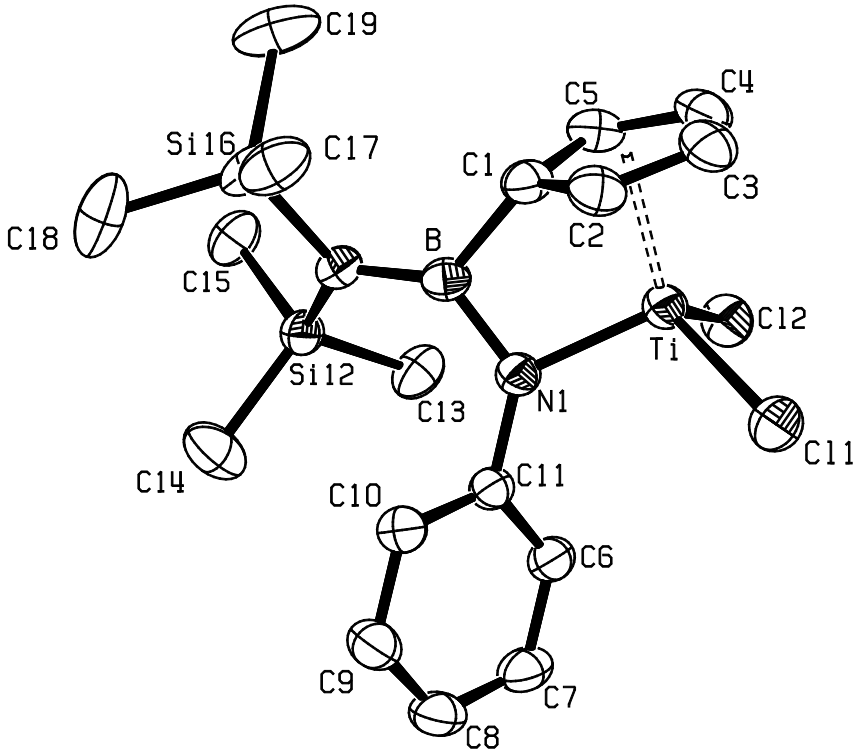

Figure 36. ORTEP representation of [Ti{η^5:η^1-(C_5H_4)B(N{$SiMe_3$}$_2$)NPh}Cl_2] (**116**) in the solid state; thermal ellipsoids are drawn at the 30% probability level; hydrogen atoms are omitted for clarity.

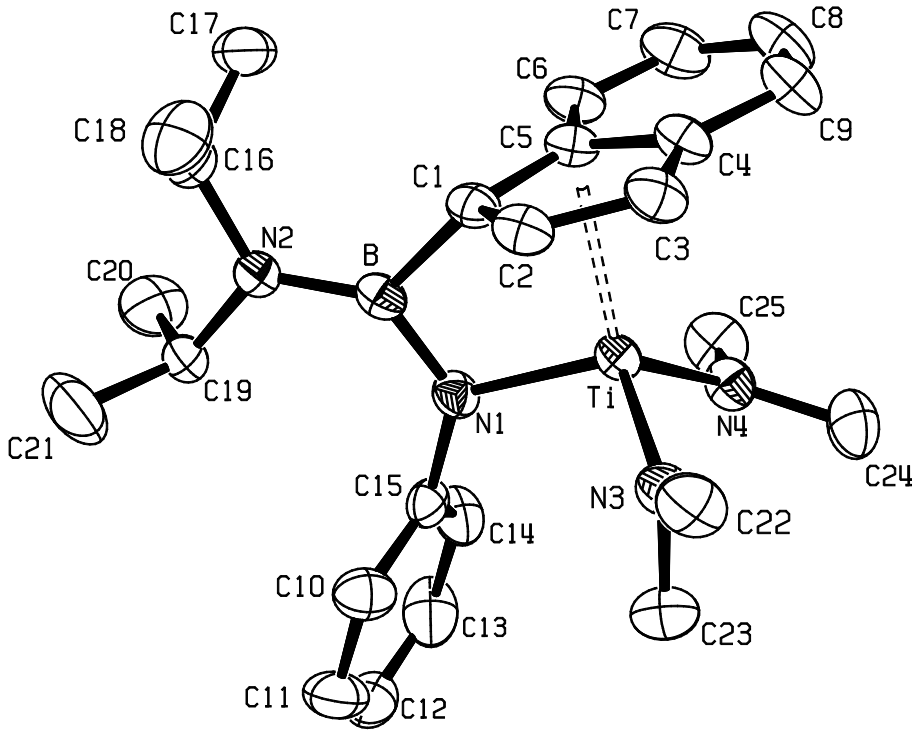

Figure 37. ORTEP representation of [Ti{η^5:η^1-(C_9H_6)B(N*i*Pr_2)NPh}(NMe_2)$_2$] (**117**) in the solid state; thermal ellipsoids are drawn at the 50% probability level; hydrogen atoms are omitted for clarity.

Table 1. Comparative selected geometric parameters for complexes **37**, **70**, **116** and **117**.

	37 [R1 = C(12), R2 = C(15)]	**70 (mol A)** [R1 = C(12), R2 = C(15)]	**70 (mol B)** [R1 = C(12'), R2 = C(15')]	**116** [R1 = Si(12), R2 = Si(16)]	**117** [R1 = C(19), R2 = C(16)]
Ti–C_5 (Å) [a]	2.027	1.989	1.995	1.992	2.054
ϕ (°) [b]	4.4	3.1	3.5	3.5	4.9
δ (Å) [c]	0.16	0.11	0.12	0.12	0.18
Ti–N(1) (Å)	2.020(2)	1.937(3)	1.930(4)	1.941(3)	2.020(2)
B–N(1) (Å)	1.428(3)	1.464(6)	1.448(6)	1.436(5)	1.428(4)
B–N(2) (Å)	1.409(3)	1.382(6)	1.386(6)	1.419(5)	1.414(4)
B–C(1) (Å)	1.603(3)	1.602(6)	1.605(6)	1.595(5)	1.610(4)
N(1)–Ti–C_5 (°) [a]	99.2	99.7	99.7	99.73	99.86
N(1)–B–N(2) (°)	131.0(2)	132.9(4)	131.4(4)	130.0(3)	130.6(3)
N(1)–B–C(1) (°)	103.57(18)	99.4(3)	100.1(3)	101.8(3)	104.0(2)
N(2)–B–C(1) (°)	125.5(2)	127.6(4)	128.5(4)	127.5(3)	125.4(3)
Σ[X–B–Y] (°) [d]	360.0	359.9	360.0	359.3	360.0
ΔB (Å) [e]	0.006	0.016	0.021	0.064	0.004
B–N(2)–R1 (°)	123.2(2)	122.8(4)	123.1(4)	122.7(2)	122.1(2)
B–N(2)–R2 (°)	122.0(2)	121.8(3)	121.6(4)	115.5(2)	123.5(2)
R1–N(2)–R2 (°)	114.8(2)	115.3(3)	115.2(3)	121.6(2)	114.4(2)
Σ[X–N(2)–Y] (°) [d]	360.0	359.9	359.9	359.8	360.0
ΔN(2) (Å) [e]	0.009	0.001	0.020	0.043	0.012
τ[B–N(2)] (°) [f]	2.1	1.7	1.9	38.0	1.3
Ti–N(1)–B (°)	102.4(2)	105.8(3)	105.8(3)	102.5(2)	102.2(2)
Ti–N(1)–Ph (°)	124.2(2)	119.5(2)	119.3(2)	127.7(2)	124.7(2)
B–N(1)–Ph (°)	131.7(2)	133.4(3)	133.6(3)	129.8(3)	131.8(2)
Σ[X–N(1)–Y] (°) [d]	358.3	358.7	358.7	360.0	358.7
ΔN(1) (Å) [e]	0.115	0.102	0.103	0.015	0.103
B–C(1)···[C_5] (°) [g]	31.9	32.2	32.4	35.2	33.0
ΔB[C_5] (Å) [h]	0.848	0.853	0.860	0.919	0.878

[a] "C_5" refers to the centroid of the five-membered aromatic ring. [b] ϕ is the angle between the normal to the [C_5] ring plane and the Ti···C_5 ring centroid vector. [c] δ is the offset of the Ti centre away from a position perpendicularly beneath the C_5 ring centroid. [d] Sum of the angles around the central atom. [e] ΔX is the deviation of atom X from the plane of its substituents. [f] Torsion angle about linkage. [g] Angle of B–C(1) bond to [C_5] ring plane. [h] Deviation of B from [C_5] plane.

In all four complexes, the geometry at titanium centre is pseudo-tetrahedral, with angles in the range 99.2(1) to 123.82(11)°, the most acute angle in each case being associated with the bite of the chelating ligand. In each structure the metal centre is slightly displaced (δ) from a position directly beneath the C_5 ring centroid such that the Ti–C_5 ring centroid vector subtends an angle (ϕ) of *ca*. 3 – 5° to the normal to the ring plane. The Ti–C_5 ring centroid and Ti–N(1) bond lengths in **37** and **117** are significantly longer than those observed in **70** and **116**, reflecting the change in

electronic environment upon formal replacement of NMe_2 for Cl. In all four structures both the B and N(2) centres have trigonal planar geometries, but whereas in **37**, **70** and **117** these two trigonal planes are nearly coplanar, in **116** the steric bulk of the $SiMe_3$ substituents forces a configuration in which the planes are mutually twisted by *ca*. 38°. This twist, however, is not accompanied by any significant lengthening of the B–N(2) bond, although there is a relatively large bend of the B–C(1) vector out of the [C_5] ring plane and a noticeably flatter geometry around N(1).

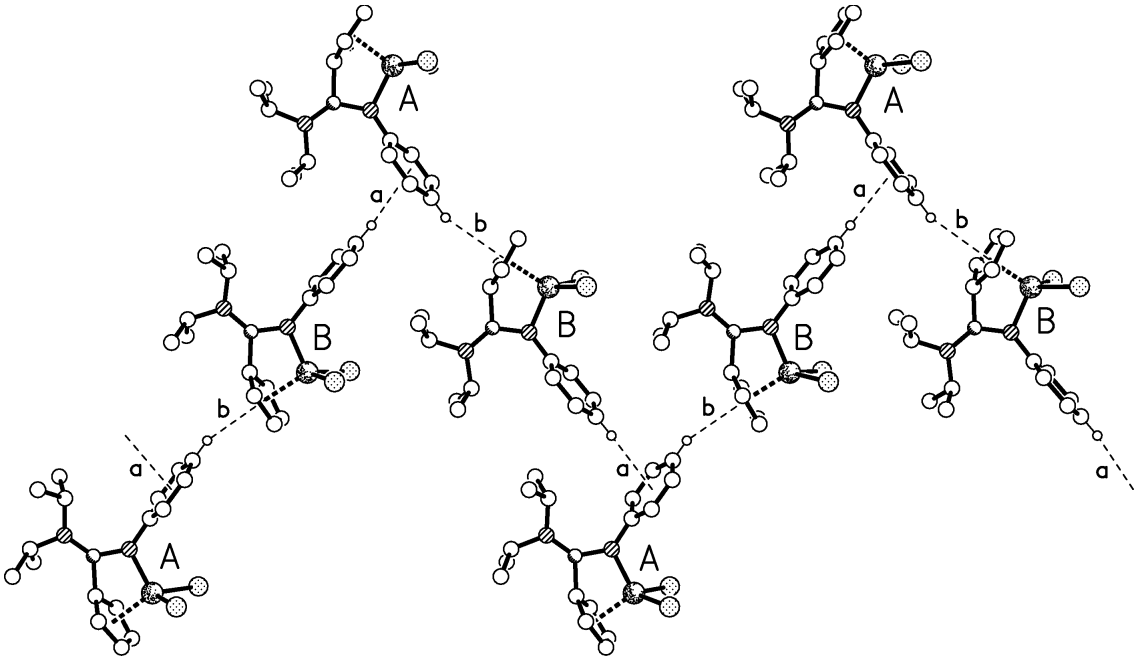

Figure 38. Part of one of the extended C–H···π linked chains of alternating **A** and **B** type molecules present in the crystals of **70**.

In the structure of **70** adjacent independent molecules are linked by C–H···π interactions to form an extended chain that propagates along the crystallographic *b* axis; the hydrogen bonding geometries [H···π] (Å) and [C–H···π] (°) are (a) 2.81, 155 and (b) 2.84, 158 (Figure 38). No significant packing interactions are observed between adjacent molecules in the crystals of **116**, the closest intermolecular contact being the approach of the C(4)–H proton in one molecule to the Cl(1) centre in another [C···Cl 3.74 Å, H···Cl 2.84 Å, C–H···Cl 158°]. There are no noteworthy intermolecular interactions in the crystals of **117**.

2.2.1.7. Reaction of [Ti{η^5:η^1-(C_5H_4)B(N*i*Pr_2)NPh}Cl_2] (70) with methylating agents

Dialkylated CGCs are the genuine pre-catalysts in the CGC catalysed polymerisation of olefins (see section 1.5.2). Potentially, these may be prepared from the dichloro substituted CGCs in a controlled reaction using various alkylating agents, *e.g.* MeLi or $AlMe_3$, and isolated prior to activation. Activation can then be achieved using a number of reagents that facilitate hydrocarbyl abstraction such as MAO, $B(C_6F_5)_3$ or $[Ph_3C^+][B(C_6F_5)_4^-]$. Commercial MAO contains substantial amounts of residual $AlMe_3$[348] and thus combines the methylating and methide abstraction agents in one mixture.

[Ti{η^5:η^1-(C_5H_4)B(N*i*Pr_2)NPh}Cl_2] (**70**) was chosen as an example to study the conversion of boron-bridged dichloro CGCs to their dimethylated derivatives and the stability of the boron bridge in the presence of methylating agents. The synthesis and isolation of the dimethyl derivatives of boron-bridged CGCs would permit the use of boranes and borates as activators in subsequent polymerisation reactions. The findings of this investigation were also expected to provide a better understanding of the catalytic performance of MAO activated boron-bridged CGCs olefin polymerisation experiments (*vide infra*).

2.2.1.7.1. Reaction of [Ti{η^5:η^1-(C_5H_4)B(N*i*Pr_2)NPh}Cl_2] (70) with MeLi

Reaction of **70** with MeLi in a toluene/Et_2O 4:1 v/v mixture at 0 °C resulted in the formation of a complicated product mixture as evidenced by ^{1}H and ^{11}B NMR spectroscopy. The components of the mixture could not be separated or unambiguously characterised. The resonances observed in the ^{11}B NMR spectrum at δ = 39.5, 28.0 and –20.5, however, indicate that the boron bridge in **70** is susceptible to reaction with MeLi under the applied conditions. Presumably, the signal at δ = 28.0, that displays a similar chemical shift as the boron atom in the starting material **70**, corresponds to a species incorporating the original chelating ligand [η^5:η^1-(C_5H_4)B(N*i*Pr_2)NPh]$^{2-}$. The signal at δ = 39.5 is characteristic of a C_2BN fragment. Such a species may arise from substitution of the amino or amido group by a methyl group. The signal at δ = –20.5 is indicative of a fourfold substituted boron centre that could be formed by nucleophilic attack at a threefold coordinated boron atom.

The reaction was repeated at –80 °C to enhance selectivity of the methylating agent. ^{1}H NMR spectroscopy again indicated formation of a complicated mixture, but the ^{11}B NMR spectrum displayed only a single new signal at δ = 28.5 that was indicative of an intact boron bridge. The dimethylated target compound could not be isolated from the mixture.

2.2.1.7.2. Reaction of [Ti{η^5:η^1-(C_5H_4)B(N*i*Pr_2)NPh}Cl_2] (70) with $AlMe_3$

Complex **70** was reacted with $AlMe_3$ under various conditions and the reaction progress monitored by means of ^{11}B NMR spectroscopy. When equimolar amounts of **70** and $AlMe_3$ (note that $AlMe_3$ may provide up to three methyl equivalents) were combined at ambient temperature, an immediately recorded ^{11}B NMR spectrum displayed a single signal at δ = 28.2 that resembles the chemical shift of the starting material {δ(^{11}B) = 28.8}. The analysis was repeated after 1 h and again the signal at δ = 28.2 was the only resonance observed. The resemblance of the signals in the starting material and the product mixture indicate comparable substitution patterns at the boron atoms, *i.e.* CBN_2, and thus reveal stability of the boron bridge under the applied conditions.

To assess the stability of the boron bridge at higher temperatures that more closely resemble the conditions applied in the polymerisation experiments, half of the reaction mixture was heated to 60 °C for 30 min and the analysis subsequently repeated. In the ^{11}B NMR spectrum, a predominant signal at δ = 86.1 was observed besides minor signals at δ = 39.9 and 28.0. The chemical shift of δ = 86.1 is consistent with the formulation of a trialkylborane, *i.e.* BMe_3,[320] that may be formed by substitution of all substituents at boron in the chelating ligand [η^5:η^1-(C_5H_4)B(N*i*Pr_2)NPh]$^{2-}$ by methyl groups, *i.e.* full degradation of the boron bridge. The resonance at δ = 39.9 may likewise arise from the substitution of either the amino or amido group in the ligand by methyl, while the signal at δ = 28.0 may correspond to residual material with an intact [η^5:η^1-(C_5H_4)B(N*i*Pr_2)NPh]$^{2-}$ ligand.

In MAO activated CGC catalysed olefin polymerisation, the co-catalyst is usually applied in large excess, *i.e.* with aluminium to transition metal ratios of greater than 500:1. Therefore, it is fair to assume that the residual $AlMe_3$ contained in commercially available MAO is present in superstoichiometric amounts relative to the

pre-catalyst. Accordingly, the other half of the initially described reaction mixture was treated with two more equivalents of $AlMe_3$ (overall Al:Ti ratio 3:1) at ambient temperature. An ^{11}B NMR spectrum recorded directly after addition of the aluminium reagent showed a minor signal at $\delta = 86.2$ besides a major signal at $\delta = 28.2$. After 24 h, a repeat of the analysis revealed complete consumption of the material that gave rise to the resonance at $\delta = 28.2$, affording only a single signal at $\delta = 86.2$. As previously stated, a resonance at $\delta = 86.2$ in the ^{11}B NMR spectrum indicates formation of a trialkylborane and hence destruction of the boron bridge in the chelating ligand $[\eta^5:\eta^1\text{-}(C_5H_4)B(N\textit{i}Pr_2)NPh]^{2-}$.

In summary, the boron bridge in **70** is stable in the presence of equimolar amounts of $AlMe_3$ at ambient temperatures. Excess $AlMe_3$ or elevated temperatures result in substitution reactions at the boron centre and in all probability destruction of the *ansa*-bridge in the chelating ligand.

2.2.1.8. Zirconium and hafnium constrained geometry complexes

The only reported zirconium complex incorporating a boron-bridged CGC type ligand is $[Zr\{\eta^5:\eta^1\text{-}(C_9H_6)B(N\textit{i}Pr_2)NPh\}_2]$ (**73**), which was formed by reaction of the dilithiated ligand precursor with $ZrCl_4$. Formation of such metallocenes by salt elimination reactions between dilithiated CGC ligand precursors and metal halides is well documented.[40, 44, 45, 46, 47] Now, for the first time, extension of the amine elimination route developed for boron-bridged titanium CGCs has afforded analogous complexes of zirconium and hafnium.

Reaction of $(\eta^1\text{-}C_5H_5)B(N\textit{i}Pr_2)N(H)Ph$ (**65**) with $[M(NMe_2)_4]$ (M = Zr, Hf) in refluxing toluene and subsequent recrystallisation yielded the corresponding CGCs $[M\{\eta^5:\eta^1\text{-}(C_5H_4)B(N\textit{i}Pr_2)NPh\}(NMe_2)_2]$ {M = Zr (**120**), Hf (**121**)} as crystalline materials (Scheme 30).

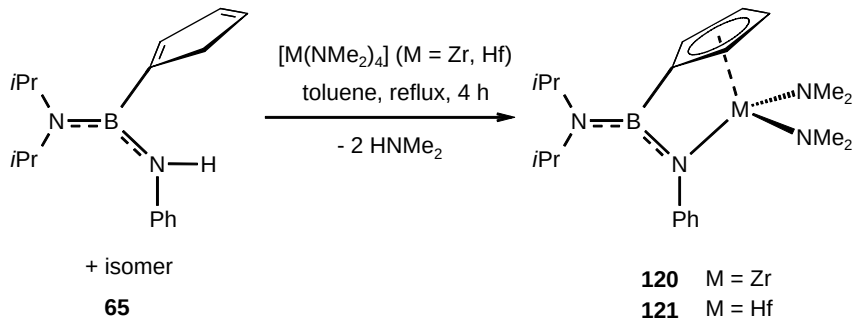

Scheme 30. Synthesis of $[M\{\eta^5:\eta^1\text{-}(C_5H_4)B(N\textit{i}Pr_2)NPh\}(NMe_2)_2]$ {M = Zr (**120**), Hf (**121**)}.

The indenyl derivative $[Zr\{\eta^5:\eta^1\text{-}(C_9H_6)B(N\textit{i}Pr_2)NPh\}(NMe_2)_2]$ (**122**) was obtained in the form of colourless crystals, after work-up, by reaction of (1-C_9H_7)B(N*i*Pr$_2$)N(H)Ph (**66**) with $[Zr(NMe_2)_4]$ in refluxing toluene (Scheme 31). Interestingly, the new indenyl complex **122** contains the same boron-bridged ligand as the previously described metallocene **73**.

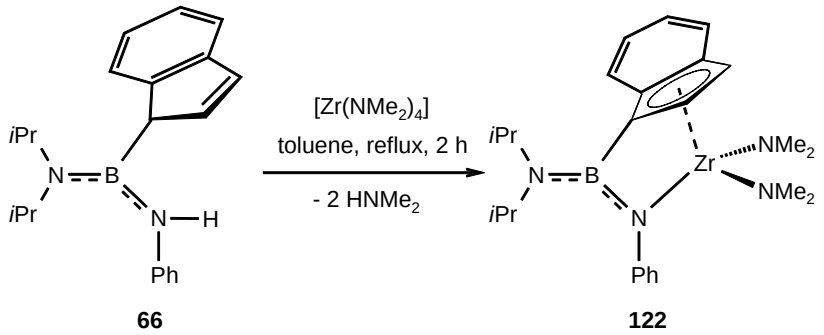

Scheme 31. Synthesis of $[Zr\{\eta^5:\eta^1\text{-}(C_9H_6)B(N\textit{i}Pr_2)NPh\}(NMe_2)_2]$ (**122**).

Complexes **120** – **122** were characterised by multinuclear 1D and 2D NMR spectroscopy and *X*-ray diffraction methods. The ^{11}B NMR chemical shifts for **120** – **122** very much resemble those of the respective ligand precursors. The ^{1}H and ^{13}C NMR spectra of **120** – **122** are unremarkable and closely resemble the spectra of the respective titanium congeners **37** and **117**. As observed for the related diamino titanium complexes **37**, **113** and **117**, the resonances corresponding to the *i*Pr$_2$N moieties of **120** – **122** in the ambient temperature ^{1}H and ^{13}C NMR spectra are significantly broadened. Such line broadening may be ascribed to a rate of rotation about the *i*Pr$_2$N–B linkage that is comparable to the NMR time scale (*vide supra*). However, in the ^{1}H and ^{13}C NMR spectra of **120** – **122** recorded at –20 °C the signals corresponding to the *i*Pr$_2$N groups are sharp and the multiplicity of the signals in the ^{1}H NMR spectra are clearly resolved. These observations are consistent with inhibition of the rotation about the *i*Pr$_2$N–B bonds in **120** – **122** on the NMR time scale at low temperatures.

Transformation of **120** – **122** into their respective dichloro derivatives was attempted by reaction with excess Me_3SiCl. In all instances, the reactions yielded colourless solids that were very poorly soluble in hexane, toluene and even dichloromethane. Consequently, samples in dichloromethane-D_2 that were sufficiently concentrated for NMR experiments could only be prepared after prolonged treatment in an ultrasonic bath. The ^1H NMR spectra displayed resonances at the chemical shifts and in roughly the integral ratios expected for the desired dichloro complexes (as judged by comparison with the ^1H NMR spectra of the titanium analogues **70** and **118**), but signals were unusually broad. The ^{11}B NMR resonances were weak due to the low concentration of the samples, but the chemical shifts {$\delta(^{11}B)$ = 28, 30.3 and 28.1, respectively} resembled those observed for the respective starting materials. The poor solubility of the products in dichloromethane stands in contrast to the good solubility of the related dichloro titanium complexes **70**, **115**, **116** and **118** in the same solvent. This in combination with the broad signals in the ^1H NMR spectrum may suggest formation of oligomeric or polymeric structures in the products.

2.2.1.9. *X*-ray crystallographic analysis of amino monoborane based zirconium and hafnium CGCs (120 – 122)

The solid-state structures of boron-bridged CGCs **120** – **122** (Figures 39 – 41) were determined by *X*-ray diffraction experiments. All three compounds crystallised in the triclinic space group $P\bar{1}$. Table 2 compares selected structural parameters of **120** – **122** with those of their respective titanium congeners **37** and **117** and the related complex [Zr{η^5:η^1-(C_9H_6)B(N*i*Pr_2)NPh}$_2$] (**73**).

The gross structures of the new complexes **120** – **122** are very similar to the structures of their respective titanium analogues **37** and **117**. All these complexes display a distorted pseudo-tetrahedral geometry at the transition metal centre. The main differences between the structures arise from the different radii of the coordinated transition metals. The larger zirconium and hafnium centres (when compared to the titanium centres) result in a lengthening of all bonds involving the metal centre. Concurrently, the N(1)–M–$Cp_{centroid}$ angles become more acute by *ca.* 5°, while the N(1)–B–C(1) angles become more obtuse by *ca.* 1.5°. In all these structures, both the B and N(2) centres have trigonal planar geometries and these trigonal planes are almost

coplanar. There are no noteworthy intermolecular interactions in the crystals of **120** – **122**.

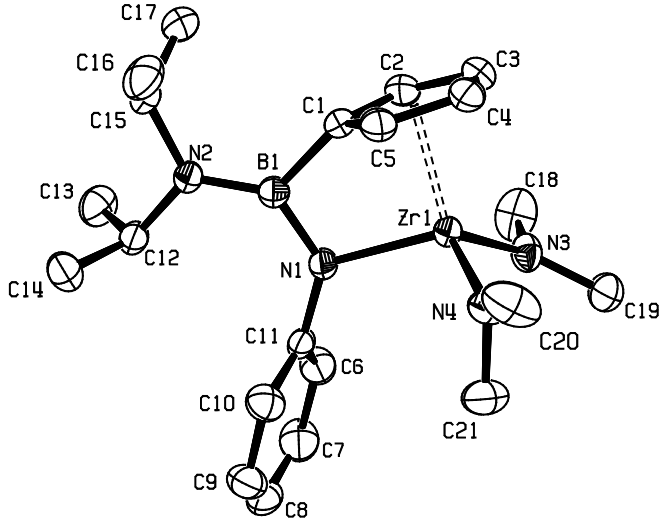

Figure 39. ORTEP representation of [Zr{η^5:η^1-(C_5H_4)B(N*i*Pr_2)NPh}(NMe_2)$_2$] (**120**) in the solid state; thermal ellipsoids are drawn at the 50% probability level; hydrogen atoms are omitted for clarity.

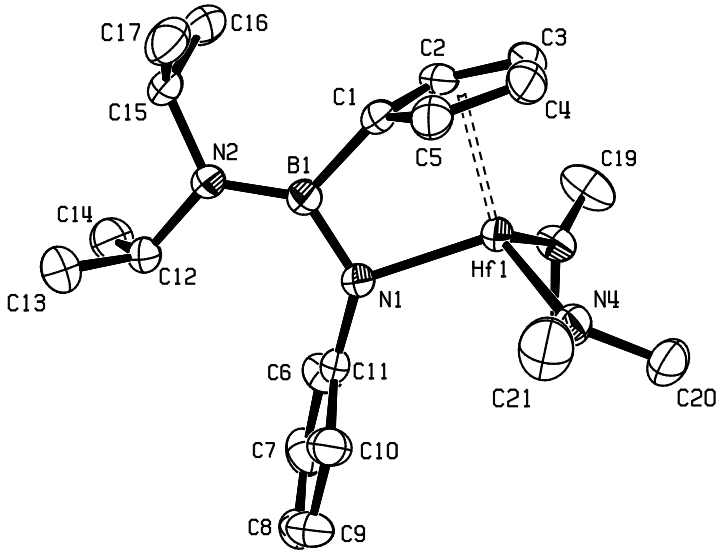

Figure 40. ORTEP representation of [Hf{η^5:η^1-(C_5H_4)B(N*i*Pr_2)NPh}(NMe_2)$_2$] (**121**) in the solid state; thermal ellipsoids are drawn at the 50% probability level; hydrogen atoms are omitted for clarity.

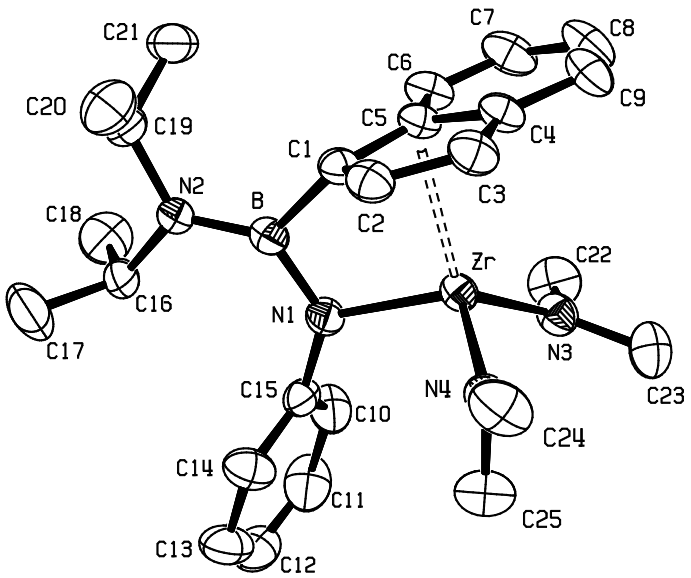

Figure 41. ORTEP representation of [Zr{η^5:η^1-(C_9H_6)B(N*i*Pr_2)NPh}(NMe_2)$_2$] (**122**) in the solid state; thermal ellipsoids are drawn at the 50% probability level; hydrogen atoms are omitted for clarity.

Comparison of the structures of **122** and **73** discloses only minor differences in the coordination of the respective linked indenyl-amido ligands to the zirconium centres. Most prominently, the Zr–$Cp_{centroid}$ distance in **73** is significantly longer and presumably results from higher electron density at the zirconium centre. The slight elongation of the Zr–N(1) distance in **73** may be similarly rationalised. These differences in bond lengths are accompanied by small changes in the other structural parameters relating to the chelating ligand, the most significant being the larger twist of the trigonal planes incorporating B and N(2) in **73** (5.1°) when compared with **122** (1.1°).

Table 2. Comparative selected geometric parameters for complexes **37**, **73**, **117**, **120**, **121** and **122**.

	37 [M = Ti, R1 = C(12), R2 = C(15)]	**120** [M = Zr, R1 = C(12), R2 = C(15)]	**121** [M = Hf, R1 = C(12), R2 = C(15)]	**117** [M = Ti, R1 = C(19), R2 = C(16)]	**122** [M = Zr, R1 = C(19), R2 = C(16)]	**73** [M = Zr, R1 = C(16), R2 = C(19)]
M–C_5 (Å) [a]	2.027	2.182	2.162	2.054	2.196	2.228
ϕ (°) [b]	4.4	4.2	3.8	4.9	4.3	5.9
δ (Å) [c]	0.16	0.16	0.14	0.18	0.16	0.23
M–N(1) (Å)	2.020(2)	2.1530(17)	2.1233(18)	2.020(2)	2.1363(14)	2.1570(18)
M–N(3) (Å)	1.9045(19)	2.0570(19)	2.0225(19)	1.915(2)	2.0469(15)	–
M–N(4) (Å)	1.913(2)	2.0314(19)	2.0415(19)	1.918(3)	2.0356(15)	–
B–N(1) (Å)	1.428(3)	1.438(3)	1.444(3)	1.428(4)	1.446(2)	1.4467(30)
B–N(2) (Å)	1.409(3)	1.408(3)	1.414(3)	1.414(4)	1.406(2)	1.4081(31)
B–C(1) (Å)	1.603(3)	1.614(3)	1.608(3)	1.610(4)	1.607(2)	1.6043(32)
N(1)–M–C_5 (°) [a]	99.2	94.1	94.9	99.9	94.9	92.7
N(1)–B–N(2) (°)	131.0(2)	130.8(2)	130.7(2)	130.6(3)	129.50(15)	130.49(21)
N(1)–B–C(1) (°)	103.57(18)	105.08(18)	105.18(18)	104.0(2)	105.45(13)	104.02(18)
N(2)–B–C(1) (°)	125.5(2)	124.14(19)	124.2(2)	125.4(3)	125.04(15)	125.44(20)
Σ[X–B–Y] (°) [d]	360.0	360.0	360.0	360.0	360.0	360.0
ΔB (Å) [e]	0.006	0.007	0.006	0.004	0.006	0.018
B–N(2)–R1 (°)	123.2(2)	122.89(18)	123.14(18)	122.1(2)	122.52(14)	122.38(19)
B–N(2)–R2 (°)	122.0(2)	122.72(18)	122.37(19)	123.5(2)	123.14(14)	123.23(20)
R1–N(2)–R2 (°)	114.8(2)	114.38(17)	114.45(17)	114.4(2)	114.30(13)	114.39(20)
Σ[X–N(2)–Y] (°) [d]	360.0	360.0	360.0	360.0	360.0	360.0
ΔN(2) (Å) [e]	0.009	0.009	0.016	0.012	0.017	0.001
τ[B–N(2)] (°) [f]	2.1	2.2	2.1	1.3	1.1	5.1
M–N(1)–B (°)	102.4(2)	103.37(13)	103.14(14)	102.2(2)	103.06(10)	102.60(14)
M–N(1)–Ph (°)	124.2(2)	123.15(13)	123.88(14)	124.7(2)	124.70(10)	126.55(14)
B–N(1)–Ph (°)	131.7(2)	131.99(18)	131.59(19)	131.8(2)	131.53(13)	130.55(19)
Σ[X–N(1)–Y] (°) [d]	358.3	358.5	358.6	358.7	359.3	359.7
ΔN(1) (Å) [e]	0.115	0.110	0.106	0.103	0.076	0.050
B–C(1)···[C_5] (°) [g]	31.9	29.4	30.4	33.0	30.5	28.4
ΔB[C_5] (Å) [h]	0.848	0.792	0.814	0.878	0.816	0.764

[a] "C_5" refers to the centroid of the five-membered aromatic ring. [b] ϕ is the angle between the normal to the [C_5] ring plane and the M···C_5 ring centroid vector. [c] δ is the offset of the M centre away from a position perpendicularly beneath the C_5 ring centroid. [d] Sum of the angles around the central atom. [e] ΔX is the deviation of atom X from the plane of its substituents. [f] Torsion angle about linkage. [g] Angle of B–C(1) bond to [C_5] ring plane. [h] Deviation of B from [C_5] plane.

2.2.1.10. Attempted syntheses of other amino monoborane-bridged CGCs

Limitations of the previously described amine elimination reaction for the synthesis of amino monoborane-bridged CGCs were not only encountered for the reaction of (η^1-C_5H_5)B(N*i*Pr$_2$)N(H)R (R = alkyl) with [Ti(NMe$_2$)$_4$]. Thus, (1-C_9H_7)B(N*i*Pr$_2$)N(H)*i*Pr (**83**), (9-$C_{13}H_9$)B(N*i*Pr$_2$)N(H)Ph (**88**) and (η^1-

$C_5Me_4H)B(NiPr_2)N(H)Ph$ (**90**) showed no reaction with $[Ti(NMe_2)_4]$ in refluxing toluene. The inertness of **83** under the applied conditions is rather surprising given that the related ligand precursors (η^1-C_5H_5)B(N*i*Pr$_2$)N(H)*i*Pr (**77**) and (1-C_9H_7)B(N*i*Pr$_2$)N(H)Ph (**66**) readily react with $[Ti(NMe_2)_4]$. The lack of reactivity of compounds **88** and **90** may be attributed to the lower acidity of the fluorenyl and tetramethylcyclopentadienyl moieties when compared to similarly substituted cyclopentadienyl or indenyl fragments. These limitations of the synthetic protocol prompted the search for an alternative approach.

(η^1-C_5H_5)B(N*i*Pr$_2$)N(H)*t*Bu (**64**) was chosen as the preferred ligand precursor to probe alternative synthetic methods, because its ^{1}H NMR spectrum is uncomplicated and that of any complexes so formed are likely to be equally simple. Coordination of the cyclopentadienyl moiety to a transition metal is expected to give rise to two characteristic pseudo-triplets corresponding to the CH groups in 2- and 3-positions relative to the boryl substituent. Such CH resonances are known to be sensitive to changes in the electronic environment at the transition metal centre. Therefore, even for closely related complexes, distinct chemical shifts for such pseudo-triplets can be expected. The resonances corresponding to the *i*Pr$_2$N (one or two doublets and one or two heptets depending on the rotational barrier about the *i*Pr$_2$N–B bond) and *t*Bu (one singlet) groups are also easily identified in the ^{1}H NMR spectra, however, their diagnostic value is limited.

Following procedures previously reported in the literature (see section 1.2.1), several synthetic approaches were assessed: (i) dimetalation/salt elimination, (ii) amine elimination using $[TiCl_2(NMe_2)_2]$ as a reagent, (iii) toluene elimination and (iv) amine assisted HCl elimination.

2.2.1.10.1. Attempted syntheses of amino monoborane-bridged CGCs *via* dimetalation/salt elimination

The dimetalation of (η^1-C_5H_5)B(N*i*Pr$_2$)N(H)*t*Bu (**64**) was attempted utilising various lithium alkyls (*n*BuLi, *t*BuLi or MeLi) in various solvents (toluene, Et_2O or mixtures thereof). The obtained product mixtures that presumably contained the dilithiated ligand precursors were then reacted with a suitable titanium source ($TiCl_4$, $[TiCl_2(NMe_2)_2]$ or $[TiCl_3(thf)_3]$ followed by oxidation with 0.5 equivalents $PbCl_2$). The reaction involving MeLi was performed using four equivalents of the base, following a

protocol reported by Resconi *et al.* that claims to suppress undesired reduction of the titanium reagent in the course of the reaction. In all cases, mixtures of two or more products containing (η^5-C_5H_4R)Ti moieties were obtained as indicated by the number of pseudo-triplets observed in the respective ^{1}H NMR spectra. Separation of the complicated mixtures was not feasible, thus preventing full characterisation of their components. However, besides the formation of the respective target compounds [Ti{η^5:η^1-(C_5H_4)B(N*i*Pr$_2$)N*t*Bu}R_2] (R = Cl, NMe_2, Me), various side products resulting from reaction of the mono-deprotonated ligand precursor and/or reactions with stoichiometries other than 1:1 between the deprotonated ligand precursor and titanium reagent are easily conceivable. To identify at least some of the possible side products, *i.e.* those resulting from 2:1 reaction of the mono-deprotonated ligand precursor with the titanium sources, the systematic synthesis of [Ti{(η^5-C_5H_4)B(N*i*Pr$_2$)N(H)*t*Bu}$_2R_2$] (R = NMe_2, Cl) by reaction of two equivalents of (η^1-C_5H_5)B(N*i*Pr$_2$)N(H)*t*Bu (**64**) with [Ti(NMe_2)$_4$] followed by reaction with excess Me_3SiCl was attempted. However, the only product of the first reaction step was the known half-sandwich complex [Ti{(η^5-C_5H_4)B(N*i*Pr$_2$)N(H)*t*Bu}(NMe_2)$_3$] (**107**) despite the excess of ligand precursor available.

The dimetalation/salt elimination route was also examined utilising the ligand precursors (9-$C_{13}H_9$)B(N*i*Pr$_2$)N(H)Ph (**88**) and (η^1-C_5Me_4H)B(N*i*Pr$_2$)N(H)Ph (**90**). Compound **88** was reacted with two equivalents of lithium alkyls in various solvents (*n*BuLi in toluene/Et_2O 1:1 v/v, MeLi in Et_2O, *t*BuLi in toluene) and subsequently with $ZrCl_4$. After work-up, samples of the resulting product mixtures showed, amongst others, resonances corresponding to the unreacted ligand precursor (characteristic NH and BCH resonances) indicating incomplete deprotonation of **88** under the applied conditions. The desired CGC could not be obtained.

The conversion of **90** to corresponding CGCs was attempted using various versions of the dimetalation/salt elimination route (2 equivalents of *t*BuLi in toluene/Et_2O 1:1 v/v, [$TiCl_3$(thf)$_3$], 0.5 equivalents of $PbCl_2$; 2 equivalents of *t*BuLi in toluene/Et_2O 1:1 v/v, [$TiCl_2(NMe_2)_2$]; 4 equivalents of MeLi, Et_2O, $TiCl_4$). The signal patterns observed in the ^{1}H NMR spectra of the crude products obtained from these reactions were promising and vaguely agreed with the signal patterns expected for the respective target products [Ti{η^5:η^1-(C_5Me_4)B(N*i*Pr$_2$)NPh}R_2] (R = Cl, NMe_2, Me).

However, the products could not be unambiguously characterised since sufficient purification by means of recrystallisation could not be achieved.

2.2.1.10.2. Attempted synthesis of an amino monoborane-bridged CGC *via* amine elimination using $[TiCl_2(NMe_2)_2]$

$[ZrCl_2(NMe_2)_2(thf)_2]$ was reportedly used as a transition metal precursor for the synthesis of CGCs *via* amine elimination. Consequently, the reaction of the boron-bridged CGC ligand precursor **64** with the related titanium complex $[TiCl_2(NMe_2)_2]$ was attempted. The assumed higher Lewis acidity of $[TiCl_2(NMe_2)_2]$ when compared to $[Ti(NMe_2)_4]$ was expected to assist complexation of the ligand precursor prior to amine elimination. However, after refluxing the reaction mixture for 3 h in toluene, the ^{1}H NMR spectrum of an aliquot dried *in vacuo* showed only signals corresponding to the unreacted ligand precursor and unidentified decomposition products. No pseudo-triplets characteristic of complexation of the ligand precursor to the titanium centre were observed.

2.2.1.10.3. Attempted synthesis of an amino monoborane-bridged CGC *via* toluene elimination

Synthesis of the corresponding CGC was attempted by reaction of (η^1-C_5H_5)B(N*i*Pr$_2$)N(H)*t*Bu (**64**) with $[TiBz_4]$ in toluene. However, no reaction between the two reactants could be observed after 16 h at ambient temperature. Refluxing the reaction mixture only resulted in decomposition of the titanium reagent while the ligand precursor remained unchanged as evidenced by ^{1}H NMR spectroscopy.

2.2.1.10.4. Attempted syntheses of amino monoborane-bridged CGCs *via* amine assisted HCl elimination

Reaction of certain CGC ligand precursors with $TiCl_4$ in the presence of amines reportedly resulted in the formation of the corresponding CGCs. Similarly, ring closure of half-sandwich complexes such as $[Ti\{(\eta^5\text{-}C_5H_4)B(N\textit{i}Pr_2)N(H)\textit{t}Bu\}(Cl)_{3-x}(NMe_2)_x]$ (x = 0, 1) under elimination of HCl is also conceivable. Consequently, the viability of these routes for the synthesis of amino monoborane-bridged CGCs was investigated.

A solution of (η^1-C_5H_5)B(N*i*Pr$_2$)N(H)*t*Bu (**64**) in toluene was treated with $TiCl_4$ at ambient temperature. After 16 h, an aliquot that was dried *in vacuo* showed only signals correpsonding to the unreacted ligand precursor. Upon addition of 10

equivalents of NEt_3 to the mixture, formation of a small quantity of a black precipitate of unidentified constitution was observed. Subsequent analysis by means of ^1H NMR spectroscopy of another aliquot again showed only signals corresponding to the starting material **64**. The reaction mixture was then heated for several hours and the analysis repeated. This displayed two weak signals at $\delta = 5.84$ and 6.18 corresponding to a (η^5-C_5H_4R)Ti moiety besides predominant signals corresponding to the unreacted ligand precursor. Apparently, reaction of **64** with $TiCl_4$ is very slow under the applied conditions and whether the desired compound is formed appears questionable. Accordingly, the reaction procedure was modified by using 1,8-diazabicyclo[5.4.0]undecene-7 (DBU) instead of NEt_3. DBU is widely applied as a very strong, largely non-nucleophilic base[349, 350, 351, 352] and therefore seemed suitable as a replacement for NEt_3 to accelerate the HCl elimination from **64** and $TiCl_4$. However, addition of DBU to a solution of **64** and $TiCl_4$ resulted in immediate formation of a ruby-red precipitate that was found to be virtually insoluble in aliphatic and aromatic hydrocarbons as well as dichloromethane. The supernatant solution was analysed by ^1H and ^{11}B NMR spectroscopy but the signals were too weak to be assigned to any distinctive species. In a control experiment, DBU was reacted with an equimolar amount of $TiCl_4$, instantly affording a ruby-red precipitate of similar solubility to the aforementioned solid. This apparently fast reaction between DBU and $TiCl_4$, resulting in a practically insoluble material, may dominate even in the presence of the ligand precursor **64** and consequently prevent formation of the corresponding CGC.

Following similar protocols, [Ti{(η^5-C_5H_4)B(N*i*Pr$_2$)N(H)*t*Bu}(Cl)$_2$(NMe$_2$)] (**111**) was treated with NEt_3 and DBU respectively to initiate ring closure under elimination of HCl. Thus, 5 equivalents of NEt_3 were added to a solution of **111** in toluene. After heating the mixture to 90 °C for 16 h, an aliquot was removed, dried *in vacuo* and analysed by ^1H NMR spectroscopy. The ^1H NMR spectrum revealed consumption of *ca.* 50% of the starting material **111** and formation of at least three new compounds incorporating (η^5-C_5H_4R)Ti fragments, as evidenced by the number of pseudo-triplets observed. Obviously, the conversion proceeds rather unselective and is therefore without practical use. The reaction was repeated utilising one equivalent of DBU as a base. After 6 h at ambient temperature, no reaction had occurred as was apparent from the ^1H NMR spectroscopic analysis of an aliquot that displayed only signals corresponding to the starting materials. The mixture was then heated to 80 °C

for 16 h and the analysis was repeated. The ^{1}H NMR spectrum indicated formation of a complicated product mixture. Separation and characterisation of the components of the mixture was not feasible.

[Ti{(η^5-C_5H_4)B(N*i*Pr$_2$)N(H)*t*Bu}Cl$_3$] would also appear as a suitable precursor for the formation of a CGC under HCl elimination. Consequently, synthesis of this compound was attempted *via* mono-deprotonation of the corresponding ligand precursor **64** and subsequent reaction with $TiCl_4$. The difference in acidity of the C_5H_5 and NH*t*Bu moieties in **64** as demonstrated in the reaction of **64** with [Ti(NMe$_2$)$_4$] should permit selective deprotonation of the C_5H_5 group under suitable conditions. When the reaction was conducted with *n*BuLi as a base and hexane as a solvent, beside the presence of significant amounts of the unreacted ligand precursor, one product was observed in the ^{1}H NMR spectrum that incorporates a (η^5-C_5H_4R)Ti fragment. Apparently, these conditions do not facilitate complete deprotonation of **64**. Therefore, the reaction was repeated utilising *n*BuLi as a base and a toluene/Et$_2$O 1:1 v/v mixture as solvent. ^{1}H NMR spectroscopy of the crude product of this reaction indicated formation of a compound bearing a (η^5-C_5H_4R)Ti moiety. However, different chemical shifts corroborate a different constitution to the product obtained from the reaction performed in hexane. Repeating the reaction using *t*BuLi as a base and toluene as a solvent resulted in a mixture of the two previously observed products. Sufficient purification of the obtained products for unambiguous characterisation could not be accomplished. It may be assumed that one of the observed products is indeed the target compound [Ti{(η^5-C_5H_4)B(N*i*Pr$_2$)N(H)*t*Bu}Cl$_3$], while the other may be [Ti{(η^5-C_5H_4)B(N*i*Pr$_2$)N(H)*t*Bu}$_2$Cl$_2$] resulting from a 2:1 reaction of the deprotonated ligand precursor with $TiCl_4$. The reaction was also repeated utilising K[N(SiMe$_3$)$_2$], as this had been reported to mono-deprotonate **64**, however, a complicated product mixture was obtained.

2.2.2. Attempted syntheses of diborane(4)-bridged CGCs

[2]Borametallocenophanes of zirconium and hafnium were recently reported to produce high molecular weight polyethylene with high activity. Thus, the synthesis of related CGCs incorporating a [2]bora *ansa*-bridge appeared to be a promising target. To this aim, the complexation of the diborane(4) based ligand precursor (η^1-

$C_5H_5)(BNMe_2)_2\{N(H)Ph\}$ (**92**) to a titanium centre was attempted utilising the (i) amine elimination, (ii) toluene elimination and (iii) dimetalation/salt elimination approaches.

2.2.2.1. Attempted syntheses of a diborane(4)-bridged CGC *via* amine elimination

Considering the successful application of the amine elimination approach to the synthesis of amino monoborane-bridged CGCs, it appeared as the obvious method for the attempted preparation of diborane(4)-bridged CGCs.

Utilising the reaction conditions established for the synthesis of amino monoborane-bridged CGCs, (η^1-$C_5H_5)(BNMe_2)_2\{N(H)Ph\}$ (**92**) was reacted with $[Ti(NMe_2)_4]$ in refluxing toluene. The initially yellow mixture turned black over the course of 3 h. An aliquot was then removed, dried *in vacuo* and analysed by multinuclear NMR spectroscopy. The predominant signal at $\delta = 31$ in the ^{11}B NMR spectrum was high-field shifted with respect to those of the ligand precursor at $\delta = 34.0$ and 46.0. Such a shift indicates significant changes in the immediate environment, *i.e.* substitution pattern, of the boron centres that result from undesired reactivity other than deprotonation of the ligand precursor. The ^{1}H NMR spectrum showed a large number of resonances that could not be assigned to distinct compounds, but that also evidenced the formation of a complicate product mixture.

The reaction procedure was consequently modified and less harsh conditions were applied. The reactants were combined in hexane at –20 °C, slowly warmed to ambient temperature and then stirred for 16 h. The colour of the mixture changed gradually from bright yellow to yellow-orange. The mixture was then carefully heated to 50 °C for 2 h and an additional 4 h at reflux. The colour changed further during this process to become bright red. An aliquot was removed, dried *in vacuo* and analysed by multinuclear 1D and 2D NMR spectroscopy. In addition to resonances indication formation of small quantities of side-products, the spectra were found to be consistent with the formation of the unbridged complex $[Ti\{(\eta^5$-$C_5H_4)(BNMe_2)_2(N\{H\}Ph)\}(NMe_2)_3]$ (**123**) *via* elimination of one equivalent of $HNMe_2$ (Scheme 32). Four resonances corresponding to the methyl groups of the $(BNMe_2)_2$ fragment in both the ^{1}H and ^{13}C NMR spectra, as well as four resonances corresponding to the methine groups of the cyclopentadienyl fragment in the ^{13}C NMR spectrum (accompanied by multiplets in the ^{1}H NMR spectrum integrating to four protons)

indicate that **123** adopts C_1 symmetry in solution. The formulation of **123** as the unbridged complex is further supported by the integration ratio of the protons of the $Ti(NMe_2)_3$ fragment in relation to the other signals and the observation of a broad signal at δ = 4.95 corresponding to the NH moiety. The ^{11}B NMR spectrum displays two resonances at δ = 34.9 and 43.4, which have similar chemical shifts to those for the ligand precursor **92**. The difference in chemical shift between the two resonances of 8.5 ppm, however, is significantly smaller (compared to 12.0 ppm in the ligand precursor).

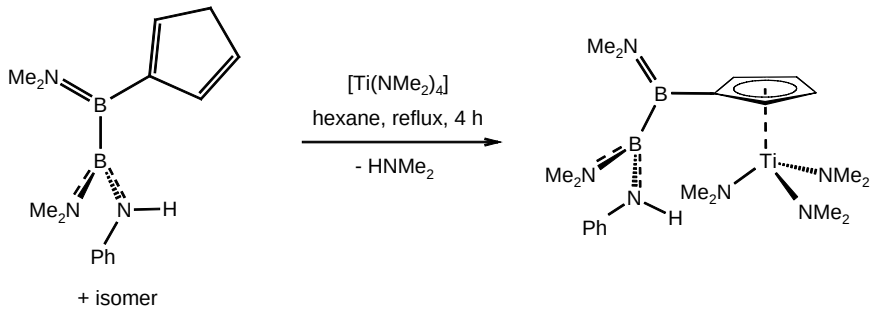

Scheme 32. Synthesis of [Ti{(η^5-C_5H_4)($BNMe_2$)$_2$(N{H}Ph)}(NMe_2)$_3$] (**123**).

The reaction mixture was subsequently refluxed for a further 20 h and the analysis repeated. In the ^1H NMR spectrum, besides some weak signals corresponding to **123** a number of more intense resonances were observed, indicating the formation of several unidentified reaction products. The ^{11}B NMR spectrum displayed two broad signals at δ = 36 and 46, resulting presumably from the superposition of resonances of various boron containing products. Evidently, prolonged heating of **123** does not facilitate selective elimination of a further equivalent of $HNMe_2$ to give the corresponding CGC.

2.2.2.2. Attempted synthesis of a diborane(4)-bridged CGC *via* toluene elimination

As an alternative to the amine elimination route, the synthesis of a diborane(4)-bridged CGC *via* toluene elimination utilising [$TiBz_4$] was attempted. Solutions of the ligand precursor **92** and [$TiBz_4$] in benzene-D_6 were combined at ambient temperature and the reaction progress was monitored by ^1H and ^{11}B NMR spectroscopy. After 16 h, the ^1H NMR spectrum displayed essentially the signals corresponding to the starting materials. However, these were accompanied by a weak signal at δ = 2.11, corresponding to the methyl group of toluene that is derived from protolytic cleavage of

a benzyl fragment from the titanium precursor. The reaction mixture was subsequently warmed to 60 °C for 22 h and the monitoring resumed. In the ^{1}H NMR spectra, the signal at δ = 2.11 was found to increase steadily in intensity, while the signal at δ = 2.80 corresponding to the methylene moiety of the titanium precursor gradually decreased and eventually vanished. In the earlier stages of the monitoring process, at least seven pseudo-triplets of various intensities were observed in the region between 5.5 – 6.5 ppm. Such pseudo-triplets are characteristic of mono-substituted cyclopentadienyl titanium complexes, *i.e.* (η^5-C_5H_4R)Ti fragments, and their multitude indicates the formation of several intermediate products. Throughout the course of the reaction, a number of signals were observed in the region typical for NMe_2 moieties on boron (2.0 – 3.0 ppm), but could not be assigned to distinct products. At the end of the 22 h period, only two pseudo-triplets of equal intensity at δ = 5.72 and 6.40 remained in the ^{1}H NMR spectrum, indicating the presence of only one final species incorporating a (η^5-C_5H_4R)Ti fragment. Moreover, four signals corresponding to the NMe_2 groups could be tentatively identified at δ = 2.26, 2.54, 2.57 and 2.62, however, certain assignment was hampered by trace impurities that give rise to resonances in the same region of the spectrum. Furthermore, integration of the signal corresponding to the methyl group of toluene with respect to the combined integrals of both pseudo-triplets afforded a ratio of 12:4, thus revealing formation of four equivalents of toluene per equivalent of (η^5-C_5H_4R)Ti. In the ^{11}B NMR spectrum, a merging of the two initial signals was observed during the course of the reaction, resulting in a signal at δ = 42.8 for the final mixture. Further characterisation of the products obtained was not possible and hence the outcome of the reaction remains unclear at this stage.

2.2.2.3. Attempted synthesis of a diborane(4)-bridged CGC *via* dimetalation/salt elimination

As a further potential route for the preparation of diborane(4)-bridged CGCs a dimetalation/salt elimination sequence was assessed. The ligand precursor **92** was sequentially reacted with two equivalents of *t*BuLi and one equivalent of [$TiCl_2(NMe_2)_2$] at –78 °C, slowly warmed to ambient temperature and then stirred for 16 h. An aliquot was dried *in vacuo* and analysed by ^{1}H and ^{11}B NMR spectroscopy. The ^{1}H NMR spectrum indicated the formation of a complicated product mixture. The ^{11}B NMR spectrum displayed a single broad resonance at δ = 37. Presumably, this

signal corresponds to a boron containing species other than the target product, since the latter would be expected to give rise to two resonances corresponding to two boron atoms with quite different substitution patterns.

2.3. Olefin polymerisation

The polymerisation of ethylene and copolymerisation of ethylene with various α-olefins or styrene are the commercially most important reactions associated with CGCs. Significant catalytic activity in the polymerisation of ethylene and styrene was also described for unbridged cyclopentadienyl amido complexes of titanium.[353, 354, 355, 356] Titanium CGCs are known to generally perform better in (co)polymerisation reactions than their zirconium and hafnium congeners. Preliminary reports on the catalytic performance of MAO activated boron-bridged CGCs stated a considerable activity of this system towards the polymerisation of ethylene and styrene.[148, 304] Consequently, a number of the previously described boron-bridged titanium CGCs (**37**, **70**, **115**, **118**) and one unbridged complex (**111**) were studied with regard to their catalytic activity in ethylene polymerisation (Figure 42). Based on the results obtained and the observations made in reactions of boron-bridged CGCs with $AlMe_3$ (*vide supra*), several of the boron-bridged CGCs (**37**, **70**, **118**) and the unbridged complex (**111**) were further investigated in styrene homopolymerisation experiments.

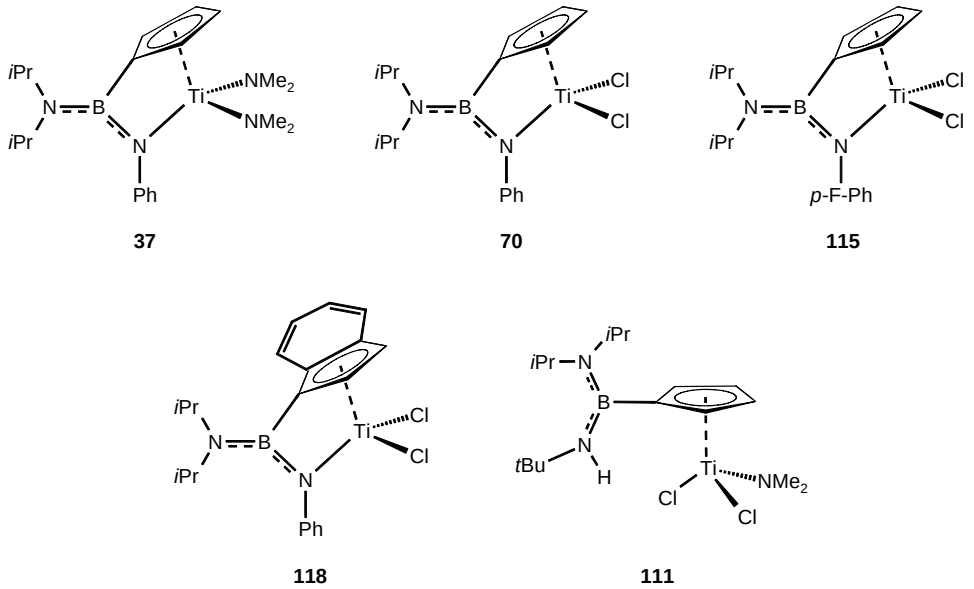

Figure 42. Complexes tested as pre-catalysts for ethylene and styrene polymerisation.

2.3.1. Ethylene polymerisation

Ethylene polymerisation experiments were performed at 30 – 80 °C using 10 – 20 μmol pre-catalyst, Al:Ti ratios of 2250:1 to 4500:1 and an ethylene pressure of 2 bar. Reaction times were in the range of 15 – 120 min. Details of the polymerisation reactions are given in the experimental section (see section 4.3.1 and Table 6).

In this study, all of the ethylene polymerisation experiments using boron-bridged CGCs afforded only small amounts of product. All products contained substantial amounts of ashes (Al_2O_3) as indicated by the poor solubility of the products and consequently weak detector responses in GPC experiments.[357] The amount of polymeric product may then be estimated from the detector responses in the respective GPC experiments relative to the expected detector response for fully soluble samples.[358] Using such an estimation, the highest polymer yield (0.72 g) and polymerisation activity {17 kg PE / (mol Ti × bar ethylene × h)} is determined for reaction PE29-1 utilising pre-catalyst **115** (60 °C, 20 μmol pre-catalyst, aluminium to titanium ratio 2250:1, 60 min). According to a rating scheme proposed by Gibson *et al.* such an activity may be regarded as low to moderate. A comparison with activity data reported in the literature is difficult as not only variations of temperature or reactant concentrations, but even modifications in stirring rate and reactor design significantly affect the polymer yields and constitution.[33, 34] The classification of the boron-bridged CGCs, however, as catalysts with low activity seems appropriate considering the ethylene polymerisation results obtained with a range of zirconocenes using the same reactor system and very similar reaction conditions {*e.g.* 60 °C, 10 μmol pre-catalyst, Al:Zr ratio 4500:1, 2 bar ethylene, 60 min; activity for [Cp_2ZrCl_2]: 700 kg PE / (mol Zr × bar ethylene × h); activity for [{(η^5-C_5H_4)$_2$BN*i*Pr$_2$}$ZrCl_2$]: 700 kg PE / (mol Zr × bar ethylene × h)} as well as reported results obtained with CGCs under comparable conditions {*e.g.* 50 °C, 15 μmol pre-catalyst, Al:Ti ratio 500:1, 2 bar ethylene, 30 min; activity for [{η^5:η^1-(C_5Me_4)$(CH_2)_2$N*t*Bu}$TiCl_2$]: 4200 kg PE / (mol Ti × bar ethylene × h)}.

The low activities of the boron-bridged CGCs in the above described ethylene polymerisation experiments prevented a characterisation of the kinetic profile of the reaction by means of a yield *vs.* reaction time correlation.

GPC results for distinct PE samples obtained from the aforementioned experiments appear to be well reproducible despite the low concentrations applied.[359] The reproducibility of determined polymer weights between two polymerisation runs under identical conditions, however, is rather poor (compare PE29-1 *vs.* PE29-2; PE29-3 *vs.* PE29-4; PE29-5 *vs.* PE29-6; PE30-1 *vs.* PE30-2; PE30-3 *vs.* PE30-4; PE30-5 *vs.* PE30-6). This lack of reproducibility renders comparison between the catalytic systems employed in this study rather difficult. Systems based on pre-catalyst **70** (PE26-x, x = 1 – 6) appear to produce a polymer with higher molecular mass than the systems involving pre-catalysts **115** and **118** (PE29-x and PE30-x, x = 1 – 6). Neither a valid correlation between aluminium to titanium ratio and molecular mass, nor titanium concentration and molecular mass could be determined due to the poor reproducibility and resulting broad scattering of determined molecular weights.

The M_w / M_n ratio for all analysed PE samples exceeds 2.0, the value expected for coordination polymerisation on a true single site catalyst.[360] M_w / M_n ratios reach values of up to 15, indicating the presence of several constitutionally differing catalytically active species.

The unbridged complex **111** was also examined as a ethylene polymerisation pre-catalyst. Reaction conditions were comparable to those applied in the polymerisation experiments involving boron-bridged CGCs. Neither polymeric nor oligomeric products were detectable by means of GPC and GC-MS, respectively. Evidently, complex **111** is not a suitable catalyst precursor for ethylene oligomerisation or polymerisation.

The low catalytic activity of boron-bridged CGCs in ethylene polymerisation experiments may be explained in conjunction with the results obtained from the reaction of boron-bridged CGCs with $AlMe_3$. The latter experiments demonstrated instability of the boron bridge in the presence of equimolar amounts of $AlMe_3$ at elevated temperature or in the presence of superstoichiometric amounts of $AlMe_3$ at ambient temperature. Considering this instability, a fast destruction of the boron bridge under the applied reaction conditions must be assumed. A half-sandwich complex appears a reasonable product of this decomposition pathway. An analogous structural motif is found in the unbridged, boryl substituted complex **111** and this was proven to be virtually inactive towards the polymerisation of ethylene in the presence of MAO

(PE23-x, x = 1 – 6). This lack of reactivity is as well consistent with the observation that half-sandwich complexes such as [$CpTiCl_3$], [$IndTiCl_3$] and [Cp^*TiCl_3] are generally poor ethylene polymerisation catalysts.

Presumably, the small amounts of PE obtained from MAO activated boron-bridged CGCs are formed by catalytically active species in the early stages of the reaction, *i.e.* active species with an intact boron bridge. Reaction of the boron bridge with $AlMe_3$ then rapidly produces half-sandwich complexes that have a very low or no activity at all.

2.3.2. Styrene polymerisation

The previous section described the ethylene polymerisation activity of catalytic systems based on boron-bridged CGCs activated with MAO. The observed low activity was attributed to the formation of unbridged half-sandwich complexes that are formed by reaction of $AlMe_3$ with the boron bridge. As MAO activated titanium half-sandwich complexes are known to be excellent styrene polymerisation catalysts,[361, 362, 363] a number of the aforementioned complexes were studied in styrene polymerisation experiments (see section 4.3.2 and Table 7).

Styrene polymerisation experiments were performed in Schlenk tubes at 50 – 80 °C using 10 μmol pre-catalyst, Al:Ti ratios of 500:1 to 2000:1, a styrene concentration of 1.74 mol/l and a reaction time of 60 min, following a modified literature procedure.[364] For comparison, several styrene polymerisation experiments were performed using [$CpTiCl_3$] as a pre-catalyst. Details of the polymerisation reactions are given in the experimental section.

All products obtained in this study contained substantial amounts of low molecular weight material as indicated by the respective GPC traces. As a consequence, precipitation of the polymer in methanol gave only very low yields, *i.e.* only the high molecular weight component was precipitated. Utilising an alternative work-up procedure involving evaporation of the solvent *in vacuo* allowed the recovery of both the high and low molecular weight fractions. However, this procedure resulted in larger ash (Al_2O_3) contents in the product as was evidenced by its partial insolubility.

Under identical conditions, the highest styrene polymerisation activity is observed for the catalytic system based on the unbridged complex **111** (PS5-1), while

the boron-bridged indenyl complex **118** (PS6-1) gives rise to a catalytic system with similar activity to the benchmark [$CpTiCl_3$] (PS4-x, x = 1, 3). Using pre-catalysts **37** (PS1-x, x = 6, 7) and **70** (PS-2-x, x = 1 – 5) very low product yields were achieved, probably due to the attempted precipitation of the polymer (*vide supra*). A higher Al:Ti ratio seems to moderately affect the activity (compare PS5-x, x = 1 – 4 and PS6-x, x = 1 – 4), though the distribution of yields obtained prevents a final conclusion from being drawn.

An interpretation of the molecular weights of the polymers obtained, as determined by GPC, is difficult since all polymers (particularly PS6-x, x = 1 – 5) contain significant amounts of low molecular weight material that is not included in the calculation of M_w and M_n. Naturally, the M_n values are affected more by changes in the low molecular weight fraction, while M_w is affected more by changes in the high molecular weight component. Consequently, the calculated M_n values in this study can be expected to be significantly higher than the real M_n values. Overestimation of the M_n values then also results in underestimation of the polydispersity of the polymer samples, as expressed by the M_w / M_n ratios.

Evidently, the catalytic system based on the unbridged complex **111** (PS5-x, x = 1 – 3) gives the highest molecular weight in the present study. The molecular weight distribution for PS obtained with this system appears to be narrow with M_w / M_n values close to 2. This suggests the predominance of a single catalytically active species. The catalytic system based on the bridged indenyl complex **118** (PS6-x, x = 1 – 5) produces the PS with the lowest molecular weight. Considering the high content of low molecular weight material in these samples, M_w / M_n values presumably exceed 2 significantly, indicating the presence of several catalytically active species in this system.

The good activity of the catalytic system based on the boron-bridged complex **118** for the homopolymerisation of styrene further supports the previously stated assumption that the boron-bridged CGCs react with $AlMe_3$ to give half-sandwich complexes that resemble species known to be good styrene polymerisation catalysts but poor ethylene polymerisation catalysts.

Chapter 3. Summary and outlook

Numerous new boron-bridged CGC ligand precursors have been prepared by sequential substitution of suitable dihaloborane precursors with one equivalent of a cyclopentadienide derivative and one equivalent of an amide. This route proved to be highly flexible in the choice of cyclopentadienide and amide, allowing facile variation of the substituents. The newly synthesised compounds include aminoborane based ligand precursors **77** – **80**, **83** – **85**, **87**, **88** and **90**, diaminodiborane(4) based ligand precursors **92** and **94** as well as ferrocenylborane based ligand precursors **101** and **102** (Figure 43).

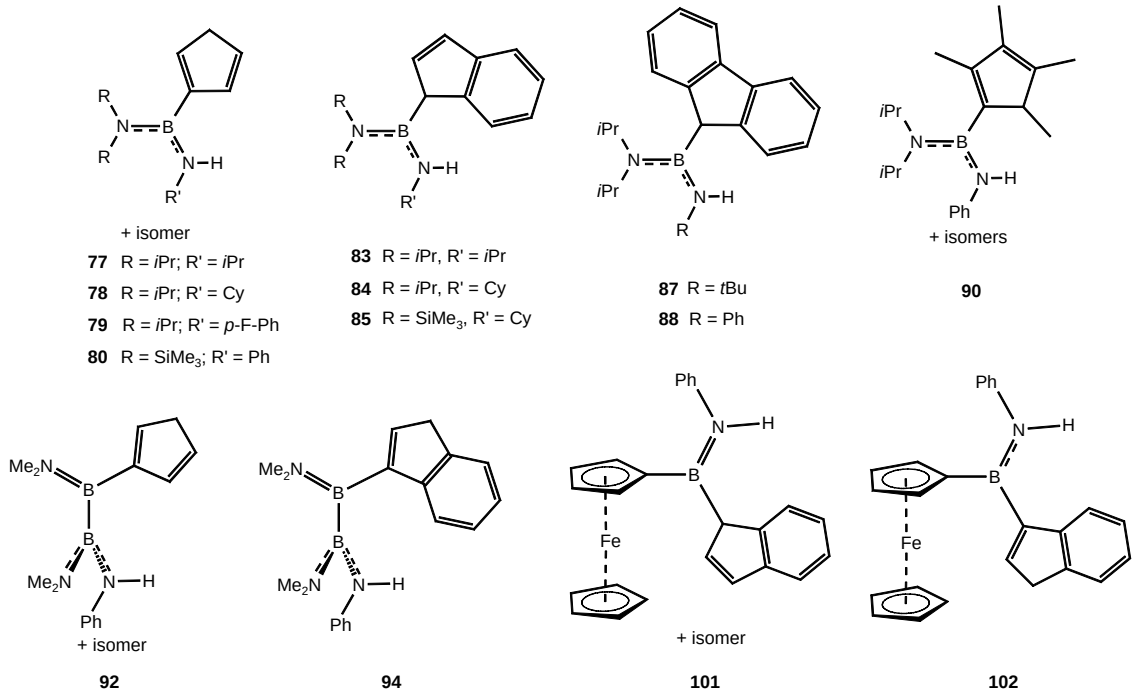

Figure 43. Newly synthesised boron-bridged ligand precursors.

Complexation of Group 4 metals with aminoborane based ligand precursors combining cyclopentadienyl and indenyl substituents, respectively, with anilido or 4-fluoroanilido moieties was achieved *via* reaction of the ligand precursors with the respective Group 4 metal tetraamides yielding the new boron-bridged CGCs **113**, **114**, **117** and **120** – **122** (Figure 44). However, aminoborane based NHR (R = alkyl) substituted ligand precursors reacted with $[Ti(NMe_2)_4]$ only under elimination of one equivalent of amine, resulting in the corresponding half-sandwich complexes **105** – **107** (Figure 45); that is the amine donor did not undergo metathesis with the amide group bound to the transition metal. This observation was attributed to the significantly lower

acidity of the NHR group where R is alkyl than where R is phenyl or 4-fluorophenyl. The half-sandwich complex **105** may be converted to the corresponding CGC **119** (Figure 44) by prolonged heating, while the related half-sandwich complex **107** decomposed under the same conditions.

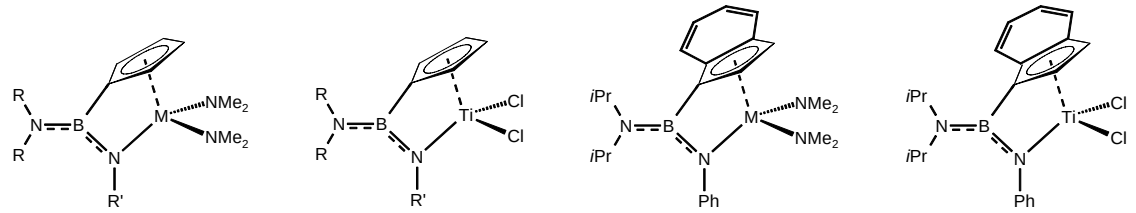

113 R = *i*Pr, R' = *p*-F-Ph, M = Ti
114 R = $SiMe_3$, R' = Ph, M = Ti
119 R = *i*Pr, R' = *i*Pr, M = Ti
120 R = *i*Pr, R' = Ph, M = Zr
121 R = *i*Pr, R' = Ph, M = Hf

115 R = *i*Pr, R' = *p*-F-Ph
116 R = $SiMe_3$, R' = Ph

117 M = Ti
122 M = Zr

118

Figure 44. Newly synthesised boron-bridged CGCs.

The diamido titanium CGCs **113**, **114** and **117** were readily converted to their dichloro congeners **115**, **116** and **118** (Figure 44) by reaction with excess Me_3SiCl, while the diamido zirconium and hafnium CGCs **120** – **122** yielded poorly soluble and hence, inadequately characterised products under comparable conditions. The half-sandwich complexes **105** and **107** reacted with excess Me_3SiCl to give the dichloro derivatives **110** and **111** (Figure 45); the corresponding trichloro derivatives were not formed even after prolonged reaction times. Metalation procedures other than amine elimination, *e.g.* dilithiation/salt elimination sequences and amine assisted HCl elimination, were assessed for a variety of aminoborane based ligand precursors, but conditions could not be optimised to yield the desired pure boron-bridged CGCs by these means.

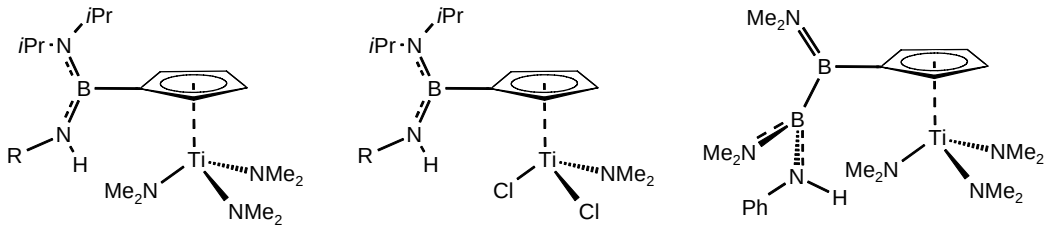

105 R = *i*Pr
106 R = Cy
107 R = *t*Bu

110 R = *i*Pr
111 R = *t*Bu

123

Figure 45. Newly synthesised boryl substituted half-sandwich complexes.

Interestingly, both half-sandwich complexes **110** and **111** partially hydrolysed to give the same product, **112**, that exhibits a unique $B_2O_3Ti_2$ core (Figure 46).

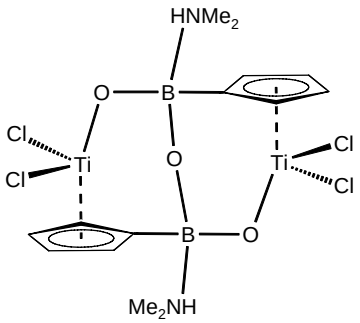

112

Figure 46. Product derived from partial hydrolysis of **110** and **111**, respectively.

The complexation of Group 4 metals with the diaminodiborane(4) based ligand precursor **92** proved problematic. Amine elimination utilising $[Ti(NMe_2)_4]$ yielded only the half-sandwich complex **123** (Figure 45). Heating of **123** resulted in decomposition rather than controlled elimination of a further equivalent of amine. Dilithiation/salt elimination sequences involving **92** yielded mixtures of several products that could not be separated.

Assessment of the reactivity of the boron-bridged CGC **70** with LiMe and $AlMe_3$ revealed that the boron bridge is susceptible to nucleophilic attack from such alkylating agents. The reaction of **70** with LiMe at –80 °C resulted in a mixture of products with an intact boron bridge, however, the dimethyl derivative of **70** could not be isolated. At 0 °C, complex **70** reacted with LiMe under nucleophilic attack of the bridging boron atom. While the boron bridge in **70** appeared to be stable in the presence of stoichiometric amounts of $AlMe_3$ at ambient temperature for at least 1 h, elevated temperatures or superstoichiometric amounts of $AlMe_3$ resulted in a fast degradation of the bridging moiety.

These findings are rather disappointing in the light that the most commonly applied co-catalyst in CGC catalysed polymerisation reactions, MAO, contains significant amounts of $AlMe_3$. Therefore, destruction of the boron bridge in boron-bridged CGCs under polymerisation conditions that usually involve a large excess of MAO (and consequently a large excess of $AlMe_3$) and high temperature has to be assumed. Indeed, the boron-bridged CGCs **37**, **70**, **115** and **118** were found to be poor

ethylene polymerisation catalysts, but good styrene polymerisation catalysts when activated with MAO. Such polymerisation characteristics would appear to arise from degradation of the linking moiety between the cyclopentadienyl and amido fragments, as CGCs are known to be highly active in ethylene homopolymerisation but have a low activity towards homopolymerisation of styrene, whereas half-sandwich complexes such as [$CpTiCl_3$] are poor ethylene homopolymerisation catalysts while being superior styrene polymerisation catalysts. The boryl substituted half-sandwich complex **111** was as well tested as a polymerisation catalyst and found virtually inactive towards the polymerisation of ethylene, but displayed a higher activity than [$CpTiCl_3$] towards the polymerisation of styrene.

Based on the aforementioned results, four important fields for further research on boron-bridged CGCs can be identified: (i) additional studies on the complexation of boron-bridged CGC ligand precursors to Group 4 metals to prepare boron-bridged CGCs with substitution pattern that are yet inaccessible (this particularly includes CGCs with diaminodiborane(4) and ferrocenylborane based ligands); (ii) the selective synthesis of dialkyl derivatives of boron-bridged CGCs that would allow the use of $B(C_6F_5)_3$ and [Ph_3C^+][$B(C_6F_5)_4^-$] instead of MAO as co-catalysts in olefin polymerisation reactions, thus preventing degradation of the bridging moiety under polymerisation conditions; (iii) extension of the synthetic methods to the preparation of boron-bridged CGCs of Group 3 metals and the lanthanides; and (iv) the application of boron-bridged Group 3 and 4 CGCs for the catalysis of organic transformations other than polymerisation reactions, particularly those that do not require the use of alkylating agents.

Chapter 4. Experimental

4.1. General considerations

All manipulations were carried out under an atmosphere of dry nitrogen or argon using standard Schlenk line and dry-box techniques. Solvents were dried by standard procedures,[365] distilled under nitrogen and stored over molecular sieves.

4.1.1. Instrumentation

NMR experiments were performed on either a Bruker Avance 500 spectrometer, a Bruker AM500 spectrometer, a Bruker DPX-400 spectrometer, a Bruker DRX 300 spectrometer, a JEOL-EX270, with Delta upgrade, spectrometer or a Bruker Avance 200 spectrometer. All NMR experiments were performed at ambient temperature unless otherwise stated. All NMR chemical shifts are reported in ppm. Chemical shifts for ^{1}H and ^{13}C-{^{1}H} NMR spectra were referenced to internal solvent resonances and are reported relative to $SiMe_4$. Assignments were made from the analysis of ^{13}C-APT, ^{13}C-DEPT, ^{1}H,^{1}H-COSY and ^{1}H,^{13}C-HMQC-COSY NMR experiments and by comparison with previously published compounds. Chemical shifts for ^{11}B-{^{1}H}, ^{19}F-{^{1}H} and ^{29}Si-{^{1}H} NMR spectra were referenced to $BF_3{\cdot}OEt_2$, CCl_3F and $SiMe_4$, respectively, as external standards. Mass spectra were recorded either on a Finnigan MAT 95, a Thermo Finnigan Trio 1000, or a Micromass Platform II spectrometer. GC-MS was performed on a Hewlett Packard G 1800A GCD instrument equipped with an HP 5 capillary column, 50 m, and mass selective detector. IR spectroscopy was recorded as dichloromethane solutions and performed on a Bruker Vector 22 FT-IR spectrometer and IR spectroscopic bands are reported in cm^{-1}.

4.1.2. Starting materials

NaCp,[366] Li[C_5Me_4H], iPr$_2$NBCl$_2$,[367] (Me$_3$Si)$_2$NBCl$_2$,[368] FcBBr$_2$, FcB(η^1-C_5H_5)$_2$, FcB(1-C_9H_7)$_2$, FcB(3-C_9H_7)$_2$, (Me$_2$N)$_2$B$_2$Cl$_2$,[369] (η^1-C_5H_5)B(NiPr$_2$)Cl, (η^1-C_5H_5)B(NiPr$_2$)N(H)tBu, (η^1-C_5H_5)B(NiPr$_2$)N(H)Ph, (1-C_9H_7)B(NiPr$_2$)Cl, (1-C_9H_7)B(NiPr$_2$)N(H)Ph, (1-C_9H_7)(BNMe$_2$)$_2$Cl, [Ti(NMe$_2$)$_4$],[370] [Zr(NMe$_2$)$_4$], [Hf(NMe$_2$)$_4$], [TiCl$_2$(NMe$_2$)$_2$],[371] [TiCl$_3$(thf)$_3$],[372] [TiBz$_4$],[373] [CpTiCl$_3$],[374] [Ti{η^5:η^1-(C_5H_4)B(NiPr$_2$)NPh}(NMe$_2$)$_2$], and [Ti{η^5:η^1-(C_5H_4)B(NiPr$_2$)NPh}Cl$_2$] were synthesised according to published procedures. Lithium indenide and lithium fluorenide were prepared by lithiation of indene and fluorene, respectively, with one

equivalent of *n*BuLi (as a solution in hexane) and subsequently isolated by filtration. Lithiation of primary amines {*i*PrNH$_2$, CyNH$_2$, *t*BuNH$_2$, PhNH$_2$, (*p*-F-Ph)NH$_2$} was performed by addition of one equivalent of *n*BuLi (as a solution in hexane) to a solution of the amine in toluene and stirring at ambient temperature for 6 to 16 h. For polymerisation experiments ethylene 8.2 was purchased from Messer Griesheim and used as supplied. Styrene for polymerisation experiments was distilled twice from CaH$_2$, then stored at –30 °C. MAO for the activation of pre-catalysts in polymerisation experiments was supplied by Crompton, Bergkamen, Germany, as a 10 weight-% solution in toluene and was used as supplied. All other reagents were purchased from commercial sources and used as supplied.

4.2. Synthesis of compounds

4.2.1. Ligand precursors

4.2.1.1. Amino monoborane based cyclopentadienyl substituted ligand precursors

4.2.1.1.1. Synthesis of (η^1-C$_5$H$_5$)B(N*i*Pr$_2$)Cl (75)

*i*Pr$_2$NBCl$_2$ (3.09 g, 17.0 mmol) in hexane (15 mL) was added dropwise to a suspension of NaCp (1.59 g, 17.9 mmol) in hexane (35 mL) at 0 °C. The mixture was then stirred at ambient temperature for 2.5 h, the precipitate was removed by filtration and washed with hexane. All volatiles were then removed *in vacuo* from the combined filtrate and washings to yield pure **75** (3.55 g, 16.8 mmol, 99%) as a single isomer.

^{1}H NMR (270 MHz, toluene-D$_8$): δ = 0.90 (d, $^3J_{H\text{-}H}$ = 6.7 Hz, 3H, Me), δ = 0.91 (d, $^3J_{H\text{-}H}$ = 6.7 Hz, 3H, Me), 1.39 (d, $^3J_{H\text{-}H}$ = 6.9 Hz, 6H, Me), 3.16 (m, 2H, CH$_{2\ Cp}$), 3.27 (m, 1H, CH$_{i\text{Pr}}$), 4.12 (m, 1H, CH$_{i\text{Pr}}$), 6.47 (pd, 2H, CH$_{Cp}$), 6.84 (pt, 1H, CH$_{Cp}$).

^{13}C NMR (126 MHz, toluene-D$_8$): δ = 21.9 (Me), 23.4 (Me), 46.6 (CH$_{i\text{Pr}}$), 46.8 (CH$_{2\ Cp}$), 51.1 (CH$_{i\text{Pr}}$), 132.9 (CH$_{Cp}$), 137.7 (CH$_{Cp}$), 140.8 (CH$_{Cp}$), BC resonance not observed.

^{11}B NMR (87 MHz, toluene-D$_8$): δ = 33.9.

MS (EI$^+$) *m*/*z* (%): 211 (34) [M^+], 196 (100) [M^+ – Me], 154 (14) [M^+ – Me – *i*Pr], 118 (15) [M^+ – Me – *i*Pr_2 – HCl].

4.2.1.1.2. Synthesis of (η^1-C_5H_5)B{N($SiMe_3$)$_2$}Cl (76)

Following the same procedure as for **75**, $(Me_3Si)_2NBCl_2$ (1.76 g, 7.27 mmol) was reacted with NaCp (0.68 g, 7.64 mmol) to yield pure **76** quantitatively (1.57 g, 7.25 mmol) as a mixture of **va** and **vh** isomers (isomer ratio approximately 7:1, assignment of constitutional isomers to the two sets of NMR spectroscopic data not possible) in the form of a pale yellow oil.

^{1}H NMR (250 MHz, chloroform-D): [major isomer]: δ = 0.22 (s, 18H, $SiMe_3$), 3.22 (m, 2H, CH_2), 6.59 – 6.63 (m, 1H, CH_{Cp}), 6.76 – 6.80 (m, 1H, CH_{Cp}), 7.13 – 7.16 (m, 1H, CH_{Cp});

[minor isomer]: δ = 0.24 (s, 18H, $SiMe_3$), 3.09 (m, 2H, CH_2), 6.41 – 6.47 (m, 1H, CH_{Cp}), 6.69 – 6.75 (m, 1H, CH_{Cp}), 6.89 – 6.92 (m, 1H, CH_{Cp}).

^{13}C NMR (101 MHz, chloroform-D): [isomer mixture]: δ = 3.2 ($SiMe_3$), 3.7 ($SiMe_3$), 41.6 (CH_2), 45.6 (CH_2), 132.2 (CH_{Cp}), 132.8 (CH_{Cp}), 133.2 (CH_{Cp}), 133.3 (CH_{Cp}), 141.2 (CH_{Cp}), 146.4 (CH_{Cp}), BC resonance not observed.

^{11}B NMR (128 MHz, chloroform-D): [isomer mixture]: δ = 43.5.

MS (CI$^+$) *m*/*z* (%): 272 (80) [M^+ + H], 236 (32) [M^+ – Cl], 162 (57) [M^+ – HCl – $SiMe_3$].

4.2.1.1.3. Synthesis of (η^1-C_5H_5)B(N*i*Pr_2)N(H)*i*Pr (77)

A freshly prepared solution of lithium *iso*propyl amide (1.10 g, 17.0 mmol) in toluene (30 mL) was added dropwise to a solution of (η^1-C_5H_5)B(N*i*Pr_2)Cl (**75**) (3.09 g, 17.0 mmol) in hexane (40 mL) at 0 °C. The reaction mixture was allowed to warm to ambient temperature and was subsequently stirred for 16 h. LiCl that was precipitated was filtered off, solvents were removed *in vacuo* at ambient temperature and the residue was distilled *in vacuo* over a short path at elevated temperature. Pure **77** (1.56 g, 6.7 mmol, 39%) as a mixture of **va** and **vh** isomers (ratio 5:4, assignment of constitutional isomers to the two sets of NMR spectroscopic data not possible) was obtained in the form of a white crystalline solid (melting point 35 °C).

^{1}H NMR (200 MHz, benzene-D_6): [major isomer]: δ = 0.98 (d, $^3J_{H\text{-}H}$ = 6.4 Hz, 6H, Me_{NHiPr}), 1.09 (d, $^3J_{H\text{-}H}$ = 6.9 Hz, 12H, Me_{NiPr_2}), 3.09 (m, 2H, CH_2), 3.11 (m, 1H, CH_{NHiPr}), 3.34 (m, 2H, CH_{NiPr_2}), 6.50-6.70 (m, 3H, CH_{Cp}), NH resonance not observed;

[minor isomer]: δ = 1.03 (d, $^3J_{H\text{-}H}$ = 6.4 Hz, 6H, Me_{NHiPr}), 1.14 (d, $^3J_{H\text{-}H}$ = 6.9 Hz, 12H, Me_{NiPr_2}), 2.91 (m, 2H, CH_2), 3.31 (m, 1H, CH_{NHiPr}), 3.44 (m, 2H, CH_{NiPr_2}), 6.40 – 6.50 (m, 2H, CH_{Cp}), 6.76 – 6.89 (m, 1H, CH_{Cp}), NH resonance not observed.

^{13}C NMR (101 MHz, benzene-D_6): [major isomer]: δ = 23.3 (Me_{NiPr_2}), 27.5 (Me_{NHiPr}), 44.7 (CH_{NiPr_2}), 46.3 (br, CH_{NHiPr}), 46.5 (CH_2 $_{Cp}$), 133.6 (CH_{Cp}), 133.8 (CH_{Cp}), 134.9 (CH_{Cp}), BC resonance not observed;

[minor isomer]: δ = 23.4 (Me_{NiPr_2}), 27.5 (Me_{NHiPr}), 43.2 (CH_2 $_{Cp}$), 44.6 (CH_{NiPr_2}), 46.3 (br, CH_{NHiPr}), 132.3 (CH_{Cp}), 135.5 (CH_{Cp}), 137.4 (CH_{Cp}), BC resonance not observed.

^{11}B NMR (64 MHz, benzene-D_6): δ = 29.6.

MS (EI$^+$) *m*/*z* (%): 234 (20) [M^+], 219 (100) [M^+ – Me], 134 (20) [M^+ – N*i*Pr$_2$], 86 (88) [$C_6H_{14}^+$].

IR 3439 w ν(NH).

4.2.1.1.4. Synthesis of (η^1-C_5H_5)B(N*i*Pr$_2$)N(H)Cy (78)

A pale yellow solution of (η^1-C_5H_5)B(N*i*Pr$_2$)Cl (**75**) (3.75 g, 20.6 mmol) in hexane (30 mL) was added dropwise to a colourless suspension of lithium cyclohexyl amide (2.16 g, 20.6 mmol) in toluene (20 mL) at 0 °C. The mixture was stirred at ambient temperature over night, the precipitated LiCl was removed by centrifugation and the solvent was evaporated *in vacuo*. The residual oily, amber coloured crude product was distilled *in vacuo* at 105 °C (oil bath temperature) to yield **78** as a mixture of **va** and **vh** isomers (isomer ratio approximately 1:1, assignment of constitutional isomers to the two sets of NMR spectroscopic data not possible) in the form of a colourless oil (3.38 g, 12.3 mmol, 60%) that crystallised at –30 °C.

^{1}H NMR (270 MHz, benzene-D_6): [isomer mixture]: δ = 1.11 (d, $^{3}J_{H\text{-}H}$ = 6.9 Hz, 12H, Me), 1.16 (d, $^{3}J_{H\text{-}H}$ = 6.9 Hz, 12H, Me), 0.90 – 1.25 (br m, 6H, $CH_{2\ Cy}$), 1.30 – 1.45 (br m, 2H, $CH_{2\ Cy}$), 1.50 – 1.65 (br m, 4H, $CH_{2\ Cy}$), 1.75 – 1.93 (br m, 4H, $CH_{2\ Cy}$), 2.55 – 2.80 (br m, 4H, $CH_{2\ Cy}$), 2.85 – 3.00 (br m, 2H, NCH), 2.90 (m, 2H, $CH_{2\ Cp}$), 3.09 (m, 2H, $CH_{2\ Cp}$), 3.33 (m, 2H, $CH_{i\text{Pr}}$), 3.46 (m, 2H, $CH_{i\text{Pr}}$), 6.4 – 6.9 (m, 6H, CH_{Cp}), NH resonance not observed.

^{13}C NMR (68 MHz, benzene-D_6): [isomer mixture]: δ = 23.0 (Me), 23.1 (Me), 25.4 ($CH_{2\ Cy}$), 25.4 ($CH_{2\ Cy}$), 25.8 ($CH_{2\ Cy}$), 25.9 ($CH_{2\ Cy}$), 38.1 ($CH_{2\ Cy}$), 43.0 ($CH_{2\ Cp}$), 46.0 ($CH_{i\text{Pr}}$), 46.1 ($CH_{i\text{Pr}}$), 46.3 ($CH_{2\ Cp}$), 51.4 (NCH), 51.5 (NCH), 132.0 (CH_{Cp}), 133.3 (CH_{Cp}), 133.6 (CH_{Cp}), 134.7 (CH_{Cp}), 135.3 (CH_{Cp}), 137.2 (CH_{Cp}), BC resonance not observed.

^{11}B NMR (87 MHz, benzene-D_6): [isomer mixture]: δ = 29.3.

MS (EI$^+$) *m*/*z* (%): 274 (19) [M^+], 259 (100) [M^+ – Me], 231 (6) [M^+ – *i*Pr], 174 (8) [M^+ – *i*Pr$_2$N].

IR 3435 w ν(NH).

4.2.1.1.5. Synthesis of (η^1-C_5H_5)B(N*i*Pr$_2$)N(H)(*p*-F-Ph) (79)

(η^1-C_5H_5)B(N*i*Pr$_2$)Cl (**75**) (3.11 g, 17.1 mmol) was dissolved in hexane (30 mL) and freshly prepared lithium *para*-fluoro-anilide (2.00 g, 17.1 mmol) as a suspension in toluene (30 mL) was added dropwise at 0 °C. The mixture was allowed to warm to ambient temperature and was subsequently stirred over night. The pale brown precipitate was removed by centrifugation. All solvents were then removed *in vacuo* at ambient temperature. The resulting yellow oil was distilled over a short path *in vacuo* at 120 °C to give **79** (3.47 g, 12.1 mmol, 71%) as a colourless oil that solidified over night at ambient temperature. The product consisted of a mixture of **va** and **vh** isomers (isomer ratio approximately 2:1, assignment of constitutional isomers to the two sets of NMR spectroscopic data not possible).

^{1}H NMR (500 MHz, benzene-D_6): [major isomer]: δ = 1.06 (d, 12H, Me), 2.83 (m, 2H, $CH_{2\ Cp}$), 3.44 (br m, 2H, $CH_{i\text{Pr}}$), 4.89 (br s, 1 H, NH), 6.44 – 6.73 (m, 7H, $CH_{Cp/p\text{-F-Ph}}$);

[minor isomer]: δ = 1.09 (d, 12H, Me), 2.77 (m, 2H, $CH_{2\ Cp}$), 3.44 (br m, 2H, $CH_{i\mathrm{Pr}}$), 4.93 (br s, 1 H, NH), 6.32 – 6.73 (m, 7H, $CH_{Cp/p\text{-F-Ph}}$).

^{13}C NMR (126 MHz, benzene-D_6): [major isomer]: δ = 23.4 (Me), 45.6 ($CH_{2\ Cp}$), 46.4 (br, $CH_{i\mathrm{Pr}}$), 115.4 (d, $^2J_{C\text{-}F}$ = 22.2 Hz, *m*-$CH_{p\text{-F-Ph}}$), 121.4 (d, $^3J_{C\text{-}F}$ = 8.3 Hz, *o*-$CH_{p\text{-F-Ph}}$), 133.4 (CH_{Cp}), 135.7 (CH_{Cp}), 138.3 (CH_{Cp}), 141.9 (d, $^4J_{C\text{-}F}$ = 2.8 Hz, *ipso*-$CH_{p\text{-F-Ph}}$), 157.8 (d, $^1J_{C\text{-}F}$ = 237 Hz, CF), BC resonance not observed;

[minor isomer]: δ = 23.8 (Me), 43.3 ($CH_{2\ Cp}$), 46.4 (br, $CH_{i\mathrm{Pr}}$), 115.1 (d, $^2J_{C\text{-}F}$ = 22.1 Hz, *m*-$CH_{p\text{-F-Ph}}$), 122.5 (d, $^3J_{C\text{-}F}$ = 8.3 Hz, *o*-$CH_{p\text{-F-Ph}}$), 132.9 (CH_{Cp}), 136.9 (CH_{Cp}), 138.4 (CH_{Cp}), 141.8 (d, $^4J_{C\text{-}F}$ = 2.8 Hz, *ipso*-$CH_{p\text{-F-Ph}}$), 157.9 (d, $^1J_{C\text{-}F}$ = 238 Hz, CF), BC resonance not observed.

^{19}F NMR (376 MHz, benzene-D_6): [major isomer]: δ = –124.4;

[minor isomer]: δ = –124.4.

^{11}B NMR (64 MHz, benzene-D_6): [isomer mixture]: δ = 29.9.

MS (EI$^+$) *m*/*z* (%): 286 (8) [M^+], 271 (26) [M^+ – Me], 173 (24) [M^+ – *p*-F-Ph-NH_2], 111 (100) [*p*-F-Ph-NH_2^+], 44 (99) [$C_3H_8^+$].

4.2.1.1.6. Synthesis of (η^1-C_5H_5)B{N($SiMe_3$)$_2$}N(H)Ph (80)

A suspension of lithium anilide (0.76 g, 7.64 mmol, 1.05 equivalents) in toluene (30 mL) was added dropwise to a solution of (η^1-C_5H_5)B{N($SiMe_3$)$_2$}Cl (**76**) (1.57 g, 7.25 mmol) in hexane (25 mL) at 0 °C. After allowing the mixture to warm to ambient temperature, the reaction mixture was stirred for 16 h. The precipitated LiCl was removed by filtration and the solvent was evaporated *in vacuo* to yield **80** as a mixture of **va** and **vh** isomers (isomer ratio approximately 3:1, assignment of constitutional isomers to the two sets of NMR spectroscopic data not possible) in the form of a yellow oil (1.58 g, 4.81 mmol, 66%). An attempt to further purify the product by distillation at 105 °C (oil bath temperature) *in vacuo* resulted only in decomposition as evidenced by darkening of the oil.

^{1}H NMR (250 MHz, chloroform-D): [major isomer]: δ = 0.10 (s, 18H, $SiMe_3$), 3.00 (m, 2H, CH_2), 5.69 (br s, 1H, NH), 6.64 – 7.26 (m, 8H, $CH_{Cp/Ph}$);

[minor isomer]: δ = 0.14 (s, 18H, $SiMe_3$), 3.07 (m, 2H, CH_2), 5.69 (br s, 1H, NH), 6.64 – 7.26 (m, 8H, $CH_{Cp/Ph}$).

^{13}C NMR (63 MHz, chloroform-D): [isomer mixture]: δ = 2.9 ($SiMe_3$), 3.2 ($SiMe_3$), 43.1 (CH_2), 44.1 (CH_2), 120.6 ($CH_{Cp/Ph}$), 122.3 ($CH_{Cp/Ph}$), 122.3 ($CH_{Cp/Ph}$), 122.4 ($CH_{Cp/Ph}$), 128.7 ($CH_{Cp/Ph}$), 129.0 ($CH_{Cp/Ph}$), 133.1 ($CH_{Cp/Ph}$), 138.0 ($CH_{Cp/Ph}$), 139.7 ($CH_{Cp/Ph}$), 143.8 ($CH_{Cp/Ph}$), 144.0 ($CH_{Cp/Ph}$), 144.8 ($CH_{Cp/Ph}$), BC resonance not observed.

^{11}B NMR (128 MHz, chloroform-D): [isomer mixture]: δ = 34.3.

MS (CI$^+$) *m*/*z* (%): 329 (100) [M^+ + H], 253 (49) [M^+ – $SiMe_3$ – 2H], 236 (26) [M^+ – HNPh].

4.2.1.2. Amino monoborane based indenyl subsituted ligand precursors

4.2.1.2.1. Synthesis of (1-C_9H_7)B{N($SiMe_3$)$_2$}Cl (82)

Following essentially the same procedure as outlined for **75**, reaction of $(Me_3Si)_2NBCl_2$ (3.16 g, 13.1 mmol) and lithium indenide (1.60 g, 13.1 mmol) yielded **82** (4.15 g, 12.9 mmol) almost quantitatively as a pale yellow oil.

^{1}H NMR (270 MHz, toluene-D_8): δ = 0.26 (s, 18H, $SiMe_3$), 3.75 (br s, 1H, BCH), 6.40 – 7.45 (m, 6H, CH_{Ind}).

^{13}C NMR (101 MHz, toluene-D_8): δ = 4.7 ($SiMe_3$), 53.7 (br, BCH), 122.4 (CH_{Ind}), 124.2 (CH_{Ind}), 125.3 (CH_{Ind}), 127.2 (CH_{Ind}), 133.6 (CH_{Ind}), 137.1 (CH_{Ind}), 145.9 (*quaternary* C_{Ind}), 146.8 (*quaternary* C_{Ind}).

^{11}B NMR (87 MHz, toluene-D_8): δ = 47.2.

MS (EI$^+$) *m*/*z* (%): 321 (1) [M^+], 306 (8) [M^+ – Me], 286 (2) [M^+ – Cl], 206 (27) [M^+ – C_9H_7], 115 (27) [$C_9H_7^+$], 98 (100) [M^+ – C_9H_7 – $SiMe_3$].

4.2.1.2.2. Synthesis of (1-C_9H_7)B(N*i*Pr$_2$)N(H)*i*Pr (83)

A suspension of lithium *iso*propyl amide (0.77 g, 11.9 mmol) in hexane (30 mL) was added dropwise to a solution of (1-C_9H_7)B(N*i*Pr$_2$)Cl (**81**) (3.12 g, 11.9 mmol) in toluene (30 mL) at 0 °C. After warming to ambient temperature, the mixture was stirred for 16 h. Precipitated LiCl was removed by centrifugation and all volatiles were

removed *in vacuo*. Recrystallisation from hexane at –30 °C afforded **83** (1.18 g, 4.2 mmol, 35%) in the form of colourless crystals.

^{1}H NMR (300 MHz, dichloromethane-D_2, –50 °C): δ = 0.08 (d, 3H, $^{3}J_{H\text{-}H}$ = 6.5 Hz, CH_3), 0.60 (d, 3H, $^{3}J_{H\text{-}H}$ = 6.5 Hz, CH_3), 1.16 (d, 6H, $^{3}J_{H\text{-}H}$ = 6.7 Hz, CH_3), 1.18 (d, 3H, $^{3}J_{H\text{-}H}$ = 6.2 Hz, CH_3), 1.23 (d, 3H, $^{3}J_{H\text{-}H}$ = 6.3 Hz, CH_3), 1.50 (m, 1H, $CH_{i\text{Pr}}$), 2.68 (d, 1H, $^{3}J_{H\text{-}H}$ = 9.3 Hz, BCH), 2.93 (m, 1H, $CH_{i\text{Pr}}$), 3.49 (br s, 1H, NH), 3.72 (m, 1H, $CH_{i\text{Pr}}$), 6.7 – 7.0 (m, 2H, $CH_{\text{Ind-5-ring}}$), 7.1 – 7.5 (m, 4H, $CH_{\text{Ind-6-ring}}$).

^{13}C NMR (75 MHz, dichloromethane-D_2, –50 °C): δ = 20.9 (Me), 22.7 (Me), 24.1 (Me), 24.4 (Me), 28.0 (Me), 28.3 (Me), 43.5 ($CH_{i\text{Pr}}$), 44.7 ($CH_{i\text{Pr}}$), 47.3 ($CH_{i\text{Pr}}$), 99.5 (br, BCH), 121.6 ($CH_{\text{Ind-6-ring}}$), 124.0 ($CH_{\text{Ind-6-ring}}$), 124.5 ($CH_{\text{Ind-6-ring}}$), 125.4 ($CH_{\text{Ind-6-ring}}$), 129.9 ($CH_{\text{Ind-5-ring}}$), 141.5 ($CH_{\text{Ind-5-ring}}$), 145.5 (*quaternary* C_{Ind}), 150.0 (*quaternary* C_{Ind}).

^{11}B NMR (64 MHz, benzene-D_6): δ = 30.0.

MS (EI$^+$) *m*/*z* (%): 283 (18) [M^+ – H], 268 (10) [M^+ – Me – H], 169 (100) [M^+ – C_9H_7], 43 (73) [$C_3H_7^+$].

4.2.1.2.3. Synthesis of (1-C_9H_7)B(N*i*Pr$_2$)N(H)Cy (84)

A solution of (1-C_9H_7)B(N*i*Pr$_2$)Cl (**81**) (2.75 g, 10.5 mmol) in toluene (25 mL) was added dropwise to a white suspension of lithium cyclohexyl amide (15.0 mmol, 1.4 equivalents) in toluene/diethyl ether (3:1 v/v, 30 mL) at 0 °C. Stirring at ambient temperature for 16 h afforded a yellow suspension. After removal of the precipitated LiCl by centrifugation and the solvent *in vacuo*, the crude product was obtained as a dark yellow oil. Colourless crystals formed at –30 °C and pure **84** (3.06 g, 9.45 mmol, 90%) was obtained after washing with cold hexane and drying the solid *in vacuo*.

^{1}H NMR (270 MHz, toluene-D_8): δ = 0.70 – 2.05 (m, 10H, CH_2), 1.18 (d, $^{3}J_{H\text{-}H}$ = 6.9 Hz, 6H, Me), 1.28 (d, $^{3}J_{H\text{-}H}$ = 6.7 Hz, 6H, Me), 2.78 (m, 1H, $CH_{i\text{Pr}}$), 2.93 (m, 1H, CH_{Cy}), 3.41 (m, 1H, $CH_{i\text{Pr}}$), 3.61 (m, 1H, BCH), 6.30 – 7.95 (m, 6H, CH_{Ind}), NH resonance not observed.

^{13}C NMR (68 MHz, toluene-D_8): δ = 23.2 (Me), 24.1 (Me), 25.4 (CH_2), 25.8 (CH_2), 25.9 (CH_2), 38.1 (CH_2), 38.2 (CH_2), 45.1 ($CH_{i\text{Pr}}$), 50.7 ($CH_{i\text{Pr}}$), 51.3 (CH_{Cy}),

120.9 (CH_{Ind}), 123.1 (CH_{Ind}), 124.0 (CH_{Ind}), 124.9 (CH_{Ind}), 129.4 (CH_{Ind}), 139.7 (CH_{Ind}), 145.0 (*quarternary* C_{Ind}), 149.3 (*quarternary* C_{Ind}), BC resonance not observed.

^{11}B NMR (87 MHz, toluene-D_8): δ = 29.2.

MS (EI$^+$) *m*/*z* (%): 324 (40) [M^+], 309 (100) [M^+ – Me], 209 (99) [M^+ – Ind], 115 (23) [Ind^+].

4.2.1.2.4. Synthesis of (1-C_9H_7)B{N($SiMe_3$)$_2$}N(H)Cy (85)

A pale yellow solution of (1-C_9H_7)B{N($SiMe_3$)$_2$}Cl (**82**) (1.29 g, 4.00 mmol) in hexane (15 mL) was added to an off-white suspension of lithium cyclohexyl amide (0.53 g, 5.00 mmol, 1.25 equivalents) in toluene/diethyl ether (3:1 v/v, 20 mL) at 0 °C. Upon addition of the chloroborane the colour of the suspension changed almost immediately to bright yellow. The mixture was stirred for 16 h at ambient temperature. The LiCl formed was then removed by centrifugation and the solvent was evaporated *in vacuo* to yield the crude product **85** as a dark yellow oil (1.32 g, 3.44 mmol, 86%).

^{1}H NMR (270 MHz, toluene-D_8): δ = 0.24 (s, 9H, $SiMe_3$), 0.26 (s, 9H, $SiMe_3$), 0.80 – 2.05 (m, 10H, CH_2), 3.17 (m, 1H, BCH), 3.50 (m, 1H, NCH), 6.60 – 7.80 (m, 6H, CH_{Ind}), NH resonance not observed.

^{13}C NMR (68 MHz, toluene-D_8): δ = 3.2 ($SiMe_3$), 3.7 ($SiMe_3$), 25.0 (CH_2), 25.5 (CH_2), 25.6 (CH_2), 36.5 (CH_2), 39.6 (CH_2), 49.9 (CH_{Cy}), 116.6 (CH_{Ind}), 121.5 (CH_{Ind}), 124.0 (CH_{Ind}), 124.2 (CH_{Ind}), 126.1 (CH_{Ind}), 144.7 (CH_{Ind}), 145.2 (*quaternary* C_{Ind}), 147.8 (*quaternary* C_{Ind}), BC resonance not observed.

^{11}B NMR (87 MHz, toluene-D_8): δ = 32.9.

MS (EI$^+$) *m*/*z* (%): 384 (19) [M^+], 369 (40) [M^+ – Me], 287 (100) [M^+ – NCy], 269 (40) [M^+ – Ind], 171 (28) [M^+ – HNCy – Ind], 98 (32) [$HNCy^+$].

4.2.1.3. Amino monoborane based fluorenyl substituted ligand precursors

4.2.1.3.1. Synthesis of (9-$C_{13}H_9$)B(N*i*Pr_2)N(H)*t*Bu (87)

A suspension of lithium fluorenide (4.30 g, 25.0 mmol) in hexane (50 mL) was treated with a solution of *i*Pr_2NBCl_2 (4.55 g, 25.0 mmol) in hexane (20 mL) at 0 °C. The suspension was allowed to warm to ambient temperature and then stirred for 16 h.

Precipitated LiCl was removed by centrifugation. Subsequently, lithium *tert*-butyl amide (1.98 g, 25.0 mmol) in a hexane/toluene (1:2 v/v, 30 mL) was added dropwise to the supernatant at 0 °C. The mixture was again warmed to ambient temperature and stirred for 16 h. Precipitated LiCl was removed by centrifugation and all volatiles were removed *in vacuo* to give a colourless solid. According to ^{11}B NMR spectroscopy and GC-MS of this solid, the target compound was formed in *ca.* 25% yield in addition to a number of side products. Two subsequent recrystallisation steps from hexane and then toluene at ambient temperature yielded the pure product **87** (1.18 g, 13.6 %).

^{1}H NMR (300 MHz, dichloromethane-D_2, –30 °C): δ = 0.05 (d, $^{3}J_{H\text{-}H}$ = 6.7 Hz, 6H, Me$_{i\text{Pr}}$), 1.20 (d, $^{3}J_{H\text{-}H}$ = 7.1 Hz, 6H, Me$_{i\text{Pr}}$), 1.44 (m, $^{3}J_{H\text{-}H}$ = 6.7 Hz, 1H, CH$_{i\text{Pr}}$), 1.46 (s, 9H, Me$_{t\text{Bu}}$), 2.87 (m, $^{3}J_{H\text{-}H}$ = 7.1 Hz, 1H, CH$_{i\text{Pr}}$), 3.36 (s, 1H, BCH), 4.21 (s, 1H, NH), 7.2 – 7.9 (m, 8H, CH$_{Flu}$).

^{13}C NMR (75 MHz, dichloromethane-D_2, –30 °C): δ = 20.9 (Me$_{i\text{Pr}}$), 24.3 (Me$_{i\text{Pr}}$), 34.7 (Me$_{t\text{Bu}}$), 43.2 (CH$_{i\text{Pr}}$), 47.6 (CH$_{i\text{Pr}}$), 49.4 (*quaternary* C$_{t\text{Bu}}$), 120.7 (CH$_{Flu}$), 125.0 (CH$_{Flu}$), 125.9 (CH$_{Flu}$), 127.1 (CH$_{Flu}$), 141.7 (*quaternary* C$_{Flu}$), 150.1 (*quaternary* C$_{Flu}$), BC resonance not observed.

^{11}B NMR (64 MHz, benzene-D_6): δ = 30.2.

MS (EI$^+$) *m*/*z* (%): 347 (3) [M^+ – H], 333 (10) [M^+ – Me], 183 (100) [$M^+ - C_{13}H_9$], 165 (19) [$C_{13}H_9^+$], 127 (33) [$M^+ - C_{13}H_8 - C_4H_9$].

4.2.1.3.2. Synthesis of (9-$C_{13}H_9$)B(N*i*Pr$_2$)N(H)Ph (88)

A solution of *i*Pr$_2$NBCl$_2$ (3.27 g, 18.0 mmol) in hexane (20 mL) was added dropwise to a yellow suspension of lithium fluorenide (3.10 g, 18.0 mmol) in hexane (30 mL) at 0 °C. The mixture was stirred at 0 °C for 30 min, then allowed to warm to ambient temperature and stirred for a further 16 h. The LiCl formed was removed by centrifugation. The remaining yellow solution was concentrated and added dropwise to a suspension of lithium anilide (1.98 g, 20.0 mmol, 1.11 equivalents) in hexane (30 mL) at 0 °C. After stirring for another 16 h the white precipitate was removed by centrifugation and the yellow supernatant was concentrated *in vacuo*. Cooling to 4 °C afforded pure **88** (2.05 g, 5.58 mmol, 31%) as a colourless crystalline solid.

^{1}H NMR (270 MHz, chloroform-D): δ = 0.28 (br s, 6H, Me), 1.26 (br s, 6H, Me), 3.00 (m, 1H, $CH_{i\mathrm{Pr}}$), 3.60 (m, 1H, $CH_{i\mathrm{Pr}}$), 4.29 (s, 1H, BCH), 5.37 (br s, 1H, NH), 6.8 – 7.9 (m, 13H, $CH_{\mathrm{Flu/Ph}}$).

^{13}C NMR (68 MHz, toluene-D_8): δ = 23.5 (Me), 45.3 ($CH_{i\mathrm{Pr}}$), 118.8 ($CH_{\mathrm{Flu/Ph}}$), 120.1 ($CH_{\mathrm{Flu/Ph}}$), 123.8 ($CH_{\mathrm{Flu/Ph}}$), 124.0 ($CH_{\mathrm{Flu/Ph}}$), 125.4 ($CH_{\mathrm{Flu/Ph}}$), 126.4 ($CH_{\mathrm{Flu/Ph}}$), 128.8 ($CH_{\mathrm{Flu/Ph}}$), 141.4 (*quaternary* C_{Flu}), 148.9 (*quaternary* C_{Flu}), BC resonance not observed.

^{11}B NMR (87 MHz, chloroform-D): δ = 30.8.

MS (EI$^+$) *m*/*z* (%): 368 (49) [M^+], 353 (29) [M^+ – Me], 202 (100) [$M^+ - C_{13}H_{10}$], 165 (60) [$C_{13}H_9^+$].

4.2.1.4. Amino monoborane based tetramethylcyclopentadienyl substituted ligand precursors

4.2.1.4.1. Synthesis of (η^1-C_5Me_4H)B(N*i*Pr$_2$)Cl (89)

A solution of $i\mathrm{Pr_2NBCl_2}$ (1.33 g, 7.3 mmol) in hexane (10 mL) was added dropwise to a suspension of Li[C_5Me_4H] (1.04 g, 7.3 mmol) in hexane (50 mL) at 0 °C. The reaction mixture was allowed to warm to room temperature and was subsequently stirred. Reaction progress was monitored by ^{11}B NMR spectroscopy. After 7 d, the signal corresponding to the dichloroborane precursor at δ = 30.2 had completely disappeared and only the resonances of the target product at δ = 37.6 and of a minor by-product at δ = 24.1 were observed. Precipitated LiCl was removed by centrifugation and all volatiles were removed *in vacuo* to yield crude **89** (1.89 g, 7.08 mmol, 97%) in the form of a yellow oil. ^{1}H and ^{13}C NMR spectra were complex and full interpretation was not possible, however, they suggested the formation of a mixture of **va** and **vh** isomers. By GC-MS, only trace impurities of unknown constitution were detected; isomers of **89** were not resolved.

^{11}B NMR (64 MHz, benzene-D_6): [mixture of isomers] δ = 37.6.

MS (EI$^+$) *m*/*z* (%): 267 (30) [M^+], 167 (21) [M^+ – N*i*Pr$_2$], 146 (100) [$M^+ - C_5Me_4H$].

4.2.1.4.2. Synthesis of (η^1-C_5Me_4H)B(N*i*Pr$_2$)N(H)Ph (90)

A solution of (η^1-C_5Me_4H)B(N*i*Pr$_2$)Cl (**89**) (1.89 g, 7.08 mmol) in hexane (20 mL) was added to a freshly prepared suspension of lithium anilide in toluene (40 mL) at 0 °C. The mixture was subsequently stirred for 16 h at ambient temperature to give a yellow, slightly cloudy solution. All volatiles were removed *in vacuo* to yield a brown oil. The residue was extracted with hexane, the residual solid removed by centrifugation and the solvent again removed *in vacuo* to yield crude **90** (2.01 g, 6.23 mmol, 88 %) as a brown oil. ^{1}H and ^{13}C NMR spectra were complex due to a large number of isomers and could not be interpreted. However, the ^{11}B NMR spectrum showed only a single signal at δ = 30.4 consistent with the target compound and GC-MS indicated that 15% (η^1-C_5Me_4H)B{N(H)Ph}$_2$ was the only notable impurity.

^{11}B NMR (64 MHz, benzene-D_6): [mixture of isomers] δ = 30.4.

MS (EI$^+$) *m*/*z* (%): 324 (19) [M$^+$], 280 (7) [M$^+$ – H – *i*Pr], 203 (100) [M$^+$ – C_5Me_4H].

4.2.1.5. Diborane(4) based ligand precursors

4.2.1.5.1. Synthesis of (η^1-C_5H_5)(BNMe$_2$)$_2$Cl (91)

A solution of $(Me_2N)_2B_2Cl_2$ (2.45 g, 16.1 mmol) was dissolved in hexane (10 mL) and added to a suspension of NaCp (1.50 g, 16.9 mmol) in toluene (40 mL) at 0 °C. The reaction mixture was stirred for 2 h at 0 °C, then for a further 21 h at ambient temperature. The reaction progress was monitored by ^{11}B NMR spectroscopy. The signal corresponding to the starting material at δ = 38.4 gradually diappeared while a new signal corresponding to the product appeared at δ ~ 42. After complete disappearance of the signal corresponding to the starting material the reaction mixture was worked-up. Precipitated NaCl and excess NaCp were removed by centrifugation and all volatiles were evaporated *in vacuo* to give the target compound **91** as a mixture of **va** and **vh** isomers (isomer ratio approximately 5:2, assignment of constitutional isomers to the two sets of NMR spectroscopic data not possible) in the form of a pale yellow oil (2.31 g, 11.0 mmol, 68.3%) that crystallised at –30 °C.

^{1}H NMR (200 MHz, benzene-D_6): [major isomer]: δ = 2.49 (s, 3H, Me), 2.64 (s, 3H, Me), 2.71 (s, 3H, Me), 2.72 (s, 3H, Me), 3.12 (m, 2H, CH_2), 6.57 – 6.59 (m, 1H, CH_{Cp}), 6.65 – 6.68 (m, 1H, CH_{Cp}), 6.91 – 6.93 (m, 1H, CH_{Cp});

[minor isomer]: δ = 2.51 (s, 3H, Me), 2.67 (s, 3H, Me), 2.70 (s, 3H, Me), 2.77 (s, 3H, Me), 2.88 (m, 2H, CH_2), 6.42 – 6.45 (m, 1H, CH_{Cp}), 6.63 – 6.64 (m, 1H, CH_{Cp}), 6.88 – 6.91 (m, 1H, CH_{Cp}).

^{13}C NMR (75 MHz, benzene-D_6): [major isomer]: δ = 37.5 (Me), 40.3 (Me), 41.9 (Me), 45.1 (Me), 46.7 (CH_2), 133.6 (CH_{Cp}), 137.3 (CH_{Cp}), 142.5 (CH_{Cp}), BC resonance not observed;

[minor isomer]: δ = 37.5 (Me), 40.4 (Me), 41.9 (Me), 43.4 (CH_2), 44.6 (Me), 132.5 (CH_{Cp}), 136.9 (CH_{Cp}), 139.8 (CH_{Cp}), BC resonance not observed.

^{11}B NMR (64 MHz, benzene-D_6): [isomer mixture]: δ = 41.5 ($\omega_{1/2}$ = 245 Hz).

MS (EI$^+$) *m*/*z* (%): 210 (77) [M^+], 195 (14) [M^+ – Me], 165 (17) [M^+ – $HNMe_2$], 145 (16) [M^+ – C_5H_5], 119 (75) [M^+ – $ClBNMe_2$ – H], 99 (100) [$B(NMe_2)_2^+$], 90 (61) [M^+ – $(C_5H_5)BNMe_2$].

4.2.1.5.2. Synthesis of (η^1-C_5H_5)$(BNMe_2)_2${N(H)Ph} (92)

(η^1-C_5H_5)$(BNMe_2)_2$Cl (**91**) (1.37 g, 6.52 mmol) was dissolved in hexane (30 mL) and added dropwise to a suspension of Li[NHPh] (6.52 mmol) in toluene (30 mL) at 0 °C. The reaction mixture was stirred for 1 h at 0 °C and subsequently for 16 h at ambient temperature. Precipitated LiCl was removed by centrifugation and all volatiles were evaporated *in vacuo* to yield the crude product as a pale yellow oil. This oil was distilled over a short path *in vacuo* at 80-100 °C to yield **92** as a mixture of **va** and **vh** isomers (isomer ratio approximately 3:1, assignment of constitutional isomers to the two sets of NMR spectroscopic data not possible) in the form of a colourless oil (0.87 g, 3.26 mmol, 50.0%).

^{1}H NMR (300 MHz, benzene-D_6): [major isomer]: δ = 2.36 (s, 3H, Me), 2.63 (s, 3H, Me), 2.80 (s, 3H, Me), 2.81 (s, 3H, Me), 3.10 (m, 2H, CH_2), 4.90 (br s, 1H, NH), 6.50 – 6.55 (m, 1H, CH_{Cp}), 6.60 – 6.65 (m, 1H, CH_{Cp}), 6.90 (m, 1H, CH_{Cp}), 6.75 – 7.20 (m, 5H, CH_{Ph});

[minor isomer]: δ = 2.69 (s, 3H, Me), 2.76 (s, 3H, Me), 2.79 (s, 3H, Me), 2.81 (s, 3H, Me), 2.82 (m, 2H, CH_2), 4.90 (br s, 1H, NH), 6.35 – 6.40 (m, 1H, CH_{Cp}), 6.50 (m, 1H, CH_{Cp}), 6.85 (m, 1H, CH_{Cp}), 6.75 – 7.20 (m, 5H, CH_{Ph}).

^{13}C NMR (75 MHz, benzene-D_6): [major isomer]: δ = 35.5 (Me), 40.4 (Me), 42.1 (Me), 44.9 (Me), 46.8 (CH_2), 118.2 (*o*-CH_{Ph}), 119.9 (*p*-CH_{Ph}), 129.3 (*m*-CH_{Ph}), 133.6 (CH_{Cp}), 136.7 (CH_{Cp}), 140.9 (CH_{Cp}), 147.6 (*ipso*-CH_{Ph}), BC resonance not observed;

[minor isomer]: δ = 40.5 (Me), 42.2 (Me), 42.6 (Me), 43.3 (CH_2), 44.5 (Me), 118.2 (*o*-CH_{Ph}), 119.9 (*p*-CH_{Ph}), 129.4 (*m*-CH_{Ph}), 132.2 (CH_{Cp}), 137.4 (CH_{Cp}), 139.3 (CH_{Cp}), 147.6 (*ipso*-CH_{Ph}), BC resonance not observed.

^{11}B NMR (64 MHz, benzene-D_6): [isomer mixture]: δ = 34.0 (BN_2), 46.0 (CBN).

MS (EI$^+$) *m*/*z* (%): 266 (100) [M^+ – H], 221 (25) [M^+ – $HNMe_2$ – H], 147 (88) [M^+ – $(C_5H_5)BNMe_2$].

IR 3399 w ν(NH).

4.2.1.5.3. Synthesis of (3-C_9H_7)($BNMe_2$)$_2$Cl (93)

(1-C_9H_7)($BNMe_2$)$_2$Cl (1.48 g, 5.68 mmol) was dissolved in toluene (20 mL) and NEt_3 (0.06 g, 0.6 mmol) was added. After stirring the solution for 2 d at ambient temperature, the solvent and amine were removed *in vacuo* to yield **93** in quantitative yield.

Analytical data for (3-C_9H_7)($BNMe_2$)$_2$Cl have been previously reported.

4.2.1.5.4. Synthesis of (3-C_9H_7)($BNMe_2$)$_2${N(H)Ph} (94)

(3-C_9H_7)($BNMe_2$)$_2$Cl (**93**) (1.48 g, 5.68 mmol) was dissolved in toluene (20 mL) and added dropwise to a suspension of Li[NHPh] (5.68 mmol) in toluene (40 mL) at 0 °C. The suspension was stirred for 1 h at 0 °C and for additional 16 h at ambient temperature. Precipitated LiCl was removed by centrifugation and all volatiles were removed *in vacuo* to yield the crude product as a brown oil. The brown oil was diluted with toluene (4 mL) and hexane (2 mL) were added to precipitate **94** as a white solid. The precipitate was separated from the supernatant by centrifugation and dried *in vacuo* to yield pure **94** (1.42 g, 4.55 mmol, 80%).

^{1}H NMR (300 MHz, benzene-D_6): δ = 2.31 (s, 3H, Me), 2.70 (s, 3H, Me), 2.73 (s, 3H, Me), 2.87 (s, 3H, Me), 3.11 (d, $^3J_{H\text{-}H}$ = 1.9 Hz, 2H, CH_2), 4.87 (br s, 1H, NH), 6.35 (t, $^3J_{H\text{-}H}$ = 1.9 Hz, 1H, $CH_{Ind\text{-}5\text{-}ring}$), 6.80 – 6.90 (m, 1H, *p*-CH_{Ph}), 6.98 – 7.07 (m, 2H, *o*-CH_{Ph}), 7.10 – 7.15 (m, 1H, $CH_{Ind\text{-}6\text{-}ring}$), 7.18 – 7.25

(m, 2H, *m*-CH_{Ph}), 7.26 – 7.40 (m, 2H, $CH_{Ind\text{-}6\text{-}ring}$), 7.50 – 7.58 (m, 1H, $CH_{Ind\text{-}6\text{-}ring}$).

^{13}C NMR (75 MHz, benzene-D_6): δ = 35.6 (Me), 40.6 (CH_2), 41.7 (Me), 42.4 (Me), 44.4 (Me), 118.5 (*p*-CH_{Ph}), 120.2 (*o*-CH_{Ph}), 122.8 ($CH_{Ind\text{-}6\text{-}ring}$), 124.0 ($CH_{Ind\text{-}6\text{-}ring}$), 124.2 ($CH_{Ind\text{-}6\text{-}ring}$), 126.3 ($CH_{Ind\text{-}6\text{-}ring}$), 129.4 (*m*-$CH_{Ph}$), 138.5 ($CH_{Ind\text{-}5\text{-}ring}$), 145.0 (*ipso*-$C_{Ph}$), 147.5 (*quaternary* C_{Ind}), 148.7 (*quaternary* C_{Ind}), BC resonance not observed.

^{11}B NMR (64 MHz, benzene-D_6): δ = 34.3 (BN_2), 48.0 (BCN).

MS (EI$^+$) *m*/*z* (%): 317 (50) [M^+], 302 (19) [M^+ – Me], 272 (31) [M^+ – $HNMe_2$], 147 (100) [$(Me_2N)BN(H)Ph^+$], 132 (81) [$(Me_2N)BN(H)Ph^+$ – Me].

IR 3398 w ν(NH).

4.2.1.6. Ferrocenyl borane based ligand precursors and related reactions

4.2.1.6.1. Reaction of [$FcBBr_2$] with NaCp

A solution of [$FcBBr_2$] (1.14 g, 3.2 mmol) in pentane (20 mL) was added dropwise to a suspension of NaCp (0.26 g, 2.9 mmol) in pentane (20 mL) at 0 °C. The resulting red-brown suspension was allowed to warm to ambient temperature and was subsequently stirred for 16 h. Precipitated NaBr was removed by centrifugation and all volatiles were removed *in vacuo* to yield a red oil. ^{1}H, ^{11}B and ^{13}C NMR spectra showed signals corresponding to [$FcB(\eta^1\text{-}C_5H_5)_2$] as the predominant product and unreacted [$FcBBr_2$]. Furthermore, in the ^{13}C NMR spectrum a set of signals of low intensity was detected that may correspond to [$FcB(\eta^1\text{-}C_5H_5)Br$] ($\delta(^{13}C)$ = 46.6 (CH_2), 70.4 ($CH_{C_5H_5Fe}$), 71.4 ($CH_{C_5H_4B}$), 76.4 ($CH_{C_5H_4B}$), 134.2 ($CH_{C_5H_5B}$), 143.2 ($CH_{C_5H_5B}$), 152.4 ($CH_{C_5H_5B}$), CB resonance not observed).

4.2.1.6.2. Reaction of [$FcBBr_2$] with LiInd

[$FcBBr_2$] (0.44 g, 1.2 mmol) was dissolved in toluene (3 mL), cooled to –80 °C and added to a suspension of LiInd (0.15 g, 1.2 mmol) in toluene (10 mL) that was also cooled to –80 °C. After 45 min, an aliquot was removed, diluted with benzene-D_6 and a ^{11}B NMR spectrum was recorded. The spectrum displayed a signal at δ = 45.2 that was attributed to [$FcBBr_2$] and a broad signal at δ = 60.7 that may indicate formation of

[FcB(1-C_9H_7)Br]. The reaction mixture was allowed to warm to ambient temperature and the monitoring process repeated. The latter ^{11}B NMR spectrum revealed formation of an additional product in high yield giving rise to a signal at δ = 38.3. Separation of the components of the reaction mixture was not possible.

4.2.1.6.3. Reaction of [$FcBBr_2$] with [BH_3·SMe_2]

[$FcBBr_2$] (99 mg, 0.28 mmol) was dissolved in benzene-D_6 (0.5 mL). One drop of [BH_3·SMe_2] (2 M solution in toluene) was added and ^{1}H and ^{11}B NMR (proton coupled) spectra were recorded immediately. In both spectra, signals corresponding to [$BBrH_2$·SMe_2] {δ(^{11}B) = –11.3, triplet; δ(^{1}H) = 1.32, singlet, SMe_2} and [BBr_2H·SMe_2] {δ(^{11}B) = –8.1, doublet; δ(^{1}H) = 1.34, singlet, SMe_2} were detected besides other signals for unidentified compounds {δ(^{11}B) = 42.3, singlet; δ(^{1}H) = 3.95, singlet; 4.01, singlet; 4.37, singlet; integral ratios *ca.* 5:1:4}. After 16 h, a repeat analysis indicated the presence of diborane(6) {δ(^{11}B) = 16.9; triplet of triplets, $^1J_{B-H_{bridging}}$ = 48 Hz, $^1J_{B-H_{terminal}}$ = 134 Hz}, [$BBrH_2$·SMe_2], [BBr_2H·SMe_2], [$FcBBr_2$] and an unidentified product {δ(^{11}B) = 54.5, broad singlet; δ(^{1}H) = 4.00, singlet; 4.45, pseudo-triplet; 4.71, pseudo-triplet; integral ratio *ca.* 5:2:2}.

4.2.1.6.4. Reaction of [$FcBBr_2$] with [$FcBR_2$] (R = η^1-C_5H_5, 1-C_9H_7, 3-C_9H_7) in the presence of [BH_3·SMe_2]

Equal molar quantities of [$FcBBr_2$] and [$FcBR_2$] (R = η^1-C_5H_5, 1-C_9H_7, 3-C_9H_7) were separately dissolved and the solutions combined (for quantities and solvents see Table 3). ^{1}H and ^{11}B NMR spectra were recorded on the mixture and showed only signals corresponding to the two respective starting materials. *Ca*. 20 mol-% [BH_3·SMe_2] (as a 2 M solution in toluene) were then added and reaction progress was monitored by ^{1}H and ^{11}B NMR spectroscopy. In all cases, reaction pathways were complex and resulted in a large number of products as evidenced by complicated NMR spectra and the components of the product mixtures could neither be separated nor identified.

Table 3. Reaction conditions for the conversion of [$FcBBr_2$] with [$FcBR_2$] in the presence of 20 mol-% [$BH_3{\cdot}SMe_2$].

R in [$FcBR_2$]	Quantity [$FcBR_2$] / [$FcBBr_2$]	Solvent	Volume of solvent
η^1-C_5H_5	0.43 mmol	benzene-D_6	1 mL
1-C_9H_7	0.56 mmol	toluene	10 mL
3-C_9H_7	0.59 mmol	toluene	10 mL

4.2.1.6.5. Synthesis of [(η^5-C_5H_5)Fe{η^5-C_5H_4B(Br)N(H)*t*Bu}] (98)

[$FcBBr_2$] (1.44 g, 4.05 mmol) was dissolved in toluene (30 mL), cooled to –80 °C and a suspension of Li[NH*t*Bu] (0.32 g, 4.05 mmol) in toluene (30 mL) was added dropwise over a 45 min period. After stirring the mixture for 1 h at –80 °C, it was allowed to warm to ambient temperature and stirred for a further 1 h. The pale yellow precipitate was removed by centrifugation. All volatiles were then removed *in vacuo* to yield **98** (1.32 g, 3.79 mmol, 94%) as an isomeric mixture (presumably *E* and *Z* isomers with respect to the substituents of the B=N fragment; isomer ratio *ca*. 10:1; assignment of *E* and *Z* conformation to the two sets of NMR spectroscopic data not possible) in the form of a red oil that crystallised on standing at ambient temperature.

^{1}H NMR (400 MHz, benzene-D_6): [major isomer]: δ = 1.29 (s, 9H, Me_{tBu}), 4.06 (s, 5H, $CH_{C_5H_5}$), 4.23 (pt, 2H, $CH_{C_5H_4B}$), 4.32 (pt, 2H, $CH_{C_5H_4B}$), 4.54 (br s, 1H, NH);

[minor isomer]: δ = 1.27 (s, 9H, Me_{tBu}), 4.06 (s, 5H, $CH_{C_5H_5}$), 4.22 (pt, 2H, $CH_{C_5H_4B}$), 4.31 (pt, 2H, $CH_{C_5H_4B}$), 4.59 (br s, 1H, NH).

^{13}C NMR (101 MHz, benzene-D_6): [major isomer]: δ = 32.0 (Me_{tBu}), 51.4 (*quaternary* C_{tBu}), 69.5 ($CH_{C_5H_5}$), 72.6 ($CH_{C_5H_4B}$), 73.6 ($CH_{C_5H_4B}$), BC resonance not observed;

[minor isomer]: δ = 31.9 (Me_{tBu}), 50.8 (*quaternary* C_{tBu}), 69.4 ($CH_{C_5H_5}$), 72.5 ($CH_{C_5H_4B}$), 73.2 ($CH_{C_5H_4B}$), BC resonance not observed.

^{11}B NMR (64 MHz, benzene-D_6): [mixture of isomers]: δ = 35.3.

4.2.1.6.6. Synthesis of [(η^5-C_5H_5)Fe{η^5-C_5H_4B(Br)N(H)Ph}] (99)

Following essentially the same procedure as for **98**, [$FcBBr_2$] (2.19 g, 6.16 mmol) was reacted with Li[NHPh] (0.61 g, 6.16 mmol) in toluene (80 mL). After work-up, **99** (2.02 g, 5.49 mmol, 89%) was obtained in the form of a red oil. The ^{1}H and ^{13}C NMR spectra at ambient temperature showed very broad signals, probably due to interconversion of two isomers. At low temperatures, two sets of signals were resolved in the ^{1}H and ^{13}C NMR spectra, corresponding to two isomers (presumably *E* and *Z* isomers with respect to the substituents of the B=N fragment) in approximately a 5:2 ratio (assignment of *E* and *Z* conformation to the two sets of NMR spectroscopic data not possible).

^{1}H NMR (300 MHz, dichloromethane-D_2, –30 °C): [major isomer]: δ = 4.24 (s, 5H, $CH_{C_5H_5}$), 4.53 – 4.58 (m, 4H, $CH_{C_5H_4B}$), 6.59 (br s, 1H, NH), 7.16 – 7.40 (m, 5H, CH_{Ph}).

[minor isomer]: δ = 4.11 (pt, 2H, $CH_{C_5H_4B}$), 4.14 (s, 5H, $CH_{C_5H_5}$), 4.42 (pt, 2H, $CH_{C_5H_4B}$), 6.50 (br s, 1H, NH), 7.16 – 7.40 (m, 5H, CH_{Ph}).

^{13}C NMR (75 MHz, dichloromethane-D_2, –30 °C): [major isomer]: δ = 69.2 ($CH_{C_5H_5}$), 73.2 ($CH_{C_5H_4B}$), 73.5 ($CH_{C_5H_4B}$), 123.7 (*o*-CH_{Ph}), 125.0 (*p*-CH_{Ph}), 128.7 (*m*-CH_{Ph}), 141.4 (*ipso*-C_{Ph}), CB resonance not observed.

[minor isomer]: δ = 69.5 ($CH_{C_5H_5}$), 73.0 ($CH_{C_5H_4B}$), 76.1 ($CH_{C_5H_4B}$), 124.1 (*o*-CH_{Ph}), 125.0 (*p*-CH_{Ph}), 128.9 (*m*-CH_{Ph}), 141.5 (*ipso*-C_{Ph}), BC resonance not observed.

^{11}B NMR (64 MHz, dichloromethane-D_2): [mixture of isomers]: δ = 36.7.

4.2.1.6.7. Synthesis of [(η^5-C_5H_5)Fe{η^5-C_5H_4B(η^1-C_5H_5)N(H)Ph}] (100)

Procedure A: A suspension of NaCp (0.10 g, 1.14 mmol, 2 equivalents) in toluene (15 mL) was cooled to –80 °C and a solution of [(η^5-C_5H_5)Fe{η^5-C_5H_4B(Br)N(H)Ph}] (**99**) (0.21 g, 0.57 mmol) in toluene (5 mL) was added dropwise over a period of 5 min. The reaction mixture was allowed to warm to ambient temperature and was subsequently stirred for 16 h. All solids (NaBr and excess NaCp)

were removed by centrifugation and all volatiles were removed *in vacuo* to yield an orange coloured oil (0.18 g).

Procedure B: [(η^5-C_5H_5)Fe{η^5-$C_5H_4B(Br)N(H)Ph$}] (**99**) (0.31 g, 0.84 mmol) was dissolved in toluene (20 mL) and cooled to –80 °C. A solution of NaCp (0.075g, 0.84 mmol) in toluene/thf (1:1 v/v, 20 mL) was added dropwise over a period of 15 min. The colour of the reaction mixture changed from red to yellow-orange during the addition. After 2 h at –80 °C, the reaction mixture was warmed to ambient temperature and all volatiles were removed *in vacuo* to yield an orange oil. The oil was dissolved in toluene (30 mL), insoluble NaBr was removed by centrifugation and the solvent was removed again *in vacuo* to yield an orange oil.

The products obtained by the two procedures showed virtually identical ^{1}H and ^{11}B NMR spectra. The signals in the ^{1}H NMR spectra were very poorly resolved and signals could not be assigned. The ^{11}B NMR signal at δ = 40 may be attributed to the formation of the target product **100**.

4.2.1.6.8. Synthesis of [(η^5-C_5H_5)Fe{η^5-$C_5H_4B(1\text{-}C_9H_7)N(H)Ph$}] (101)

A solution of [(η^5-C_5H_5)Fe{η^5-$C_5H_4B(Br)N(H)Ph$}] (**99**) (0.78 g, 2.11 mmol) in toluene (40 mL) was cooled to –70 °C and added to solid LiInd (0.26 g, 2.11 mmol). The mixture was allowed to warm to ambient temperature and subsequently stirred for 16 h. Precipitated LiBr was removed by centrifugation and all volatiles were removed *in vacuo* to yield a red oil that solidified at ambient temperature. Pure **101** (0.68 g, 1.68 mmol, 80%) was obtained as orange coloured crystals suitable for *X*-ray structure determination by recrystallisation from toluene at –30 °C. At ambient temperature, solution ^{1}H and ^{13}C NMR spectra showed two sets of signals corresponding to two isomers of **101** (presumably *E* and *Z* isomers with respect to the substituents of the B=N fragment) in approximately a 5:2 ratio (assignment of *E* and *Z* conformation to the two sets of NMR spectroscopic data not possible).

^{1}H NMR (500 MHz, benzene-D_6): [major isomer]: δ = 4.02 (s, 5H, $CH_{C_5H_5}$), 4.11 (BCH), 4.15 (s, 1H, $CH_{C_5H_4B}$), 4.18 (s, 1H, $CH_{C_5H_4B}$), 4.19 (s, 2H, $CH_{C_5H_4B}$), 5.41 (s, 1H, NH), 6.6 – 7.7 (m, 11H, $CH_{Ph/Ind}$);

[minor isomer]: δ = 3.67 (s, 1H, $CH_{C_5H_4B}$), 3.84 (s, 1H, $CH_{C_5H_4B}$), 3.93 (s, 5H, $CH_{C_5H_5}$), 4.03 (s, 2H, $CH_{C_5H_4B}$), 4.26 (BCH), 6.27 (s, 1H, NH), 6.9 – 7.5 (m, 11H, $CH_{Ph/Ind}$).

^{13}C NMR (126 MHz, benzene-D_6): [major isomer]: δ = 49.7 (BCH), 69.0 ($CH_{C_5H_5}$), 72.7 ($CH_{C_5H_4B}$), 72.8 ($CH_{C_5H_4B}$), 75.5 ($CH_{C_5H_4B}$), 75.9 ($CH_{C_5H_4B}$), 121.9 ($CH_{Ph/Ind}$), 124.0 ($CH_{Ph/Ind}$), 124.7 ($CH_{Ph/Ind}$), 124.9 ($CH_{Ph/Ind}$), 126.0 ($CH_{Ph/Ind}$), 126.3 ($CH_{Ph/Ind}$), 128.7 ($CH_{Ph/Ind}$), 130.4 ($CH_{Ph/Ind}$), 138.9 ($CH_{Ph/Ind}$), 143.5 (*quaternary* C_{Ind}), 145.6 (*quaternary* C_{Ind}), 148.1 (*ipso*-C_{Ph}), $BC_{C_5H_4B}$ resonance not observed;

[minor isomer]: δ = 46.2 (BCH), 69.0 ($CH_{C_5H_5}$), 71.8 ($CH_{C_5H_4B}$), 71.9 ($CH_{C_5H_4B}$), 72.4 ($CH_{C_5H_4B}$), 73.1 ($CH_{C_5H_4B}$), 121.3 ($CH_{Ph/Ind}$), 124.3 ($CH_{Ph/Ind}$), 124.4 ($CH_{Ph/Ind}$), 124.5 ($CH_{Ph/Ind}$), 124.8 ($CH_{Ph/Ind}$), 125.9 ($CH_{Ph/Ind}$), 128.6 ($CH_{Ph/Ind}$), 129.4 ($CH_{Ph/Ind}$), 130.8 ($CH_{Ph/Ind}$), 143.3 (*quaternary* C_{Ind}), 146.0 (*quaternary* C_{Ind}), 148.7 (*ipso*-C_{Ph}), $BC_{C_5H_4B}$ resonance not observed.

^{11}B NMR (64 MHz, benzene-D_6): [mixture of isomers]: δ = 42.9.

4.2.1.6.9. Synthesis of [(η^5-C_5H_5)Fe{η^5-C_5H_4B(3-C_9H_7)N(H)Ph}] (102)

[(η^5-C_5H_5)Fe{η^5-C_5H_4B(1-C_9H_7)N(H)Ph}] (**101**) (0.15 g, 0.37 mmol) was dissolved in toluene (20 mL), neat NEt_3 (0.05 mL, 0.37 mmol) added and the reaction mixture stirred for 16 h at ambient temperature. All volatiles were removed *in vacuo* to yield **102** (0.15 g, 0.37 mmol, 100%) in the form of a red oil.

^{1}H NMR (500 MHz, benzene-D_6): δ = 3.31 (m, 2H, $CH_{2\ Ind}$), 4.05 (s, 5H, $CH_{C_5H_5}$), 4.29 (m, 2H, $CH_{C_5H_4B}$), 4.31 (m, 2H, $CH_{C_5H_4B}$), 6.33 – 7.40 (m, 10H, $CH_{Ph/Ind}$), NH resonance not observed.

^{13}C NMR (126 MHz, benzene-D_6): δ = 41.0 ($CH_{2\ Ind}$), 68.9 ($CH_{C_5H_5}$), 72.8 ($CH_{C_5H_4B}$), 74.0 ($CH_{C_5H_4B}$), 121.7 ($CH_{Ph/Ind}$), 122.9 ($CH_{Ph/Ind}$), 123.2 ($CH_{Ph/Ind}$), 123.9 ($CH_{Ph/Ind}$), 124.6 ($CH_{Ph/Ind}$), 126.4 ($CH_{Ph/Ind}$), 129.1 ($CH_{Ph/Ind}$), 140.2

($CH_{Ph/Ind}$), 144.1 (*quaternary* C_{Ind}), 144.4 (*quaternary* C_{Ind}), 147.9 (*ipso*-C_{Ph}), BC resonances not observed.

^{11}B NMR (64 MHz, benzene-D_6): δ = 41.5.

4.2.1.6.10. Synthesis of [(η^5-C_5H_5)Fe{η^5-C_5H_4B(N{H}*t*Bu)$_2$}] (103)

A solution of Li[NH*t*Bu] (0.24 g, 3.04 mmol, 2.0 equivalents) in toluene (20 mL) was added to a solution of [$FcBBr_2$] (0.54 g, 1.52 mmol) in toluene (35 mL) at –70 °C. Within 30 min at –70 °C, the mixture formed a bright yellow-orange coloured suspension. The mixture was then stirred for an additional 30 min at –70 °C and subsequently for 16 h at ambient temperature. Precipitated LiBr was removed by centrifugation and all volatiles were removed *in vacuo* to yield **103** (0.44 g) as an orange coloured oil. ^{1}H and ^{13}C NMR spectra showed the presence of significant amounts (*ca.* 25%) of an additional product for which the formulation [{–(Fc)B–N(*t*Bu)–}$_3$] is consistent with the data.

^{1}H NMR (200 MHz, benzene-D_6): [major product]: δ = 1.22 (s, 18H, Me_{tBu}), 3.37 (br s, 2H, NH), 4.07 (s, 5H, $CH_{C_5H_5}$), 4.13 (pt, 2H, $CH_{C_5H_4B}$), 4.29 (pt, 2H, $CH_{C_5H_4B}$);

[minor product]: δ = 1.23 (s, 9H, Me_{tBu}), 4.04 (s, 5H, $CH_{C_5H_5}$), 4.22 (pt, 2H, $CH_{C_5H_4B}$), 4.26 (pt, 2H, $CH_{C_5H_4B}$).

^{13}C NMR (101 MHz, benzene-D_6): [major product]: δ = 33.3 (Me_{tBu}), 48.7 (*quaternary* C_{tBu}), 68.9 ($CH_{C_5H_5}$), 69.3 ($CH_{C_5H_4B}$), 74.1 ($CH_{C_5H_4B}$), BC resonance not observed;

[minor product]: δ = 33.1 (Me_{tBu}), 50.0 (*quaternary* C_{tBu}), 68.8 ($CH_{C_5H_5}$), 71.4 ($CH_{C_5H_4B}$), 72.4 ($CH_{C_5H_4B}$), BC resonance not observed.

^{11}B NMR (64 MHz, benzene-D_6): [major product]: δ = 29.3;

[minor product]: δ = 42.6.

4.2.1.6.11. Synthesis of [(η^5-C_5H_5)Fe{η^5-C_5H_4B(N{H}Ph)$_2$}] (104)

[$FcBBr_2$] (0.62 g, 1.74 mmol) was dissolved in toluene (40 mL) and cooled to –80 °C. A suspension of Li[NHPh] (0.34 g, 3.48 mmol, 2.0 equivalents) in toluene (40

mL) was then added dropwise and the reaction mixture stirred for 2 h at –80 °C before warming to ambient temperature and stirring for a further 16 h. Precipitated LiBr was removed by centrifugation and all volatiles were removed *in vacuo* to yield **104** (0.60 g, 1.57 mmol, 91%) as a red oil.

^{1}H NMR (500 MHz, benzene-D_6): δ = 3.98 (s, 5H, $CH_{C_5H_5}$), 4.14 (pt, 2H, $CH_{C_5H_4B}$), 4.18 (pt, 2H, $CH_{C_5H_4B}$), 5.42 (br s, 2H, NH), 6.30 – 7.10 (m, 10H, CH_{Ph}).

^{13}C NMR (126 MHz, benzene-D_6): δ = 69.1 ($CH_{C_5H_5}$), 71.1 ($CH_{C_5H_4B}$), 74.1 ($CH_{C_5H_4B}$), 115.1 (*p*-CH_{Ph}), 121.9 (*o*-CH_{Ph}), 129.3 (*m*-CH_{Ph}), 144.3 (*ipso*-C_{Ph}), BC resonance not observed.

^{11}B NMR (64 MHz, benzene-D_6): δ = 31.5.

4.2.2. Complex synthesis

4.2.2.1. Amino monoborane based non-chelating titanium complexes

4.2.2.1.1. Synthesis of [Ti{(η^5-C_5H_4)B(N*i*Pr$_2$)N(H)*i*Pr}(NMe$_2$)$_3$] (105)

The ligand precursor (η^1-C_5H_5)B(N*i*Pr$_2$)N(H)*i*Pr (**77**) (1.56 g, 6.67 mmol) was dissolved in toluene (30 mL) and neat [Ti(NMe$_2$)$_4$] (1.50 g, 6.67 mmol) was added by syringe at 0 °C. The resulting yellow solution was allowed to warm to ambient temperature and no colour change was observed. The reaction mixture was then heated to 70 °C during which the colour changed slowly to light orange. Upon subsequent reflux for 3 h the mixture further darkened in colour. After cooling to ambient temperature, all volatiles were removed *in vacuo* to yield **105** (2.50 g, 6.06 mmol, 91%) in the form of a dark red oil.

^{1}H NMR (200 MHz, benzene-D_6): δ = 1.10 (d, $^{3}J_{H\text{-}H}$ = 6.3 Hz, 6H, Me_{iPr}), 1.16 (d, $^{3}J_{H\text{-}H}$ = 6.8 Hz, 12H, Me_{iPr}), 3.18 (s, 18H, NMe_2), 3.53 – 3.75 (m, 3H, CH_{iPr}), 5.96 (pt, 2H, CH_{Cp}), 6.42 (pt, 2H, CH_{Cp}), NH resonance not observed.

^{13}C NMR (101 MHz, benzene-D_6): δ = 23.8 (Me_{iPr}), 28.0 (Me_{iPr}), 44.2 (CH_{iPr}), 46.4 (br, CH_{iPr}), 50.4 (NMe_2), 111.2 (CH_{Cp}), 120.0 (CH_{Cp}), BC resonance not observed.

^{11}B NMR (64 MHz, benzene-D_6): δ = 28.8.

MS (EI$^+$) *m/z* (%): 369 (7) [M^+ – NMe_2], 323 (6) [M^+ – 2 $HNMe_2$], 234 (13) [$(C_5H_5)B(NiPr_2)N(H)iPr^+$], 219 (55) [$(C_5H_5)B(NiPr_2)N(H)iPr^+$ – Me], 86 (100) [iPr_2^+].

IR 3441 w ν(NH).

4.2.2.1.2. Synthesis of [Ti{(η^5-C_5H_4)B(N*i*Pr$_2$)N(H)Cy}(NMe$_2$)$_3$] (106)

Following essentially the same procedure as described for **105**, (η^1-C_5H_5)B(N*i*Pr$_2$)N(H)Cy (**78**) (0.75 g, 2.73 mmol) was reacted with [Ti(NMe_2)$_4$] (0.61 g, 2.73 mmol) in toluene (20 mL). The reaction mixture was refluxed for 3 h during which the colour changed from yellow to dark red. The solvent was removed *in vacuo* to give **106** as a dark red oil (1.23 g, 2.70 mmol, 99%).

^{1}H NMR (270 MHz, toluene-D_8): δ = 1.19 (d, $^3J_{H\text{-}H}$ = 6.7 Hz, 12H, Me_{iPr}), 0.90 – 2.00 (m, 10H, CH_2), 3.18 (s, 18H, NMe_2), 3.55 – 3.75 (m, 2H, CH_{iPr}), 5.93 (pt, 2H, CH_{Cp}), 6.36 (pt, 2H, CH_{Cp}), NH resonance not observed.

^{13}C NMR (68 MHz, toluene-D_8): δ = 23.7 (Me_{iPr}), 25.8 (CH_2), 26.3 (CH_2), 38.7 (CH_2), 46.5 (CH_{Cy}), 50.3 (NMe_2), 51.2 (CH_{iPr}), 111.3 (CH_{Cp}), 119.7 (CH_{Cp}), BC resonance not observed.

^{11}B NMR (87 MHz, toluene-D_8): δ = 28.3.

MS (CI$^+$) *m/z* (%): 454 (5) [M^+ + H], 409 (71) [M^+ – $HNMe_2$], 275 (20) [$(C_5H_5)B(NiPr_2)N(H)Cy + H^+$].

IR 3441 w ν(NH).

4.2.2.1.3. Synthesis of [Ti{(η^5-C_5H_4)B(N*i*Pr$_2$)N(H)*t*Bu}(NMe$_2$)$_3$] (107)

Following the same procedure as for the synthesis of **105**, (η^1-C_5H_5)B(N*i*Pr$_2$)N(H)*t*Bu (**64**) (0.64 g, 2.58 mmol) was reacted with [Ti(NMe_2)$_4$] (0.58 g, 2.58 mmol) in toluene (20 mL). The mixture was refluxed for 2 h, then all volatiles were removed *in vacuo* to yield pure **107** (1.10 g, 2.55 mmol, 99%) in the form of a red oil.

^{1}H NMR (200 MHz, benzene-D_6): δ = 1.16 (d, 12H, Me_{iPr}), 1.19 (s, 9H, Me_{tBu}), 3.18 (s, 18H, NMe_2), 3.51 (m, 2H, CH_{iPr}), 5.91 (pt, 2H, CH_{Cp}), 6.46 (pt, 2H, CH_{Cp}), NH resonance not observed.

^{13}C NMR (75 MHz, benzene-D_6): δ = 24.0 (Me_{tBu}), 34.1 (Me_{iPr}), 46.4 (br, CH_{iPr}), 49.7 (*quaternary* C_{tBu}), 50.5 (NMe_2), 111.0 (CH_{Cp}), 120.9 (CH_{Cp}), BC resonance not observed.

^{11}B NMR (64 MHz, benzene-D_6): δ = 29.1.

MS (CI^+) *m*/*z* (%): 383 (100) [$M^+ - NMe_2$], 339 (80) [$M^+ - 2\ NMe_2$], 183 (47) [$M^+ - Ti(NMe_2)_3 - C_5H_4$].

IR 3456 w ν(NH).

4.2.2.1.4. Synthesis of [Ti{(η^5-C_5H_4)B(N*i*Pr$_2$)N(H)*i*Pr}Cl(NMe$_2$)$_2$] (108)

[Ti{(η^5-C_5H_4)B(N*i*Pr$_2$)N(H)*i*Pr}(NMe_2)$_3$] (**105**) (0.27 g, 0.65 mmol) was dissolved in hexane (10 mL) and neat Me_3SiCl (0.72 g, 6.5 mmol, 10 equivalents) was added. The red mixture was stirred for 16 h at ambient temperature. ^{1}H NMR spectroscopy on a dried sample revealed almost full conversion to the mono-chlorinated product. All volatiles were consequently removed *in vacuo* to give **108** (0.26 g, 0.64 mmol, 98%) in virtually quantitative yield as a red oil that was slightly contaminated by the corresponding dichloro complex **110**.

^{1}H NMR (400 MHz, benzene-D_6): δ = 1.07 (d, $^3J_{H\text{-}H}$ = 6.3 Hz, 6H, Me_{NHiPr}), 1.15 (d, $^3J_{H\text{-}H}$ = 6.8 Hz, 12H, Me_{NiPr_2}), 3.16 (s, 12H, NMe_2), 3.58 (m, 3H, CH_{iPr}), 5.95 (pt, 2H, CH_{Cp}), 6.47 (pt, 2H, CH_{Cp}), NH resonance not observed.

^{13}C NMR (101 MHz, benzene-D_6): δ = 23.6 (Me_{NiPr_2}), 27.7 (Me_{NHiPr}), 44.5 (CH_{NHiPr}), 46.6 (br, CH_{NiPr_2}), 48.9 (NMe_2), 113.9 (CH_{Cp}), 121.8 (CH_{Cp}), BC resonance not observed.

^{11}B NMR (64 MHz, benzene-D_6): δ = 28.9.

4.2.2.1.5. Synthesis of [Ti{(η^5-C_5H_4)B(N*i*Pr$_2$)N(H)*i*Pr}Cl$_2$(NMe$_2$)] (110)

[Ti{(η^5-C_5H_4)B(N*i*Pr$_2$)N(H)*i*Pr}Cl(NMe_2)$_2$] (**108**) (0.20 g, 0.49 mmol) was dissolved in hexane (10 mL) and neat Me_3SiCl (0.72 g, 6.5 mmol, 13 equivalents) was added. The resulting red solution was stirred for 48 h at ambient temperature. ^{1}H NMR spectroscopy on a dried sample indicated full conversion to the dichlorinated product. Consequently, all volatiles were removed *in vacuo* to yield **110** (0.18 g, 0.46 mmol, 93%) in the form of a red oil.

^{1}H NMR (400 MHz, benzene-D_6): δ = 1.08 (d, $^3J_{H\text{-}H}$ = 6.3 Hz, 6H, Me_{NHiPr}), 1.16 (d, $^3J_{H\text{-}H}$ = 6.8, 12H, Me_{NiPr_2}), 3.41 (m, $^3J_{H\text{-}H}$ = 6.3 Hz, 1H, CH_{NHiPr}), 3.45 (m, $^3J_{H\text{-}H}$ = 6.8 Hz, 2H, CH_{NiPr_2}), 3.63 (s, 6H, NMe_2), 6.47 (pt, 2H, CH_{Cp}), 6.64 (pt, 2H, CH_{Cp}), NH resonance not observed.

^{13}C NMR (101 MHz, benzene-D_6): δ = 23.3 (Me_{NiPr_2}), 27.4 (Me_{NHiPr}), 44.5 (CH_{NHiPr}), 46.7 (br, CH_{NiPr_2}), 52.6 (NMe_2), 120.6 (CH_{Cp}), 124.9 (CH_{Cp}), BC resonance not observed.

^{11}B NMR (64 MHz, benzene-D_6): δ = 27.8.

IR 3438 w ν(NH).

4.2.2.1.6. Synthesis of [Ti{(η^5-C_5H_4)B(N*i*Pr$_2$)N(H)*t*Bu}Cl$_2$(NMe$_2$)] (111)

[Ti{(η^5-C_5H_4)B(N*i*Pr$_2$)N(H)*t*Bu}(NMe_2)$_3$] (**107**) (0.83 g, 1.95 mmol) was dissolved in hexane (20 mL) to give a bright orange solution. Neat Me_3SiCl (2.11 g, 19.5 mmol, 10 equivalents) was added and the resulting mixture was stirred at ambient temperature for 6 h. ^{1}H NMR spectroscopy on a small aliquot dried *in vacuo* indicated almost full conversion to the dichloro complex. All volatiles were subsequently removed *in vacuo* to afford a red oil. Recrystallisation from hexane at 4 °C afforded bright red crystals of pure **111** in almost quantitative yield (0.74 g, 1.80 mmol, 92%).

^{1}H NMR (200 MHz, benzene-D_6): δ = 1.01 (s, 9H, Me_{tBu}), 1.07 (d, $^3J_{H\text{-}H}$ = 6.8 Hz, 12H, Me_{iPr}), 3.06 (br s, 1H, NH), 3.29 (m, $^3J_{H\text{-}H}$ = 6.8 Hz, 2H, CH_{iPr}), 3.49 (s, 6H, NMe_2), 6.30 (pt, 2H, CH_{Cp}), 6.59 (pt, 2H, CH_{Cp}).

^{13}C NMR (101 MHz, benzene-D_6): δ = 23.4 (Me_{iPr}), 34.0 (Me_{tBu}), 47.2 (br, CH_{iPr}), 49.7 (*quaternary* C_{tBu}), 52.8 (NMe_2), 120.3 (CH_{Cp}), 125.5 (CH_{Cp}), BC resonance not observed.

^{11}B NMR (64 MHz, benzene-D_6): δ = 28.2.

IR 3450 w ν(NH).

4.2.2.1.7. Formation of [{$TiCl_2(\mu$-{$OB(NHMe_2)$-η^5-C_5H_4})}$_2$-μ-O] (112) by partial hydrolysis of [Ti{(η^5-C_5H_4)B(N*i*Pr$_2$)N(H)R}$Cl_2(NMe_2)$] {R = *i*Pr (110), *t*Bu (111)}

An unsealed GC-MS vial containing a solution of [Ti{(η^5-C_5H_4)B(N*i*Pr$_2$)N(H)*i*Pr}$Cl_2(NMe_2)$] (**110**) in dichloromethane was allowed to stand for 4 weeks at ambient temperature. During this period, yellow crystals formed which were identified as [{$TiCl_2(\mu$-{$OB(NHMe_2)$-η^5-C_5H_4})}$_2$-μ-O] (**112**) by *X*-ray diffraction experiments. This product presumably arises from partial hydrolysis of the starting material. Characterisation by multinuclear NMR spectroscopy was not possible due to poor solubility in common NMR solvents.

Under the same conditions **111** hydrolyses to form the same complex **112**, as determined by *X*-ray diffraction methods.

4.2.2.2. Amino monoborane based constrained geometry complexes of titanium

4.2.2.2.1. Synthesis of [Ti{η^5:η^1-(C_5H_4)B(N*i*Pr$_2$)N(*p*-F-Ph)}$(NMe_2)_2$] (113)

(η^1-C_5H_5)B(N*i*Pr$_2$)N(H)(*p*-F-Ph) (**79**) (0.68 g, 2.38 mmol) was dissolved in toluene (30 mL) and neat [$Ti(NMe_2)_4$] (0.53 g, 2.38 mmol) was added by syringe at ambient temperature. The resulting solution changed colour from yellow to orange within minutes and darkened to become dark red-brown after 15 min at reflux temperature. The reaction mixture was stirred for a further 1 h under reflux. All volatiles were removed *in vacuo* to yield the pure product **113** (0.97 g, 2.31 mmol, 97%) as an orange coloured solid.

^{1}H NMR (200 MHz, benzene-D_6): δ = 0.91 (br m, 6H, $Me_{i\text{Pr}}$), 1.56 (br m, 6H, $Me_{i\text{Pr}}$), 2.89 (s, 12H, NMe_2), 3.20 (br m, 1H, $CH_{i\text{Pr}}$), 3.54 (br m, 1H, $CH_{i\text{Pr}}$), 5.94 (pt, 2H, CH_{Cp}), 6.22 (pt, 2H, CH_{Cp}), 6.65 – 6.92 (m, 4H, $CH_{p\text{-F-Ph}}$).

^{13}C NMR (101 MHz, benzene-D_6): δ = 21.7 (br s, $Me_{i\text{Pr}}$), 27.4 (br s, $Me_{i\text{Pr}}$), 44.6 (br s, $CH_{i\text{Pr}}$), 46.5 (br s, $CH_{i\text{Pr}}$), 47.9 (s, NMe_2), 114.9 (d, $^2J_{C\text{-F}}$ = 22 Hz, *m*-$CH_{p\text{-F-Ph}}$), 116.0 (s, CH_{Cp}), 120.0 (s, CH_{Cp}), 124.8 (d, $^3J_{C\text{-F}}$ = 7.2 Hz, *o*-$CH_{p\text{-F-Ph}}$), 151.6 (d, $^4J_{C\text{-F}}$ = 2.4 Hz, *ipso*-$C_{p\text{-F-Ph}}$), 158.7 (d, $^1J_{C\text{-F}}$ = 238 Hz, CF), BC resonance not observed.

^{11}B NMR (64 MHz, benzene-D_6): δ = 28.0.

^{19}F NMR (376 MHz, benzene-D_6): $\delta = -123.3$.

4.2.2.2.2. Synthesis of [Ti{η^5:η^1-(C_5H_4)B(N{$SiMe_3$}$_2$)NPh}(NMe_2)$_2$] (114)

Following essentially the same procedure as for the preparation of **113**, (η^1-C_5H_5)B{N($SiMe_3$)$_2$}N(H)Ph (1.51 g, 4.60 mmol) was reacted with [Ti(NMe_2)$_4$] (1.03 g, 4.60 mmol). After removing all volatiles *in vacuo*, **114** (2.10 g, 4.55 mmol, 99%) was obtained in the form of a dark red oil.

^{1}H NMR (400 MHz, toluene-D_8): $\delta = 0.40$ (s, 18H, $SiMe_3$), 3.09 (s, 12H, NMe_2), 6.04 (pt, 2H, CH_{Cp}), 6.29 (pt, 2H, CH_{Cp}), 7.0 – 7.4 (m, 5H, CH_{Ph}).

^{13}C NMR (101 MHz, toluene-D_8): $\delta = 3.9$ ($SiMe_3$), 47.4 (NMe_2), 115.6 (CH_{Cp}), 120.1 (CH_{Cp}), 121.7 (CH_{Ph}), 124.0 (CH_{Ph}), 128.7 (CH_{Ph}), 153.2 (*ipso*-C_{Ph}), BC resonance not observed.

^{11}B NMR (87 MHz, toluene-D_8): $\delta = 33.0$.

^{29}Si NMR (99 MHz, toluene-D_8): $\delta = 0.27$.

MS (CI^+) *m*/*z* (%): 329 (8) [(C_5H_5)B{N($SiMe_3$)$_2$}N(H)Ph + H^+] and ligand fragments.

4.2.2.2.3. Synthesis of [Ti{η^5:η^1-(C_5H_4)B(N*i*Pr_2)NPh}Cl_2] (70)

Following the literature procedure, a solution of [Ti{η^5:η^1-(C_5H_4)B(N*i*Pr_2)NPh}(NMe_2)$_2$] (**37**) (0.17 g, 0.42 mmol) in hexane (10 mL) was reacted with neat Me_3SiCl (0.50 g, 4.60 mmol, 11 equivalents) at 0 °C. The mixture was allowed to warm to ambient temperature and stirred for 16 h. The yellow-orange precipitate was collected by filtration, washed with hexane and dried *in vacuo*. Recrystallisation from CH_2Cl_2 at 4 °C yielded **70** (0.16 g, 0.42 mmol, 98%) as orange crystals suitable for *X*-ray diffraction experiments.

Analytical data for **70** have been previously reported.

4.2.2.2.4. Synthesis of [Ti{η^5:η^1-(C_5H_4)B(N*i*Pr_2)N(*p*-F-Ph)}Cl_2] (115)

[Ti{η^5:η^1-(C_5H_4)B(N*i*Pr_2)N(*p*-F-Ph)}(NMe_2)$_2$] (**113**) (0.41 g, 0.98 mmol) was dissolved in hexane (20 mL) and neat Me_3SiCl (1.06 g, 9.8 mmol, 10 equivalents) were added by syringe at 0 °C. After a few minutes, the colour changed from red-brown to bright orange and after 2 h a yellow precipitate had formed. The reaction mixture was

stored for 1 year at ambient temperature before work-up. All volatiles were removed *in vacuo*. The red residue was re-dissolved in dichloromethane, concentrated and stored at –30 °C for recrystallisation. Pure **115** (0.23 g, 0.57 mmol, 58%) was obtained in the form of bright red microcrystals.

^{1}H NMR (500 MHz, dichloromethane-D_2): δ = 0.91 (d, $^{3}J_{H\text{-}H}$ = 6.7 Hz, 6H, Me_{iPr}), 1.54 (d, $^{3}J_{H\text{-}H}$ = 6.9 Hz, 6H, Me_{iPr}), 3.14 (m, $^{3}J_{H\text{-}H}$ = 6.7 Hz, 1H, CH_{iPr}), 3.42 (m, $^{3}J_{H\text{-}H}$ = 6.9 Hz, 1H, CH_{iPr}), 6.44 (pt, 2H, CH_{Cp}), 7.08 (pt, 2H, CH_{Cp}), 6.84 – 7.10 (m, 4H, $CH_{p\text{-}F\text{-}Ph}$).

^{13}C NMR (126 MHz, dichloromethane-D_2): δ = 21.3 (s, Me_{iPr}), 27.6 (s, Me_{iPr}), 45.2 (s, CH_{iPr}), 47.2 (s, CH_{iPr}), 116.3 (d, $^{2}J_{C\text{-}F}$ = 23 Hz, *m*-$CH_{p\text{-}F\text{-}Ph}$), 124.1 (d, $^{3}J_{C\text{-}F}$ = 8.3 Hz, *o*-$CH_{p\text{-}F\text{-}Ph}$), 124.3 (s, CH_{Cp}), 127.3 (s, CH_{Cp}), 148.4 (d, $^{4}J_{C\text{-}F}$ = 3.7 Hz, *ipso*-$C_{p\text{-}F\text{-}Ph}$), 160.7 (d, $^{1}J_{C\text{-}F}$ = 245 Hz, CF), BC resonance not observed.

^{11}B NMR (64 MHz, dichloromethane-D_2): δ = 28.1.

^{19}F NMR (376 MHz, dichloromethane-D_2): δ = –119.1.

4.2.2.2.5. Synthesis of [Ti{η^5:η^1-(C_5H_4)B(N{$SiMe_3$}$_2$)NPh}Cl_2] (116)

Following the same procedure as for the synthesis of **70**, [Ti{η^5:η^1-(C_5H_4)B(N{$SiMe_3$}$_2$)NPh}(NMe_2)$_2$] (**114**) (1.19 g, 2.57 mmol) was reacted with excess Me_3SiCl (2.79 g, 25.5 mmol, 10 equivalents) in hexane (30 mL). After removal of all volatiles *in vacuo*, recrystallisation from hexane at ambient temperature yielded pure **116** as orange prismatic and needle shaped crystals (0.78 g, 1.75 mmol, 68%).

^{1}H NMR (270 MHz, benzene-D_6): δ = 0.10 (s, 9H, $SiMe_3$), 0.20 (s, 9H, $SiMe_3$), 5.96 (pt, 1H, CH_{Cp}), 6.07 (pt, 1H, CH_{Cp}), 6.31 (pt, 1H, CH_{Cp}), 6.61 (pt, 1H, CH_{Cp}), 6.75 – 7.45 (m, 5H, CH_{Ph}).

^{13}C NMR (68 MHz, benzene-D_6): δ = 3.7 ($SiMe_3$), 3.9 ($SiMe_3$), 119.0 ($CH_{Cp/Ph}$), 121.2 ($CH_{Cp/Ph}$), 122.7 ($CH_{Cp/Ph}$), 123.1 ($CH_{Cp/Ph}$), 123.3 ($CH_{Cp/Ph}$), 126.2 ($CH_{Cp/Ph}$), 126.5 ($CH_{Cp/Ph}$), 152.7 (*ipso*-C_{Ph}), BC resonance not observed.

^{11}B NMR (87 MHz, benzene-D_6): δ = 33.1.

^{29}Si NMR (54 MHz, benzene-D_6): δ = 1.7 (s, $SiMe_3$), 5.6 (s, $SiMe_3$).

MS (CI$^+$) *m*/*z* (%): 445 (54) [M^+], 329 (29) [$(C_5H_5)B\{N(SiMe_3)_2\}N(H)Ph + H^+$], 236 (20) [$(Me_3Si)_2NBCpH^+$], 162 (60) [$(Me_3Si)_2NH_2^+$].

4.2.2.2.6. Synthesis of [Ti{η^5:η^1-(C_9H_6)B(N*i*Pr$_2$)NPh}(NMe_2)$_2$] (117)

Employing essentially the same procedure described for the preparation of **113**, a solution of (1-C_9H_7)B(N*i*Pr$_2$)N(H)Ph (**66**) (0.87 g, 2.73 mmol) in toluene was treated with neat Ti(NMe_2)$_4$ (0.61 g, 2.73 mmol) and refluxed for 4 h. After all volatiles were removed *in vacuo*, recrystallisation twice from hexane first at –30 °C and subsequently at 4 °C afforded **117** (1.00 g, 2.21 mmol, 81%) as orange crystals.

^{1}H NMR (270 MHz, benzene-D_6): δ = 0.91 (br d, 3H, Me$_{i\text{Pr}}$), 1.03 (br d, 3H, Me$_{i\text{Pr}}$), 1.64 (br d, 6H, Me$_{i\text{Pr}}$), 2.29 (s, 6H, NMe_2), 3.08 (s, 6H, NMe_2), 3.28 (m, 1H, CH$_{i\text{Pr}}$), 3.73 (m, 1H, CH$_{i\text{Pr}}$), 6.2 – 7.8 (m, 11H, CH$_{\text{Ind/Ph}}$).

^{13}C NMR (68 MHz, benzene-D_6): δ = 22.8 (Me$_{i\text{Pr}}$), 22.0 (Me$_{i\text{Pr}}$), 27.0 (Me$_{i\text{Pr}}$), 27.7 (Me$_{i\text{Pr}}$), 44.5 (CH$_{i\text{Pr}}$), 46.4 (NMe_2), 47.0 (CH$_{i\text{Pr}}$), 49.5 (NMe_2), 107.4 (CH$_{\text{Ind/Ph}}$), 120.4 (CH$_{\text{Ind/Ph}}$), 121.4 (CH$_{\text{Ind/Ph}}$), 123.2 (CH$_{\text{Ind/Ph}}$), 123.4 (CH$_{\text{Ind/Ph}}$), 123.6 (CH$_{\text{Ind/Ph}}$), 124.4 (CH$_{\text{Ind/Ph}}$), 125.0 (CH$_{\text{Ind/Ph}}$), 126.8 (CH$_{\text{Ind/Ph}}$), 128.8 (*quarternary* C$_{\text{Ind}}$), 132.0 (*quarternary* C$_{\text{Ind}}$), 155.4 (*ipso*-C$_{\text{Ph}}$), BC resonance not observed.

^{11}B NMR (87 MHz, benzene-D_6): δ = 27.7.

MS (CI$^+$) *m*/*z* (%): 319 (40) [$(C_9H_7)B(N\textit{i}Pr_2)N(H)Ph + H^+$] and ligand fragments.

4.2.2.2.7. Synthesis of [Ti{η^5:η^1-(C_9H_6)B(N*i*Pr$_2$)NPh}Cl_2] (118)

Utilising the same procedure as for the synthesis of **70**, [Ti{η^5:η^1-(C_9H_6)B(N*i*Pr$_2$)NPh}(NMe_2)$_2$] (**12**) (0.20 g, 0.44 mmol) was reacted with excess Me_3SiCl (0.48 g, 4.4 mmol, 10 equivalents). After work-up, recrystallisation from toluene at –30 °C yielded pure **118** as red microcrystals (0.17 g, 0.39 mmol, 87%).

^{1}H NMR (270 MHz, benzene-D_6): δ = 0.74 (d, $^3J_{\text{H-H}}$ = 6.7 Hz, 3H, Me), 0.79 (d, $^3J_{\text{H-H}}$ = 6.7, 3H, Me), 1.40 (d, $^3J_{\text{H-H}}$ = 6.9, 3H, Me), 1.44 (d, $^3J_{\text{H-H}}$ = 6.9, 3H, Me), 3.13 (m, $^3J_{\text{H-H}}$ = 6.9, 1H, CH$_{i\text{Pr}}$), 3.39 (m, $^3J_{\text{H-H}}$ = 6.7, 1H, CH$_{i\text{Pr}}$), 6.3 – 7.7 (m, 11H, CH$_{\text{Ind/Ph}}$).

^{13}C NMR (101 MHz, chloroform-D): δ = 21.4 (Me), 21.7 (Me), 27.2 (Me), 27.7 (Me), 44.6 ($CH_{i\mathrm{Pr}}$), 47.0 ($CH_{i\mathrm{Pr}}$), 116.4 ($CH_{\mathrm{Ind/Ph}}$), 121.8 ($CH_{\mathrm{Ind/Ph}}$), 125.1 ($CH_{\mathrm{Ind/Ph}}$), 126.2 ($CH_{\mathrm{Ind/Ph}}$), 127.5 ($CH_{\mathrm{Ind/Ph}}$), 128.0 ($CH_{\mathrm{Ind/Ph}}$), 128.5 ($CH_{\mathrm{Ind/Ph}}$), 129.2 ($CH_{\mathrm{Ind/Ph}}$), 129.4 ($CH_{\mathrm{Ind/Ph}}$), 133.5 (*quaternary* C_{Ind}), 134.8 (*quaternary* C_{Ind}), 151.8 (*ipso*-C_{Ph}), BC resonance not observed.

^{11}B NMR (87 MHz, benzene-D_6): δ = 28.0.

MS (EI$^+$) *m*/*z* (%): 314 (100) [$M^+ - TiCl_2 - 2$ H].

4.2.2.2.8. Synthesis of [Ti{η^5:η^1-(C_5H_4)B(N*i*Pr$_2$)N*i*Pr}(NMe_2)$_2$] (119)

Procedure A: Neat [Ti{η^5-(C_5H_4)B(N*i*Pr$_2$)N(H)*i*Pr}(NMe_2)$_3$] (**105**) (1.15 g, 2.78 mmol) was heated to 135-150 °C (oil bath temperature). Samples of the dark red reaction mixture were taken frequently and subjected to ^{1}H NMR spectroscopy. After 2 h, signal integral ratios indicated *ca.* 25% conversion to the bridged target product **119** and the reaction mixture appeared to be virtually free of by-products. After 9 h, conversion was determined to be *ca.* 45%, still with only minor traces of by-products. After 33 h, however, although conversion had risen to *ca.* 75% the reaction mixture became almost black in colour and significant amounts of by-products were detected. Separation of the reaction components by recrystallisation from toluene and hexane at various temperatures was unsuccessful.

Procedure B: [Ti{η^5:η^1-(C_5H_4)B(N*i*Pr$_2$)N(H)*i*Pr}(NMe_2)$_3$] (**105**) (0.25 g, 0.60 mmol) was dissolved in toluene (20 mL). The resulting red solution was refluxed and reaction progress was monitored by ^{1}H NMR spectroscopy. After 20 h, conversion was *ca.* 35% according to intregral ratios. After 68 h, the conversion was virtually complete and only negligible traces of by-products were detected. All volatiles were removed *in vacuo* to yield **119** (0.18 g, 0.49 mmol, 82%) as a red oil. Separation of the reaction components by recrystallisation from different solvents at various temperatures was unsuccessful.

^{1}H NMR (200 MHz, benzene-D_6): δ = 1.31 (d, $^3J_{\mathrm{H\text{-}H}}$ = 6.3 Hz, 6H, $Me_{\mathrm{TiN}i\mathrm{Pr}}$), 1.36 (d, $^3J_{\mathrm{H\text{-}H}}$ = 6.8 Hz, 12H, $Me_{\mathrm{N}i\mathrm{Pr}_2}$), 2.99 (s, 12H, NMe_2), 3.59 (m, $^3J_{\mathrm{H\text{-}H}}$ = 6.8 Hz, 2H, $CH_{\mathrm{N}i\mathrm{Pr}_2}$), 4.07 (m, $^3J_{\mathrm{H\text{-}H}}$ = 6.3 Hz, 2H, $CH_{\mathrm{TiN}i\mathrm{Pr}}$), 5.78 (pt, 2H, CH_{Cp}), 6.17 (pt, 2H, CH_{Cp}).

^{13}C NMR (75 MHz, benzene-D_6): δ = 25.1 (Me_{NiPr_2}), 27.4 (Me_{TiNiPr}), 46.5 (CH_{NiPr_2}), 48.8 (NMe_2), 53.3 (CH_{TiNiPr}), 114.9 (CH_{Cp}), 119.6 (CH_{Cp}), BC resonance not observed.

^{11}B NMR (64 MHz, benzene-D_6): δ = 29.1.

4.2.2.3. Amino monoborane based constrained geometry complexes of zirconium and hafnium

4.2.2.3.1. Synthesis of [Zr{η^5:η^1-(C_5H_4)B(N*i*Pr$_2$)NPh}(NMe_2)$_2$] (120)

Solutions of the ligand precursor (η^1-C_5H_5)B(N*i*Pr$_2$)N(H)Ph (**65**) (0.64 g, 2.39 mmol) and [$Zr(NMe_2)_4$] (0.64 g, 2.39 mmol), both in toluene (20 mL), were combined at ambient temperature. During reflux for 4 h, the initially almost colourless solution became bright yellow in colour. All volatiles were removed *in vacuo*, the dark yellow residue was re-dissolved in hexane, concentrated and stored for recrystallisation at ambient temperature. Large colourless crystals of **120** (0.74 g, 1.67 mmol, 70%) were obtained after several hours.

^{1}H NMR (300 MHz, dichloromethane-D_2, –20 °C): δ = 0.86 (d, $^3J_{H\text{-}H}$ = 6.7 Hz, 6H, Me_{iPr}), 1.40 (d, $^3J_{H\text{-}H}$ = 6.9 Hz, 6H, Me_{iPr}), 2.75 (s, 12H, NMe_2), 3.19 (m, $^3J_{H\text{-}H}$ = 6.9 Hz, 1H, CH_{iPr}), 3.38 (m, $^3J_{H\text{-}H}$ = 6.7 Hz, 1H, CH_{iPr}), 6.04 (pt, 2H, CH_{Cp}), 6.50 (pt, 2H, CH_{Cp}), 6.64 – 6.71 (m, 2H, *o*-CH_{Ph}), 6.77 – 6.85 (m, 1H, *p*-CH_{Ph}), 7.07 – 7.16 (m, 2H, *m*-CH_{Ph}).

^{13}C NMR (75 MHz, dichloromethane-D_2, –20 °C): δ = 21.2 (Me_{iPr}), 26.8 (Me_{iPr}), 43.1 (NMe_2), 43.9 (CH_{iPr}), 46.0 (CH_{iPr}), 98.6 (BC), 113.6 (CH_{Cp}), 118.5 (CH_{Cp}), 120.3 (*p*-CH_{Ph}), 123.9 (*o*-CH_{Ph}), 128.2 (*m*-CH_{Ph}), 153.5 (*ipso*-C_{Ph}).

^{11}B NMR (64 MHz, benzene-D_6): δ = 27.8.

MS (EI$^+$) *m*/*z* (%): 444 (35) [M^+], 401 (63) [$M^+ - C_3H_7$], 356 (100) [$M^+ - 2\ NMe_2$], 313 (15) [$M^+ - 2\ NMe_2 - C_3H_7$], 299 (20) [$M^+ - 2\ NMe_2 - N$*i*Pr], 270 (22) [$M^+ - 2\ NMe_2 - 2\ C_3H_7$], 256 (31) [$M^+ - 2\ NMe_2 - N$*i*Pr$_2$], 44 (64) [$NMe_2^+$].

4.2.2.3.2. Synthesis of [Hf{η^5:η^1-(C_5H_4)B(N*i*Pr$_2$)NPh}(NMe_2)$_2$] (121)

A solution of the ligand precursor (η^1-C_5H_5)B(N*i*Pr$_2$)N(H)Ph (**65**) (0.86 g, 3.21 mmol) in toluene (20 mL) was combined with a solution of [$Hf(NMe_2)_4$] (1.14 g, 3.21

mmol) in toluene (20 mL) to give a pale yellow mixture. This was refluxed for 4 h, changing colour to bright yellow. All volatiles were removed *in vacuo*, the residue was re-dissolved in toluene and stored at –30 °C for recrystallisation. Pure **121** (1.06 g, 1.99 mmol, 62%) was obtained in the form of colourless crystals that were suitable for an *X*-ray structure determination.

^{1}H NMR (300 MHz, dichloromethane-D_2, –20 °C): δ = 0.85 (d, $^{3}J_{H\text{-}H}$ = 6.7 Hz, 6H, Me$_{i\text{Pr}}$), 1.40 (d, $^{3}J_{H\text{-}H}$ = 6.9 Hz, 6H, Me$_{i\text{Pr}}$), 2.77 (s, 12H, NMe_2), 3.20 (m, $^{3}J_{H\text{-}H}$ = 6.9 Hz, 1H, CH$_{i\text{Pr}}$), 3.36 (m, $^{3}J_{H\text{-}H}$ = 6.7 Hz, 1H, CH$_{i\text{Pr}}$), 6.02 (pt, 2H, CH$_{Cp}$), 6.49 (pt, 2H, CH$_{Cp}$), 6.65 – 6.72 (m, 2H, *o*-CH$_{Ph}$), 6.78 – 6.85 (m, 1H, *p*-CH$_{Ph}$), 7.08 – 7.16 (m, 2H, *m*-CH$_{Ph}$).

^{13}C NMR (75 MHz, dichloromethane-D_2, –20 °C): δ = 21.1 (Me$_{i\text{Pr}}$), 26.7 (Me$_{i\text{Pr}}$), 43.0 (NMe_2), 43.9 (CH$_{i\text{Pr}}$), 46.1 (CH$_{i\text{Pr}}$), 98.6 (BC), 113.2 (CH$_{Cp}$), 118.0 (CH$_{Cp}$), 120.6 (*p*-CH$_{Ph}$), 124.2 (*o*-CH$_{Ph}$), 128.1 (*m*-CH$_{Ph}$), 153.2 (*ipso*-C$_{Ph}$).

^{11}B NMR (64 MHz, benzene-D_6): δ = 27.2.

4.2.2.3.3. Synthesis of [Zr{η^5:η^1-(C_9H_6)B(N*i*Pr$_2$)NPh}(NMe_2)$_2$] (122)

A solution of [Zr(NMe_2)$_4$] (0.51 g, 1.92 mmol) in toluene (10 mL) was added to a solution of (1-C_9H_7)B(N*i*Pr$_2$)N(H)Ph (**66**) (0.61 g, 1.92 mmol) in toluene (20 mL). The reaction mixture was refluxed for 2 h, over which time the colour changed from colourless to bright orange. Subsequently, all volatiles were removed *in vacuo*, the residue was dissolved in hexane and stored at –80 °C. Pure **122** (0.53 g, 1.08 mmol, 56%) was obtained in the form of a colourless microcrystalline material. Recrystallisation from hexane at 4 °C yielded crystals of **122** suitable for *X*-ray diffraction experiments.

^{1}H NMR (300 MHz, dichloromethane-D_2, –20 °C): δ = 0.94 (d, $^{3}J_{H\text{-}H}$ = 6.7 Hz, 3H, Me$_{i\text{Pr}}$), 0.99 (d, $^{3}J_{H\text{-}H}$ = 6.7 Hz, 3H, Me$_{i\text{Pr}}$), 1.47 (d, $^{3}J_{H\text{-}H}$ = 6.8 Hz, 3H, Me$_{i\text{Pr}}$), 1.48 (d, $^{3}J_{H\text{-}H}$ = 6.8 Hz, 3H, Me$_{i\text{Pr}}$), 1.96 (s, 6H, NMe_2), 2.89 (s, 6H, NMe_2), 3.32 (m, $^{3}J_{H\text{-}H}$ = 6.8 Hz, 1H, CH$_{i\text{Pr}}$), 3.51 (m, $^{3}J_{H\text{-}H}$ = 6.7 Hz, 1H, CH$_{i\text{Pr}}$), 6.35 – 7.78 (m, 11H, CH$_{Ind/Ph}$).

^{13}C NMR (75 MHz, dichloromethane-D_2, –20 °C): δ = 21.2 (Me$_{i\text{Pr}}$), 21.5 (Me$_{i\text{Pr}}$), 26.5 (Me$_{i\text{Pr}}$), 27.0 (Me$_{i\text{Pr}}$), 40.7 (NMe_2), 43.9 (CH$_{i\text{Pr}}$), 44.3 (NMe_2), 46.5 (CH$_{i\text{Pr}}$), 102.2 (CH$_{Ind\text{-}5\text{-}ring}$), 120.2 (*p*-CH$_{Ph}$), 122,8 (CH$_{Ind\text{-}6\text{-}ring}$), 123.1 (*o*-CH$_{Ph}$),

123.3 ($CH_{Ind\text{-}5\text{-}ring}$), 123.8 ($CH_{Ind\text{-}6\text{-}ring}$), 124.1 ($CH_{Ind\text{-}6\text{-}ring}$), 124.8 ($CH_{Ind\text{-}6\text{-}ring}$), 127.7 (*quaternary* C_{Ind}), 128.2 (*m*-CH_{Ph}), 131.0 (*quaternary* C_{Ind}), 153.2 (*ipso*-C_{Ph}), BC resonance not observed.

^{11}B NMR (64 MHz, benzene-D_6): δ = 28.5.

4.2.2.3.4. Reaction of [Zr{η^5:η^1-(C_5H_4)B(N*i*Pr_2)NPh}(NMe_2)$_2$] (120) with Me_3SiCl

[Zr{η^5:η^1-(C_5H_4)B(N*i*Pr_2)NPh}(NMe_2)$_2$] (**120**) (0.20 mg, 0.45 mmol) was dissolved in hexane (20 mL) and a large excess of Me_3SiCl (0.43 mL, 3.96 mmol, 9 equivalents) was added. Within hours, a precipitate had formed. The reaction mixture was subsequently stirred at ambient temperature for 4 d. All volatiles were removed *in vacuo* to yield an off-white powder (0.18 g). Solubility of the powder in dichloromethane was very poor and only prolonged treatment (30 min) of a sample in dichloromethane-D_2 in an ultrasonic bath provided a solution that was sufficiently concentrated for NMR spectroscopy. Resonances at chemical shifts expected for the desired dichlorocomplex were detected in roughly the right integral ratios, but were unusually broad.

^{1}H NMR (200 MHz, dichloromethane-D_2): δ = 0.6 – 1.0 (br s, 6 H, Me), 1.2 – 1.6 (br s, 6 H, Me), 3.1 – 3.4 (br s, 2 H, $CH_{i\text{Pr}}$), 6.2 – 7.4 (m, 9 H, $CH_{Cp/Ph}$).

^{11}B NMR (64 MHz, dichloromethane-D_2): δ = 28.

4.2.2.3.5. Reaction of [Hf{η^5:η^1-(C_5H_4)B(N*i*Pr_2)NPh}(NMe_2)$_2$] (121) with Me_3SiCl

[Hf{η^5:η^1-(C_5H_4)B(N*i*Pr_2)NPh}(NMe_2)$_2$] (**121**) (0.50 g, 0.94 mmol) was dissolved in hexane (20 mL) and a large excess of neat Me_3SiCl (1.08 g, 10.0 mmol, 11 equivalents) was added at ambient temperature. A white precipitate formed in the initially clear solution within hours. The reaction mixture was stirred for 4 d at ambient temperature. All volatiles were subsequently removed *in vacuo* to yield a white powder (0.46 g), that was soluble in dichloromethane only after prolonged treatment in an ultrasonic bath. In toluene, significant solubility was only observed at high temperatures. An attempt to recrystallise the material from refluxing toluene by slow cooling in an oil bath failed. Only with prolonged treatment in an ultrasonic bath, a sample in dichloromethane-D_2 that was sufficiently concentrated for NMR experiments

could be obtained. Signal integral ratios and chemical shifts in the ^{1}H NMR spectrum were as expected for the dichlorinated target compound, but all signals were unusually broad.

^{1}H NMR (200 MHz, dichloromethane-D_2): δ = 0.6 – 1.0 (br s, 6 H, Me), 1.2 – 1.6 (br s, 6 H, Me), 3.1 – 3.4 (br s, 2 H, $CH_{i\mathrm{Pr}}$), 6.1 – 7.4 (m, 9 H, $CH_{\mathrm{Cp/Ph}}$).

^{11}B NMR (64 MHz, dichloromethane-D_2): δ = 28.1.

4.2.2.3.6. Reaction of [Zr{η^5:η^1-(C_9H_6)B(N*i*Pr$_2$)NPh}(NMe_2)$_2$] (122) with Me_3SiCl

[Zr{η^5:η^1-(C_9H_6)B(N*i*Pr$_2$)NPh}(NMe_2)$_2$] (**122**) (0.20 g, 0.40 mmol) was dissolved in hexane (10 mL) and neat Me_3SiCl (0.43 mL, 3.96 mmol, 10 equivalents) was added at ambient temperature. Within hours, formation of a white precipitate was observed. After stirring the reaction mixture for further 4 d at ambient temperature, all volatiles were removed *in vacuo* to yield an off-white powder (0.16 g). Solubility of this residue was poor even in dichloromethane and only by prolonged treatment in an ultrasonic bath a solution sufficiently concentrated for NMR spectroscopy could be obtained. Chemical shifts and integral ratios in the ^{1}H NMR spectrum were as expected for the dichlorinated target compound, however, all signals were unusually broad even at low temperatures (–20 °C).

^{1}H NMR (200 MHz, dichloromethane-D_2, –20 °C): δ = 0.5 – 0.9 (br s, 6 H, Me), 1.1 – 1.6 (br s, 6 H, Me), 2.8 – 3.5 (br s, 2 H, $CH_{i\mathrm{Pr}}$), 6.0 – 8.0 (m, 11 H, $CH_{\mathrm{Ind/Ph}}$).

^{11}B NMR (64 MHz, dichloromethane-D_2): δ = 30.3.

4.2.2.4. Transformations of [Ti{η^5:η^1-(C_5H_4)B(N*i*Pr$_2$)NPh}Cl_2] (70)

4.2.2.4.1. Reaction of [Ti{η^5:η^1-(C_5H_4)B(N*i*Pr$_2$)NPh}Cl_2] (70) with MeLi

Reaction A: [Ti{η^5:η^1-(C_5H_4)B(N*i*Pr$_2$)NPh}Cl_2] (**70**) (0.14 g, 0.36 mmol) was dissolved in toluene/Et_2O (4:1 v/v, 25 mL) to give a dark orange solution. The mixture was cooled to 0 °C and MeLi (0.45 mL of a 1.6 M solution in Et_2O, 0.72 mmol) added by syringe. Within minutes, the mixture darkened and became brown although no precipitate was observed. After 2 h at 0 °C, an aliquot was taken, all volatiles were removed *in vacuo* and the residue was re-dissolved in benzene-D_6. ^{1}H and ^{11}B NMR

spectroscopy on the sample both showed signals corresponding to a mixture of compounds, with those in the ^{11}B NMR spectrum at δ = 39.5, 28.0 and –20.5 being indicative of reaction with the boron bridge.

Reaction B: [Ti{η^5:η^1-(C_5H_4)B(N*i*Pr$_2$)NPh}Cl_2] (**70**) (67.4 mg, 0.175 mmol) was dissolved in toluene (10 mL) to give a bright yellow solution. The mixture was cooled to –80 °C, partially precipitating the orange starting material. MeLi (2.2 mL of a 0.16 M solution in toluene/Et_2O, 0.35 mmol) were added over a period of 10 min. The mixture was allowed to warm to ambient temperature and was subsequently stirred over night. This resulted in a slow colour change from yellow to orange and the formation of a small quantity of colourless precipitate. All volatiles were removed *in vacuo*, the residue was re-dissolved in hexane and the precipitate was removed by centrifugation. Recrystallisation by concentrating the supernatant and storing it at –30 °C was unsuccessful. A sample dried *in vacuo* displayed a large number of peaks in the ^{1}H NMR spectrum indicative of a mixture of compounds, but a single signal in the ^{11}B NMR spectrum at δ = 28.5 that is indicative of an intact boron bridge.

4.2.2.4.2. Reaction of [Ti{η^5:η^1-(C_5H_4)B(N*i*Pr$_2$)NPh}Cl_2] (70) with $AlMe_3$

Reaction A: Benzene-D_6 (0.5 mL) was added to [Ti{η^5:η^1-(C_5H_4)B(N*i*Pr$_2$)NPh}Cl_2] (**70**) (7.7 mg, 20 µmol) affording a cloudy orange coloured solution. ^{11}B NMR spectroscopy on the sample showed a single signal at δ = 28.8. $AlMe_3$ (1.4 mg, 20 µmol, as a solution in 0.5 mL toluene) was added at ambient temperature, resulting in immediate dissolution of the orange residue and a colour change to pale yellow-green. The ^{11}B NMR spectrum of the sample, recorded directly after addition of the $AlMe_3$, displayed a single signal at δ = 28.2. The same signal was observed after 1 h at ambient temperature.

Reaction B: Half of the mixture of reaction A was heated to 60 °C for 30 min, resulting in a colour change to yellow-brown. A ^{11}B NMR spectrum recorded subsequently exhibited a strong signal at δ = 86.1 besides minor signals at δ = 28 and 39.9.

Reaction C: Half of the mixture of reaction A was treated with $AlMe_3$ (1.4 mg, 20 µmol, as a solution in 0.5 mL toluene) at ambient temperature. In an ^{11}B NMR spectrum recorded immediately after addition of the $AlMe_3$, an additional signal at δ =

86.2 was apparent besides the signal at δ = 28.2 for the starting material. After 24 h at ambient temperature, the ^{11}B NMR spectrum showed only a single signal at δ = 86.2.

4.2.2.5. Further reactions with amino monoborane based ligand precursors

4.2.2.5.1. Attempted synthesis of [Ti{(η^5-C_5H_4)B(N*i*Pr$_2$)N(H)*t*Bu}Cl$_3$]

(η^1-C_5H_5)B(N*i*Pr$_2$)N(H)*t*Bu (**64**) (0.31 g, 1.25 mmol) was dissolved in hexane (40 mL) and 1 equivalent of *n*BuLi (0.50 mL of a 2.5 M solution in hexane, 1.25 mmol) was added at 0 °C. The reaction mixture was slowly warmed to ambient temperature and subsequently stirred for 4 h. The resulting mixture was then added over a period of 30 min to a solution of $TiCl_4$ (0.24 g, 1.25 mmol) in hexane (100 mL) at –70 °C. After attaining ambient temperature, the reaction mixture was stirred for 16 h. All volatiles were removed *in vacuo*, the residue was extracted with hexane and any insoluble material was removed by centrifugation. The solvent was again removed *in vacuo* and the resulting residue was analysed by ^{1}H NMR spectroscopy. The ^{1}H NMR spectrum displayed pseudo-triplets at δ = 6.36 and 6.86, presumably corresponding to the target compound [LTiCl_3]. However, this compound is the minor component in a mixture with the unreacted ligand precursor.

Using essentially the same procedure, the reaction was repeated with modification of the solvents and/or the deprotonation agent. In all of these reaction, the products could not be sufficiently purified to allow for full characterisation. Reaction conditions and observations are summarised in Table 4.

Table 4. Attempted syntheses of [Ti{(η^5-C_5H_4)B(N*i*Pr$_2$)N(H)*t*Bu}Cl_3].

Deprotonation agent	Solvent	Observations
*n*BuLi	hexane	one product (pt @ 6.36, 6.86 ppm) beside unreacted ligand precursor
*n*BuLi	toluene/Et_2O, 1:1 v/v	one predominant product (pt @ 6.24, 6.85 ppm) beside unidentified material
*t*BuLi	toluene	two products (pt @ 6.36, 6.86 and 6.24, 6.85 ppm, respectively)
K[N($SiMe_3$)$_2$]	toluene	complicated product mixture

4.2.2.5.2. Attempted double deprotonation of (η^1-C_5H_5)B(N*i*Pr$_2$)N(H)*t*Bu (64) and subsequent reactions with titanium compounds

(η^1-C_5H_5)B(N*i*Pr$_2$)N(H)*t*Bu (**64**) (0.47 g, 1.89 mmol) was dissolved in toluene (40 mL), cooled to 0 °C and 2 equivalents *t*BuLi (2.22 mL of a 1.7 M solution in pentane, 3.78 mmol) were added slowly. The reaction mixture was allowed to attain ambient temperature and was then stirred for 16 h. $TiCl_4$ (0.36 g, 1.89 mmol) was dissolved in toluene (40 mL), the solution was cooled to –80 °C and the mixture containing the deprotonated ligand precursor was added over a period of 30 min. The reaction mixture was allowed to warm slowly to ambient temperature and was then stirred for 2 h. All volatiles were removed *in vacuo*, the residue was extracted with toluene and any insoluble material was removed by centrifugation. The volume of the solution was reduced to dryness *in vacuo* and the resulting residue was analysed by ^{1}H NMR spectroscopy. The ^{1}H NMR spectrum showed pseudo-triplets for two compounds with (η^5-C_5H_4R)Ti moieties at δ = 5.79, 6.56 and 6.04, 6.32, respectively. The separation of these compounds was not feasible.

The same procedure was followed whilst varying the solvents, deprotonation agents and/or titanium sources. In some cases, the titanium(III) compound [$TiCl_3(thf)_3$] was utilised, followed by oxidation with 0.5 equivalents $PbCl_2$ to oxidise the resulting compounds to titanium(IV) species. In none of these reactions could the product mixtures be separated to allow full characterisation of the components. Table 5 summarises reaction conditions and observations.

Table 5. Attempted syntheses of [Ti{η^5:η^1-(C_5H_4)B(N*i*Pr$_2$)N*t*Bu}R_2] (R = Cl, NMe_2).

Deprotonation agent	Solvent	Titanium source	Observations
*t*BuLi	toluene	$TiCl_4$	two products (pt @ 5.79, 6.56 and 6.04, 6.32 ppm, respectively)
MeLi (4 equivalents)	Et_2O	$TiCl_4$	large number of products
*n*BuLi	toluene/Et_2O, 1:1 v/v	[$TiCl_2(NMe_2)_2$]	five products
*t*BuLi	toluene	[$TiCl_2(NMe_2)_2$]	five products
*t*BuLi	toluene/Et_2O, 1:1 v/v	[$TiCl_2(NMe_2)_2$]	two products (pt @ 5.90, 6.53 and 6.30, 6.59 ppm, respectively)
*n*BuLi	toluene/Et_2O, 1:1 v/v	1) [$TiCl_3(thf)_3$] 2) 0.5 $PbCl_2$	large number of products
*t*BuLi	toluene	1) [$TiCl_3(thf)_3$] 2) 0.5 $PbCl_2$	large number of products

4.2.2.5.3. Attempted complex formation from (η^1-C_5H_5)B(N*i*Pr$_2$)N(H)*t*Bu (64) using additional bases

(η^1-C_5H_5)B(N*i*Pr$_2$)N(H)*t*Bu (**64**) (0.46 g, 1.85 mmol) was dissolved in toluene (10 mL) and neat $TiCl_4$ was added at ambient temperature. The reaction mixture was stirred for 16 h at ambient temperature. An aliquot was taken, all volatiles were removed *in vacuo* and a ^{1}H NMR spectrum was recorded. This only exhibited signals corresponding to the unreacted ligand precursor. NEt_3 (1.87 g, 18.5 mmol, 10 equivalents) were added, immediately resulting in the formation of a black precipitate. The resulting mixture was stirred for 24 h at ambient temperature, another sample was prepared as above and analysed by ^{1}H NMR spectroscopy. This displayed again only signals corresponding to the ligand precursor. The reaction mixture was then heated to 100 °C (oil bath temperature) for 4 h and the analysis repeated. The ^{1}H NMR spectrum

showed some weak pseudo-triplets at δ = 5.84 and 6.18 besides dominant signals corresponding to the ligand precursor.

The reaction was repeated utilising 1,8-diazabicyclo[5.4.0]undecene-7 (DBU). However, addition of 2 equivalents DBU to a solution containing the ligand precursor and $TiCl_4$ resulted in immediate formation of a ruby-red precipitate. The precipitate was found to be virtually insoluble in dichloromethane. ^{1}H and ^{11}B NMR spectroscopy on the supernatant solution displayed only very weak signals that could not be assigned. In a control experiment, reaction of $TiCl_4$ with an equimolar amount of DBU also afforded a ruby-red precipitate that exhibited similar solubility characteristics.

4.2.2.5.4. Attempted 2:1 reaction of (η^1-C_5H_5)B(N*i*Pr$_2$)N(H)*t*Bu (64) with [Ti(NMe$_2$)$_4$]

[$Ti(NMe_2)_4$] (0.16 g, 0.70 mmol) and 2 equivalents (η^1-C_5H_5)B(N*i*Pr$_2$)N(H)*t*Bu (**64**) (0.35 g, 1.41 mmol, 2 equivalents) were co-dissolved in toluene (20 mL) and refluxed for 9 h. All volatiles were subsequently removed *in vacuo*. The ^{1}H NMR spectrum of the residue showed only signals corresponding to [Ti{(η^5-C_5H_4)B(N*i*Pr$_2$)N(H)*t*Bu}$(NMe_2)_3$] (**107**) and the unreacted ligand precursor, but no signals consistent with the formation of the desired product [Ti{(η^5-C_5H_4)B(N*i*Pr$_2$)N(H)*t*Bu}$_2(NMe_2)_2$].

4.2.2.5.5. Attempted reaction of (η^1-C_5H_5)B(N*i*Pr$_2$)N(H)*t*Bu (64) with [TiCl$_2$(NMe$_2$)$_2$]

(η^1-C_5H_5)B(N*i*Pr$_2$)N(H)*t*Bu (**64**) (0.27 g, 1.09 mmol) and [$TiCl_2(NMe_2)_2$] (0.23 g, 1.09 mmol) were separately dissolved in toluene (10 mL), the solutions were combined and the resulting mixture was refluxed for 3 h. All volatiles were removed *in vacuo* and a sample was analysed by ^{1}H NMR spectroscopy. The ^{1}H NMR spectrum displayed mainly signals corresponding to the unreacted ligand precursor beside signals of some unidentified decomposition products. No pseudo-triplets characteristic for complexation of the C_5 ring were observed.

4.2.2.5.6. Attempted reaction of (η^1-C_5H_5)B(N*i*Pr$_2$)N(H)*t*Bu (64) with [TiBz$_4$]

Separate solutions of the ligand precursor (η^1-C_5H_5)B(N*i*Pr$_2$)N(H)*t*Bu (**64**) (0.22 g, 0.89 mmol) and [$TiBz_4$] (0.37 g, 0.89 mmol) in toluene (40 mL) were combined at –

80 °C. After attaining ambient temperature, a sample was taken and subjected to ^{1}H NMR spectroscopy. The spectrum showed only signals corresponding to the unreacted starting material. After 16 h at ambient temperature, the ^{1}H NMR spectrum of another sample was essentially unchanged. Therefore, the reaction mixture was refluxed for 2.5 h. The ^{1}H NMR spectrum of another sample indicated complete decomposition of the titanium compound while the ligand precursor remained unchanged.

4.2.2.5.7. Attempted reaction of (1-C_9H_7)B(N*i*Pr$_2$)N(H)*i*Pr (83) with [Ti(NMe$_2$)$_4$]

(1-C_9H_7)B(N*i*Pr$_2$)N(H)*i*Pr (**83**) (1.13 g, 3.98 mmol) and [Ti(NMe$_2$)$_4$] (0.89 g, 3.98 mmol) were co-dissolved in toluene (30 mL). The reaction mixture was refluxed for 2 h, changing colour slowly from bright yellow to orange. All volatiles were removed *in vacuo*. The ^{1}H NMR spectrum displayed only the signals corresponding to the unreacted ligand precursor.

4.2.2.5.8. Attempted reaction of (η^1-$C_{13}H_9$)B(N*i*Pr$_2$)N(H)Ph (88) with [Ti(NMe$_2$)$_4$]

(9-$C_{13}H_9$)B(N*i*Pr$_2$)N(H)Ph (**88**) (0.58 g, 1.57 mmol) was dissolved in toluene (40 mL), neat [Ti(NMe$_2$)$_4$] (0.35 g, 1.57 mmol) was added and the reaction mixture was refluxed for 3 h. All volatiles were removed *in vacuo* and a sample of the residue was analysed by ^{1}H NMR spectroscopy. The ^{1}H NMR spectrum showed only signals corresponding to the unreacted ligand precursor and some traces of [Ti(NMe$_2$)$_4$].

4.2.2.5.9. Attempted dilithiation of (9-$C_{13}H_9$)B(N*i*Pr$_2$)N(H)Ph (88) with RLi

(9-$C_{13}H_9$)B(N*i*Pr$_2$)N(H)Ph (**88**) (0.12 g, 0.33 mmol) was dissolved in toluene/Et_2O (10:1 v/v, 50 mL) to give a pale yellow solution. The solution was cooled to 0 °C and 2 equivalents of *n*BuLi (0.41 mL of a 1.6 M solution in hexane, 0.66 mmol) were added dropwise. After addition of a few drops, the colour of the solution changed to bright orange. The mixture was stirred at ambient temperature for 16 h, then it was cooled to –78 °C and $ZrCl_4$ (0.08 g, 0.33 mmol) added. The reaction mixture was allowed to warm to ambient temperature and subsequently stirred for 24 h. All volatiles were removed *in vacuo*, the residue was re-dissolved in chloroform, insoluble material was removed by centrifugation and the solvent was again removed *in vacuo*. ^{1}H NMR spectroscopy on a sample showed the unreacted ligand precursor to be the main

component of the product mixture as indicated by its characteristic BCH ($\delta(^1H)$ = 4.29) and NH ($\delta(^1H)$ = 5.37) resonances.

The reaction procedure was repeated twice, once using MeLi as a base and neat Et_2O as a solvent and once utilising *t*BuLi as a base and hexane as a solvent. In both cases, ^1H NMR spectra after work-up showed resonances corresponding to the BCH and NH protons of the unreacted ligand precursor, indicating that this compound was one of the main components of the product mixture.

4.2.2.5.10. Attempted reaction of (η^1-C_5Me_4H)B(N*i*Pr$_2$)N(H)Ph (90) with [Ti(NMe$_2$)$_4$]

(η^1-C_5Me_4H)B(N*i*Pr$_2$)N(H)Ph (**90**) (0.57 g, 1.76 mmol) was dissolved in toluene (40 mL) and neat [Ti(NMe$_2$)$_4$] (0.39 g, 1.76 mmol) was added. The mixture was refluxed for 3 h. All volatiles were removed *in vacuo* and a ^1H NMR spectrum was recorded. The ^1H NMR spectrum showed only signals corresponding to the ligand precursor and residual [Ti(NMe$_2$)$_4$].

4.2.2.5.11. Attempted double deprotonation of (η^1-C_5Me_4H)B(N*i*Pr$_2$)N(H)Ph (90) and subsequent reactions with titanium compounds

Reaction A: (η^1-C_5Me_4H)B(N*i*Pr$_2$)N(H)Ph (**90**) (0.35 g, 1.07 mmol) was dissolved in toluene/Et_2O (1:1 v/v, 40 mL), cooled to –80 °C and 2 equivalents of *t*BuLi (1.26 mL of a 1.7 M solution in pentane, 2.14 mmol) diluted with toluene (10 mL) were added dropwise. The mixture was allowed to warm to ambient temperature and stirred for 16 h. The resulting mixture was then added dropwise to a solution of [$TiCl_2(NMe_2)_2$] (0.22 g, 1.07 mmol) in toluene (30 mL) at –80 °C. After warming to ambient temperature the mixture was stirred for a further 16 h. Subsequently, all solids were removed by centrifugation and all volatiles *in vacuo*. The crude product was analysed by ^1H and ^{11}B NMR spectroscopy. The ^1H NMR spectrum displayed a signal pattern that may correspond to the target compound [Ti{η^5:η^1-(C_5Me_4)B(N*i*Pr$_2$)NPh}(NMe$_2$)$_2$] and the only resonance observed in the ^{11}B NMR spectrum at δ = 27.7 is consistent with this formulation. However, attempts to further purify the crude product by means of recrystallisation were unsuccessful and hence, unambiguous characterisation was not possible.

^{1}H NMR (200 MHz, benzene-D_6): δ = 0.95 (d, $^{3}J_{H\text{-}H}$ = 6.7 Hz, 6H, Me$_{i\text{Pr}}$), 1.54 (d, $^{3}J_{H\text{-}H}$ = 6.8 Hz, 6H, Me$_{i\text{Pr}}$), 1.93 (s, 6H, $Me_{C_5Me_4}$), 2.11 (s, 6H, $Me_{C_5Me_4}$), 2.95 (s, 12H, NMe_2), 3.57 (m, 1H, $CH_{i\text{Pr}}$), 3.73 (m, 1H, $CH_{i\text{Pr}}$), 6.8 – 7.4 (m, 5H, CH_{Ph}).

^{11}B NMR (64 MHz, benzene-D_6): δ = 27.7.

Reaction B: (η^1-C_5Me_4H)B(N*i*Pr_2)N(H)Ph (**90**) (0.33 g, 1.02 mmol) was dissolved in toluene/Et_2O (1:1 v/v, 40 mL), cooled to –80 °C and 2 equivalents of *t*BuLi (1.20 mL of a 1.7 M solution in pentane, 2.04 mmol) diluted with toluene (10 mL) were added dropwise. The mixture was warmed to ambient temperature and stirred for 16 h. The resulting mixture was cooled to –80 °C and solid [$TiCl_3(thf)_3$] (0.38 g, 1.02 mmol) was added at once. The reaction mixture was then warmed to ambient temperature and stirred for 2 h. Subsequently, solid $PbCl_2$ (0.14 g, 0.51 mmol) was added and the mixture stirred for a further 16 h. All solids were removed by centrifugation and all volatiles *in vacuo* to yield the crude product. Recrystallisation from toluene yielded a pale yellow solid. Analysis of the product by means of ^{1}H NMR spectroscopy was inconclusive, while the ^{11}B NMR spectrum displayed a single signal at δ = 29.0.

Reaction C: (η^1-C_5Me_4H)B(N*i*Pr_2)N(H)Ph (**90**) (0.36 g, 1.12 mmol) was dissolved in Et_2O (30 mL), cooled to –80 °C and 2 equivalents of MeLi (1.40 mL of a 1.6 M solution in Et_2O, 2.24 mmol) in Et_2O (10 mL) were added dropwise. The mixture was allowed to warm to ambient temperature. The mixture was again cooled to –80 °C and 2 further equivalents of MeLi (1.40 mL of a 1.6 M solution in Et_2O, 2.24 mmol) in Et_2O (10 mL) were added followed by dropwise addition of $TiCl_4$ (0.21 g, 1.12 mmol) in toluene (10 mL). The reaction mixture was warmed to ambient temperature and stirred for 16 h. Subsequently, all solids were removed by centrifugation and all volatiles *in vacuo*. Attempts to further purify the crude product by means of recrystallisation were unsuccessful. ^{1}H NMR spectroscopy of the crude product was inconclusive, while the ^{11}B NMR spectrum displayed a single resonance at δ = 27.3.

4.2.2.6. Further reactions of amino monoborane based non-chelating titanium complexes

4.2.2.6.1. Attempted amine elimination from [Ti{(η^5-C_5H_4)B(N*i*Pr$_2$)N(H)*t*Bu}(NMe$_2$)$_3$] (107)

Neat [Ti{(η^5-C_5H_4)B(N*i*Pr$_2$)N(H)*t*Bu}(NMe$_2$)$_3$] (**107**) (50 mg, 0.12 mmol) was heated to 135 °C for 16 h. The dark brown residue was dissolved in benzene-D_6 and analysed by ^{1}H NMR spectroscopy. The ^{1}H NMR spectrum indicated complete decomposition of the starting material.

4.2.2.6.2. Attempted HCl elimination from [Ti{(η^5-C_5H_4)B(N*i*Pr$_2$)N(H)*i*Pr}Cl$_2$(NMe$_2$)] (110) by addition of bases

[Ti{(η^5-C_5H_4)B(N*i*Pr$_2$)N(H)*i*Pr}Cl$_2$(NMe$_2$)] (**110**) (0.53 g, 1.33 mmol) was dissolved in toluene (10 mL) and excess NEt_3 (0.67 g, 6.65 mmol) added. The reaction mixture was heated to 90 °C for 16 h. A sample was taken, all volatiles were removed *in vacuo*, the residue was dissolved in benzene-D_6 and analysed by ^{1}H NMR spectroscopy. The ^{1}H NMR spectrum showed *ca*. 50% consumption of the starting material and formation of at least three new compounds bearing (η^5-C_5H_4R)Ti moieties as judged by the characteristic pseudo-triplets.

Virtually the same procedure was followed using [Ti{(η^5-C_5H_4)B(N*i*Pr$_2$)N(H)*i*Pr}Cl$_2$(NMe$_2$)] (**110**) (0.24 g, 0.60 mmol) and 1 equivalent DBU (0.09 g, 0.60 mmol) in toluene in toluene (10 mL). The reaction mixture was stirred for 6 h at ambient temperature. ^{1}H NMR spectroscopy on an aliquot dried *in vacuo* showed only signals corresponding to the starting materials. The mixture was subsequently heated to 80 °C for 16 h. Another aliquot was taken, all volatiles were removed *in vacuo* and a ^{1}H NMR spectrum was recorded. This indicated formation of a complex product mixture.

4.2.2.7. Diborane(4) based complexes and related reactions

4.2.2.7.1. Reaction of (η^1-C_5H_5)(BNMe$_2$)$_2${N(H)Ph} (92) with [Ti(NMe$_2$)$_4$]

Reaction A: (η^1-C_5H_5)(BNMe$_2$)$_2${N(H)Ph} (**92**) (0.22 g, 0.82 mmol) was dissolved in toluene (20 mL) and an equal amount of neat [Ti(NMe$_2$)$_4$] (0.18 g, 0.82 mmol) was added at ambient temperature. The resulting bright yellow solution was

refluxed for 3 h to give an almost black mixture. A sample was taken, dried *in vacuo* and analysed by ^{1}H and ^{11}B NMR spectroscopy. The ^{1}H NMR spectrum showed a large number of signals that could not be assigned, whereas the ^{11}B NMR spectrum displayed a prominent signal at $\delta = 31$ that indicated decomposition of the ligand precursor ($\delta(^{11}B) = 34.0, 46.0$).

Reaction B: $[Ti(NMe_2)_4]$ (0.41 g, 1.84 mmol) was dissolved in hexane (150 mL) and cooled to *ca*. –20 °C. The ligand precursor **92** (0.49 g, 1.84 mmol) as a solution in hexane (20 mL) was added dropwise during the course of 1 h. No immediate colour change was observed after addition. The mixture was allowed to warm slowly to ambient temperature and was subsequently stirred for 16 h, gradually changing colour from bright yellow to yellow-orange. The mixture was then heated for 2 h to *ca*. 50 °C and for a further 4 h at reflux, changing colour to bright red. An aliquot was removed, dried *in vacuo* and analysed by multinuclear NMR spectroscopy. ^{1}H, ^{11}B and ^{13}C NMR spectra were consistent with the unbridged complex $[Ti\{(\eta^5\text{-}C_5H_4)(BNMe_2)_2(N\{H\}Ph)\}(NMe_2)_3]$ (**123**) and showed only traces of impurities.

^{1}H NMR (200 MHz, benzene-D_6): δ = 2.44 (br s, 3H, Me_{NBNMe}), 2.69 (br s, 3H, Me_{NBNMe}), 2.89 (s, 3H, Me_{CBNMe}), 2.98 (s, 3H, Me_{CBNMe}), 3.11 (s, 18H, Me_{TiNMe}), 4.95 (br s, 1H, NH), 5.89 – 5.94 (m, 1H, CH_{Cp}), 6.02 – 6.07 (m, 1H, CH_{Cp}), 6.32 – 6.40 (m, 2H, CH_{Cp}), 6.75 – 7.13 (m, 5H, CH_{Ph}).

^{13}C NMR (75 MHz, benzene-D_6): δ = 36.0 (Me_{NBNMe}), 40.7 (Me_{CBNMe}), 42.3 (Me_{NBNMe}), 45.4 (Me_{CBNMe}), 50.2 (Me_{TiNMe}), 111.5 (CH_{Cp}), 112.8 (CH_{Cp}), 118.4 (CH_{Cp}), 118.6 ($CH_{o\text{-}Ph}$), 119.7 ($CH_{p\text{-}Ph}$), 121.8 (CH_{Cp}), 129.3 ($CH_{m\text{-}Ph}$), 147.4 (*ipso*-C_{Ph}), BC resonance not observed.

^{11}B NMR (64 MHz, benzene-D_6): $\delta = 34.9$ (NBN), 43.4 (CBN).

Reaction C: The solution of crude **123** in hexane (obtained from aforementioned reaction B) was refluxed for another 20 h. The ^{1}H NMR spectrum of a sample displayed weak signals for the unbridged complex **123** as well as a number of more intense signals arising from unidentified reaction products. The ^{11}B NMR spectrum showed one very broad signal at $\delta = 36$ and a weaker, equally broad resonance at $\delta = 46$.

4.2.2.7.2. Reaction of (η^1-C_5H_5)($BNMe_2$)$_2${N(H)Ph} (92) with [$TiBz_4$]

A solution of [$TiBz_4$] (0.15 g, 0.37 mmol) in benzene-D_6 (0.5 mL) was added to a solution of (η^1-C_5H_5)($BNMe_2$)$_2${N(H)Ph} (**92**) (0.10 g, 0.37 mmol) in the same solvent (0.5 mL). After 16 h at ambient temperature, a ^{1}H NMR spectrum was recorded, indicating the formation of small quantities of toluene. The mixture was subsequently heated to 60 °C and the reaction progress was monitored by ^{1}H and ^{11}B NMR spectroscopy during a period of 22 h. The signal at δ = 2.11 in the ^{1}H NMR spectrum corresponding to the Me resonance of toluene increased steadily in intensity, while the signal at δ = 2.80 corresponding to the methylene group of the starting material [$TiBz_4$] gradually decreased and eventually vanished. In the region between 5.5 – 6.5 ppm of the ^{1}H NMR spectra recorded in the earlier stages of the monitoring period, at least seven pseudo-triplets of various intensities could be observed. In the mixture that was obtained after 22 h at 60 °C, only two pseudo-triplets were observed at δ = 5.72 and 6.40. In the region of the ^{1}H NMR spectrum that is typical for NMe_2 groups on boron (2.0 – 3.0 ppm) a number of signals was observed at all stages of the monitoring process that could not be assigned to distinct compounds. Integrals of the signal corresponding to the Me group on toluene and the two combined pseudo-triplets were in the ratio of 12:4. In the ^{11}B NMR spectrum, a merging of the two initial signals corresponding to the ligand precursor {δ(^{11}B) = 34.0, 46.0} was observed in the course of the reaction, resulting in a signal at δ = 42.8 for the final mixture.

4.2.2.7.3. Reaction of (η^1-C_5H_5)($BNMe_2$)$_2${N(H)Ph} (92) with *t*BuLi and [$Ti(NMe_2)_2Cl_2$]

Ligand precursor (η^1-C_5H_5)($BNMe_2$)$_2${N(H)Ph} (**92**) (0.45 g, 1.69 mmol) was dissolved in hexane (50 mL), cooled to –78 °C and 2 equivalents of *t*BuLi (2.0 mL of a 1.7 M solution in pentane, 3.4 mmol) were added by syringe. The reaction mixture was allowed to warm to ambient temperature and subsequently stirred for 16 h. The resulting mixture was then cooled to –78 °C and [$Ti(NMe_2)_2Cl_2$] (0.35 g, 1.69 mmol) as a solution in toluene (20 mL) added dropwise. The resulting brown mixture was slowly warmed to ambient temperature and then stirred over night. A sample was taken, dried *in vacuo* and subjected to ^{1}H and ^{11}B NMR spectroscopy. The ^{1}H NMR spectrum indicated formation of a complex product mixture and no signals could be assigned. The ^{11}B NMR spectrum showed only one signal at δ = 37.

4.3. Polymerisation reactions

4.3.1. Ethylene polymerisation

Ethylene polymerisation reactions were performed in a 500 mL double-walled glass autoclave fitted with external heating, a dropping funnel and magnetic stirrer bar. The dry autoclave was flushed with argon for 5 min prior to use. Toluene (200 mL) and a specific amount of MAO solution (15 – 30 mL) were added to the autoclave, while a toluene solution containing a specific amount of the respective catalyst precursor (10 – 20 μmol) was added to the dropping funnel. The toluene/MAO mixture was heated to the desired reaction temperature (30 – 80 °C). At the same time, ethylene at a pressure of 2 bar was introduced to the reaction vessel until the toluene/MAO solution was saturated as evidenced by zero-flow of ethylene. The polymerisation reaction was initialised by adding the catalyst precursor solution to the toluene/MAO mixture *via* the dropping funnel. Ethylene pressure was held constant at 2 bar throughout the polymerisation process. After a specific time (15 min – 2 h), the polymerisation reaction was stopped by addition of acidified methanol (50 mL, 10 vol-% hydrochloric acid). The mixture was cooled down to ambient temperature, then added to methanol (800 mL) to precipitate the polymer. To complete the precipitation, the mixture was stirred for 1 h before filtering. The obtained precipitate was washed with toluene and methanol, then dried at elevated temperature. Reaction conditions and analytical results are summarised in Table 6.

4.3.2. Styrene polymerisation

Styrene polymerisation experiments were performed in 100 mL Schlenk bottles following a modified literature procedure. Specific amounts of toluene, catalyst precursor and MAO (total volume 40 mL, amount of catalyst precursor 10 μmol, amount of MAO solution 3.3 – 13.2 mL) were added to a Schlenk bottle. The reaction vessel was placed in an oil bath that was heated to a specific temperature (30 – 70 °C). After a 15 min introductory period, styrene (10.0 mL, giving a 1.74 M styrene solution in toluene) were added by syringe to start the polymerisation reaction. The reaction mixture was stirred at the specified temperature for 1 h. The polymerisation reaction was stopped by addition of acidified methanol (50 mL, 10 vol-% hydrochloric acid). Further work-up followed either of two procedures as indicated. (1) The reaction mixture was added to methanol (300 mL) to precipitate the produced polymer. The

precipitate was filtered off, washed with methanol and subsequently dried at elevated temperature. (2) All volatiles were removed *in vacuo* and the residue was dried to completion at elevated temperature.

In a few experiments, the order of addition of the reactants was changed. Where indicated, a mixture of toluene, styrene and MAO was heated to the desired temperature and after 15 min, a solution containing a specific amount of the respective catalyst precursor was added to start the polymerisation reaction.

Reaction conditions and analytical results are summarised in Table 7.

4.3.3. Polymer analysis

4.3.3.1. Gel permeation chromatography

Polymer analyses for selected polyethylene and polystyrene samples by gel permeation chromatography (GPC) were performed by Steve Holding of RAPRA Technology, Shropshire, UK following a standardised protocol. GPC experiments were performed on a Polymer Laboratories PL220 instrument employing PLgel guard plus 2 x mixed bed-B, 30 cm, 10 microns, columns and both a refractive index and a Viscotek differential pressure detector.

For polyethylene samples, 1,2,4-trichlorobenzene with anti-oxidant at 160 °C was used as a solvent at a nominal flow-rate of 1.0 mL/min. For polystyrene samples, tetrahydrofuran with anti-oxidant at 30 °C was used as a solvent at a nominal flow-rate of 1.0 mL/min.

GPC samples of polyethylene were prepared by adding 15 mL of solvent to 15 mg of a polymer sample and heating for 40 min at 190 °C, with shaking. The sample solutions were filtered through a glass filter pad into autosampler vials, which were placed in a heated sample compartment on the instrument. After an initial delay of 30 min to allow the first solution to equilibrate thermally, injection of part of the contents of each vial was carried out automatically.

GPC samples of polystyrene were prepared by adding 10 mL of solvent to 20 mg of a polymer sample. The solutions were left for at least 4 h to dissolve. After thorough mixing the solutions were filtered through a 0.2 micron polyamide membrane,

with glass-fibre pre-filter and transferred into sample vials, that were then placed in an autosampler.

The GPC system used was calibrated with polystyrene. For polyethylene samples, a mathematical procedure involving the use of literature viscosity constants has been applied to the calibration to allow for the difference in chemical type between the sample and the calibrants. The following Mark-Houwink parameters have been applied: polystyrene, $a = 0.707$, $\log K = -3.917$; polyethylene, $a = 0.725$, $\log K = -3.391$.

4.3.3.2. GC-MS of polymerisation mixtures

GC-MS experiments were performed on selected ethylene polymerisation mixtures to establish the content of ethylene oligomers. Samples were prepared by diluting the reaction mixture with dichloromethane (low temperature cut-off) or tridecane (high temperature cut-off). No low molecular ethylene oligomers were detected in any of the performed experiments.

4.3.3.3. Thermogravimetry and differential scanning calorimetry

Analyses by means of thermogravimetry (TGA) and differential scanning calorimetry (DSC) were performed on a DuPont 9000 thermoanalyser equipped with a TGA 951 or DSC 910 kit, respectively. TGA and DSC diagrams for the obtained precipitate from polymerisation experiment PE23-4 (as an example of a low yield ethylene polymerisation experiment) and MAO hydrolysis experiments were obtained. These diagrams were virtually identical.

Table 6. Reaction conditions and analytical results of ethylene polymerisation experiments.

Identifier	Catalyst	time / min	temperature / °C	[catalyst] / µmol	[MAO] / mmol	Recovered precipitate / g	M_w [a]	M_n [a]	M_w / M_n [a]	Peak area [a]
PE23-1	**111**	60	60	10	45	3.05	–	–	–	–
PE23-2	**111**	60	60	10	45	3.74	–	–	–	–
PE23-3	**111**	120	60	10	45	3.34	–	–	–	–
PE23-4[b,c]	**111**	15	60	10	45	3.30	n.d.r.	n.d.r.	n. d. r.	0
PE23-5[b]	**111**	15	30	10	45	3.35	n.d.r.	n.d.r.	n. d. r.	0
PE23-6[b]	**111**	15	80	10	45	3.11	n.d.r.	n.d.r.	n. d. r.	0
PE25-1	**37**	60	60	10	45	4.07	n.d.r.[d]	n.d.r.[d]	n. d. r.	0
PE25-2	**37**	60	60	10	45	4.74	4,800 4,630	1,780 1,890	2.7 2.5	1 1
PE25-3	**37**	60	60	10	45	1.59	–	–	–	–
PE25-4	**37**	60	80	10	45	0.56	–	–	–	–
PE25-5	**37**	120	60	10	45	1.38	–	–	–	–
PE26-1	**70**	60	60	10	45	3.16	372,000 245,000	109,000 54,500	3.4 4.5	1 1
PE26-2	**70**	60	60	10	22.5	1.35	n. d. r.	n. d. r.	n. d. r.	0
PE26-3	**70**	60	60	20	45	3.65	274,000 281,000	87,500 104,000	3.1 2.7	1.7 1.9
PE26-4	**70**	60	80	20	45	3.15	141,000 77,500	23,500 21,000	6.0 3.7	2.1 1.1
PE26-5	**70**	120	80	20	45	3.38	130,000 130,000	14,500 14,500	8.9 9.0	1 1
PE26-6	**70**	60	60	10	45	3.06	n. d. r.	n. d. r.	n. d. r.	0
PE29-1	**115**	60	60	20	45	3.39	39,500 39,100	9,670 9,900	4.1 4.0	9 10

Table 6 (continued). Reaction conditions and analytical results of ethylene polymerisation experiments.

Identifier	Catalyst	time / min	temperature / °C	[catalyst] / µmol	[MAO] / mmol	Recovered precipitate / g	M_w [a]	M_n [a]	M_w / M_n [a]	Peak area [a]
PE29-2	**115**	60	60	20	45	2.27	27,200 27,300	6,090 6,070	4.5 4.5	4 4
PE29-3	**115**	60	60	20	22.5	0.88	51,600 51,900	5,510 5,340	9.4 9.7	1 1
PE29-4	**115**	60	60	20	22.5	1.29	–	–	–	–
PE30-1	**118**	60	60	20	45	3.06	75,200 76,500	7,860 8,530	9.6 9.0	1 1
PE30-2	**118**	60	60	20	45	3.30	40,200 39,100	5,770 5,610	7.0 7.0	1 1
PE30-3	**118**	60	60	20	22.5	1.13	52,500 53,300	7,040 7,100	7.5 7.5	2 2
PE30-4	**118**	60	60	20	22.5	1.24	72,600 73,200	5,170 4,970	14 15	1 1
PE30-5	**118**	60	60	10	45	2.65	82,900 83,100	6,440 6,200	13 13	1 1
PE30-6	**118**	60	60	10	45	3.08	59,500 59,300	6,220 6,280	9.6 9.5	1 1

n.d.r. = no RI detector response; a) results of two GPC runs; b) reaction mixture analysed by GC-MS; c) obtained precipitate analysed by TGA and DSC; d) samples contained traces of high molecular weight material as evidenced by differential pressure chromatography.

Table 7. Reaction conditions and analytical results of styrene polymerisation experiments.

Identifier	Work-up procedure	Catalyst	time / min	temperature / °C	[catalyst] / µmol	[MAO] / mmol	Recovered precipitate / g	M_w [a,b]	M_n [a,b]	M_w / M_n [a,b]	Peak area [a]
PS1-6	1	**37**	60	50	10	10.0	0.53	–	–	–	–
PS1-7[c]	1	**37**	60	50	10	5.0	0.09	–	–	–	–
PS2-1	1	**70**	60	50	10	5.0	0.08	–	–	–	–
PS2-2	1	**70**	60	50	10	10.0	0.53	21,900 21,800	10,800 10,500	2.0 2.1	9 10
PS2-3[d]	1	**70**	60	50	10	20.0	1.75	21,100 19,600	11,300 10,100	1.9 1.9	1.2 1.1
PS2-4	1	**70**	60	80	10	20.0	1.61	16,700 16,900	8,740 8,940	1.9 1.9	12 12
PS2-5[c]	1	**70**	60	50	10	20.0	1.44	13,900 13,700	6,070 6,060	2.3 2.3	13 14
PS4-1	2	[$CpTiCl_3$]	60	50	10	5.0	2.16	7,470 7,440	2,960 3,010	2.5 2.5	15 15
PS4-2	1	[$CpTiCl_3$]	60	50	10	10.0	0.15	–	–	–	–
PS4-3	2	[$CpTiCl_3$]	60	80	10	5.0	2.03	17,500 17,400	9,140 9,020	1.9 1.9	21 22
PS4-4[c]	2	[$CpTiCl_3$]	60	50	10	10.0	1.89	–	–	–	–
PS5-1	2	**111**	60	50	10	5.0	2.63	35,000 34,400	17,200 16,400	2.0 2.1	5 5
PS5-2	2	**111**	60	50	10	10.0	4.43	28,500 29,100	15,100 15,000	1.9 1.9	3 3
PS5-3	2	**111**	60	50	10	20.0	4.57	24,100 24,100	13,400 13,600	1.8 1.8	2 2
PS5-4	2	**111**	60	80	10	20.0	3.76	21,000 21,100	9,560 9,510	2.2 2.2	9 10

Table 7 (continued). Reaction conditions and analytical results of styrene polymerisation experiments.

Identifier	Work-up procedure	Catalyst	time / min	temperature / °C	[catalyst] / µmol	[MAO] / mmol	Recovered precipitate / g	M_w [a,b]	M_n [a,b]	M_w / M_n [a,b]	Peak area [a]
PS5-5[c]	2	**111**	60	50	10	20.0	5.23	16,500 16,400	6,530 6,780	2.5 2.4	3 3
PS6-1	2	**118**	60	50	10	5.0	1.93	6,190 6,280	3,300 3,290	1.9 1.9	5 5
PS6-2	2	**118**	60	50	10	10.0	2.19	5,740 4,950	1,370 1,320	4.2 3.7	4 4
PS6-3	2	**118**	60	50	10	20.0	3.53	5,720 5,680	3,430 3,370	1.7 1.7	1 2
PS6-4	2	**118**	60	80	10	20.0	4.43	12,600 12,600	4,790 4,760	2.6 2.6	7 8
PS6-5[c]	2	**118**	60	50	10	20.0	3.52	4,870 4,660	2,910 2,870	1.7 1.6	1 1

a) results of two GPC runs; b) all samples contained traces of high molecular weight material as evidenced by differential pressure chromatography, however, these traces were not included in the computation of molecular weight data; c) a mixture of toluene, styrene and MAO was heated to the desired temperature and after 15 min, a solution containing a specified amount of the respective catalyst precursor was added to start the polymerisation reaction; d) GPC performed on 1,2,4-trichlorobenzene solutions at 160 °C.

References

[1] PlasticsEurope Deutschland (Eds.), *Plastics Business Data and Charts*, Frankfurt, 2005, http://www.vke.de.

[2] K. Ziegler, E. Holzkamp, H. Breil, H. Martin, *Angew. Chem.* **1955**, *67*, 541.

[3] K. Ziegler, *Angew. Chem.* **1964**, *76*, 545.

[4] G. Natta, P. Corradini, *Atti Accad. Naz. Lincci Mem. Cl. Sci. Fis. Mat. Nat. Sez. II*, **1955**, 5, 73.

[5] G. Natta, *Angew. Chem.* **1956**, *68*, 393.

[6] G. Natta, *Angew. Chem.* **1964**, *76*, 553.

[7] J. P. Hogan, R. L. Banks, Belg. Pat. 530 617 (1955).

[8] M. P. McDaniel, *Adv. Catal.* **1985**, *33*, 47 and references therein.

[9] B. M. Weckhuysen, R. A. Schoonheydt, *Catal. Today*, **1999**, *51*, 215 and references therein.

[10] H. H. Brintzinger, D. Fischer, R. Mülhaupt, B. Rieger, R. Waymouth, *Angew. Chem.* **1995**, *107*, 1255; *Angew. Chem. Int. Ed. Engl.* **1995**, *34*, 1143 and references therein.

[11] W. Kaminsky, *J. Chem. Soc.*, *Dalton Trans.* **1998**, 1413.

[12] K. Soga, T. Shiono, *Prog. Polym. Sci.* **1997,** *22*, 1503.

[13] W. Kaminsky, M. Arndt, *Adv. Polym. Sci.* **1997**, *127*, 143.

[14] M. Bochmann, *J. Chem. Soc., Dalton Trans.* **1996**, 255.

[15] G. Fink, R. Mülhaupt, H. H. Brintzinger (Eds.), *Ziegler Catalysts*, Springer, Berlin, 1995.

[16] H. Sinn, W. Kaminsky, H.-J. Vollmer, *Angew. Chem.* **1980**, *92*, 396; *Angew. Chem. Int. Ed. Engl.* **1980**, *19*, 390.

[17] W. Kaminsky, *Macromol. Chem. Phys*. **1996**, *197*, 3907.

[18] A. Togni, R. L. Halterman (Eds.), *Metallocenes*, Wiley-VCH, Weinheim, 1998.

[19] J. A. Ewen, *J. Am. Chem. Soc.* **1984**, *106*, 6355.

[20] H. Schnutenhaus, H. H. Brintzinger, *Angew. Chem.* **1979**, *91*, 837; *Angew. Chem. Int. Ed. Engl.* **1979**, *18*, 777.

[21] F. R. W. P. Wild, M. Wasiucionek, G. Huttner, H. H. Brintzinger, *J. Organomet. Chem.* **1985**, *288*, 63.

[22] W. Kaminsky, K. Külper, H. H. Brintzinger, F. R. W. P. Wild, *Angew. Chem.* **1985**, *97*, 507; *Angew. Chem. Int. Ed. Engl.* **1985**, *24*, 507.

[23] P. J. Shapiro, E. Bunel, W. Schaefer, J. E. Bercaw, *Organometallics*, **1990**, *9*, 867.

[24] W. E. Piers, P. J. Shapiro, E. E. Bunel, J. E. Bercaw, *Synlett*, **1990**, 74.

[25] J. Okuda, *Chem. Ber*. **1990**, *123*, 1649.

[26] P. N. Stevens, F. J. Timmers, D. R. Wilson, G. F. Schmidt, P. N. Nickias, R. K. Rosen, G. W. Knight, S. Lai, *Eur. Pat. Appl*. **1991**, EP-416815-A2.

[27] J. M. Canich, G. G. Hlatky, H. W. Turner, *PCT Appl*. **1992**, WO 92-00333.

[28] D. W. Carpenetti, L. Kloppenburg, J. T. Kupec, J. L. Petersen, *Organometallics*, **1996**, *15*, 1572; correction in: *Organometallics*, **1996**, *15*, 2668.

[29] P.-J. Sinnema, L. v. d. Veen, A. L. Spek, N. Veldman, J. H. Teuben, *Organometallics*, **1997**, *16*, 4245.

[30] D. B. Millward, A. P. Cole, R. M. Waymouth, *Organometallics*, **2000**, *19*, 1870.

[31] P. S. Chum, W. J. Kruper, M. J. Guest, *Adv. Mater.* **2000**, *12*, 1759.

[32] A. L. McKnight, R. M. Waymouth, *Chem. Rev.* **1998**, *98*, 2587.

[33] J. Okuda, T. Eberle. In: A. Togni, R. L. Halterman (Eds.), *Metallocenes*, Vol. 1, Wiley-VCH, Weinheim, 1998, p. 415.

[34] G. J. P. Britovsek, V. C. Gibson, D. F. Wass, *Angew. Chem.* **1999**, *111*, 448; *Angew. Chem. Int. Ed.* **1999**, *38*, 428.

[35] V. C. Gibson, S. K. Spitzmesser, *Chem. Rev.* **2003**, *103*, 283.

[36] A. K. Hughes, A. Meetsma, J. H. Teuben, *Organometallics*, **1993**, *12*, 1936.

[37] A. L. McKnight, M. A. Masood, R. M. Waymouth, D. A. Straus, *Organometallics*, **1997**, *16*, 2879.

[38] H. V. R. Dias, Z. Wang, S. G. Bott, *J. Organomet. Chem.* **1996**, *508*, 91.

[39] J. Okuda, F. J. Schattenmann, S. Wocadlo, W. Massa, *Organometallics*, **1995**, *14*, 789.

[40] L. Duda, G. Erker, R. Fröhlich, F. Zippel, *Eur. J. Inorg. Chem.* **1998**, 1153.

[41] F. Amor, J. Okuda, *J. Organomet. Chem.* **1996**, *520*, 245.

[42] L. Resconi, I. Camurati, C. Grandini, M. Rinaldi, N. Mascellani, O. Traverso, *J. Organomet. Chem.* **2002**, *664*, 5.

[43] A. K. Hughes, A. J. Kingsley, *J. Chem. Soc., Dalton Trans.* **1997**, 4139.

[44] H. G. Alt, K. Föttinger, W. Milius, *J. Organomet. Chem.* **1999**, *572*, 21.

[45] U. Böhme, K.-H. Thiele, *J. Organomet. Chem.* **1994**, *472*, 39.

[46] K. E. du Plooy, U. Moll, S. Wocadlo, W. Massa, J. Okuda, *Organometallics*, **1995**, *14*, 3129.

[47] J. Okuda, F. Amor, K. E. du Plooy, T. Eberle, K. C. Hultzsch, T. P. Spaniol, *Polyhedron*, **1998**, *17*, 1073.

[48] H. Braunschweig, C. von Koblinski, F. M. Breitling, K. Radacki, C. Hu, L. Wesemann, T. Marx, I. Pantenburg, *Inorg. Chim. Acta*, **2003**, *350*, 467.

[49] W. A. Herrmann, M. J. A. Morawietz, *J. Organomet. Chem.* **1994**, *482*, 169.

[50] P.-J. Sinnema, K. Liekelema, O. K. B. Staal, B. Hessen, J. H. Teuben, *J. Mol. Catal. A: Chem.* **1998**, *128*, 143.

[51] W. A. Herrmann, M. J. A. Morawietz, T. Priermeier, *Angew. Chem.* **1994**, *106*, 2025; *Angew. Chem. Int. Ed. Engl.* **1994**, *33*, 1946.

[52] Y.-X. Chen, T. J. Marks, *Organometallics*, **1997**, *16*, 3649.

[53] P. T. Gomes, M. L. H. Green, A. M. Martins, P. Mountford, *J. Organomet. Chem.* **1997**, *541*, 121.

[54] P. T. Gomes, M. L. H. Green, A. M. Martins, *J. Organomet. Chem.* **1998**, *551*, 133.

[55] J. R. Ascenso, A. R. Dias, J. A. Fernandes, A. M. Martins, S. S. Rodrigues, *Inorg. Chim. Acta*, **2003**, *356*, 279.

[56] S. Ciruelos, T. Cuenca, R. Gómez, P. Gómez-Sal, A. Manzanero, P. Royo, *Organometallics*, **1996**, *15*, 5577.

[57] J. Okuda, S. Verch, T. P. Spaniol, R. Stürmer, *Chem. Ber.* **1996**, *129*, 1429.

[58] J. Okuda, K. E. du Plooy, W. Massa, H.-C. Kang, U. Rose, *Chem. Ber.* **1996**, *129*, 275.

[59] S. Ciruelos, A. Sebastián, T. Cuenca, P. Gómez-Sal, A. Manzanero, P. Royo, *J. Organomet. Chem.* **2000**, *604*, 103.

[60] A. B. Vázquez, P. Royo, E. Herdtweck, *J. Organomet. Chem.* **2003**, *683*, 155.

[61] J. Stroot, W. Saak, D. Haase, R. Beckhaus, *Z. Anorg. Allg. Chem.* **2002**, *628*, 755.

[62] R. Gómez, P. Gómez-Sal, A. Martín, A. Núñez, P. A. del Real, P. Royo, *J. Organomet. Chem.* **1998**, *564*, 93.

[63] W.-P. Leung, F.-Q. Song, Z.-Y. Zhou, F. Xue, T. C. W. Mak, *J. Organomet. Chem.* **1999**, *575*, 232.

[64] R. E. v. H. Spence, W. E. Piers, *Organometallics*, **1995**, *14*, 4617.

[65] F. Amor, A. Butt, K. du Plooy, T. Spaniol, J. Okuda, *J. Organomet. Chem.* **1998**, *558*, 139.

[66] J. Jin, D. R. Wilson, E. Y.-X. Chen, *Chem. Commun.* **2002**, 708.

[67] T. Eberle, T. P. Spaniol, J. Okuda, *Eur. J. Inorg. Chem.* **1998**, 237.

[68] F. Amor, K. E. du Plooy, T. P. Spaniol, J. Okuda, *J. Organomet. Chem.* **1998**, *558*, 139.

[69] D. D. Devore, F. J. Timmers, D. L. Hasha, T. J. Marks, P. A. Deck, C. L. Stern, *Organometallics*, **1995**, *14*, 3132.

[70] M. Dahlmann, J. Schottek, R. Fröhlich, D. Kunz, M. Nissinen, G. Erker, G. Fink, R. Kleinschmidt, *J. Chem. Soc., Dalton Trans.* **2000**, 1881.

[71] L. F. Braun, T. Dreier, M. Christy, J. L. Petersen, *Inorg. Chem.* **2004**, *43*, 3976.

[72] A. Spannenberg, W. Baumann, S. Becke, U. Rosenthal, *Organometallics*, **2002**, *21*, 1512.

[73] B. Rhodes, J. C. W. Chien, J. S. Wood, A. Chandrasekaran, M. D. Rausch, *Appl. Organomet. Chem.* **2002**, *16*, 323.

[74] G. Martínez, P. Royo, E. Herdtweck, *J. Organomet. Chem.* **2005**, *690*, 952.

[75] J. Zemánek, P. Štěpnička, K. Fejfarová, R. Gyepes, I. Císařová, M. Horáček, J. Kubišta, V. Varga, K. Mach, *Collect. Czech. Chem. Commun.* **2001**, *66*, 605.

[76] M. F. N. N. Carvalho, K. Mach, A. R. Dias, J. F. Mano, M. M. Marques, A. M. Soares, A. J. L. Pombeiro, *Inorg. Chem. Commun.* **2003**, *6*, 331.

[77] H. G. Alt, A. Reb, K. Kundu, *J. Organomet. Chem.* **2001**, *628*, 211.

[78] J. Klosin, W. J. Kruper, Jr., P. N. Nickias, G. R. Roof, P. De Waele, K. A. Abboud, *Organometallics*, **2001**, *20*, 2663.

[79] A. Razavi, U. Thewalt, *J. Organomet. Chem.* **2001**, *621*, 267.

[80] S. Gentil, N. Pirio, P. Meunier, J. C. Gallucci, J. D. Schloss, L. A. Paquette, *Organometallics*, **2000**, *19*, 4169.

[81] G. Xu, E. Ruckenstein, *Macromolecules*, **1998**, *31*, 4724.

[82] A. Sebastián, P. Royo, P. Gómez-Sal, E. Herdtweck, *Inorg. Chim. Acta*, **2003**, *350*, 511.

[83] A. R. Lavoie, R. M. Waymouth, *Tetrahedron*, **2004**, *60*, 7147.

[84] C. Grandini, I. Camurati, S. Guidotti, N. Mascellani, L. Resconi, I. E. Nifant'ev, I. A. Kashulin, P. V. Ivchenko, P. Mercandelli, A. Sironi, *Organometallics*, **2004**, *23*, 344.

[85] H. G. Alt, A. Reb, W. Milius, A. Weis, *J. Organomet. Chem.* **2001**, *628*, 169.

[86] A. Reb, H. G. Alt, *J. Mol. Catal. A: Chem.* **2001**, *174*, 35.

[87] J. Cano, P. Royo, M. Lanfranchi, M. A. Pellinghelli, A. Tiripicchio, *Angew. Chem.* **2001**, *113*, 2563; *Angew. Chem. Int. Ed.* **2001**, *40*, 2495.

[88] J. Cano, P. Royo, H. Jacobsen, O. Blacque, H. Berke, E. Herdtweck, *Eur. J. Inorg. Chem.* **2003**, 2463.

[89] M. Sudupe, J. Cano, P. Royo, E. Herdtweck, *Eur. J. Inorg. Chem.* **2004**, 3074.

[90] J. Cano, M. Sudupe, P. Royo, M. E. G. Mosquera, *Organometallics*, **2005**, *24*, 2424.

[91] H. G. Alt, R. Ernst, I. K. Böhmer, *J. Organomet. Chem.* **2002**, *658*, 259.

[92] L. Li, M. V. Metz, H. Li, M.-C. Chen, T. J. Marks, L. Liable-Sands, A. L. Rheingold, *J. Am. Chem. Soc.* **2002**, *124*, 12725.

[93] S. K. Noh, J. Lee, D.-H. Lee, *J. Organomet. Chem.* **2003**, *667*, 53.

[94] J. Wang, H. Li, N. Guo, L. Li, C. L. Stern, T. J. Marks, *Organometallics*, **2004**, *23*, 5112.

[95] S. K. Noh, W. L. Jiang, D. H. Lee, *Macromol. Res.* **2004**, *12*, 100.

[96] S. J. Brown, X. Gao, D. G. Harrison, L. Koch, R. E. v. H. Spence, G. P. A. Yap, *Organometallics*, **1998**, *17*, 5445.

[97] A. J. Ashe, III, X. Fang, J. W. Kampf, *Organometallics*, **1999**, *18*, 1363.

[98] S. Feng, J. Klosin, W. J. Kruper, Jr., M. H. McAdon, D. R. Neithamer, P. N. Nickias, J. T. Patton, D. R. Wilson, K. A. Abboud, C. L. Stern, *Organometallics*, **1999**, *18*, 1159.

[99] J. Okuda, S. Verch, R. Stürmer, T. P. Spaniol, *J. Organomet. Chem.* **2000**, *605*, 55.

[100] F. Amor, T. P. Spaniol, J. Okuda, *Organometallics*, **1997**, *16*, 4765.

[101] F. Amor, A. Butt, K. E. du Plooy, T. P. Spaniol, J. Okuda, *Organometallics*, **1998**, *17*, 5836.

[102] G. Jiménez, E. Rodríguez, P. Gómez-Sal, P. Royo, T. Cuenca, M. Galakhov, *Organometallics*, **2001**, *20*, 2459.

[103] G. Jiménez, P. Royo, T. Cuenca, E. Herdtweck, *Organometallics*, **2002**, *21*, 2189.

[104] S. Arndt, K. Beckerle, K. C. Hultzsch, P.-J. Sinnema, P. Voth, T. P. Spaniol, J. Okuda, *J. Mol. Catal. A: Chem.* **2002**, *190*, 215.

[105] J. Okuda, T. Eberle, T. P. Spaniol, V. Piquet-Fauré, *J. Organomet. Chem.* **1999**, *591*, 127.

[106] J. Okuda, S. Verch, R. Stürmer, T. P. Spaniol, *Chirality*, **2000**, *12*, 472.

[107] J. T. Park, S. C. Yoon, B.-J. Bae, W. S. Seo, I.-H. Suh, T. K. Han, J. R. Park, *Organometallics*, **2000**, *19*, 1269.

[108] V. Tabernero, T. Cuenca, E. Herdtweck, *J. Organomet. Chem.* **2002**, *663*, 173.

[109] A. I. Licht, H. G. Alt, *J. Organomet. Chem.* **2003**, *684*, 91.

[110] M. H. Lee, J.-W. Hwang, Y. Kim, Y. Han, Y. Do, *Organometallics*, **2000**, *19*, 5514.

[111] M. Horáček, P. Štěpnička, J. Kubišta, K. Fejfarová, R. Gyepes, K. Mach, *Organometallics*, **2003**, *22*, 861.

[112] S. Wang, Q. Yang, T. C. W. Mak, Z. Xie, *Organometallics*, **1999**, *18*, 4478.

[113] G. Zi, H.-W. Li, Z. Xie, *Organometallics*, **2002**, *21*, 1136.

[114] G. Zi, H.-W. Li, Z. Xie, *Organometallics*, **2002**, *21*, 3850.

[115] Y. Wang, H. Wang, H. Wang, H.-S. Chan, Z. Xie, *J. Organomet. Chem.* **2003**, *683*, 39.

[116] S. Wang, H.-W. Li, Z. Xie, *Organometallics*, **2004**, *23*, 2469.

[117] S. Wang, H.-W. Li, Z. Xie, *Organometallics*, **2004**, *23*, 3780.

[118] H. Wang, H.-S. Chan, J. Okuda, Z. Xie, *Organometallics*, **2005**, *24*, 3118.

[119] K. Kunz, G. Erker, S. Döring, R. Fröhlich, G. Kehr, *J. Am. Chem. Soc.* **2001**, *123*, 6181.

[120] S. Bredeau, G. Altenhoff, K. Kunz, S. Döring, S. Grimme, G. Kehr, G. Erker, *Organometallics*, **2004**, *23*, 1836.

[121] T. Ishiyama, T. Mizuta, K. Miyoshi, H. Nakazawa, *Chem. Lett.* **2003**, *32*, 70.

[122] O. Tardif, Z. Hou, M. Nishiura, T. Koizumi, Y. Wakatsuki, *Organometallics*, **2001**, *20*, 4565.

[123] G. Altenhoff, S. Bredeau, G. Erker, G. Kehr, O. Kataeva, R. Fröhlich, *Organometallics*, **2002**, *21*, 4084.

[124] T. Ishiyama, T. Mizuta, K. Miyoshi, H. Nakazawa, *Organometallics*, **2003**, *22*, 1096.

[125] O. Tardif, M. Nishiura, Z. Hou, *Tetrahedron*, **2003**, *59*, 10525.

[126] T. Ishiyama, K. Miyoshi, H. Nakazawa, *J. Mol. Catal. A: Chem.* **2004**, *221*, 41.

[127] S. Ciruelos, T. Cuenca, R. Gómez, P. Gómez-Sal, A. Manzanero, P. Royo, *Polyhedron*, **1998**, *17*, 1055.

[128] Y.-X. Chen, P.-F. Fu, C. L. Stern, T. J. Marks, *Organometallics*, **1997**, *16*, 5958.

[129] For a review on this class of compounds and related cyclopentadienyl complexes bearing pendant *O*-donors see: U. Siemeling, *Chem. Rev.* **2000**, *100*, 1495.

[130] Y. Qian, J. Huang, X. Chen, G. Li, W. Chen, B. Li, X. Jin, Q. Yang, *Polyhedron*, **1994**, *13*, 1105.

[131] A. Rau, S. Schmitz, G. Luft, *J. Organomet. Chem.* **2000**, *608*, 71.

[132] L. E. Turner, M. G. Thorn, P. E. Fanwick, I. P. Rothwell, *Chem. Commun.* **2003**, 1034.

[133] Y. Zhang, J. Wang, Y. Mu, Z. Shi, C. Lü, Y. Zhang, L. Qiao, S. Feng, *Organometallics*, **2003**, *22*, 3877.

[134] Y. Zhang, Y. Mu, C. Lü, G. Li, J. Xu, Y. Zhang, D. Zhu, S. Feng, *Organometallics*, **2004**, *23*, 540.

[135] L. E. Turner, M. G. Thorn, P. E. Fanwick, I. P. Rothwell, *Organometallics*, **2004**, *23*, 1576.

[136] B. Rieger, *J. Organomet. Chem.* **1991**, *420*, C17.

[137] J. Christoffers, R. G. Bergman, *Angew. Chem.* **1995**, *107*, 2423; *Angew. Chem. Int. Ed. Engl.* **1995**, *34*, 2266.

[138] G. Trouvé, D. A. Laske, A. Meetsma, J. H. Teuben, *J. Organomet. Chem.* **1996**, *511*, 255.

[139] E. E. C. G. Gielens, J. Y. Tiesnitsch, B. Hessen, J. H. Teuben, *Organometallics*, **1998**, *17*, 1652.

[140] R. W. Baker, B. J. Wallace, *Chem. Commun.* **1999**, 1405.

[141] S. D. R. Christie, K. W. Man, R. J. Whitby, A. M. Z. Slawin, *Organometallics*, **1999**, *18*, 348.

[142] D. Hüerländer, R. Fröhlich, G. Erker, *J. Chem. Soc., Dalton Trans.* **2002**, 1513.

[143] J. Wang, C. Zheng, J. A. Maguire, N. S. Hosmane, *Organometallics*, **2003**, *22*, 4839.

[144] P. J. Shapiro, *Coord. Chem. Rev.* **2002**, *231*, 67 and references therein.

[145] C. E. Zachmanoglou, A. Docrat, B. M. Bridgewater, G. Parkin, C. G. Brandow, J. E. Bercaw, C. N. Jardine, M. Lyall, J. C. Green, J. B. Keister, *J. Am. Chem. Soc.* **2002**, *124*, 9525.

[146] K. Kunz, G. Erker, G. Kehr, R. Fröhlich, H. Jacobsen, H. Berke, O. Blacque, *J. Am. Chem. Soc.* **2002**, *124*, 3316.

[147] A. B. Vázquez, P. Royo, *J. Organomet. Chem.* **2003**, *671*, 172.

[148] H. Braunschweig, C. von Koblinski, U. Englert, *Chem. Commun.* **2000**, 1049.

[149] A. Bertuleit, M. Könemann, L. Duda, G. Erker, R. Fröhlich, *Topics Catal.* **1999**, *7*, 37.

[150] K. Kunz, G. Erker, S. Döring, S. Bredeau, G. Kehr, R. Fröhlich, *Organometallics*, **2002**, *21*, 1031.

[151] V. V. Kotov, E. V. Avtomonov, J. Sundermeyer, K. Harms, D. A. Lemenovskii, *Eur. J. Inorg. Chem.* **2002**, 678.

[152] A. A. Trifonov, T. P. Spaniol, J. Okuda, *Organometallics*, **2001**, *20*, 4869.

[153] P. Foster, J. C. W. Chien, M. D. Rausch, *J. Organomet. Chem.* **1997**, *545*, 35.

[154] D. van Leusen, D. J. Beetstra, B. Hessen, J. H. Teuben, *Organometallics*, **2000**, *19*, 4084.

[155] A. K. Hughes, S. M. B. Marsh, J. A. K. Howard, P. S. Ford, *J. Organomet. Chem.* **1997**, *528*, 195.

[156] P. J. Shapiro, W. D. Cotter, W. P. Schaefer, J. A. Labinger, J. E. Bercaw, *J. Am. Chem. Soc.* **1994**, *116*, 4623.

[157] Y. Mu, W. E. Piers, M.-A. MacDonald, M. J. Zaworotko, *Can. J. Chem.* **1995**, *73*, 2233.

[158] K. C. Hultzsch, T. P. Spaniol, J. Okuda, *Angew. Chem.* **1999**, *111*, 163; *Angew. Chem. Int. Ed.* **1999**, *38*, 227.

[159] K. C. Hultzsch, P.Voth, K. Beckerle, T. P. Spaniol, J. Okuda, *Organometallics*, **2000**, *19*, 228.

[160] S. Arndt, P. Voth, T. P. Spaniol, J. Okuda, *Organometallics*, **2000**, *19*, 4690.

[161] M. Nishiura, Z. Hou, Y. Wakatsuki, T. Yamaki, T. Miyamoto, *J. Am. Chem. Soc.* **2003**, *125*, 1184.

[162] E. Kirillov, L. Toupet, C. W. Lehmann, A. Razavi, J.-F. Carpentier, *Organometallics*, **2003**, *22*, 4467.

[163] Z. Hou, T. Koizumi, M. Nishiura, Y. Wakatsuki, *Organometallics*, **2001**, *20*, 3323.

[164] J. T. Golden, D. N. Kazul'kin, B. L. Scott, A. Z. Voskoboynikov, C. J. Burns, *Organometallics*, **2003**, *22*, 3971.

[165] B. D. Stubbert, C. L. Stern, T. J. Marks, *Organometallics*, **2003**, *22*, 4836.

[166] P. T. Witte, A. Meetsma, B. Hessen, *Organometallics*, **1999**, *18*, 2944.

[167] Kaminsky, W., Hinrichs, B., Rehder, D., *Polymer*, **2002**, *43*, 7225.

[168] P. T. Witte, A. Meetsma, B. Hessen, P. H. M. Budzelaar, *J. Am. Chem. Soc.* **1997**, *119*, 10561.

[169] W. A. Herrmann, W. Baratta, *J. Organomet. Chem.* **1996**, *506*, 357.

[170] M. I. Alcalde, M. P. Gómez-Sal, P. Royo, *Organometallics*, **1999**, *18*, 546.

[171] S. Gómez-Ruiz, T. Höcher, S. Prashar, E. Hey-Hawkins, *Organometallics*, **2005**, *24*, 2061.

[172] R. Arteaga-Müller, J. Sánchez-Nieves, P. Royo, M. E. G. Mosquera, *Polyhedron* **2005**, in press.

[173] Y. Liang, G. P. A. Yap, A. L. Rheingold, K. H. Theopold, *Organometallics*, **1996**, *15*, 5284.

[174] W. A. Herrmann, W. Baratta, M. J. A. Morawietz, *J. Organomet. Chem.* **1995**, *497*, C4.

[175] T.-F. Wang, C.-Y. Lai, C.-C. Hwu, Y.-S. Wen, *Organometallics*, **1997**, *16*, 1218.

[176] T.-F. Wang, C.-C. Hwu, C.-W. Tsai, Y.-S. Wen, *Organometallics*, **1998**, *17*, 131.

[177] J. M. Pietryga, J. D. Gorden, C. L. B. Macdonald, A. Voigt, R. J. Wiacek, A. H. Cowley, *J. Am. Chem. Soc.* **2001**, *123*, 7713.

[178] J. M. Pietryga, J. N. Jones, L. A. Mullins, R. J. Wiacek, A. H. Cowley, *Chem. Commun.* **2003**, 2072.

[179] R. J. Wiacek, C. L. B. Macdonald, J. N. Jones, J. M. Pietryga, A. H. Cowley, *Chem. Commun.* **2003**, 430.

[180] See references 15 – 34 in ref. 32 and references 29 – 41 in ref. 35.

[181] P. Cossee, *J. Catal.* **1964**, *3*, 80.

[182] E. J. Arlman, P. Cossee, *J. Catal.* **1964**, *3*, 99.

[183] T. K. Woo, L. Fan, T. Ziegler, *Organometallics*, **1994**, *13*, 432.

[184] T. K. Woo, L. Fan, T. Ziegler, *Organometallics*, **1994**, *13*, 2252.

[185] L. Fan, D. Harrison, T. K. Woo, T. Ziegler, *Organometallics*, **1995**, *14*, 2018.

[186] T. K. Woo, P. M. Margl, J. C. W. Lohrenz, P. E. Blöchl, T. Ziegler, *J. Am. Chem. Soc.* **1996**, *118*, 13021.

[187] G. Lanza, I. L. Fragalà, T. J. Marks, *J. Am. Chem. Soc.* **1998**, *120*, 8257.

[188] M. S. W. Chan, K. Vanka, C. C. Pye, T. Ziegler, *Organometallics*, **1999**, *18*, 4624.

[189] G. Lanza, I. L. Fragalà, T. J. Marks, *Organometallics*, **2001**, *20*, 4006.

[190] G. Lanza, I. L. Fragalà, T. J. Marks, *Organometallics*, **2002**, *21*, 5594.

[191] Z. Xu, K. Vanka, T. Ziegler, *Organometallics*, **2004**, *23*, 104.

[192] S. H. Yang, J. Huh, W. H. Jo, *Macromolecules*, **2005**, 38, 1402.

[193] R. Kleinschmidt, Y. Griebenow, G. Fink, *J. Mol. Catal. A: Chem.* **2000**, *157*, 83.

[194] G. Lanza, I. L. Fragalà, T. J. Marks, *J. Am. Chem. Soc.* **2000**, *122*, 12764.

[195] J. C. Stevens, *Stud. Surf. Sci. Catal.* **1996**, *101*, 11.

[196] K. Soga, T. Uozumi, S. Nakamura, T. Toneri, T. Teranishi, T. Sano, T. Arai, T. Shiono, *Macromol. Chem. Phys.* **1996**, *197*, 4237.

[197] T. K. Woo, P. M. Margl, T. Ziegler, P. E. Blöchl, *Organometallics*, **1997**, *16*, 3454.

[198] W.-J. Wang, D. Yan, S. Zhu, A. E. Hamielec, *Macromolecules*, **1998**, *31*, 8677.

[199] M. Nele, J. B. P. Soares, *Macromol. Theory Simul.* **2002**, *11*, 939.

[200] E. Y.-X. Chen, T. J. Marks, *Chem. Rev.* **2000**, *100*, 1391 and references therein.

[201] H. Sinn, W. Kaminsky, H. Höcker (Eds.), *Alumoxanes*, Macromolecular Symposia 97, Hüthig & Wepf, Heidelberg 1995.

[202] S. S. Reddy, S. Sivaram, *Prog. Polym. Sci.* **1995**, *20*, 309.

[203] For a structure elucidation of the active species in MAO activated CGCs based on ^{1}H and ^{13}C NMR spectroscopy see: K. P. Bryliakov, E. P. Talsi, M. Bochmann, *Organometallics*, **2004**, *23*, 149.

[204] T. Shiomura, T. Asanuma, T. Sunaga, *Macromol. Rapid Commun.* **1997**, *18*, 169.

[205] W. E. Piers, T. Chivers, *Chem. Soc. Rev.* **1997**, *26*, 345 and references therein.

[206] X. Yang, C. L. Stern, T. J. Marks, *J. Am. Chem. Soc.* **1991**, *113*, 3623.

[207] X. Yang, C. L. Stern, T. J. Marks, *J. Am. Chem. Soc.* **1994**, *116*, 10015.

[208] For a review on weakly coordinating anions see: I. Krossing, I. Raabe, *Angew. Chem.* **2004**, *116*, 2116; *Angew. Chem. Int. Ed.* **2004**, *43*, 2066.

[209] F. Song, R. D. Cannon, S. J. Lancaster, M. Bochmann, *J. Mol. Catal. A: Chem.* **2004**, *218*, 21.

[210] P. A. Deck, C. L. Beswick, T. J. Marks, *J. Am. Chem. Soc.* **1998**, *120*, 1772.

[211] T. Shiomura, T. Asanuma, N. Inoue, *Macromol. Rapid Commun.* **1996**, *17*, 9.

[212] H. Hagihara, T. Shiono, T. Ikeda, *Macromolecules*, **1998**, *31*, 3184.

[213] T. Hasan, A. Ioku, K. Nishii, T. Shiono, T. Ikeda, *Macromolecules*, **2001**, *34*, 3142.

[214] A. Ioku, T. Hasan, T. Shiono, T. Ikeda, *Macromol. Chem. Phys.* **2002**, *203*, 748.

[215] A. Ioku, T. Shiono, T. Ikeda, *Appl. Catal. A: General*, **2002**, *226*, 15.

[216] T. Hasan, T. Shiono, T. Ikeda, *Macromol. Symp.* **2004**, *213*, 123.

[217] E. Y.-X. Chen, W. J. Kruper, G. Roof, D. R. Wilson, *J. Am. Chem. Soc.* **2001**, *123*, 745.

[218] Y.-X. Chen, C. L. Stern, T. J. Marks, *J. Am. Chem. Soc.* **1997**, *119*, 2582.

[219] A. H. Cowley, G. S. Hair, B. G. McBurnett, R. A. Jones, *Chem. Commun.* **1999**, 437.

[220] G. S. Hair, R. A. Jones, A. H. Cowley, V. Lynch, *Inorg. Chem.* **2001**, *40*, 1014.

[221] F. Hannig, R. Fröhlich, K. Bergander, G. Erker, J. L. Petersen, *Organometallics*, **2004**, *23*, 4495.

[222] M. Dahlmann, G. Erker, K. Bergander, *J. Am. Chem. Soc.* **2000**, *122*, 7986.

[223] J. C. Stevens, *Stud. Surf. Sci. Catal.* **1994**, *89*, 277.

[224] On the contrary, for $(CH_2)_n$ (n = 2, 3) bridged systems, a higher activity was observed for the longer bridge (corresponding to a less acute $Cp_{centroid}$–M–N angle), see ref. 50.

[225] C. Janiak. In: A. Togni, R. L. Halterman (Eds.), *Metallocenes*, Vol. 2, Wiley-VCH, Weinheim, 1998, p. 547.

[226] J. Suhm, M. J. Schneider, R. Mülhaupt, *J. Mol. Catal. A: Chem.* **1998**, *128*, 215.

[227] A. Malmberg, J. Liimatta, A. Lehtinen, B. Löfgren, *Macromolecules*, **1999**, *32*, 6687.

[228] H. Li, L. Li, T. J. Marks, L. Liable-Sands, A. L. Rheingold, *J. Am. Chem. Soc.* **2003**, *125*, 10788.

[229] M. Galimberti, N. Mascellani, F. Piemontesi, I. Camurati, *Macromol. Rapid Commun.* **1999**, *20*, 214.

[230] K. Nishii, T. Shiono, T. Ikeda, *Macromol. Rapid Commun.* **2004**, *25*, 1029.

[231] K. Nishii, T. Matsumae, E. O. Dare, T. Shiono, T. Ikeda, *Macromol. Chem. Phys.* **2004**, *205*, 363.

[232] C. De Rosa, F. Auriemma, O. Ruiz de Ballesteros, L. Resconi, A. Fait, E. Ciaccia, I. Camurati, *J. Am. Chem. Soc.* **2003**, *125*, 10913.

[233] C. De Rosa, F. Auriemma, O. Ruiz de Ballesteros, *Macromolecules*, **2003**, *36*, 7607.

[234] P.-J. Sinnema, B. Hessen, J. H. Teuben, *Macromol. Rapid. Commun.* **2000**, *21*, 562.

[235] G. Xu, D. Cheng, *Macromolecules*, **2001**, *34*, 2040.

[236] M. Kamigaito, T. K. Lal, R. M. Waymouth, *J. Polym. Sci. A: Polym. Chem.* **2000**, *38*, 4649.

[237] J. M. Santos, M. R. Ribeiro, M. F. Portela, H. Cramail, A. Deffieux, *Macromol. Chem. Phys.* **2001**, *202*, 3043.

[238] J. M. Santos, M. R. Ribeiro, M. F. Portela, H. Cramail, A. Deffieux, A. Antiñolo, A. Otero, S. Prashar, *Macromol. Chem. Phys.* **2002**, *203*, 139.

[239] A. Tsuchida, C. Bolln, F. G. Sernetz, H. Frey, R. Mülhaupt, *Macromolecules*, **1997**, *30*, 2818.

[240] J.-F. Lahitte, F. Peruch, F. Isel, P. J. Lutz, *Macromol. Symp.* **2004**, *213*, 253.

[241] X. Zhang, B. Hessen, *Chem. Commun.* **2002**, 2862.

[242] D.-H. Lee, K.-B. Yoon, H.-J. Kim, S.-S. Woo, S. K. Noh, *J. Appl. Polym. Sci.* **1998**, *67*, 2187.

[243] J. Ren, G. R. Hatfield, *Macromolecules*, **1995**, *28*, 2588.

[244] F. G. Sernetz, R. Mülhaupt, R. M. Waymouth, *Macromol. Chem. Phys.* **1996**, *197*, 1071.

[245] F. G. Sernetz, R. Mülhaupt, F. Amor, T. Eberle, J. Okuda, *J. Polym. Sci. A: Polym. Chem.* **1997**, *35*, 1571.

[246] K. Nomura, H. Okumura, T. Komatsu, N. Naga, Y. Imanishi, *J. Mol. Catal. A: Chem.* **2002**, *190*, 225.

[247] R. Skeřil, P. Šindelář, Z. Salajka, V. Varga, I. Císařová, J. Pinkas, M. Horáček, K. Mach, *J. Mol. Catal. A: Chem.* **2004**, *224*, 97.

[248] G. Xu, *Macromolecules*, **1998**, *31*, 2395.

[249] N. Guo, L. Li, T. J. Marks, *J. Am. Chem. Soc.* **2004**, *126*, 6542.

[250] S. K. Noh, Y. Yang, W. S. Lyoo, *J. Appl. Polym. Sci.* **2003**, *90*, 2469.

[251] S. K. Noh, M. Lee, D. H. Kum, K. Kim, W. S. Lyoo, D.-H. Lee, *J. Polym. Sci. A: Polym. Chem.* **2004**, *42*, 1712.

[252] T. C. Chung, H. L. Lu, *J. Polym. Sci. A, Polym. Chem.* **1997**, *35*, 575.

[253] T. C. Chung, H. L. Lu, *J. Polym. Sci. A: Polym. Chem.* **1998**, *36*, 1017.

[254] F. G. Sernetz, R. Mülhaupt, *J. Polym. Sci. A: Polym. Chem.* **1997**, *35*, 2549.

[255] H. L. Lu, S. Hong, T. C. Chung, *Macromolecules*, **1998**, *31*, 2028.

[256] F. G. Sernetz, R. Mülhaupt, R. M. Waymouth, *Polym. Bull.* **1997**, *38*, 141.

[257] C. Janiak, P. G. Lassahn, *J. Mol. Catal. A, Chem.* **2001**, *166*, 193 and references therein.

[258] D. Ruchatz, G. Fink, *Macromolecules*, **1998**, *31*, 4669.

[259] D. Ruchatz, G. Fink, *Macromolecules*, **1998**, *31*, 4674.

[260] D. Ruchatz, G. Fink, *Macromolecules*, **1998**, *31*, 4681.

[261] D. Ruchatz, G. Fink, *Macromolecules*, **1998**, *31*, 4684.

[262] A. L. McKnight, R. M. Waymouth, *Macromolecules*, **1999**, *32*, 2816.

[263] I. Tritto, C. Marestin, L. Boggioni, L. Zetta, A. Provasoli, D. R. Ferro, *Macromolecules*, **2000**, *33*, 8931.

[264] B. A. Harrington, D. J. Crowther, *J. Mol. Catal. A: Chem.* **1998**, *128*, 79.

[265] I. Tritto, C. Marestin, L. Boggioni, M. C. Sacchi, H.-H. Brintzinger, D. R. Ferro, *Macromolecules*, **2001**, *34*, 5770.

[266] K. Thorshaug, R. Mendichi, L. Boggioni, I. Tritto, S. Trinkle, C. Friedrich, R. Mülhaupt, *Macromolecules*, **2002**, *35*, 2903.

[267] E.-G. Kim, M. L. Klein, *Organometallics*, **2004**, *23*, 3319.

[268] H. Lasarov, T. T. Pakkanen, *Macromol. Rapid. Commun.* **2001**, *22*, 434.

[269] R. Manivannan, G. Sundararajan, W. Kaminsky, *Macromol. Rapid Commun.* **2000**, *21*, 968.

[270] R. Manivannan, G. Sundararajan, W. Kaminsky, *J. Mol. Catal. A: Chem.* **2000**, *160*, 85.

[271] A. R. Lavoie, M. H. Ho, R. M. Waymouth, *Chem. Commun.* **2003**, 864.

[272] T. R. Jensen, J. J. O'Donnell, III, T. J. Marks, *Organometallics*, **2004**, *23*, 740.

[273] S. Ikai, J. Yamashita, Y. Kai, M. Murakami, T. Yano, Y. Qian, J. Huang, *J. Mol. Catal. A: Chem.* **1999**, *140*, 115.

[274] W. Kaminsky, B. Hinrichs, D. Rehder, *Polymer*, **2002**, *43*, 7225.

[275] W. Kaminsky, B. Hinrichs, *Macromol. Symp.* **2003**, *195*, 39.

[276] L. S. Boffa, B. M. Novak, *Chem. Rev.* **2000**, *100*, 1479.

[277] M. M. Marques, S. G. Correia, J. R. Ascenso, A. F. G. Ribeiro, P. T. Gomes, A. R. Dias, P. Foster, M. D. Rausch, J. C. W. Chien, *J. Polym. Sci. A: Polym. Chem.* **1999**, *37*, 2457.

[278] H. Nguyen, A. P. Jarvis, M. J. G. Lesley, W. M. Kelly, S. S. Reddy, N. J. Taylor, S. Collins, *Macromolecules*, **2000**, *33*, 1508.

[279] A. Rodriguez-Delgado, W. R. Mariott, E. Y.-X. Chen, *Macromolecules*, **2004**, *37*, 3092.

[280] J. Jin, E. Y.-X. Chen, *Macromol. Chem. Phys.* **2002**, *203*, 2329.

[281] E. A. Bijpost, R. Duchateau, J. H. Teuben, *J. Mol. Catal. A: Chem.* **1995**, *95*, 121.

[282] D. B. Millward, G. Sammis, R. M. Waymouth, *J. Org. Chem.* **2000**, *65*, 3902.

[283] R. A. Stockland, Jr., S. R. Foley, R. F. Jordan, *J. Am. Chem. Soc.* **2003**, *125*, 796.

[284] A. K. Dash, T. R. Jensen, C. L. Stern, T. J. Marks, *J. Am. Chem. Soc.* **2004**, *126*, 12528.

[285] V. M. Arredondo, S. Tian, F. E. McDonald, T. J. Marks, *J. Am. Chem. Soc.* **1999**, *121*, 3633.

[286] S. Tian, V. M. Arredondo, C. L. Stern, T. J. Marks, *Organometallics*, **1999**, *18*, 2568.

[287] M. Nishiura, Z. Hou, *J. Mol. Catal. A: Chem.* **2004**, *213*, 101.

[288] For a review on boron-bridged Group 4 *ansa*-metallocenes see: P. J. Shapiro, *Eur. J. Inorg. Chem.* **2001**, 321.

[289] H. Braunschweig, M. Kraft, K. Radacki, S. Stellwag, *Z. Anorg. Allg. Chem.* **2005**, accepted for publication.

[290] J. A. Klang, D. B. Collum, *Organometallics*, **1988**, *7*, 1532.

[291] S. A. Larkin, J. T. Golden, P. J. Shapiro, G. P. A. Yap, D. M. J. Foo, A. L. Rheingold, *Organometallics*, **1996**, *15*, 2393.

[292] D. S. Stelck, P. J. Shapiro, N. Basickes, *Organometallics*, **1997**, *16*, 4546.

[293] C. T. Burns, D. S. Stelck, P. J. Shapiro, A. Vij, K. Kunz, A. L. Rheingold, *Organometallics*, **1999**, *18*, 5432.

[294] M. T. Reetz, M. Willuhn, C. Psiorz, R. Goddard, *Chem. Commun*. **1999**, 1103.

[295] K. A. Rufanov, V. V. Kotov, N. B. Kazennova, D. A. Lemenovskii, E. V. Avtomonov, J. Lorberth, *J. Organomet. Chem.* **1996**, *525*, 287.

[296] H. Braunschweig, C. von Koblinski, R. Wang, *Eur. J. Inorg. Chem.* **1999**, 69.

[297] H. Braunschweig, C. von Koblinski, M. Mamuti, U. Englert, R. Wang, *Eur. J. Inorg. Chem.* **1999**, 1899.

[298] A. J. Ashe, III, X. Fang, J. W. Kampf, *Organometallics*, **1999**, *18*, 2288.

[299] A. J. Ashe, III, X. Fang, A. Hokky, J. W. Kampf, *Organometallics*, **2004**, *23*, 2197.

[300] H. Braunschweig, M. Kraft, K. Radacki, S. Stellwag, *Eur. J. Inorg. Chem.* **2005**, 2754.

[301] For a recent review on aminoboranediyl bridged metallocenes and CGCs see: H. Braunschweig, F. M. Breitling, E. Gullo, M. Kraft, *J. Organomet. Chem.* **2003**, *680*, 31.

[302] H. Braunschweig, M. Gross, M. Kraft, M. O. Kristen, D. Leusser, J. Am. Chem. Soc. 2005, 127, 3282.

[303] H. Braunschweig, M. Kraft, M. Homberger, F. M. Breitling, A. J. P. White, U. Englert, D. J. Williams, *Appl. Organomet. Chem.* **2003**, *17*, 421.

[304] C. von Koblinski, Ph.D. Thesis, Aachen, 2000.

[305] H. Braunschweig, F. M. Breitling, M. Homberger, C. von Koblinski, A. J. P. White, D. J. Williams, *Z. Anorg. Allg. Chem.* **2003**, *629*, 2244.

[306] M. Homberger, Ph.D. Thesis, Aachen, 2002.

[307] P. Jutzi, *Chem. Rev.* **1986**, *86*, 983.

[308] P. Paetzold, H. Grundke, *Chem. Ber.* **1971**, *104*, 1136.

[309] G. E. Herberich, A. Fischer, *Organometallics*, **1996**, *15*, 58.

[310] E. Barday, B. Frange, B. Hanquet, G. E. Herberich, *J. Organomet. Chem.* **1999**, *572*, 225.

[311] J. Knizek, I. Krossing, H. Nöth, W. Ponikwar, *Eur. J. Inorg. Chem.* **1998**, 505.

[312] K. Rufanov, E. Avtomonov, N. Kazennova, V. Kotov, A. Khvorost, D. Lemenovskii, J. Lorberth, *J. Organomet. Chem.* **1997**, *536-537*, 361.

[313] R. Duchateau, S. J. Lancaster, M. Thornton-Pett, M. Bochmann, *Organometallics*, **1997**, *16*, 4995.

[314] For an exception see ref. 313 and I. D. Gridnev, A. Meller, *Main Group Metal Chem.* **1998**, *21*, 271.

[315] H. Braunschweig, C. von Koblinski, M. Neugebauer, U. Englert, X. Zheng, *J. Organomet. Chem.* **2001**, *619*, 305.

[316] B. M. Mikhailov, T. K. Baryshnikova, V. S. Bogdanov, *Zh. Obsch. Khim.* **1973**, *43*,1949.

[317] G. E. Herberich, E. Barday, A. Fischer, *J. Organomet. Chem.* **1998**, *567*, 127.

[318] F. A. Bovey, L. Jelinski, P. A. Mirau, *Nuclear Magnetic Resonance Spectroscopy*, 2. ed., Academic Press, San Diego, 1988.

[319] B. Wrackmeyer, *Prog. NMR Spectrosc.* **1979**, *12*, 227.

[320] H. Nöth, B. Wrackmeyer, *Nuclear Magnetic Resonance*, *Spectroscopy of Boron Compounds*. In: P. Diehl, E. Fluck, R. Kosfeld (Eds.), *NMR*, *Basic Principles and Progress*, Vol. 14, Springer, Berlin, 1978.

[321] H. Friebolin, *Basic one and two dimensional NMR spectroscopy*, 2. ed., VCH, Weinheim, 1992.

[322] A. J. Ashe, III, W. Klein, R. Rousseau, *J. Organomet. Chem.* **1994**, *468*, 21 and references therein.

[323] B. Wrackmeyer, U. Dörfler, M. Herberhold, *Z. Naturforschung B*, **1993**, *48*, 121.

[324] Synthesis of a CGC bearing a pendent ferrocenyl moiety has been previously reported: L. Schwink, P. Knochel, T. Eberle, J. Okuda, *Organometallics*, **1998**, *17*, 7.

[325] M. Kraft, Ph.D. Thesis, Würzburg, 2005.

[326] S. Guo, F. Peters, F. F. de Biani, J. W. Bats, E. Herdtweck, P. Zanello, M. Wagner, *Inorg. Chem.* **2001**, *40*, 4928.

[327] R. Köster, M. A. Grassberger, *Liebigs Ann. Chem.* **1968**, *719*, 169.

[328] L. I. Zakharkin, A. I. Kovredov, *Izv. Akad. Nauk SSSR*, **1962**, *12*, 2247.

[329] H. C. Brown, A. B. Levy, *J. Organomet. Chem.* **1972**, *44*, 233.

[330] D. Fest, C. D. Habben, A. Meller, G. M. Sheldrick, D. Stalke, F. Pauer, *Chem. Ber.* **1990**, *123*, 703.

[331] H.-J. Koch, H. W. Roesky, R. Bohra, M. Noltemeyer, H.-G. Schmidt, *Angew. Chem.* **1992**, *104*, 612; *Angew. Chem.*, *Int. Ed. Engl.* **1992**, *31*, 598.

[332] D. R. Manke, D. G. Nocera, *Inorg. Chim. Acta*, **2003**, *345*, 235.

[333] D. R. Manke, D. G. Nocera, *Inorg. Chem.* **2003**, *42*, 4431.

[334] D. R. Manke, Z.-H. Loh, D. G. Nocera, *Inorg. Chem.* **2004**, *43*, 3618.

[335] K. Ma, H.-W. Lerner, S. Scholz, J. W. Bats, M. Bolte, M. Wagner, *J. Organomet. Chem.* **2002**, *664*, 94.

[336] M. Scheibitz, M. Bolte, J. W. Bats, H.-W. Lerner, I. Nowik, R. H. Herber, A. Krapp, M. Lein, M. C. Holthausen, M. Wagner, *Chem. Eur. J.* **2005**, *11*, 584.

[337] A. Appel, F. Jäkle, T. Priermeier, R. Schmid, M. Wagner, *Organometallics*, **1996**, *15*, 1188.

[338] J. Silver, D. A. Davies, R. M. G. Roberts, M. Herberhold, U. Dörfler, B. Wrackmeyer, *J. Organomet. Chem.* **1999**, *590*, 71.

[339] D. M. Giolando, K. Kirschbaum, L. J. Graves, U. Bolle, *Inorg. Chem*. **1992**, *31*, 3887.

[340] Y. Bai, M. Noltemeyer, H. W. Roesky, *Z. Naturforsch. B: Chem. Sci.* **1991**, *46*, 1357.

[341] R. M. Pupi, J. N. Coalter, J. L. Petersen, *J. Organomet. Chem.* **1995**, *497*, 17.

[342] Y. Bai, H. W. Roesky, M. Noltemeyer, *Z. Anorg. Allg. Chem.* **1991**, *595*, 21.

[343] S. Ciruelos, T. Cuenca, P. Gómez-Sal, A. Manzanero, P. Royo, *Organometallics*, **1995**, *14*, 177.

[344] A. V. Churakov, D. A. Lemenovskii, L. G. Kuz'mina, *J. Organomet. Chem.* **1995**, *489*, C81.

[345] R. Fandos, A. Meetsma, J. H. Teuben, *Organometallics*, **1991**, *10*, 59.

[346] D. C. Bradley, M. H. Chisholm, *Acc. Chem. Res.* **1976**, *9*, 273.

[347] J. C. Green, M. Payne, E. A. Seddon, R. A. Andersen, *J. Chem. Soc.*, *Dalton Trans.* **1982**, 887.

[348] According to the certificate of analysis, the MAO solution supplied by Crompton, Bergkamen, Germany that was used in the present study contains 34.5% of the overall aluminium in the form of free and associated $AlMe_3$. Even after heating a MAO solution *in vacuo* for several hours, significant amounts (3.5%) of $AlMe_3$ are retained in the mixture, see: L. Resconi, S. Bossi, L. Abis, *Macromolecules*, **1990**, *23*, 4489.

[349] H. Oedinger, F. Möller, *Angew. Chem.* **1967**, *79*, 53; *Angew. Chem., Int. Ed. Engl.* **1967**, *16*, 76.

[350] H. Oedinger, F. Möller, K. Eiter, *Synthesis*, **1972**, 591.

[351] P. Wolkoff, *J. Org. Chem.* **1982**, *47*, 1944.

[352] I. Hermecz. In: A. R. Katritzky (Ed.), *Advances in Heterocyclic Chemistry*, Academic Press, New York, 1987, p. 83.

[353] P.-J. Sinnema, T. P. Spaniol, J. Okuda, *J. Organomet. Chem.* **2000**, *598*, 179.

[354] K. Nomura, K. Fujii, *Organometallics*, **2002**, *21*, 3042.

[355] K. Nomura, K. Fujii, *Stud. Surf. Sci. Catal.* **2003**, *145*, 121.

[356] K. Nomura, K. Fujii, *Macromolecules*, **2003**, *36*, 2633.

[357] Low solubility of polymers could, in principle, also result from (i) very high molecular masses or (ii) cross-linked polymers. The former is highly unlikely due to the substantial amounts of the known chain transfer agent $AlMe_3$ present in the reaction mixture. The latter was never described for CGCs and is not consistent with the generally assumed mechanism for olefin polymerisation with activated CGCs and may therefore be excluded.

[358] Fully soluble PE samples give a detector response with a peak area of *ca.* 45; private communication by S. Holding, RAPRA Technology, Shropshire, UK.

[359] In the GPC analyses, a sample material to solvent ratio was applied that is usually used for completely soluble polymer samples. Due to the poor solubility of samples obtained in the present study, polymer concentrations in the solutions injected into the GPC system were therefore much lower than those generally employed.

[360] P. J. Flory, *Principles of Polymer Chemistry*, Cornell University Press, Ithaca, 1986.

[361] N. Ishihara, M. Kuramoto, M. Uoi, *Macromolecules*, **1988**, *21*, 3356.

[362] N. Tomotsu, N. Ishihara, T. H. Newman, M. T. Malanga, *J. Mol. Catal. A: Chem.* **1998**, *128*, 167.

[363] J. Schellenberg, N. Tomotsu, *Prog. Polym. Sci.* **2002**, *27*, 1925.

[364] B. Huang, K. Cao, B.-G. Li, S. Zhu, *J. Appl. Polym. Sci.* **2004**, *94*, 1449.

[365] D. D. Perrin, W. L. F. Armarego, D. R. Perrin, *Purification of Laboratory Chemicals*, 2. ed., Pergamon Press, Oxford 1980.

[366] T. K. Panda, M. T. Gamer, P. W. Roesky, *Organometallics*, **2003**, *22*, 877.

[367] W. Gerrard, H. R. Hudson, E. F. Mooney, *J. Chem. Soc.* **1960**, 5168.

[368] P. Geymayer, E. G. Rochow, U. Wannegat, *Angew. Chem.* **1964**, *76*, 499.

[369] H. Nöth, H. Schick, W. Meister, *J. Organomet. Chem.* **1964**, *1*, 401.

[370] D. C. Bradley, I. M. Thomas, *J. Chem. Soc.* **1960**, 3857.

[371] E. Benzing, W. Kornicker, *Chem. Ber.* **1961**, 2263.

[372] L. E. Manzer, *Inorg. Synth.* **1982**, *21*, 135.

[373] U. Zucchini, E. Albizzati, U. Giannini, *J. Organomet. Chem.* **1971**, *26*, 357.

[374] A. M. Cardoso, R. J. H. Clark, S. Moorhouse, *J. Chem. Soc., Dalton Trans.* **1980**, 1156.

Appendix: *X*-ray structure determination

Table 8. Crystal data and structure refinement for **70**.

Empirical formula	$C_{17}H_{23}BCl_2N_2Ti$
Formula weight	384.98
Temperature	183(2) K
Wavelength	0.71073 Å
Crystal system	Monoclinic
Space group	P2(1)/c
Unit cell dimensions	a = 12.575(2) Å
	b = 18.8522(15) Å
	c = 16.8556(13) Å
	α = 90°
	β = 109.247(11)°
	γ = 90°
Volume	3772.5(8) $Å^3$
Z	8
Density (calculated)	1.356 Mg/m^3
Absorption coefficient	0.736 mm^{-1}
F(000)	1600
Crystal size	0.50 x 0.40 x 0.13 mm^3
Theta range for data collection	2.03 to 25.00°
Index ranges	0<=h<=14, 0<=k<=22, -20<=l<=18
Reflections collected	6944
Independent reflections	6624 [R(int) = 0.0346]
Absorption correction	None
Refinement method	Full-matrix least-squares on F^2
Data / restraints / parameters	5767 / 0 / 391
Goodness-of-fit on F^2	0.998
Final R indices [I>2sigma(I)]	R1 = 0.0502, wR2 = 0.0967
R indices (all data)	R1 = 0.1072, wR2 = 0.1203
Largest diff. peak and hole	0.307 and -0.267 $e.Å^{-3}$
CCDC reference number	225922

Table 9. Atomic coordinates ($\times 10^4$) and equivalent isotropic displacement parameters ($Å^2 \times 10^3$) for **70**. U(eq) is defined as one third of the trace of the orthogonalised U_{ij} tensor.

	x	y	z	U(eq)
Ti	4087(1)	6157(1)	6581(1)	20(1)
Cl(1)	5152(1)	6943(1)	6163(1)	35(1)
Cl(2)	2801(1)	6850(1)	6888(1)	35(1)
N(1)	5028(3)	5694(2)	7595(2)	21(1)
N(2)	5369(3)	4339(2)	7888(2)	23(1)
B	4933(4)	4933(3)	7411(3)	22(1)
C(1)	4102(4)	4958(2)	6458(3)	23(1)
C(2)	4457(4)	5245(2)	5805(3)	27(1)
C(3)	3553(5)	5625(3)	5237(3)	35(1)
C(4)	2624(4)	5572(2)	5522(3)	35(1)
C(5)	2952(4)	5158(2)	6259(3)	29(1)
C(6)	5385(2)	6500(2)	8795(2)	33(1)
C(7)	6117(3)	6928(2)	9404(2)	44(1)
C(8)	7247(3)	6967(2)	9469(2)	48(2)
C(9)	7644(2)	6577(2)	8926(2)	42(1)
C(10)	6912(2)	6148(2)	8317(2)	32(1)
C(11)	5782(2)	6109(1)	8251(2)	24(1)
C(12)	6090(4)	4380(2)	8781(3)	28(1)
C(13)	5570(5)	3999(3)	9360(3)	39(1)
C(14)	7284(4)	4095(3)	8894(3)	37(1)
C(15)	5137(4)	3607(2)	7533(3)	28(1)
C(16)	5572(5)	3488(2)	6809(3)	36(1)
C(17)	3888(4)	3414(3)	7303(3)	37(1)
Ti'	10969(1)	4383(1)	3454(1)	19(1)
Cl(1')	9913(1)	5166(1)	3885(1)	30(1)
Cl(2')	12279(1)	5064(1)	3157(1)	32(1)
N(1')	9995(3)	3981(2)	2415(2)	24(1)
N(2')	9603(3)	2666(2)	1987(2)	25(1)
B'	10066(4)	3220(3)	2534(3)	22(1)
C(1')	10902(4)	3180(2)	3486(3)	21(1)
C(2')	10546(4)	3434(2)	4154(3)	26(1)
C(3')	11454(4)	3771(2)	4757(3)	30(1)
C(4')	12390(4)	3733(3)	4483(3)	31(1)
C(5')	12063(4)	3364(2)	3710(3)	28(1)
C(6')	9622(2)	4846(2)	1265(2)	35(1)
C(7')	8887(3)	5309(2)	706(2)	52(2)
C(8')	7776(3)	5362(2)	686(2)	56(2)
C(9')	7400(2)	4951(2)	1225(2)	46(1)
C(10')	8135(2)	4488(2)	1784(2)	33(1)
C(11')	9246(2)	4435(1)	1804(2)	25(1)
C(12')	8849(4)	2777(2)	1110(3)	27(1)
C(13')	9306(5)	2430(3)	469(3)	43(1)
C(14')	7644(4)	2534(3)	982(3)	40(1)
C(15')	9795(4)	1909(2)	2260(3)	30(1)
C(16')	9346(5)	1744(2)	2975(3)	39(1)
C(17')	11029(5)	1699(3)	2465(4)	45(1)

Table 10. Anisotropic displacement parameters ($Å^2 \times 10^3$) for **70**. The anisotropic displacement factor exponent takes the form: $-2\pi^2[h^2 a^{*2} U_{11} + ... + 2 h k a^* b^* U_{12}]$.

	U_{11}	U_{22}	U_{33}	U_{23}	U_{13}	U_{12}
Ti	20(1)	19(1)	19(1)	-1(1)	4(1)	2(1)
Cl(1)	34(1)	32(1)	43(1)	5(1)	16(1)	-2(1)
Cl(2)	31(1)	34(1)	40(1)	-3(1)	14(1)	10(1)
N(1)	23(2)	20(2)	17(2)	0(1)	2(1)	1(1)
N(2)	25(2)	19(2)	22(2)	-2(1)	3(1)	0(1)
B	17(2)	25(2)	22(2)	-4(2)	4(2)	1(2)
C(1)	27(2)	17(2)	23(2)	-5(2)	4(2)	1(2)
C(2)	33(2)	27(2)	24(2)	-5(2)	11(2)	3(2)
C(3)	48(3)	32(3)	17(2)	-4(2)	-1(2)	3(2)
C(4)	30(3)	28(2)	32(2)	-12(2)	-9(2)	4(2)
C(5)	23(2)	28(2)	32(2)	-10(2)	3(2)	-3(2)
C(6)	44(3)	28(2)	25(2)	1(2)	10(2)	6(2)
C(7)	76(4)	24(2)	25(2)	-4(2)	8(3)	11(2)
C(8)	64(4)	26(2)	33(3)	-1(2)	-13(3)	-13(2)
C(9)	39(3)	38(3)	40(3)	-2(2)	3(2)	-14(2)
C(10)	29(2)	33(2)	31(2)	0(2)	6(2)	-4(2)
C(11)	32(2)	17(2)	17(2)	0(2)	2(2)	1(2)
C(12)	32(2)	22(2)	24(2)	-4(2)	2(2)	0(2)
C(13)	45(3)	44(3)	27(2)	8(2)	9(2)	7(2)
C(14)	26(2)	46(3)	34(2)	-2(2)	2(2)	1(2)
C(15)	34(2)	17(2)	28(2)	-1(2)	3(2)	-1(2)
C(16)	41(3)	24(2)	43(3)	-8(2)	14(2)	-1(2)
C(17)	37(3)	26(2)	43(3)	-1(2)	8(2)	-10(2)
Ti'	21(1)	17(1)	17(1)	-1(1)	5(1)	-2(1)
Cl(1')	30(1)	29(1)	31(1)	-4(1)	11(1)	5(1)
Cl(2')	33(1)	33(1)	31(1)	-1(1)	13(1)	-11(1)
N(1')	29(2)	21(2)	21(2)	2(1)	4(2)	-1(2)
N(2')	27(2)	22(2)	28(2)	-4(2)	11(2)	-2(2)
B'	19(2)	22(2)	23(2)	-1(2)	4(2)	-2(2)
C(1')	23(2)	17(2)	22(2)	2(2)	5(2)	-1(2)
C(2')	28(2)	22(2)	27(2)	9(2)	7(2)	-3(2)
C(3')	40(3)	26(2)	20(2)	5(2)	6(2)	2(2)
C(4')	26(2)	28(2)	31(2)	1(2)	-2(2)	4(2)
C(5')	26(2)	24(2)	30(2)	0(2)	6(2)	0(2)
C(6')	47(3)	28(2)	25(2)	2(2)	4(2)	-11(2)
C(7')	79(5)	31(3)	31(3)	9(2)	-3(3)	-13(3)
C(8')	66(4)	34(3)	42(3)	4(2)	-15(3)	8(3)
C(9')	44(3)	40(3)	39(3)	-5(2)	-9(2)	14(2)
C(10')	37(3)	31(2)	27(2)	-1(2)	4(2)	2(2)
C(11')	35(2)	18(2)	16(2)	-1(2)	1(2)	1(2)
C(12')	30(2)	25(2)	23(2)	-6(2)	4(2)	-1(2)
C(13')	47(3)	51(3)	34(3)	-17(2)	19(2)	-14(3)
C(14')	29(2)	48(3)	38(3)	-11(2)	5(2)	-2(2)
C(15')	29(2)	21(2)	36(2)	-8(2)	5(2)	0(2)
C(16')	46(3)	19(2)	53(3)	7(2)	18(2)	-2(2)
C(17')	37(3)	34(3)	57(3)	-14(2)	6(2)	7(2)

Table 11. Bond lengths [Å] for **70**.

Ti-N(1)	1.937(3)	Ti'-N(1')	1.930(4)
Ti-Cl(1)	2.260(2)	Ti'-Cl(1')	2.2588(14)
Ti-Cl(2)	2.2677(15)	Ti'-Cl(2')	2.2707(15)
Ti-C(1)	2.271(4)	Ti'-C(1')	2.271(4)
Ti-C(2)	2.298(4)	Ti'-C(2')	2.300(4)
Ti-C(5)	2.317(5)	Ti'-C(5')	2.319(5)
Ti-C(3)	2.364(4)	Ti'-C(3')	2.376(4)
Ti-C(4)	2.371(4)	Ti'-C(4')	2.379(4)
Ti-B	2.727(5)	Ti'-B'	2.710(5)
N(1)-C(11)	1.430(4)	N(1')-C(11')	1.428(4)
N(1)-B	1.464(6)	N(1')-B'	1.448(6)
N(2)-B	1.382(6)	N(2')-B'	1.386(6)
N(2)-C(12)	1.480(5)	N(2')-C(12')	1.485(5)
N(2)-C(15)	1.495(5)	N(2')-C(15')	1.496(6)
B-C(1)	1.602(6)	B'-C(1')	1.605(6)
C(1)-C(5)	1.423(6)	C(1')-C(2')	1.425(7)
C(1)-C(2)	1.424(7)	C(1')-C(5')	1.425(6)
C(2)-C(3)	1.415(7)	C(2')-C(3')	1.405(6)
C(3)-C(4)	1.405(8)	C(3')-C(4')	1.401(7)
C(4)-C(5)	1.410(7)	C(4')-C(5')	1.414(7)
C(6)-C(7)	1.39	C(6')-C(7')	1.39
C(6)-C(11)	1.39	C(6')-C(11')	1.39
C(7)-C(8)	1.39	C(7')-C(8')	1.39
C(8)-C(9)	1.39	C(8')-C(9')	1.39
C(9)-C(10)	1.39	C(9')-C(10')	1.39
C(10)-C(11)	1.39	C(10')-C(11')	1.39
C(12)-C(13)	1.522(7)	C(12')-C(14')	1.528(7)
C(12)-C(14)	1.545(7)	C(12')-C(13')	1.529(7)
C(15)-C(16)	1.509(7)	C(15')-C(16')	1.522(7)
C(15)-C(17)	1.533(7)	C(15')-C(17')	1.526(7)

Table 12. Bond angles [°] for **70**.

N(1)-Ti-Cl(1)	108.56(12)	C(5)-Ti-B	62.5(2)
N(1)-Ti-Cl(2)	109.44(12)	C(3)-Ti-B	94.1(2)
Cl(1)-Ti-Cl(2)	103.52(6)	C(4)-Ti-B	93.9(2)
N(1)-Ti-C(1)	67.06(15)	C(11)-N(1)-B	133.4(3)
Cl(1)-Ti-C(1)	126.93(13)	C(11)-N(1)-Ti	119.5(2)
Cl(2)-Ti-C(1)	128.49(13)	B-N(1)-Ti	105.8(3)
N(1)-Ti-C(2)	89.1(2)	B-N(2)-C(12)	122.8(4)
Cl(1)-Ti-C(2)	93.52(13)	B-N(2)-C(15)	121.8(3)
Cl(2)-Ti-C(2)	148.67(13)	C(12)-N(2)-C(15)	115.3(3)
C(1)-Ti-C(2)	36.3(2)	N(2)-B-N(1)	132.9(4)
N(1)-Ti-C(5)	89.4(2)	N(2)-B-C(1)	127.6(4)
Cl(1)-Ti-C(5)	147.40(13)	N(1)-B-C(1)	99.4(3)
Cl(2)-Ti-C(5)	95.26(13)	N(2)-B-Ti	175.6(3)
C(1)-Ti-C(5)	36.1(2)	N(1)-B-Ti	43.1(2)
C(2)-Ti-C(5)	58.9(2)	C(1)-B-Ti	56.3(2)
N(1)-Ti-C(3)	123.5(2)	C(5)-C(1)-C(2)	105.6(4)
Cl(1)-Ti-C(3)	89.43(14)	C(5)-C(1)-B	121.4(4)
Cl(2)-Ti-C(3)	117.71(14)	C(2)-C(1)-B	121.2(4)
C(1)-Ti-C(3)	59.9(2)	C(5)-C(1)-Ti	73.7(2)
C(2)-Ti-C(3)	35.3(2)	C(2)-C(1)-Ti	72.9(2)
C(5)-Ti-C(3)	58.1(2)	B-C(1)-Ti	87.7(3)
N(1)-Ti-C(4)	123.5(2)	C(3)-C(2)-C(1)	109.2(4)
Cl(1)-Ti-C(4)	117.5(2)	C(3)-C(2)-Ti	74.9(3)
Cl(2)-Ti-C(4)	90.31(13)	C(1)-C(2)-Ti	70.8(2)
C(1)-Ti-C(4)	59.7(2)	C(4)-C(3)-C(2)	107.8(4)
C(2)-Ti-C(4)	58.4(2)	C(4)-C(3)-Ti	73.0(3)
C(5)-Ti-C(4)	35.0(2)	C(2)-C(3)-Ti	69.8(2)
C(3)-Ti-C(4)	34.5(2)	C(3)-C(4)-C(5)	107.8(4)
N(1)-Ti-B	31.12(14)	C(3)-C(4)-Ti	72.5(3)
Cl(1)-Ti-B	122.94(12)	C(5)-C(4)-Ti	70.4(3)
Cl(2)-Ti-B	123.90(12)	C(4)-C(5)-C(1)	109.5(4)
C(1)-Ti-B	35.95(14)	C(4)-C(5)-Ti	74.6(3)
C(2)-Ti-B	62.7(2)	C(1)-C(5)-Ti	70.2(2)
C(7)-C(6)-C(11)	120.0	Cl(2')-Ti'-C(3')	119.63(13)
C(6)-C(7)-C(8)	120.0	C(1')-Ti'-C(3')	59.5(2)
C(7)-C(8)-C(9)	120.0	C(2')-Ti'-C(3')	34.9(2)
C(10)-C(9)-C(8)	120.0	C(5')-Ti'-C(3')	58.0(2)
C(9)-C(10)-C(11)	120.0	N(1')-Ti'-C(4')	123.9(2)
C(10)-C(11)-C(6)	120.0	Cl(1')-Ti'-C(4')	118.79(13)
C(10)-C(11)-N(1)	119.3(2)	Cl(2')-Ti'-C(4')	91.50(13)
C(6)-C(11)-N(1)	120.6(2)	C(1')-Ti'-C(4')	59.5(2)
N(2)-C(12)-C(13)	112.2(4)	C(2')-Ti'-C(4')	58.0(2)
N(2)-C(12)-C(14)	110.7(4)	C(5')-Ti'-C(4')	35.0(2)
C(13)-C(12)-C(14)	111.2(4)	C(3')-Ti'-C(4')	34.3(2)
N(2)-C(15)-C(16)	112.7(4)	N(1')-Ti'-B'	30.93(14)
N(2)-C(15)-C(17)	111.6(4)	Cl(1')-Ti'-B'	122.21(12)
C(16)-C(15)-C(17)	112.0(4)	Cl(2')-Ti'-B'	121.92(12)
N(1')-Ti'-Cl(1')	106.53(13)	C(1')-Ti'-B'	36.25(14)
N(1')-Ti'-Cl(2')	108.12(13)	C(2')-Ti'-B'	62.6(2)
Cl(1')-Ti'-Cl(2')	104.35(5)	C(5')-Ti'-B'	63.07(15)
N(1')-Ti'-C(1')	67.2(2)	C(3')-Ti'-B'	93.9(2)

Table 12 (continued). Bond angles [°] for **70**.

Cl(1')-Ti'-C(1')	127.91(13)	C(4')-Ti'-B'	94.2(2)
Cl(2')-Ti'-C(1')	127.22(13)	C(11')-N(1')-B'	133.6(3)
N(1')-Ti'-C(2')	88.6(2)	C(11')-N(1')-Ti'	119.3(2)
Cl(1')-Ti'-C(2')	94.76(13)	B'-N(1')-Ti'	105.8(3)
Cl(2')-Ti'-C(2')	149.31(12)	B'-N(2')-C(12')	123.1(4)
C(1')-Ti'-C(2')	36.3(2)	B'-N(2')-C(15')	121.6(4)
N(1')-Ti'-C(5')	90.2(2)	C(12')-N(2')-C(15')	115.2(3)
Cl(1')-Ti'-C(5')	148.94(13)	N(2')-B'-N(1')	131.4(4)
Cl(2')-Ti'-C(5')	94.58(13)	N(2')-B'-C(1')	128.5(4)
C(1')-Ti'-C(5')	36.2(2)	N(1')-B'-C(1')	100.1(3)
C(2')-Ti'-C(5')	58.9(2)	N(2')-B'-Ti'	173.8(4)
N(1')-Ti'-C(3')	122.7(2)	N(1')-B'-Ti'	43.3(2)
Cl(1')-Ti'-C(3')	91.09(13)	C(1')-B'-Ti'	56.8(2)
C(2')-C(1')-C(5')	105.7(4)	C(4')-C(5')-Ti'	74.8(3)
C(2')-C(1')-B'	120.1(4)	C(1')-C(5')-Ti'	70.1(2)
C(5')-C(1')-B'	122.0(4)	C(7')-C(6')-C(11')	120.0
C(2')-C(1')-Ti'	72.9(2)	C(8')-C(7')-C(6')	120.0
C(5')-C(1')-Ti'	73.7(2)	C(9')-C(8')-C(7')	120.0
B'-C(1')-Ti'	86.9(2)	C(8')-C(9')-C(10')	120.0
C(3')-C(2')-C(1')	109.3(4)	C(9')-C(10')-C(11')	120.0
C(3')-C(2')-Ti'	75.5(3)	C(10')-C(11')-C(6')	120.0
C(1')-C(2')-Ti'	70.7(2)	C(10')-C(11')-N(1')	118.6(3)
C(4')-C(3')-C(2')	108.1(4)	C(6')-C(11')-N(1')	121.3(3)
C(4')-C(3')-Ti'	73.0(3)	N(2')-C(12')-C(14')	112.2(4)
C(2')-C(3')-Ti'	69.6(2)	N(2')-C(12')-C(13')	112.2(4)
C(3')-C(4')-C(5')	107.9(4)	C(14')-C(12')-C(13')	111.0(4)
C(3')-C(4')-Ti'	72.7(2)	N(2')-C(15')-C(16')	111.9(4)
C(5')-C(4')-Ti'	70.2(3)	N(2')-C(15')-C(17')	111.5(4)
C(4')-C(5')-C(1')	109.0(4)	C(16')-C(15')-C(17')	112.5(4)

Table 13. Crystal data and structure refinement for **83**.

Empirical formula	$C_{18}H_{29}BN_2$
Formula weight	284.24
Temperature	173(2) K
Wavelength	0.71073 Å
Crystal system	Monoclinic
Space group	P2(1)/n
Unit cell dimensions	a = 8.1029(8) Å
	b = 14.0352(14) Å
	c = 15.6679(15) Å
	α = 90°
	β = 100.503(2)°
	γ = 90°
Volume	1752.0(3) $Å^3$
Z	4
Density (calculated)	1.073 Mg/m^3
Absorption coefficient	0.062 mm^{-1}
F(000)	620
Crystal size	0.25 x 0.20 x 0.09 mm^3
Theta range for data collection	1.96 to 26.15°
Index ranges	-10<=h<=10, -17<=k<=17, -19<=l<=19
Reflections collected	14804
Independent reflections	3484 [R(int) = 0.0315]
Completeness to theta = 26.15°	99.8 %
Absorption correction	Empirical
Max. and min. transmission	1. and 0.883715
Refinement method	Full-matrix least-squares on F^2
Data / restraints / parameters	3484 / 0 / 190
Goodness-of-fit on F^2	1.020
Final R indices [I>2sigma(I)]	R1 = 0.0460, wR2 = 0.1100
R indices (all data)	R1 = 0.0607, wR2 = 0.1189
Largest diff. peak and hole	0.225 and -0.205 $e.Å^{-3}$

Table 14. Atomic coordinates ($\times 10^4$) and equivalent isotropic displacement parameters ($Å^2 \times 10^3$) for **83**. U(eq) is defined as one third of the trace of the orthogonalised U_{ij} tensor.

	x	y	z	U(eq)
N(1)	676(1)	1213(1)	1022(1)	34(1)
N(2)	2566(1)	593(1)	2323(1)	30(1)
C(19)	-960(2)	1080(1)	3021(1)	30(1)
C(31)	4140(2)	841(1)	2019(1)	35(1)
C(11)	-742(2)	510(1)	2234(1)	29(1)
C(21)	-871(2)	1378(1)	397(1)	33(1)
C(41)	2839(2)	184(1)	3203(1)	34(1)
C(12)	-1020(2)	-488(1)	2524(1)	36(1)
C(14)	-1320(2)	461(1)	3666(1)	35(1)
C(18)	-847(2)	2054(1)	3173(1)	40(1)
B(1)	932(2)	771(1)	1847(1)	28(1)
C(13)	-1361(2)	-504(1)	3326(1)	39(1)
C(17)	-1097(2)	2398(1)	3969(1)	51(1)
C(32)	4392(2)	1918(1)	1972(1)	48(1)
C(22)	-1756(2)	2283(1)	595(1)	43(1)
C(43)	3713(2)	876(1)	3888(1)	48(1)
C(33)	4334(2)	324(1)	1187(1)	53(1)
C(15)	-1542(2)	817(1)	4468(1)	47(1)
C(23)	-470(2)	1414(1)	-516(1)	44(1)
C(42)	3729(2)	-775(1)	3254(1)	51(1)
C(16)	-1431(2)	1787(2)	4607(1)	55(1)

Table 15. Anisotropic displacement parameters ($Å^2 \times 10^3$) for **83**. The anisotropic displacement factor exponent takes the form: $-2\pi^2[h^2 a^{*2} U_{11} + ... + 2 h k a^* b^* U_{12}]$.

	U_{11}	U_{22}	U_{33}	U_{23}	U_{13}	U_{12}
N(1)	25(1)	42(1)	35(1)	6(1)	7(1)	-1(1)
N(2)	25(1)	32(1)	32(1)	3(1)	7(1)	-1(1)
C(19)	19(1)	39(1)	33(1)	1(1)	3(1)	3(1)
C(31)	23(1)	43(1)	40(1)	2(1)	5(1)	-2(1)
C(11)	24(1)	33(1)	30(1)	2(1)	3(1)	-1(1)
C(21)	32(1)	36(1)	29(1)	2(1)	3(1)	-4(1)
C(41)	26(1)	39(1)	36(1)	8(1)	3(1)	0(1)
C(12)	30(1)	35(1)	43(1)	-1(1)	7(1)	-5(1)
C(14)	21(1)	49(1)	35(1)	6(1)	6(1)	3(1)
C(18)	33(1)	39(1)	46(1)	-1(1)	5(1)	3(1)
B(1)	27(1)	26(1)	30(1)	-3(1)	6(1)	-1(1)
C(13)	30(1)	41(1)	47(1)	11(1)	9(1)	-5(1)
C(17)	43(1)	50(1)	59(1)	-17(1)	6(1)	8(1)
C(32)	38(1)	49(1)	56(1)	10(1)	10(1)	-12(1)
C(22)	38(1)	50(1)	40(1)	4(1)	5(1)	8(1)
C(43)	45(1)	59(1)	37(1)	2(1)	-2(1)	-5(1)
C(33)	32(1)	75(1)	56(1)	-12(1)	17(1)	2(1)
C(15)	34(1)	73(1)	36(1)	5(1)	11(1)	6(1)
C(23)	57(1)	45(1)	31(1)	1(1)	8(1)	1(1)
C(42)	41(1)	42(1)	68(1)	18(1)	7(1)	7(1)
C(16)	45(1)	81(1)	41(1)	-18(1)	10(1)	11(1)

Table 16. Bond lengths [Å] for **83**.

N(1)-B(1)	1.4153(19)	C(11)-B(1)	1.626(2)
N(1)-C(21)	1.4629(17)	C(21)-C(22)	1.518(2)
N(2)-B(1)	1.4187(18)	C(21)-C(23)	1.524(2)
N(2)-C(41)	1.4732(17)	C(41)-C(42)	1.522(2)
N(2)-C(31)	1.4822(17)	C(41)-C(43)	1.523(2)
C(19)-C(18)	1.388(2)	C(12)-C(13)	1.337(2)
C(19)-C(14)	1.404(2)	C(14)-C(15)	1.394(2)
C(19)-C(11)	1.5066(19)	C(14)-C(13)	1.453(2)
C(31)-C(33)	1.525(2)	C(18)-C(17)	1.387(2)
C(31)-C(32)	1.529(2)	C(17)-C(16)	1.381(3)
C(11)-C(12)	1.5023(19)	C(15)-C(16)	1.380(3)

Table 17. Bond angles [°] for **83**.

B(1)-N(1)-C(21)	130.32(12)	N(2)-C(41)-C(42)	112.50(13)
B(1)-N(2)-C(41)	121.82(11)	N(2)-C(41)-C(43)	112.49(12)
B(1)-N(2)-C(31)	124.46(11)	C(42)-C(41)-C(43)	111.79(13)
C(41)-N(2)-C(31)	113.64(10)	C(16)-C(15)-C(14)	118.79(16)
C(18)-C(19)-C(14)	120.13(13)	C(13)-C(12)-C(11)	111.58(13)
C(18)-C(19)-C(11)	130.47(13)	C(15)-C(14)-C(19)	120.34(15)
C(14)-C(19)-C(11)	109.40(12)	C(15)-C(14)-C(13)	131.81(14)
N(2)-C(31)-C(33)	113.09(12)	C(19)-C(14)-C(13)	107.84(13)
N(2)-C(31)-C(32)	112.17(12)	C(17)-C(18)-C(19)	118.82(15)
C(33)-C(31)-C(32)	113.20(14)	N(1)-B(1)-N(2)	121.67(12)
C(12)-C(11)-C(19)	101.62(11)	N(1)-B(1)-C(11)	116.50(11)
C(12)-C(11)-B(1)	120.29(11)	N(2)-B(1)-C(11)	121.81(12)
C(19)-C(11)-B(1)	114.58(11)	C(12)-C(13)-C(14)	109.56(13)
N(1)-C(21)-C(22)	112.04(12)	C(16)-C(17)-C(18)	120.96(16)
N(1)-C(21)-C(23)	109.28(12)	C(15)-C(16)-C(17)	120.94(16)
C(22)-C(21)-C(23)	110.70(12)		

Table 18. Crystal data and structure refinement for **87**.

Empirical formula	$C_{23}H_{33}BN_2$
Formula weight	232.22
Temperature	173(2) K
Wavelength	0.71073 Å
Crystal system	Monoclinic
Space group	P2(1)/n
Unit cell dimensions	a = 9.296(6) Å
	b = 16.074(9) Å
	c = 14.548(8) Å
	$\alpha = 90°$
	$\beta = 96.940(13)°$
	$\gamma = 90°$
Volume	2158(2) $Å^3$
Z	6
Density (calculated)	1.072 Mg/m^3
Absorption coefficient	0.061 mm^{-1}
F(000)	760
Crystal size	.235 x .125 x .100 mm^3
Theta range for data collection	1.90 to 23.45°.
Index ranges	-10<=h<=10, -17<=k<=18, -16<=l<=16
Reflections collected	35199
Independent reflections	3145 [R(int) = 0.0951]
Completeness to theta = 23.45°	98.9 %
Absorption correction	Empirical
Max. and min. transmission	1. and 0.780629
Refinement method	Full-matrix least-squares on F^2
Data / restraints / parameters	3145 / 0 / 243
Goodness-of-fit on F^2	1.056
Final R indices [I>2sigma(I)]	R1 = 0.0452, wR2 = 0.0971
R indices (all data)	R1 = 0.0725, wR2 = 0.1067
Largest diff. peak and hole	0.137 and -0.131 $e.Å^{-3}$

Table 19. Atomic coordinates ($\times 10^4$) and equivalent isotropic displacement parameters ($Å^2 \times 10^3$) for **87**. U(eq) is defined as one third of the trace of the orthogonalised U_{ij} tensor.

	x	y	z	U(eq)
B	-808(2)	3076(1)	6175(2)	32(1)
C(1)	-1419(2)	2550(1)	5268(1)	32(1)
N(1)	-1555(2)	3816(1)	6369(1)	36(1)
N(2)	441(2)	2819(1)	6768(1)	33(1)
C(2)	-397(2)	2385(1)	4555(1)	33(1)
C(3)	497(2)	2936(1)	4164(1)	42(1)
C(4)	1311(2)	2653(1)	3496(1)	48(1)
C(5)	1234(2)	1829(1)	3214(1)	46(1)
C(6)	356(2)	1269(1)	3602(1)	41(1)
C(7)	-465(2)	1550(1)	4284(1)	34(1)
C(8)	-1464(2)	1114(1)	4819(1)	35(1)
C(9)	-1915(2)	285(1)	4812(1)	41(1)
C(10)	-2946(2)	49(1)	5369(2)	47(1)
C(11)	-3508(2)	621(1)	5939(2)	48(1)
C(12)	-3050(2)	1443(1)	5964(1)	42(1)
C(13)	-2029(2)	1692(1)	5403(1)	34(1)
C(20)	-2721(2)	4312(1)	5844(1)	39(1)
C(21)	-4152(2)	3832(1)	5683(2)	50(1)
C(23)	-2262(2)	4614(1)	4929(1)	49(1)
C(22)	-2947(2)	5075(1)	6445(1)	54(1)
C(30)	1130(2)	3305(1)	7570(1)	36(1)
C(31)	1727(2)	4138(1)	7282(2)	50(1)
C(32)	193(2)	3388(1)	8355(1)	46(1)
C(40)	1163(2)	2017(1)	6634(1)	41(1)
C(41)	2712(2)	2119(2)	6417(2)	62(1)
C(42)	1081(3)	1426(1)	7446(2)	61(1)

Table 20. Anisotropic displacement parameters ($Å^2 \times 10^3$) for **87**. The anisotropic displacement factor exponent takes the form: $-2\pi^2[h^2 a^{*2} U_{11} + ... + 2 h k a^* b^* U_{12}]$.

	U_{11}	U_{22}	U_{33}	U_{23}	U_{13}	U_{12}
B	33(1)	37(1)	28(1)	5(1)	8(1)	-3(1)
C(1)	30(1)	35(1)	31(1)	-1(1)	0(1)	4(1)
N(1)	40(1)	38(1)	29(1)	-3(1)	-4(1)	7(1)
N(2)	34(1)	33(1)	30(1)	-4(1)	-2(1)	2(1)
C(2)	32(1)	39(1)	27(1)	-1(1)	-1(1)	2(1)
C(3)	48(1)	40(1)	37(1)	-4(1)	7(1)	-2(1)
C(4)	48(1)	56(2)	42(1)	2(1)	11(1)	-4(1)
C(5)	42(1)	61(2)	35(1)	-8(1)	7(1)	4(1)
C(6)	38(1)	44(1)	37(1)	-8(1)	-2(1)	6(1)
C(7)	30(1)	40(1)	29(1)	-3(1)	-4(1)	4(1)
C(8)	31(1)	38(1)	33(1)	-1(1)	-6(1)	1(1)
C(9)	42(1)	39(1)	40(1)	-3(1)	-6(1)	3(1)
C(10)	46(1)	42(1)	50(1)	8(1)	-5(1)	-5(1)
C(11)	44(1)	55(2)	43(1)	10(1)	1(1)	-8(1)
C(12)	39(1)	53(2)	34(1)	-2(1)	0(1)	-2(1)
C(13)	31(1)	42(1)	28(1)	1(1)	-4(1)	1(1)
C(20)	40(1)	41(1)	34(1)	3(1)	4(1)	10(1)
C(21)	40(1)	63(2)	48(1)	9(1)	5(1)	13(1)
C(23)	52(1)	51(1)	43(1)	10(1)	7(1)	13(1)
C(22)	66(2)	49(1)	47(1)	-1(1)	6(1)	21(1)
C(30)	36(1)	39(1)	33(1)	1(1)	-3(1)	0(1)
C(31)	53(1)	52(1)	45(1)	-2(1)	-3(1)	-14(1)
C(32)	48(1)	57(2)	31(1)	-2(1)	-4(1)	-2(1)
C(40)	40(1)	41(1)	40(1)	-4(1)	-6(1)	8(1)
C(41)	46(1)	73(2)	65(2)	-12(1)	-1(1)	17(1)
C(42)	78(2)	43(1)	59(2)	5(1)	-7(1)	13(1)

Table 21. Bond lengths [Å] for **87**.

B-N(2)	1.421(3)	C(6)-C(7)	1.398(3)
B-N(1)	1.422(3)	C(7)-C(8)	1.461(3)
B-C(1)	1.612(3)	C(8)-C(9)	1.397(3)
C(1)-C(2)	1.511(3)	C(8)-C(13)	1.403(3)
C(1)-C(13)	1.513(3)	C(9)-C(10)	1.381(3)
C(1)-H(1)	0.968(17)	C(10)-C(11)	1.382(3)
N(1)-C(20)	1.482(2)	C(11)-C(12)	1.387(3)
N(1)-H(1N)	0.91(2)	C(12)-C(13)	1.383(3)
N(2)-C(40)	1.477(2)	C(20)-C(23)	1.525(3)
N(2)-C(30)	1.483(2)	C(20)-C(21)	1.531(3)
C(2)-C(3)	1.383(3)	C(20)-C(22)	1.534(3)
C(2)-C(7)	1.398(3)	C(30)-C(32)	1.524(3)
C(3)-C(4)	1.378(3)	C(30)-C(31)	1.527(3)
C(4)-C(5)	1.387(3)	C(40)-C(41)	1.520(3)
C(5)-C(6)	1.380(3)	C(40)-C(42)	1.525(3)

Table 22. Bond angles [°] for **87**.

N(2)-B-N(1)	120.32(18)	N(2)-C(30)-C(31)	112.54(15)
N(2)-B-C(1)	121.72(18)	C(32)-C(30)-C(31)	112.88(17)
N(1)-B-C(1)	117.95(18)	C(6)-C(7)-C(8)	131.26(19)
C(2)-C(1)-C(13)	101.90(16)	C(2)-C(7)-C(8)	108.62(17)
C(2)-C(1)-B	117.68(16)	C(9)-C(8)-C(13)	120.07(19)
C(13)-C(1)-B	118.16(16)	C(9)-C(8)-C(7)	131.59(19)
C(2)-C(1)-H(1)	107.4(10)	C(13)-C(8)-C(7)	108.32(17)
C(13)-C(1)-H(1)	105.0(10)	C(10)-C(9)-C(8)	119.20(19)
B-C(1)-H(1)	105.7(10)	C(9)-C(10)-C(11)	120.5(2)
B-N(1)-C(20)	133.82(17)	C(10)-C(11)-C(12)	120.8(2)
B-N(1)-H(1N)	115.8(12)	C(13)-C(12)-C(11)	119.3(2)
C(20)-N(1)-H(1N)	109.6(12)	C(12)-C(13)-C(8)	120.02(19)
B-N(2)-C(40)	121.61(16)	C(12)-C(13)-C(1)	129.40(18)
B-N(2)-C(30)	124.59(16)	C(8)-C(13)-C(1)	110.52(17)
C(40)-N(2)-C(30)	113.79(15)	N(1)-C(20)-C(23)	110.87(16)
C(3)-C(2)-C(7)	120.41(18)	N(1)-C(20)-C(21)	112.04(17)
C(3)-C(2)-C(1)	129.01(18)	C(23)-C(20)-C(21)	110.86(17)
C(7)-C(2)-C(1)	110.57(17)	N(1)-C(20)-C(22)	106.20(16)
C(4)-C(3)-C(2)	119.2(2)	C(23)-C(20)-C(22)	108.39(17)
C(3)-C(4)-C(5)	120.7(2)	C(21)-C(20)-C(22)	108.27(17)
C(6)-C(5)-C(4)	120.9(2)	N(2)-C(40)-C(41)	113.01(17)
C(5)-C(6)-C(7)	118.7(2)	N(2)-C(40)-C(42)	112.01(17)
C(6)-C(7)-C(2)	120.11(18)	C(41)-C(40)-C(42)	111.44(18)
N(2)-C(30)-C(32)	113.77(16)		

Table 23. Crystal data and structure refinement for **88**.

Empirical formula	$C_{25}H_{29}BN_2$
Formula weight	368.31
Temperature	293(2) K
Wavelength	0.71073 Å
Crystal system	Triclinic
Space group	P-1
Unit cell dimensions	a = 8.186(7) Å
	b = 11.796(7) Å
	c = 11.860(10) Å
	α = 94.26(6)°
	β = 104.17(6)°
	γ = 92.55(6)°
Volume	1105.0(15) $Å^3$
Z	2
Density (calculated)	1.107 Mg/m^3
Absorption coefficient	0.064 mm^{-1}
F(000)	396
Crystal size	0.63 x 0.50 x 0.40 mm
Theta range for data collection	1.78 to 25.00°
Index ranges	0<=h<=9, -13<=k<=13, -14<=l<=13
Reflections collected	4128
Independent reflections	3835 [R_{int} = 0.0490]
Absorption correction	None
Refinement method	Full-matrix least-squares on F^2
Data / restraints / parameters	3284 / 1 / 245
Goodness-of-fit on F^2	S = 1.046
R indices [for 2192 reflections with I>2sigma(I)]	R_1 = 0.0604, wR_2 = 0.1517
R indices (for all 3284 data)	R_1 = 0.1178, wR_2 = 0.2103
Largest diff. peak and hole	0.198 and -0.225 $eÅ^{-3}$
CCDC reference number	215175

Table 24. Atomic coordinates ($\times 10^4$) and equivalent isotropic displacement parameters ($Å^2 \times 10^3$) for **88**. U(eq) is defined as one third of the trace of the orthogonalised U_{ij} tensor.

	x	y	z	U(eq)
B	5393(4)	2632(3)	6011(3)	52(1)
N(1)	5029(3)	2415(3)	4769(2)	69(1)
N(2)	7051(3)	2637(2)	6711(2)	51(1)
C(1)	3783(3)	2816(3)	6561(2)	54(1)
C(2)	3483(3)	1973(3)	7398(3)	57(1)
C(3)	3455(5)	790(3)	7283(4)	79(1)
C(4)	3194(6)	194(4)	8203(5)	102(1)
C(5)	2962(6)	754(4)	9193(5)	102(1)
C(6)	2965(4)	1933(4)	9322(3)	80(1)
C(7)	3217(3)	2538(3)	8413(3)	58(1)
C(8)	3333(3)	3768(3)	8303(2)	53(1)
C(9)	3173(4)	4691(3)	9066(3)	65(1)
C(10)	3414(4)	5777(3)	8752(3)	74(1)
C(11)	3836(5)	5953(3)	7718(3)	73(1)
C(12)	3966(4)	5037(3)	6950(3)	63(1)
C(13)	3700(3)	3939(3)	7230(2)	51(1)
C(14)	2445(2)	3305(2)	3839(2)	63(1)
C(15)	946(2)	3278(2)	2975(2)	70(1)
C(16)	481(2)	2343(2)	2153(2)	79(1)
C(17)	1514(3)	1436(2)	2195(2)	99(2)
C(18)	3013(3)	1462(2)	3059(2)	82(1)
C(19)	3478(2)	2397(2)	3881(2)	54(1)
C(20)	8570(3)	2494(3)	6256(3)	59(1)
C(21)	8890(4)	3465(4)	5545(3)	83(1)
C(22)	8614(5)	1328(4)	5629(4)	93(1)
C(23)	7427(3)	2822(3)	8000(2)	56(1)
C(24)	8101(5)	1763(3)	8586(3)	81(1)
C(25)	8579(4)	3886(3)	8492(3)	73(1)

Table 25. Anisotropic displacement parameters ($Å^2 \times 10^3$) for **88**. The anisotropic displacement factor exponent takes the form: $-2\pi^2[h^2 a^{*2} U_{11} + ... + 2 h k a^* b^* U_{12}]$.

	U_{11}	U_{22}	U_{33}	U_{23}	U_{13}	U_{12}
B	42(2)	62(2)	50(2)	3(1)	7(1)	10(1)
N(1)	40(1)	116(2)	48(1)	-1(1)	7(1)	19(1)
N(2)	37(1)	68(2)	47(1)	4(1)	7(1)	12(1)
C(1)	35(1)	77(2)	45(1)	3(1)	2(1)	5(1)
C(2)	35(1)	70(2)	62(2)	6(1)	5(1)	2(1)
C(3)	65(2)	76(3)	94(3)	1(2)	19(2)	-3(2)
C(4)	90(3)	76(3)	145(4)	24(3)	38(3)	-5(2)
C(5)	97(3)	101(4)	121(4)	49(3)	40(3)	7(3)
C(6)	63(2)	106(3)	76(2)	27(2)	24(2)	7(2)
C(7)	34(1)	82(2)	56(2)	10(2)	7(1)	2(1)
C(8)	30(1)	79(2)	47(2)	4(1)	5(1)	8(1)
C(9)	46(2)	94(3)	52(2)	2(2)	7(1)	15(2)
C(10)	63(2)	81(3)	70(2)	-8(2)	5(2)	26(2)
C(11)	75(2)	69(2)	75(2)	10(2)	13(2)	19(2)
C(12)	57(2)	75(2)	59(2)	14(2)	13(1)	14(2)
C(13)	33(1)	69(2)	47(1)	7(1)	2(1)	12(1)
C(14)	56(2)	72(2)	55(2)	-4(1)	3(1)	7(1)
C(15)	59(2)	80(2)	63(2)	14(2)	-1(2)	11(2)
C(16)	70(2)	99(3)	55(2)	5(2)	-12(2)	12(2)
C(17)	101(3)	97(3)	74(2)	-22(2)	-21(2)	16(2)
C(18)	81(2)	85(3)	68(2)	-8(2)	-2(2)	25(2)
C(19)	44(1)	77(2)	41(1)	6(1)	7(1)	6(1)
C(20)	37(1)	83(2)	56(2)	0(1)	6(1)	17(1)
C(21)	57(2)	116(3)	85(2)	21(2)	31(2)	13(2)
C(22)	70(2)	104(3)	102(3)	-15(2)	15(2)	33(2)
C(23)	40(1)	76(2)	48(2)	3(1)	3(1)	8(1)
C(24)	83(2)	94(3)	61(2)	15(2)	0(2)	18(2)
C(25)	55(2)	94(3)	64(2)	-13(2)	11(1)	-5(2)

Table 26. Bond lengths [Å] for **88**.

B-N(2)	1.407(4)	C(8)-C(13)	1.404(4)
B-N(1)	1.431(4)	C(9)-C(10)	1.379(5)
B-C(1)	1.624(4)	C(10)-C(11)	1.380(5)
N(1)-C(19)	1.436(3)	C(11)-C(12)	1.385(5)
N(2)-C(23)	1.481(4)	C(12)-C(13)	1.382(5)
N(2)-C(20)	1.483(4)	C(14)-C(15)	1.39
C(1)-C(13)	1.505(4)	C(14)-C(19)	1.39
C(1)-C(2)	1.509(4)	C(15)-C(16)	1.39
C(2)-C(3)	1.391(5)	C(16)-C(17)	1.39
C(2)-C(7)	1.401(4)	C(17)-C(18)	1.39
C(3)-C(4)	1.395(6)	C(18)-C(19)	1.39
C(4)-C(5)	1.363(7)	C(20)-C(22)	1.520(5)
C(5)-C(6)	1.388(6)	C(20)-C(21)	1.523(5)
C(6)-C(7)	1.387(5)	C(23)-C(25)	1.523(5)
C(7)-C(8)	1.467(5)	C(23)-C(24)	1.534(5)
C(8)-C(9)	1.395(5)		

Table 27. Bond angles [°] for **88**.

N(2)-B-N(1)	121.4(3)	C(13)-C(8)-C(7)	108.3(3)
N(2)-B-C(1)	122.3(3)	C(10)-C(9)-C(8)	118.5(3)
N(1)-B-C(1)	116.3(2)	C(9)-C(10)-C(11)	121.1(3)
B-N(1)-C(19)	131.5(2)	C(10)-C(11)-C(12)	120.5(4)
B-N(2)-C(23)	121.6(2)	C(13)-C(12)-C(11)	119.8(3)
B-N(2)-C(20)	124.6(2)	C(12)-C(13)-C(8)	119.3(3)
C(23)-N(2)-C(20)	113.8(2)	C(12)-C(13)-C(1)	130.0(3)
C(13)-C(1)-C(2)	102.1(2)	C(8)-C(13)-C(1)	110.6(3)
C(13)-C(1)-B	118.4(2)	C(15)-C(14)-C(19)	120.0
C(2)-C(1)-B	116.4(2)	C(16)-C(15)-C(14)	120.0
C(3)-C(2)-C(7)	119.9(3)	C(15)-C(16)-C(17)	120.0
C(3)-C(2)-C(1)	129.4(3)	C(16)-C(17)-C(18)	120.0
C(7)-C(2)-C(1)	110.7(3)	C(19)-C(18)-C(17)	120.0
C(2)-C(3)-C(4)	118.6(4)	C(18)-C(19)-C(14)	120.0
C(5)-C(4)-C(3)	120.9(4)	C(18)-C(19)-N(1)	119.5(2)
C(4)-C(5)-C(6)	121.5(4)	C(14)-C(19)-N(1)	120.5(2)
C(7)-C(6)-C(5)	118.3(4)	N(2)-C(20)-C(22)	114.1(3)
C(6)-C(7)-C(2)	120.8(3)	N(2)-C(20)-C(21)	112.2(3)
C(6)-C(7)-C(8)	130.9(3)	C(22)-C(20)-C(21)	112.7(3)
C(2)-C(7)-C(8)	108.2(3)	N(2)-C(23)-C(25)	113.0(3)
C(9)-C(8)-C(13)	120.8(3)	N(2)-C(23)-C(24)	111.8(3)
C(9)-C(8)-C(7)	131.0(3)	C(25)-C(23)-C(24)	111.9(3)

Table 28. Crystal data and structure refinement for **101**.

Empirical formula	$C_{25}H_{22}BFeN$
Formula weight	403.10
Temperature	173(2) K
Wavelength	0.71073 Å
Crystal system	Triclinic
Space group	P-1
Unit cell dimensions	a = 7.4676(17) Å
	b = 11.346(3) Å
	c = 12.538(3) Å
	α = 77.333(4)°
	β = 82.899(5)°
	γ = 75.143(4)°
Volume	999.2(4) $Å^3$
Z	2
Density (calculated)	1.340 Mg/m^3
Absorption coefficient	0.764 mm^{-1}
F(000)	420
Crystal size	0.31 x 0.22 x 0.05 mm^3
Theta range for data collection	1.67 to 26.13°.
Index ranges	-9<=h<=9, -13<=k<=14, -15<=l<=15
Reflections collected	15166
Independent reflections	3952 [R(int) = 0.0482]
Completeness to theta = 26.13°	99.4 %
Absorption correction	Empirical
Max. and min. transmission	0.96 and 0.722
Refinement method	Full-matrix least-squares on F^2
Data / restraints / parameters	3952 / 0 / 253
Goodness-of-fit on F^2	1.068
Final R indices [I>2sigma(I)]	R1 = 0.0371, wR2 = 0.0994
R indices (all data)	R1 = 0.0419, wR2 = 0.1023
Largest diff. peak and hole	0.473 and -0.190 $e.Å^{-3}$

Table 29. Atomic coordinates ($\times 10^4$) and equivalent isotropic displacement parameters ($Å^2 \times 10^3$) for **101**. U(eq) is defined as one third of the trace of the orthogonalised U_{ij} tensor.

	x	y	z	U(eq)
Fe(1)	10207(1)	6003(1)	7674(1)	36(1)
N(1)	7250(3)	9223(2)	8294(2)	54(1)
B(1)	8941(3)	8837(2)	7696(2)	42(1)
C(11)	6507(3)	8653(2)	9328(2)	50(1)
C(12)	5079(4)	8081(3)	9361(2)	66(1)
C(13)	4310(5)	7546(3)	10352(3)	87(1)
C(14)	4958(5)	7573(3)	11303(3)	93(1)
C(15)	6363(5)	8127(3)	11298(2)	85(1)
C(16)	7175(4)	8690(3)	10300(2)	68(1)
C(21)	9339(3)	9719(2)	6544(2)	45(1)
C(22)	10790(3)	10373(2)	6687(2)	57(1)
C(23)	10132(3)	11612(2)	6483(2)	58(1)
C(24)	7048(3)	13054(2)	5788(2)	55(1)
C(25)	5369(4)	13060(2)	5450(2)	63(1)
C(26)	4884(4)	11962(3)	5456(2)	66(1)
C(27)	6090(3)	10821(2)	5812(2)	56(1)
C(28)	7795(3)	10799(2)	6137(2)	43(1)
C(29)	8278(3)	11916(2)	6130(2)	45(1)
C(31)	10431(3)	7624(2)	8051(2)	42(1)
C(32)	11993(3)	7150(2)	7333(2)	47(1)
C(33)	12926(3)	5945(2)	7841(2)	53(1)
C(34)	12000(3)	5645(2)	8882(2)	51(1)
C(35)	10479(3)	6660(2)	9018(2)	45(1)
C(41)	7717(3)	6337(2)	7007(2)	52(1)
C(42)	9210(3)	5981(2)	6241(2)	55(1)
C(43)	10243(3)	4794(2)	6690(2)	58(1)
C(44)	9396(3)	4405(2)	7742(2)	56(1)
C(45)	7837(3)	5360(2)	7934(2)	52(1)

Table 30. Anisotropic displacement parameters ($Å^2 \times 10^3$) for **101**. The anisotropic displacement factor exponent takes the form: $-2\pi^2[h^2 a^{*2} U_{11} + ... + 2 h k a^* b^* U_{12}]$.

	U_{11}	U_{22}	U_{33}	U_{23}	U_{13}	U_{12}
Fe(1)	33(1)	35(1)	39(1)	-7(1)	-3(1)	-6(1)
N(1)	55(1)	41(1)	51(1)	-1(1)	6(1)	2(1)
B(1)	47(1)	37(1)	44(1)	-11(1)	-1(1)	-12(1)
C(11)	53(1)	40(1)	42(1)	-7(1)	6(1)	7(1)
C(12)	70(2)	62(2)	61(2)	-11(1)	6(1)	-14(1)
C(13)	90(2)	75(2)	87(2)	-8(2)	28(2)	-26(2)
C(14)	105(3)	71(2)	65(2)	3(2)	32(2)	14(2)
C(15)	96(2)	86(2)	45(1)	-18(1)	-7(1)	33(2)
C(16)	64(2)	69(2)	63(2)	-24(1)	-6(1)	9(1)
C(21)	47(1)	40(1)	46(1)	-7(1)	3(1)	-11(1)
C(22)	45(1)	54(1)	69(2)	-2(1)	-3(1)	-14(1)
C(23)	60(1)	45(1)	71(2)	-3(1)	-7(1)	-21(1)
C(24)	64(2)	42(1)	51(1)	-2(1)	7(1)	-7(1)
C(25)	57(1)	59(2)	53(1)	6(1)	4(1)	2(1)
C(26)	53(1)	82(2)	54(1)	6(1)	-10(1)	-14(1)
C(27)	60(1)	64(2)	48(1)	-2(1)	-7(1)	-24(1)
C(28)	47(1)	42(1)	36(1)	-3(1)	2(1)	-11(1)
C(29)	49(1)	43(1)	41(1)	-7(1)	6(1)	-11(1)
C(31)	42(1)	40(1)	47(1)	-12(1)	-4(1)	-11(1)
C(32)	39(1)	46(1)	58(1)	-11(1)	2(1)	-16(1)
C(33)	32(1)	51(1)	76(2)	-17(1)	-9(1)	-5(1)
C(34)	51(1)	45(1)	57(1)	-8(1)	-22(1)	-4(1)
C(35)	51(1)	43(1)	42(1)	-9(1)	-11(1)	-8(1)
C(41)	41(1)	62(1)	55(1)	-9(1)	-16(1)	-10(1)
C(42)	63(1)	72(2)	38(1)	-10(1)	-8(1)	-26(1)
C(43)	58(1)	63(2)	66(2)	-37(1)	3(1)	-18(1)
C(44)	64(1)	42(1)	67(2)	-10(1)	-13(1)	-20(1)
C(45)	43(1)	69(2)	51(1)	-10(1)	-2(1)	-25(1)

Table 31. Bond lengths [Å] for **101**.

Fe(1)-C(43)	2.029(2)	C(21)-C(28)	1.496(3)
Fe(1)-C(42)	2.035(2)	C(21)-C(22)	1.508(3)
Fe(1)-C(44)	2.035(2)	C(22)-C(23)	1.342(3)
Fe(1)-C(35)	2.037(2)	C(23)-C(29)	1.439(3)
Fe(1)-C(32)	2.040(2)	C(24)-C(25)	1.370(4)
Fe(1)-C(41)	2.045(2)	C(24)-C(29)	1.393(3)
Fe(1)-C(45)	2.046(2)	C(25)-C(26)	1.381(4)
Fe(1)-C(31)	2.048(2)	C(26)-C(27)	1.391(4)
Fe(1)-C(33)	2.050(2)	C(27)-C(28)	1.378(3)
Fe(1)-C(34)	2.051(2)	C(28)-C(29)	1.402(3)
N(1)-B(1)	1.406(3)	C(31)-C(35)	1.440(3)
N(1)-C(11)	1.430(3)	C(31)-C(32)	1.446(3)
B(1)-C(31)	1.549(3)	C(32)-C(33)	1.414(3)
B(1)-C(21)	1.609(3)	C(33)-C(34)	1.414(3)
C(11)-C(12)	1.375(4)	C(34)-C(35)	1.419(3)
C(11)-C(16)	1.386(3)	C(41)-C(45)	1.413(3)
C(12)-C(13)	1.383(4)	C(41)-C(42)	1.415(3)
C(13)-C(14)	1.349(5)	C(42)-C(43)	1.403(4)
C(14)-C(15)	1.354(5)	C(43)-C(44)	1.420(3)
C(15)-C(16)	1.415(4)	C(44)-C(45)	1.408(3)

Table 32. Bond angles [°] for **101**.

C(43)-Fe(1)-C(42)	40.38(10)	C(35)-Fe(1)-C(33)	68.35(9)
C(43)-Fe(1)-C(44)	40.91(10)	C(32)-Fe(1)-C(33)	40.46(9)
C(42)-Fe(1)-C(44)	68.31(10)	C(41)-Fe(1)-C(33)	161.51(10)
C(43)-Fe(1)-C(35)	160.44(10)	C(45)-Fe(1)-C(33)	155.91(10)
C(42)-Fe(1)-C(35)	157.99(10)	C(31)-Fe(1)-C(33)	69.44(9)
C(44)-Fe(1)-C(35)	124.00(10)	C(43)-Fe(1)-C(34)	123.44(10)
C(43)-Fe(1)-C(32)	120.65(10)	C(42)-Fe(1)-C(34)	160.09(10)
C(42)-Fe(1)-C(32)	107.99(9)	C(44)-Fe(1)-C(34)	106.88(10)
C(44)-Fe(1)-C(32)	155.75(10)	C(35)-Fe(1)-C(34)	40.61(9)
C(35)-Fe(1)-C(32)	68.52(9)	C(32)-Fe(1)-C(34)	67.99(9)
C(43)-Fe(1)-C(41)	68.12(10)	C(41)-Fe(1)-C(34)	157.38(10)
C(42)-Fe(1)-C(41)	40.60(10)	C(45)-Fe(1)-C(34)	121.51(10)
C(44)-Fe(1)-C(41)	68.06(10)	C(31)-Fe(1)-C(34)	69.26(9)
C(35)-Fe(1)-C(41)	122.59(9)	C(33)-Fe(1)-C(34)	40.34(10)
C(32)-Fe(1)-C(41)	125.71(10)	B(1)-N(1)-C(11)	130.34(19)
C(43)-Fe(1)-C(45)	68.26(10)	N(1)-B(1)-C(31)	125.14(19)
C(42)-Fe(1)-C(45)	68.18(9)	N(1)-B(1)-C(21)	117.16(19)
C(44)-Fe(1)-C(45)	40.38(10)	C(31)-B(1)-C(21)	117.70(18)
C(35)-Fe(1)-C(45)	108.26(9)	C(12)-C(11)-C(16)	119.4(2)
C(32)-Fe(1)-C(45)	162.55(10)	C(12)-C(11)-N(1)	119.6(2)
C(41)-Fe(1)-C(45)	40.42(9)	C(16)-C(11)-N(1)	121.0(2)
C(43)-Fe(1)-C(31)	156.53(10)	C(11)-C(12)-C(13)	120.7(3)
C(42)-Fe(1)-C(31)	121.56(10)	C(14)-C(13)-C(12)	120.4(3)
C(44)-Fe(1)-C(31)	161.18(10)	C(13)-C(14)-C(15)	120.4(3)
C(35)-Fe(1)-C(31)	41.29(8)	C(14)-C(15)-C(16)	120.8(3)
C(32)-Fe(1)-C(31)	41.44(8)	C(11)-C(16)-C(15)	118.4(3)
C(41)-Fe(1)-C(31)	108.01(9)	C(28)-C(21)-C(22)	101.21(17)
C(45)-Fe(1)-C(31)	124.80(9)	C(28)-C(21)-B(1)	117.32(17)
C(43)-Fe(1)-C(33)	106.52(10)	C(22)-C(21)-B(1)	108.21(18)
C(42)-Fe(1)-C(33)	124.01(10)	C(23)-C(22)-C(21)	111.2(2)
C(44)-Fe(1)-C(33)	120.29(10)	C(22)-C(23)-C(29)	109.7(2)
C(25)-C(24)-C(29)	118.8(2)	C(33)-C(34)-C(35)	108.3(2)
C(24)-C(25)-C(26)	121.1(2)	C(33)-C(34)-Fe(1)	69.81(13)
C(25)-C(26)-C(27)	120.7(2)	C(35)-C(34)-Fe(1)	69.16(12)
C(28)-C(27)-C(26)	119.0(2)	C(34)-C(35)-C(31)	109.1(2)
C(27)-C(28)-C(29)	120.0(2)	C(34)-C(35)-Fe(1)	70.23(12)
C(27)-C(28)-C(21)	130.0(2)	C(31)-C(35)-Fe(1)	69.77(11)
C(29)-C(28)-C(21)	109.93(18)	C(45)-C(41)-C(42)	107.9(2)
C(24)-C(29)-C(28)	120.4(2)	C(45)-C(41)-Fe(1)	69.82(12)
C(24)-C(29)-C(23)	131.7(2)	C(42)-C(41)-Fe(1)	69.31(12)
C(28)-C(29)-C(23)	107.80(19)	C(43)-C(42)-C(41)	108.1(2)
C(35)-C(31)-C(32)	105.30(18)	C(43)-C(42)-Fe(1)	69.58(13)
C(35)-C(31)-B(1)	130.76(19)	C(41)-C(42)-Fe(1)	70.09(12)
C(32)-C(31)-B(1)	123.32(19)	C(42)-C(43)-C(44)	108.1(2)
C(35)-C(31)-Fe(1)	68.94(11)	C(42)-C(43)-Fe(1)	70.03(13)
C(32)-C(31)-Fe(1)	68.98(11)	C(44)-C(43)-Fe(1)	69.78(13)
B(1)-C(31)-Fe(1)	119.37(14)	C(45)-C(44)-C(43)	107.9(2)
C(33)-C(32)-C(31)	109.3(2)	C(45)-C(44)-Fe(1)	70.23(13)
C(33)-C(32)-Fe(1)	70.16(12)	C(43)-C(44)-Fe(1)	69.31(12)
C(31)-C(32)-Fe(1)	69.58(11)	C(44)-C(45)-C(41)	108.0(2)
C(34)-C(33)-C(32)	107.9(2)	C(44)-C(45)-Fe(1)	69.40(12)
C(34)-C(33)-Fe(1)	69.86(12)	C(41)-C(45)-Fe(1)	69.76(12)
C(32)-C(33)-Fe(1)	69.38(12)		

Table 33. Crystal data and structure refinement for **111**.

Empirical formula	$C_{17}H_{34}BCl_2N_3Ti$
Formula weight	410.08
Temperature	193(2) K
Wavelength	0.71073 Å
Crystal system	Monoclinic
Space group	C2/c
Unit cell dimensions	a = 24.325(5) Å
	b = 17.761(4) Å
	c = 12.096(2) Å
	α = 90°
	β = 119.27(3)°
	γ = 90°
Volume	4558.7(16) $Å^3$
Z	8
Density (calculated)	1.195 Mg/m^3
Absorption coefficient	0.614 mm^{-1}
F(000)	1744
Crystal size	.4 x .3 x .3 mm^3
Theta range for data collection	2.29 to 27.38°.
Index ranges	-31<=h<=31, -22<=k<=22, -15<=l<=14
Reflections collected	25618
Independent reflections	4912 [R(int) = 0.0526]
Completeness to theta = 27.38°	94.7 %
Absorption correction	Analytical
Max. and min. transmission	.8664 and .7984
Refinement method	Full-matrix least-squares on F^2
Data / restraints / parameters	4912 / 30 / 244
Goodness-of-fit on F^2	1.023
Final R indices [I>2sigma(I)]	R1 = 0.0339, wR2 = 0.0838
R indices (all data)	R1 = 0.0432, wR2 = 0.0881
Largest diff. peak and hole	0.259 and -0.390 $e.Å^{-3}$
CCDC reference number	279470

Table 34. Atomic coordinates ($\times 10^4$) and equivalent isotropic displacement parameters ($Å^2 \times 10^3$) for **111**. U(eq) is defined as one third of the trace of the orthogonalised U_{ij} tensor.

	x	y	z	U(eq)
Ti(1)	8581(1)	9246(1)	8924(1)	32(1)
Cl(1)	8747(1)	10523(1)	8935(1)	51(1)
Cl(2)	7581(1)	9210(1)	8678(1)	47(1)
B(1)	9071(1)	7263(1)	9210(3)	34(1)
N(1)	8470(1)	6911(1)	8474(2)	37(1)
N(2)	9627(1)	6865(1)	9447(3)	51(1)
N(3)	8524(1)	8959(1)	7386(2)	41(1)
C(1)	9140(1)	8092(1)	9794(2)	32(1)
C(2)	9574(1)	8674(1)	9920(2)	39(1)
C(3)	9580(1)	9230(1)	10745(3)	44(1)
C(4)	9142(1)	9028(1)	11122(2)	44(1)
C(5)	8874(1)	8334(1)	10538(2)	35(1)
C(6)	10312(1)	6899(2)	10344(3)	63(1)
C(7)	10614(2)	7361(3)	9653(6)	83(2)
C(8)	10570(2)	6115(2)	10499(7)	97(3)
C(9)	10485(2)	7278(3)	11573(5)	75(2)
C(6A)	10312(1)	6899(2)	10344(3)	63(1)
C(7A)	10579(18)	7453(16)	11440(30)	93(5)
C(8A)	10754(10)	6725(13)	9860(20)	93(5)
C(9A)	10377(12)	6104(10)	11140(20)	93(5)
C(10)	7865(1)	7310(1)	8000(2)	39(1)
C(11)	7470(1)	7033(2)	8573(3)	56(1)
C(12)	7473(1)	7326(2)	6558(3)	64(1)
C(13)	8375(1)	6098(1)	8125(3)	55(1)
C(14)	8603(2)	5859(2)	7214(5)	86(1)
C(15)	8615(2)	5598(2)	9284(4)	81(1)
C(16)	7992(2)	9372(2)	6347(3)	54(1)
C(17)	8847(1)	8500(2)	6891(3)	53(1)

Table 35. Anisotropic displacement parameters ($Å^2 \times 10^3$) for **111**. The anisotropic displacement factor exponent takes the form: $-2\pi^2[h^2 a^{*2} U_{11} + ... + 2 h k a^* b^* U_{12}]$.

	U_{11}	U_{22}	U_{33}	U_{23}	U_{13}	U_{12}
Ti(1)	34(1)	30(1)	29(1)	1(1)	12(1)	4(1)
Cl(1)	63(1)	31(1)	54(1)	1(1)	25(1)	1(1)
Cl(2)	36(1)	49(1)	54(1)	3(1)	20(1)	11(1)
B(1)	31(1)	32(1)	40(2)	1(1)	16(1)	0(1)
N(1)	29(1)	30(1)	49(1)	-4(1)	17(1)	-2(1)
N(2)	29(1)	39(1)	75(2)	-19(1)	18(1)	-1(1)
N(3)	48(1)	40(1)	33(1)	1(1)	17(1)	-4(1)
C(1)	27(1)	33(1)	32(1)	2(1)	11(1)	2(1)
C(2)	29(1)	36(1)	42(1)	1(1)	10(1)	0(1)
C(3)	40(1)	38(1)	37(1)	-5(1)	6(1)	-3(1)
C(4)	52(1)	45(1)	26(1)	-4(1)	11(1)	9(1)
C(5)	34(1)	38(1)	29(1)	4(1)	13(1)	6(1)
C(6)	27(1)	61(2)	85(2)	-21(2)	14(1)	6(1)
C(7)	47(2)	82(3)	132(5)	-6(3)	52(3)	-1(2)
C(8)	45(2)	61(2)	153(6)	-8(3)	24(3)	23(2)
C(9)	47(3)	85(4)	57(3)	-7(3)	-2(2)	24(2)
C(6A)	27(1)	61(2)	85(2)	-21(2)	14(1)	6(1)
C(10)	28(1)	39(1)	43(1)	-4(1)	12(1)	-2(1)
C(11)	42(1)	63(2)	66(2)	-13(1)	30(1)	-9(1)
C(12)	44(2)	82(2)	46(2)	6(1)	5(1)	-5(1)
C(13)	39(1)	38(1)	84(2)	-18(1)	27(1)	-9(1)
C(14)	60(2)	77(2)	122(4)	-61(2)	47(2)	-21(2)
C(15)	64(2)	39(1)	128(4)	15(2)	39(2)	2(1)
C(16)	63(2)	56(2)	34(1)	11(1)	16(1)	2(1)
C(17)	66(2)	58(2)	46(2)	-4(1)	37(1)	-4(1)

Table 36. Bond lengths [Å] for **111**.

Ti(1)-N(3)	1.867(2)	N(3)-C(17)	1.450(4)
Ti(1)-Cl(1)	2.3015(8)	N(3)-C(16)	1.482(3)
Ti(1)-Cl(2)	2.3034(9)	C(1)-C(5)	1.409(3)
Ti(1)-C(2)	2.339(2)	C(1)-C(2)	1.433(3)
Ti(1)-C(3)	2.350(3)	C(2)-C(3)	1.399(4)
Ti(1)-C(4)	2.352(3)	C(3)-C(4)	1.395(4)
Ti(1)-C(5)	2.363(2)	C(4)-C(5)	1.412(3)
Ti(1)-C(1)	2.400(2)	C(6)-C(9)	1.494(6)
B(1)-N(2)	1.427(3)	C(6)-C(8)	1.500(4)
B(1)-N(1)	1.432(3)	C(6)-C(7)	1.584(6)
B(1)-C(1)	1.605(3)	C(10)-C(11)	1.516(4)
N(1)-C(10)	1.474(3)	C(10)-C(12)	1.524(4)
N(1)-C(13)	1.490(3)	C(13)-C(15)	1.514(5)
N(2)-C(6)	1.480(3)	C(13)-C(14)	1.515(5)

Table 37. Bond angles [°] for **111**.

N(3)-Ti(1)-Cl(1)	101.66(6)	B(1)-N(1)-C(10)	123.53(16)
N(3)-Ti(1)-Cl(2)	107.67(8)	B(1)-N(1)-C(13)	124.73(18)
Cl(1)-Ti(1)-Cl(2)	101.45(3)	C(10)-N(1)-C(13)	111.71(17)
N(3)-Ti(1)-C(2)	87.15(10)	B(1)-N(2)-C(6)	138.2(2)
Cl(1)-Ti(1)-C(2)	106.93(6)	C(17)-N(3)-C(16)	110.6(2)
Cl(2)-Ti(1)-C(2)	144.53(7)	C(17)-N(3)-Ti(1)	140.64(18)
N(3)-Ti(1)-C(3)	118.07(11)	C(16)-N(3)-Ti(1)	108.66(19)
Cl(1)-Ti(1)-C(3)	84.79(6)	C(5)-C(1)-C(2)	104.9(2)
Cl(2)-Ti(1)-C(3)	131.57(8)	C(5)-C(1)-B(1)	125.5(2)
C(2)-Ti(1)-C(3)	34.72(9)	C(2)-C(1)-B(1)	128.4(2)
N(3)-Ti(1)-C(4)	143.25(9)	C(5)-C(1)-Ti(1)	71.37(12)
Cl(1)-Ti(1)-C(4)	98.77(7)	C(2)-C(1)-Ti(1)	70.10(12)
Cl(2)-Ti(1)-C(4)	97.68(8)	B(1)-C(1)-Ti(1)	132.47(15)
C(2)-Ti(1)-C(4)	57.64(10)	C(3)-C(2)-C(1)	109.5(2)
C(3)-Ti(1)-C(4)	34.53(11)	C(3)-C(2)-Ti(1)	73.06(14)
N(3)-Ti(1)-C(5)	118.84(8)	C(1)-C(2)-Ti(1)	74.71(12)
Cl(1)-Ti(1)-C(5)	133.58(6)	C(4)-C(3)-C(2)	108.0(2)
Cl(2)-Ti(1)-C(5)	87.71(6)	C(4)-C(3)-Ti(1)	72.83(14)
C(2)-Ti(1)-C(5)	57.27(9)	C(2)-C(3)-Ti(1)	72.22(13)
C(3)-Ti(1)-C(5)	57.42(9)	C(3)-C(4)-C(5)	107.5(2)
C(4)-Ti(1)-C(5)	34.84(8)	C(3)-C(4)-Ti(1)	72.64(15)
N(3)-Ti(1)-C(1)	87.41(9)	C(5)-C(4)-Ti(1)	72.99(14)
Cl(1)-Ti(1)-C(1)	141.20(6)	C(1)-C(5)-C(4)	110.0(2)
Cl(2)-Ti(1)-C(1)	111.64(6)	C(1)-C(5)-Ti(1)	74.23(13)
C(2)-Ti(1)-C(1)	35.18(7)	C(4)-C(5)-Ti(1)	72.17(14)
C(3)-Ti(1)-C(1)	58.28(8)	N(2)-C(6)-C(9)	114.5(3)
C(4)-Ti(1)-C(1)	58.18(8)	N(2)-C(6)-C(8)	107.8(3)
C(5)-Ti(1)-C(1)	34.40(8)	C(9)-C(6)-C(8)	113.4(4)
N(2)-B(1)-N(1)	119.18(19)	N(2)-C(6)-C(7)	106.3(3)
N(2)-B(1)-C(1)	118.80(19)	C(9)-C(6)-C(7)	108.3(4)
N(1)-B(1)-C(1)	122.02(19)	C(8)-C(6)-C(7)	105.9(4)
N(1)-C(10)-C(11)	113.6(2)	N(1)-C(13)-C(15)	111.7(3)
N(1)-C(10)-C(12)	113.6(2)	N(1)-C(13)-C(14)	114.6(3)
C(11)-C(10)-C(12)	110.3(2)	C(15)-C(13)-C(14)	113.4(3)

Table 38. Crystal data and structure refinement for **112**.

Empirical formula	$C_{14}H_{20}B_2Cl_4N_2O_3Ti_2$
Formula weight	523.54
Temperature	193(2) K
Wavelength	0.71073 Å
Crystal system	Monoclinic
Space group	C2/c
Unit cell dimensions	a = 17.3047(13) Å
	b = 8.9757(7) Å
	c = 14.7696(11) Å
	α = 90°
	β = 112.59(10)°
	γ = 90°
Volume	2118.0(3) Å^3
Z	4
Density (calculated)	1.642 Mg/m^3
Absorption coefficient	1.276 mm^{-1}
F(000)	1056
Crystal size	0.42 x 0.10 x 0.09 mm^3
Theta range for data collection	2.55 to 26.08°
Index ranges	-21<=h<=21, -11<=k<=11, -18<=l<=18
Reflections collected	14573
Independent reflections	2083 [R_{int} = 0.0209]
Completeness to theta = 26.08°	99.8 %
Refinement method	Full-matrix least-squares on F^2
Data / restraints / parameters	2083 / 0 / 125
Goodness-of-fit on F^2	S = 1.137
R indices [for 2014 reflections with I>2sigma(I)]	R_1 = 0.0290, wR_2 = 0.0792
R indices (for all 2083 data)	R_1 = 0.0302, wR_2 = 0.0802
Largest diff. peak and hole	0.707 and -0.232 eÅ^{-3}
CCDC reference number	279469

Table 39. Atomic coordinates ($\times 10^4$) and equivalent isotropic displacement parameters ($Å^2 \times 10^3$) for **112**. U(eq) is defined as one third of the trace of the orthogonalised U_{ij} tensor.

	x	y	z	U(eq)
Ti(1)	1227(1)	6201(1)	2207(1)	23(1)
Cl(1)	2012(1)	5792(1)	1282(1)	33(1)
Cl(2)	832(1)	8626(1)	1867(1)	38(1)
O(1)	0	3285(2)	2500	26(1)
O(2)	312(1)	5217(2)	1546(1)	24(1)
B(1)	-309(1)	4120(2)	1609(2)	25(1)
C(8)	1882(1)	4464(2)	3415(2)	29(1)
C(5)	1175(1)	4997(2)	3584(1)	25(1)
C(6)	2128(1)	6916(3)	3810(2)	37(1)
C(4)	1332(1)	6529(2)	3812(1)	30(1)
C(7)	2466(1)	5646(3)	3569(2)	36(1)
N(1)	-428(1)	2925(2)	742(1)	29(1)
C(10)	392(1)	2354(3)	776(2)	37(1)
C(9)	-982(2)	1660(3)	747(2)	38(1)

Table 40. Anisotropic displacement parameters ($Å^2 \times 10^3$) for **112**. The anisotropic displacement factor exponent takes the form: $-2\pi^2[h^2 a^{*2} U_{11} + ... + 2 h k a^* b^* U_{12}]$.

	U_{11}	U_{22}	U_{33}	U_{23}	U_{13}	U_{12}
Ti(1)	22(1)	24(1)	23(1)	2(1)	8(1)	-2(1)
Cl(1)	31(1)	39(1)	34(1)	3(1)	17(1)	2(1)
Cl(2)	42(1)	26(1)	44(1)	5(1)	15(1)	2(1)
O(1)	27(1)	24(1)	25(1)	0	8(1)	0
O(2)	24(1)	27(1)	21(1)	1(1)	7(1)	1(1)
B(1)	23(1)	25(1)	25(1)	-4(1)	9(1)	-1(1)
C(8)	24(1)	34(1)	28(1)	8(1)	7(1)	5(1)
C(5)	24(1)	29(1)	18(1)	3(1)	4(1)	1(1)
C(6)	35(1)	44(1)	25(1)	-2(1)	4(1)	-16(1)
C(4)	33(1)	32(1)	22(1)	-3(1)	10(1)	-5(1)
C(7)	20(1)	52(1)	30(1)	10(1)	4(1)	-1(1)
N(1)	29(1)	27(1)	31(1)	-4(1)	11(1)	1(1)
C(10)	37(1)	35(1)	42(1)	-8(1)	18(1)	5(1)
C(9)	41(1)	32(1)	41(1)	-12(1)	16(1)	-10(1)

Table 41. Bond lengths [Å] for **112**.

Ti(1)-O(2)	1.7473(13)	B(1)-C(5)#1	1.618(3)
Ti(1)-Cl(2)	2.2791(6)	B(1)-N(1)	1.621(3)
Ti(1)-Cl(1)	2.2969(6)	C(8)-C(7)	1.421(3)
Ti(1)-C(8)	2.312(2)	C(8)-C(5)	1.422(3)
Ti(1)-C(4)	2.325(2)	C(5)-C(4)	1.417(3)
Ti(1)-C(5)	2.3337(19)	C(5)-B(1)#1	1.618(3)
Ti(1)-C(7)	2.362(2)	C(6)-C(7)	1.388(4)
Ti(1)-C(6)	2.369(2)	C(6)-C(4)	1.422(3)
O(1)-B(1)#1	1.428(2)	N(1)-C(9)	1.488(3)
O(1)-B(1)	1.428(2)	N(1)-C(10)	1.491(3)
O(2)-B(1)	1.486(3)		

Table 42. Bond angles [°] for **112**.

O(2)-Ti(1)-Cl(2)	103.24(5)	B(1)-O(2)-Ti(1)	145.24(12)
O(2)-Ti(1)-Cl(1)	101.70(5)	O(1)-B(1)-O(2)	112.44(15)
Cl(2)-Ti(1)-Cl(1)	102.54(2)	O(1)-B(1)-C(5)#1	114.25(16)
O(2)-Ti(1)-C(8)	99.28(7)	O(2)-B(1)-C(5)#1	108.02(16)
Cl(2)-Ti(1)-C(8)	146.18(6)	O(1)-B(1)-N(1)	105.63(16)
Cl(1)-Ti(1)-C(8)	97.16(6)	O(2)-B(1)-N(1)	105.38(16)
O(2)-Ti(1)-C(4)	109.44(7)	C(5)#1-B(1)-N(1)	110.77(15)
Cl(2)-Ti(1)-C(4)	90.18(6)	C(7)-C(8)-C(5)	109.1(2)
Cl(1)-Ti(1)-C(4)	142.61(6)	C(7)-C(8)-Ti(1)	74.21(12)
C(8)-Ti(1)-C(4)	58.38(8)	C(5)-C(8)-Ti(1)	73.02(11)
O(2)-Ti(1)-C(5)	85.59(6)	C(4)-C(5)-C(8)	105.65(18)
Cl(2)-Ti(1)-C(5)	121.72(5)	C(4)-C(5)-B(1)#1	126.39(18)
Cl(1)-Ti(1)-C(5)	132.35(5)	C(8)-C(5)-B(1)#1	127.34(18)
C(8)-Ti(1)-C(5)	35.64(7)	C(4)-C(5)-Ti(1)	71.98(11)
C(4)-Ti(1)-C(5)	35.41(7)	C(8)-C(5)-Ti(1)	71.34(11)
O(2)-Ti(1)-C(7)	134.49(7)	B(1)#1-C(5)-Ti(1)	114.52(12)
Cl(2)-Ti(1)-C(7)	119.09(7)	C(7)-C(6)-C(4)	107.6(2)
Cl(1)-Ti(1)-C(7)	85.55(6)	C(7)-C(6)-Ti(1)	72.65(12)
C(8)-Ti(1)-C(7)	35.39(8)	C(4)-C(6)-Ti(1)	70.71(11)
C(4)-Ti(1)-C(7)	57.89(8)	C(5)-C(4)-C(6)	109.5(2)
C(5)-Ti(1)-C(7)	59.10(7)	C(5)-C(4)-Ti(1)	72.61(11)
O(2)-Ti(1)-C(6)	143.41(7)	C(6)-C(4)-Ti(1)	74.03(12)
Cl(2)-Ti(1)-C(6)	89.30(6)	C(6)-C(7)-C(8)	108.1(2)
Cl(1)-Ti(1)-C(6)	108.98(6)	C(6)-C(7)-Ti(1)	73.22(12)
C(8)-Ti(1)-C(6)	58.15(8)	C(8)-C(7)-Ti(1)	70.40(11)
C(4)-Ti(1)-C(6)	35.26(8)	C(9)-N(1)-C(10)	110.12(17)
C(5)-Ti(1)-C(6)	59.07(7)	C(9)-N(1)-B(1)	112.83(16)
C(7)-Ti(1)-C(6)	34.13(9)	C(10)-N(1)-B(1)	111.70(15)
B(1)#1-O(1)-B(1)	116.7(2)		

Table 43. Crystal data and structure refinement for **116**.

Empirical formula	$C_{17}H_{27}BCl_2N_2Si_2Ti$
Formula weight	445.20
Temperature	203(2) K
Wavelength	1.54178 Å
Crystal system	Monoclinic
Space group	P2(1)/c
Unit cell dimensions	a = 7.1231(11) Å
	b = 19.0371(10) Å
	c = 17.219(2) Å
	$\alpha = 90°$
	$\beta = 97.423(14)°$
	$\gamma = 90°$
Volume	2315.4(5) $Å^3$
Z	4
Density (calculated)	1.277 Mg/m^3
Absorption coefficient	6.263 mm^{-1}
F(000)	928
Crystal size	0.50 x 0.37 x 0.33 mm^3
Theta range for data collection	3.48 to 59.99°.
Index ranges	0<=h<=7, 0<=k<=21, -19<=l<=19
Reflections collected	3732
Independent reflections	3423 [R(int) = 0.0966]
Absorption correction	Ellipsoidal
Max. and min. transmission	0.1765 and 0.0329
Refinement method	Full-matrix least-squares on F^2
Data / restraints / parameters	3248 / 12 / 215
Goodness-of-fit on F^2	1.050
Final R indices [I>2sigma(I)]	R1 = 0.0493, wR2 = 0.1255
R indices (all data)	R1 = 0.0631, wR2 = 0.1454
Extinction coefficient	0.0014(3)
Largest diff. peak and hole	0.713 and -0.256 $e.Å^{-3}$
CCDC reference number	225923

Table 44. Atomic coordinates ($\times 10^4$) and equivalent isotropic displacement parameters ($Å^2 \times 10^3$) for **116**. U(eq) is defined as one third of the trace of the orthogonalised U_{ij} tensor.

	x	y	z	U(eq)
Ti	1307(1)	4727(1)	8637(1)	53(1)
Cl(1)	2699(2)	5708(1)	9147(1)	75(1)
Cl(2)	-1817(1)	4968(1)	8415(1)	72(1)
N(1)	2190(4)	4623(2)	7623(2)	52(1)
N(2)	2341(4)	3440(2)	6892(2)	52(1)
B	2412(5)	3876(2)	7564(2)	51(1)
C(1)	2447(5)	3634(2)	8452(2)	58(1)
C(2)	3661(6)	3958(2)	9077(2)	65(1)
C(3)	2651(7)	4055(3)	9721(2)	73(1)
C(4)	819(7)	3800(3)	9509(3)	73(1)
C(5)	691(6)	3525(2)	8747(2)	65(1)
C(6)	1383(3)	5739(1)	6955(1)	61(1)
C(7)	1831(4)	6266(1)	6451(2)	72(1)
C(8)	3460(4)	6213(1)	6089(2)	75(1)
C(9)	4642(3)	5633(1)	6231(2)	72(1)
C(10)	4194(3)	5107(1)	6736(2)	61(1)
C(11)	2565(3)	5160(1)	7098(1)	51(1)
Si(12)	800(2)	3604(1)	6024(1)	57(1)
C(13)	-1165(7)	4184(2)	6223(3)	76(1)
C(14)	2040(9)	4002(4)	5235(3)	98(2)
C(15)	-319(7)	2756(2)	5662(3)	80(1)
Si(16)	3748(2)	2681(1)	7005(1)	74(1)
C(17)	5935(7)	2885(3)	7680(4)	86(1)
C(18)	4543(8)	2444(4)	6040(5)	112(2)
C(19)	2452(9)	1952(3)	7417(5)	117(2)

Table 45. Anisotropic displacement parameters ($Å^2 \times 10^3$) for **116**. The anisotropic displacement factor exponent takes the form: $-2\pi^2[h^2 a^{*2} U_{11} + ... + 2 h k a^* b^* U_{12}]$.

	U_{11}	U_{22}	U_{33}	U_{23}	U_{13}	U_{12}
Ti	61(1)	52(1)	45(1)	2(1)	5(1)	-3(1)
Cl(1)	91(1)	67(1)	68(1)	-12(1)	10(1)	-17(1)
Cl(2)	63(1)	79(1)	74(1)	4(1)	10(1)	5(1)
N(1)	64(2)	47(2)	43(1)	3(1)	4(1)	0(1)
N(2)	54(2)	44(1)	60(2)	1(1)	6(1)	3(1)
B	48(2)	49(2)	56(2)	6(2)	3(2)	-1(2)
C(1)	65(2)	47(2)	59(2)	7(2)	2(2)	2(2)
C(2)	65(2)	69(2)	57(2)	12(2)	-4(2)	-1(2)
C(3)	91(3)	77(3)	48(2)	13(2)	-3(2)	3(2)
C(4)	83(3)	76(3)	61(2)	23(2)	16(2)	1(2)
C(5)	66(2)	59(2)	67(2)	16(2)	3(2)	-9(2)
C(6)	78(2)	49(2)	54(2)	-1(2)	5(2)	1(2)
C(7)	100(3)	49(2)	62(2)	8(2)	-5(2)	0(2)
C(8)	106(3)	63(2)	54(2)	9(2)	6(2)	-20(2)
C(9)	85(3)	74(3)	59(2)	4(2)	17(2)	-13(2)
C(10)	71(2)	53(2)	59(2)	2(2)	11(2)	-2(2)
C(11)	66(2)	44(2)	40(2)	1(1)	1(1)	-2(1)
Si(12)	65(1)	53(1)	52(1)	-4(1)	6(1)	-3(1)
C(13)	76(3)	65(2)	80(3)	-9(2)	-14(2)	12(2)
C(14)	113(4)	122(5)	60(2)	2(3)	14(2)	-39(3)
C(15)	79(3)	63(2)	95(3)	-20(2)	0(2)	-4(2)
Si(16)	58(1)	42(1)	117(1)	-5(1)	0(1)	4(1)
C(17)	64(2)	61(2)	128(4)	8(3)	-3(2)	9(2)
C(18)	75(3)	107(4)	153(5)	-61(4)	13(3)	16(3)
C(19)	95(4)	60(3)	186(7)	34(4)	-16(4)	-16(3)

Table 46. Bond lengths [Å] for **116**.

Ti-N(1)	1.941(3)	C(1)-C(2)	1.430(6)
Ti-Cl(1)	2.2385(12)	C(2)-C(3)	1.410(6)
Ti-Cl(2)	2.2553(13)	C(3)-C(4)	1.395(7)
Ti-C(1)	2.271(4)	C(4)-C(5)	1.404(7)
Ti-C(2)	2.281(4)	C(6)-C(7)	1.39
Ti-C(5)	2.343(4)	C(6)-C(11)	1.39
Ti-C(3)	2.362(4)	C(7)-C(8)	1.39
Ti-C(4)	2.372(4)	C(8)-C(9)	1.39
Ti-B	2.654(4)	C(9)-C(10)	1.39
N(1)-C(11)	1.413(3)	C(10)-C(11)	1.39
N(1)-B	1.436(5)	Si(12)-C(13)	1.849(5)
N(2)-B	1.419(5)	Si(12)-C(15)	1.871(5)
N(2)-Si(16)	1.755(3)	Si(12)-C(14)	1.873(5)
N(2)-Si(12)	1.764(3)	Si(16)-C(19)	1.858(6)
B-C(1)	1.595(5)	Si(16)-C(17)	1.860(5)
C(1)-C(5)	1.425(6)	Si(16)-C(18)	1.879(7)

Table 47. Bond angles [°] for **116**.

N(1)-Ti-Cl(1)	105.04(10)	C(1)-Ti-B	36.77(12)
N(1)-Ti-Cl(2)	107.19(10)	C(2)-Ti-B	64.36(13)
Cl(1)-Ti-Cl(2)	105.95(5)	C(5)-Ti-B	62.30(13)
N(1)-Ti-C(1)	67.47(13)	C(3)-Ti-B	95.32(15)
Cl(1)-Ti-C(1)	132.11(11)	C(4)-Ti-B	93.85(15)
Cl(2)-Ti-C(1)	121.65(11)	C(11)-N(1)-B	129.8(3)
N(1)-Ti-C(2)	85.59(14)	C(11)-N(1)-Ti	127.7(2)
Cl(1)-Ti-C(2)	97.81(12)	B-N(1)-Ti	102.5(2)
Cl(2)-Ti-C(2)	148.57(12)	B-N(2)-Si(16)	115.5(2)
C(1)-Ti-C(2)	36.60(15)	B-N(2)-Si(12)	122.7(2)
N(1)-Ti-C(5)	93.37(14)	Si(16)-N(2)-Si(12)	121.6(2)
Cl(1)-Ti-C(5)	149.40(11)	N(2)-B-N(1)	130.0(3)
Cl(2)-Ti-C(5)	91.19(11)	N(2)-B-C(1)	127.5(3)
C(1)-Ti-C(5)	35.93(14)	N(1)-B-C(1)	101.8(3)
C(2)-Ti-C(5)	58.9(2)	N(2)-B-Ti	160.4(3)
N(1)-Ti-C(3)	120.66(15)	N(1)-B-Ti	45.6(2)
Cl(1)-Ti-C(3)	91.63(13)	C(1)-B-Ti	58.4(2)
Cl(2)-Ti-C(3)	122.29(13)	C(5)-C(1)-C(2)	105.6(4)
C(1)-Ti-C(3)	59.9(2)	C(5)-C(1)-B	118.6(3)
C(2)-Ti-C(3)	35.3(2)	C(2)-C(1)-B	122.1(3)
C(5)-Ti-C(3)	57.8(2)	C(5)-C(1)-Ti	74.8(2)
N(1)-Ti-C(4)	125.8(2)	C(2)-C(1)-Ti	72.1(2)
Cl(1)-Ti-C(4)	117.77(13)	B-C(1)-Ti	84.8(2)
Cl(2)-Ti-C(4)	92.07(12)	C(3)-C(2)-C(1)	109.1(4)
C(1)-Ti-C(4)	59.4(2)	C(3)-C(2)-Ti	75.5(3)
C(2)-Ti-C(4)	58.2(2)	C(1)-C(2)-Ti	71.3(2)
C(5)-Ti-C(4)	34.6(2)	C(4)-C(3)-C(2)	107.7(4)
C(3)-Ti-C(4)	34.3(2)	C(4)-C(3)-Ti	73.2(2)
N(1)-Ti-B	31.90(12)	C(2)-C(3)-Ti	69.2(2)
Cl(1)-Ti-B	128.77(9)	C(3)-C(4)-C(5)	108.6(4)
Cl(2)-Ti-B	112.38(9)	C(3)-C(4)-Ti	72.5(2)
C(5)-C(4)-Ti	71.6(2)	N(2)-Si(12)-C(13)	110.6(2)
C(4)-C(5)-C(1)	108.9(4)	N(2)-Si(12)-C(15)	108.7(2)
C(4)-C(5)-Ti	73.8(2)	C(13)-Si(12)-C(15)	106.1(2)
C(1)-C(5)-Ti	69.3(2)	N(2)-Si(12)-C(14)	112.7(2)
C(7)-C(6)-C(11)	120.0	C(13)-Si(12)-C(14)	109.4(3)
C(6)-C(7)-C(8)	120.0	C(15)-Si(12)-C(14)	109.1(3)
C(7)-C(8)-C(9)	120.0	N(2)-Si(16)-C(19)	110.7(2)
C(10)-C(9)-C(8)	120.0	N(2)-Si(16)-C(17)	108.6(2)
C(9)-C(10)-C(11)	120.0	C(19)-Si(16)-C(17)	109.5(3)
C(10)-C(11)-C(6)	120.0	N(2)-Si(16)-C(18)	109.4(3)
C(10)-C(11)-N(1)	118.2(2)	C(19)-Si(16)-C(18)	112.3(4)
C(6)-C(11)-N(1)	121.8(2)	C(17)-Si(16)-C(18)	106.2(3)

Table 48. Crystal data and structure refinement for **117**.

Empirical formula	$C_{25}H_{37}BN_4Ti$
Formula weight	452.30
Temperature	203(2) K
Wavelength	0.71073 Å
Crystal system	Triclinic
Space group	P-1
Unit cell dimensions	a = 9.6645(10) Å
	b = 9.8449(13) Å
	c = 13.8532(14) Å
	α = 88.386(10)°
	β = 80.406(8)°
	γ = 75.145(9)°
Volume	1256.1(2) $Å^3$
Z	2
Density (calculated)	1.196 Mg/m^3
Absorption coefficient	0.359 mm^{-1}
F(000)	484
Crystal size	0.77 x 0.50 x 0.47 mm^3
Theta range for data collection	2.14 to 25.00°.
Index ranges	0<=h<=11, -11<=k<=11, -16<=l<=16
Reflections collected	4715
Independent reflections	4427 [R(int) = 0.0419]
Absorption correction	None
Refinement method	Full-matrix least-squares on F^2
Data / restraints / parameters	4145 / 0 / 272
Goodness-of-fit on F^2	1.016
Final R indices [I>2sigma(I)]	R1 = 0.0522, wR2 = 0.1318
R indices (all data)	R1 = 0.0743, wR2 = 0.1484
Largest diff. peak and hole	0.539 and -0.387 $e.Å^{-3}$
CCDC reference number	225924

Table 49. Atomic coordinates ($\times 10^4$) and equivalent isotropic displacement parameters ($Å^2 \times 10^3$) for **117**. U(eq) is defined as one third of the trace of the orthogonalised U_{ij} tensor.

	x	y	z	U(eq)
Ti	6971(1)	5770(1)	6925(1)	25(1)
B	8543(3)	3602(3)	7849(2)	28(1)
N(1)	7507(3)	3695(2)	7210(2)	30(1)
N(2)	9409(3)	2419(2)	8259(2)	30(1)
N(3)	7582(3)	6047(2)	5563(2)	33(1)
N(4)	4899(3)	6294(2)	7024(2)	33(1)
C(1)	8526(3)	5213(3)	8036(2)	30(1)
C(2)	9164(3)	6031(3)	7316(2)	32(1)
C(3)	8284(4)	7414(3)	7319(2)	36(1)
C(4)	7102(3)	7546(3)	8113(2)	34(1)
C(5)	7258(3)	6197(3)	8567(2)	30(1)
C(6)	6229(4)	6024(3)	9388(2)	38(1)
C(7)	5125(4)	7167(4)	9743(3)	49(1)
C(8)	4973(4)	8497(4)	9298(3)	52(1)
C(9)	5926(4)	8697(3)	8499(3)	45(1)
C(10)	8118(2)	1893(2)	5922(1)	41(1)
C(11)	7775(2)	841(2)	5433(1)	51(1)
C(12)	6441(3)	533(2)	5714(2)	51(1)
C(13)	5450(2)	1276(2)	6483(2)	56(1)
C(14)	5794(2)	2328(2)	6972(1)	41(1)
C(15)	7128(2)	2637(2)	6691(1)	30(1)
C(16)	10400(3)	2520(3)	8947(2)	37(1)
C(17)	9581(4)	3260(4)	9908(2)	46(1)
C(18)	11623(4)	3189(4)	8495(3)	55(1)
C(19)	9363(4)	964(3)	8048(2)	36(1)
C(20)	8759(5)	274(4)	8957(3)	57(1)
C(21)	10821(5)	71(4)	7553(4)	69(1)
C(22)	8602(4)	6728(3)	4981(2)	43(1)
C(23)	6962(4)	5297(4)	4919(2)	44(1)
C(24)	4173(4)	7428(4)	6439(3)	50(1)
C(25)	3853(4)	5916(4)	7800(3)	49(1)

Table 50. Anisotropic displacement parameters ($Å^2 \times 10^3$) for **117**. The anisotropic displacement factor exponent takes the form: $-2\pi^2[h^2 a^{*2} U_{11} + ... + 2 h k a^* b^* U_{12}]$.

	U_{11}	U_{22}	U_{33}	U_{23}	U_{13}	U_{12}
Ti	24(1)	24(1)	27(1)	-1(1)	0(1)	-7(1)
B	25(2)	29(1)	29(1)	-5(1)	2(1)	-9(1)
N(1)	32(1)	24(1)	35(1)	-1(1)	-6(1)	-9(1)
N(2)	30(1)	28(1)	32(1)	-3(1)	-6(1)	-5(1)
N(3)	32(1)	34(1)	31(1)	-1(1)	-1(1)	-10(1)
N(4)	25(1)	34(1)	38(1)	-2(1)	0(1)	-7(1)
C(1)	30(2)	31(1)	32(1)	-4(1)	-6(1)	-12(1)
C(2)	29(2)	37(1)	33(1)	-6(1)	1(1)	-14(1)
C(3)	43(2)	31(1)	36(1)	-1(1)	-1(1)	-19(1)
C(4)	35(2)	31(1)	36(1)	-7(1)	-2(1)	-12(1)
C(5)	33(2)	31(1)	28(1)	-4(1)	-4(1)	-13(1)
C(6)	45(2)	40(2)	31(1)	-5(1)	1(1)	-18(1)
C(7)	50(2)	53(2)	41(2)	-13(1)	11(2)	-19(2)
C(8)	49(2)	39(2)	59(2)	-22(2)	8(2)	-6(2)
C(9)	52(2)	29(1)	52(2)	-11(1)	1(2)	-10(1)
C(10)	49(2)	43(2)	37(2)	-1(1)	-6(1)	-20(2)
C(11)	75(3)	42(2)	37(2)	-8(1)	-12(2)	-17(2)
C(12)	68(3)	32(2)	64(2)	-2(1)	-36(2)	-16(2)
C(13)	44(2)	40(2)	91(3)	3(2)	-26(2)	-19(2)
C(14)	34(2)	32(1)	60(2)	-1(1)	-9(1)	-11(1)
C(15)	35(2)	22(1)	35(1)	6(1)	-13(1)	-9(1)
C(16)	33(2)	37(1)	43(2)	-1(1)	-13(1)	-8(1)
C(17)	62(2)	44(2)	37(2)	-3(1)	-16(2)	-16(2)
C(18)	38(2)	65(2)	69(2)	6(2)	-17(2)	-21(2)
C(19)	37(2)	28(1)	41(2)	-7(1)	-13(1)	-2(1)
C(20)	74(3)	44(2)	63(2)	4(2)	-17(2)	-30(2)
C(21)	56(3)	53(2)	84(3)	-29(2)	0(2)	5(2)
C(22)	51(2)	42(2)	35(2)	1(1)	7(1)	-18(2)
C(23)	46(2)	54(2)	33(2)	-4(1)	-5(1)	-17(2)
C(24)	37(2)	41(2)	66(2)	1(2)	-10(2)	0(1)
C(25)	36(2)	56(2)	54(2)	-1(2)	4(2)	-17(2)

Table 51. Bond lengths [Å] for **117**.

Ti-N(3)	1.915(2)	C(1)-C(5)	1.454(4)
Ti-N(4)	1.918(3)	C(2)-C(3)	1.408(4)
Ti-N(1)	2.020(2)	C(3)-C(4)	1.430(4)
Ti-C(1)	2.286(3)	C(4)-C(9)	1.425(4)
Ti-C(2)	2.350(3)	C(4)-C(5)	1.436(4)
Ti-C(5)	2.397(3)	C(5)-C(6)	1.418(4)
Ti-C(3)	2.422(3)	C(6)-C(7)	1.374(5)
Ti-C(4)	2.475(3)	C(7)-C(8)	1.415(5)
Ti-B	2.708(3)	C(8)-C(9)	1.362(5)
B-N(2)	1.414(4)	C(10)-C(11)	1.39
B-N(1)	1.428(4)	C(10)-C(15)	1.39
B-C(1)	1.610(4)	C(11)-C(12)	1.39
N(1)-C(15)	1.436(3)	C(12)-C(13)	1.39
N(2)-C(16)	1.482(4)	C(13)-C(14)	1.39
N(2)-C(19)	1.483(4)	C(14)-C(15)	1.39
N(3)-C(22)	1.454(4)	C(16)-C(17)	1.529(4)
N(3)-C(23)	1.464(4)	C(16)-C(18)	1.534(5)
N(4)-C(25)	1.457(4)	C(19)-C(20)	1.515(5)
N(4)-C(24)	1.460(4)	C(19)-C(21)	1.518(5)
C(1)-C(2)	1.424(4)		

Table 52. Bond angles [°] for **117**.

N(3)-Ti-N(4)	101.72(11)	C(1)-Ti-B	36.37(9)
N(3)-Ti-N(1)	109.35(10)	C(2)-Ti-B	63.18(10)
N(4)-Ti-N(1)	105.61(10)	C(5)-Ti-B	62.89(9)
N(3)-Ti-C(1)	123.58(11)	C(3)-Ti-B	94.00(10)
N(4)-Ti-C(1)	134.29(10)	C(4)-Ti-B	93.54(10)
N(1)-Ti-C(1)	67.28(10)	N(2)-B-N(1)	130.6(3)
N(3)-Ti-C(2)	91.70(11)	N(2)-B-C(1)	125.4(3)
N(4)-Ti-C(2)	152.96(10)	N(1)-B-C(1)	104.0(2)
N(1)-Ti-C(2)	91.58(10)	N(2)-B-Ti	175.5(2)
C(1)-Ti-C(2)	35.74(10)	N(1)-B-Ti	46.80(13)
N(3)-Ti-C(5)	145.79(11)	C(1)-B-Ti	57.40(14)
N(4)-Ti-C(5)	101.62(10)	B-N(1)-C(15)	131.8(2)
N(1)-Ti-C(5)	87.87(9)	B-N(1)-Ti	102.2(2)
C(1)-Ti-C(5)	36.07(10)	C(15)-N(1)-Ti	124.7(2)
C(2)-Ti-C(5)	57.52(10)	B-N(2)-C(16)	123.5(2)
N(3)-Ti-C(3)	89.15(10)	B-N(2)-C(19)	122.1(2)
N(4)-Ti-C(3)	121.63(11)	C(16)-N(2)-C(19)	114.4(2)
N(1)-Ti-C(3)	124.45(11)	C(22)-N(3)-C(23)	109.8(2)
C(1)-Ti-C(3)	59.27(10)	C(22)-N(3)-Ti	136.7(2)
C(2)-Ti-C(3)	34.29(11)	C(23)-N(3)-Ti	113.3(2)
C(5)-Ti-C(3)	57.22(10)	C(25)-N(4)-C(24)	110.5(3)
N(3)-Ti-C(4)	118.17(10)	C(25)-N(4)-Ti	126.7(2)
N(4)-Ti-C(4)	96.34(11)	C(24)-N(4)-Ti	121.2(2)
N(1)-Ti-C(4)	121.56(10)	C(2)-C(1)-C(5)	105.1(2)
C(1)-Ti-C(4)	59.01(10)	C(2)-C(1)-B	123.0(2)
C(2)-Ti-C(4)	56.64(10)	C(5)-C(1)-B	121.7(2)
C(5)-Ti-C(4)	34.23(10)	C(2)-C(1)-Ti	74.6(2)
C(3)-Ti-C(4)	33.94(10)	C(5)-C(1)-Ti	76.1(2)
N(3)-Ti-B	119.39(10)	B-C(1)-Ti	86.2(2)
N(4)-Ti-B	126.02(10)	C(3)-C(2)-C(1)	110.8(3)
N(1)-Ti-B	31.02(10)	C(3)-C(2)-Ti	75.7(2)
C(1)-C(2)-Ti	69.7(2)	C(6)-C(7)-C(8)	121.7(3)
C(2)-C(3)-C(4)	107.7(3)	C(9)-C(8)-C(7)	121.1(3)
C(2)-C(3)-Ti	70.0(2)	C(8)-C(9)-C(4)	119.2(3)
C(4)-C(3)-Ti	75.1(2)	C(11)-C(10)-C(15)	120.0
C(9)-C(4)-C(3)	133.0(3)	C(10)-C(11)-C(12)	120.0
C(9)-C(4)-C(5)	119.7(3)	C(13)-C(12)-C(11)	120.0
C(3)-C(4)-C(5)	107.3(3)	C(12)-C(13)-C(14)	120.0
C(9)-C(4)-Ti	125.0(2)	C(15)-C(14)-C(13)	120.0
C(3)-C(4)-Ti	71.0(2)	C(14)-C(15)-C(10)	120.0
C(5)-C(4)-Ti	69.91(15)	C(14)-C(15)-N(1)	120.3(2)
C(6)-C(5)-C(4)	119.5(3)	C(10)-C(15)-N(1)	119.6(2)
C(6)-C(5)-C(1)	131.6(3)	N(2)-C(16)-C(17)	112.1(3)
C(4)-C(5)-C(1)	108.9(2)	N(2)-C(16)-C(18)	113.3(3)
C(6)-C(5)-Ti	121.9(2)	C(17)-C(16)-C(18)	111.1(3)
C(4)-C(5)-Ti	75.9(2)	N(2)-C(19)-C(20)	111.6(3)
C(1)-C(5)-Ti	67.80(15)	N(2)-C(19)-C(21)	112.5(3)
C(7)-C(6)-C(5)	118.8(3)	C(20)-C(19)-C(21)	111.9(3)

Table 53. Crystal data and structure refinement for **120**.

Empirical formula	$C_{21}H_{35}BN_4Zr$
Formula weight	445.56
Temperature	173(2) K
Wavelength	0.71073 Å
Crystal system	Triclinic
Space group	P-1
Unit cell dimensions	a = 9.4986(8) Å
	b = 9.7515(8) Å
	c = 13.8010(11) Å
	α = 101.5630(10)°
	β = 103.7000(10)°
	γ = 102.6290(10)°
Volume	1168.23(17) $Å^3$
Z	2
Density (calculated)	1.267 Mg/m^3
Absorption coefficient	0.482 mm^{-1}
F(000)	468
Crystal size	0.24 x 0.24 x 0.16 mm^3
q range for data collection	1.58 to 26.18°
Index ranges	-11<=h<=11, -12<=k<=12, -17<=l<=17
Reflections collected	24671
Independent reflections	4659 [R_{int} = 0.0271]
Completeness to q = 26.18°	99.8 %
Absorption correction	Semi-empirical from equivalents
Refinement method	Full-matrix least-squares on F^2
Data / restraints / parameters	4659 / 0 / 244
Goodness-of-fit on F^2	S = 1.086
R indices [for 4427 reflections with I>2s(I)]	R_1 = 0.0315, wR_2 = 0.0916
R indices (for all 4659 data)	R_1 = 0.0328, wR_2 = 0.0927
Largest diff. peak and hole	0.655 and -0.513 $eÅ^{-3}$
CCDC reference number	278300

Table 54. Atomic coordinates ($\times 10^4$) and equivalent isotropic displacement parameters ($Å^2 \times 10^3$) for **120**. U(eq) is defined as one third of the trace of the orthogonalised U_{ij} tensor.

	x	y	z	U(eq)
Zr(1)	-195(1)	3048(1)	7005(1)	24(1)
N(1)	2221(2)	3917(2)	7441(1)	27(1)
B(1)	2486(3)	5364(3)	8077(2)	26(1)
N(2)	3831(2)	6500(2)	8555(1)	28(1)
N(3)	-756(2)	1019(2)	7261(2)	34(1)
N(4)	-1114(2)	2818(2)	5475(1)	33(1)
C(1)	852(2)	5469(2)	8175(2)	29(1)
C(2)	73(3)	4596(3)	8705(2)	34(1)
C(3)	-1498(3)	4206(3)	8212(2)	39(1)
C(4)	-1722(3)	4842(3)	7385(2)	37(1)
C(5)	-297(2)	5636(2)	7370(2)	32(1)
C(11)	3152(2)	3242(2)	6968(2)	27(1)
C(10)	3544(3)	3619(3)	6128(2)	37(1)
C(9)	4415(3)	2916(3)	5642(2)	45(1)
C(8)	4912(3)	1829(3)	5983(2)	48(1)
C(7)	4525(3)	1435(3)	6810(3)	51(1)
C(6)	3642(3)	2124(3)	7297(2)	39(1)
C(15)	3866(3)	7954(2)	9158(2)	32(1)
C(17)	3374(3)	7885(3)	10128(2)	45(1)
C(16)	2990(3)	8746(3)	8503(2)	45(1)
C(12)	5318(2)	6355(2)	8478(2)	31(1)
C(13)	6452(3)	6593(3)	9532(2)	45(1)
C(14)	5963(3)	7337(3)	7868(2)	43(1)
C(18)	-276(4)	758(3)	8277(3)	58(1)
C(19)	-1913(3)	-246(3)	6545(2)	43(1)
C(20)	-2035(3)	3425(4)	4784(2)	52(1)
C(21)	-480(3)	1802(3)	4911(2)	44(1)

Table 55. Anisotropic displacement parameters ($Å^2 \times 10^3$) for **120**. The anisotropic displacement factor exponent takes the form: $-2\pi^2[h^2 a^{*2} U_{11} + ... + 2 h k a^* b^* U_{12}]$.

	U_{11}	U_{22}	U_{33}	U_{23}	U_{13}	U_{12}
Zr(1)	22(1)	22(1)	27(1)	4(1)	7(1)	4(1)
N(1)	22(1)	23(1)	34(1)	4(1)	9(1)	5(1)
B(1)	26(1)	25(1)	28(1)	6(1)	8(1)	7(1)
N(2)	25(1)	23(1)	32(1)	4(1)	9(1)	4(1)
N(3)	29(1)	27(1)	45(1)	12(1)	10(1)	6(1)
N(4)	33(1)	40(1)	29(1)	10(1)	11(1)	16(1)
C(1)	28(1)	23(1)	32(1)	-1(1)	12(1)	4(1)
C(2)	34(1)	38(1)	28(1)	3(1)	13(1)	8(1)
C(3)	32(1)	40(1)	42(1)	1(1)	21(1)	3(1)
C(4)	26(1)	37(1)	44(1)	-2(1)	10(1)	11(1)
C(5)	32(1)	27(1)	39(1)	6(1)	14(1)	11(1)
C(11)	21(1)	23(1)	29(1)	-1(1)	4(1)	3(1)
C(10)	34(1)	42(1)	38(1)	11(1)	11(1)	15(1)
C(9)	33(1)	62(2)	36(1)	3(1)	14(1)	11(1)
C(8)	30(1)	44(1)	59(2)	-13(1)	13(1)	10(1)
C(7)	43(2)	34(1)	80(2)	11(1)	20(1)	21(1)
C(6)	39(1)	32(1)	52(1)	13(1)	17(1)	14(1)
C(15)	30(1)	23(1)	38(1)	0(1)	10(1)	3(1)
C(17)	47(2)	40(1)	40(1)	-5(1)	18(1)	1(1)
C(16)	47(2)	25(1)	58(2)	6(1)	10(1)	10(1)
C(12)	25(1)	24(1)	38(1)	2(1)	7(1)	4(1)
C(13)	34(1)	44(1)	48(2)	6(1)	1(1)	11(1)
C(14)	38(1)	41(1)	55(2)	12(1)	23(1)	7(1)
C(18)	60(2)	49(2)	62(2)	27(1)	3(2)	11(1)
C(19)	43(1)	29(1)	55(2)	6(1)	20(1)	3(1)
C(20)	52(2)	83(2)	41(1)	30(1)	21(1)	38(2)
C(21)	48(2)	48(2)	35(1)	4(1)	13(1)	21(1)

Table 56. Bond lengths [Å] for **120**.

Zr(1)-N(4)	2.0314(19)	N(4)-C(20)	1.444(3)
Zr(1)-N(3)	2.0570(19)	N(4)-C(21)	1.457(3)
Zr(1)-N(1)	2.1531(17)	C(1)-C(5)	1.424(3)
Zr(1)-C(1)	2.420(2)	C(1)-C(2)	1.427(3)
Zr(1)-C(2)	2.444(2)	C(2)-C(3)	1.414(3)
Zr(1)-C(5)	2.501(2)	C(3)-C(4)	1.401(4)
Zr(1)-C(3)	2.533(2)	C(4)-C(5)	1.412(3)
Zr(1)-C(4)	2.559(2)	C(11)-C(6)	1.390(3)
Zr(1)-C(21)	2.825(3)	C(11)-C(10)	1.390(3)
Zr(1)-B(1)	2.852(2)	C(10)-C(9)	1.389(4)
N(1)-C(11)	1.414(3)	C(9)-C(8)	1.372(4)
N(1)-B(1)	1.438(3)	C(8)-C(7)	1.377(4)
B(1)-N(2)	1.408(3)	C(7)-C(6)	1.393(4)
B(1)-C(1)	1.614(3)	C(15)-C(16)	1.521(3)
N(2)-C(12)	1.476(3)	C(15)-C(17)	1.527(3)
N(2)-C(15)	1.482(3)	C(12)-C(14)	1.521(3)
N(3)-C(19)	1.452(3)	C(12)-C(13)	1.530(3)
N(3)-C(18)	1.458(4)		

Table 57. Bond angles [°] for **120**.

N(4)-Zr(1)-N(3)	107.51(8)	N(2)-B(1)-N(1)	130.8(2)
N(4)-Zr(1)-N(1)	110.48(7)	N(2)-B(1)-C(1)	124.14(19)
N(3)-Zr(1)-N(1)	110.27(7)	N(1)-B(1)-C(1)	105.08(18)
N(4)-Zr(1)-C(1)	119.29(8)	N(2)-B(1)-Zr(1)	176.86(16)
N(3)-Zr(1)-C(1)	132.02(8)	N(1)-B(1)-Zr(1)	47.25(10)
N(1)-Zr(1)-C(1)	63.73(7)	C(1)-B(1)-Zr(1)	57.96(10)
N(4)-Zr(1)-C(2)	140.96(8)	B(1)-N(2)-C(12)	122.88(18)
N(3)-Zr(1)-C(2)	100.43(8)	B(1)-N(2)-C(15)	122.73(18)
N(1)-Zr(1)-C(2)	83.71(7)	C(12)-N(2)-C(15)	114.38(17)
C(1)-Zr(1)-C(2)	34.11(8)	C(19)-N(3)-C(18)	110.6(2)
N(4)-Zr(1)-C(5)	89.11(8)	C(19)-N(3)-Zr(1)	125.13(17)
N(3)-Zr(1)-C(5)	149.19(8)	C(18)-N(3)-Zr(1)	123.02(17)
N(1)-Zr(1)-C(5)	86.57(7)	C(20)-N(4)-C(21)	111.3(2)
C(1)-Zr(1)-C(5)	33.58(8)	C(20)-N(4)-Zr(1)	141.28(17)
C(2)-Zr(1)-C(5)	54.55(8)	C(21)-N(4)-Zr(1)	107.02(15)
N(4)-Zr(1)-C(3)	116.03(8)	C(5)-C(1)-C(2)	105.4(2)
N(3)-Zr(1)-C(3)	95.45(8)	C(5)-C(1)-B(1)	124.00(19)
N(1)-Zr(1)-C(3)	115.72(7)	C(2)-C(1)-B(1)	121.1(2)
C(1)-Zr(1)-C(3)	55.78(7)	C(5)-C(1)-Zr(1)	76.35(12)
C(2)-Zr(1)-C(3)	32.95(8)	C(2)-C(1)-Zr(1)	73.89(12)
C(5)-Zr(1)-C(3)	53.74(8)	B(1)-C(1)-Zr(1)	87.63(12)
N(4)-Zr(1)-C(4)	88.03(8)	C(3)-C(2)-C(1)	109.4(2)
N(3)-Zr(1)-C(4)	120.31(8)	C(3)-C(2)-Zr(1)	76.98(13)
N(1)-Zr(1)-C(4)	117.20(7)	C(1)-C(2)-Zr(1)	72.01(12)
C(1)-Zr(1)-C(4)	55.33(7)	C(4)-C(3)-C(2)	107.7(2)
C(2)-Zr(1)-C(4)	53.98(8)	C(4)-C(3)-Zr(1)	75.04(13)
C(5)-Zr(1)-C(4)	32.38(7)	C(2)-C(3)-Zr(1)	70.07(13)
C(3)-Zr(1)-C(4)	31.93(9)	C(3)-C(4)-C(5)	108.0(2)
N(4)-Zr(1)-C(21)	29.55(7)	C(3)-C(4)-Zr(1)	73.03(13)
N(3)-Zr(1)-C(21)	91.34(8)	C(5)-C(4)-Zr(1)	71.58(12)
N(1)-Zr(1)-C(21)	94.55(7)	C(4)-C(5)-C(1)	109.4(2)
C(1)-Zr(1)-C(21)	135.25(8)	C(4)-C(5)-Zr(1)	76.04(13)
C(2)-Zr(1)-C(21)	167.99(8)	C(1)-C(5)-Zr(1)	70.07(12)
C(5)-Zr(1)-C(21)	113.54(8)	C(6)-C(11)-C(10)	117.9(2)
C(3)-Zr(1)-C(21)	144.06(8)	C(6)-C(11)-N(1)	120.7(2)
C(4)-Zr(1)-C(21)	117.58(8)	C(10)-C(11)-N(1)	121.3(2)
N(4)-Zr(1)-B(1)	117.71(8)	C(9)-C(10)-C(11)	121.1(2)
N(3)-Zr(1)-B(1)	127.11(7)	C(8)-C(9)-C(10)	120.6(3)
N(1)-Zr(1)-B(1)	29.38(7)	C(9)-C(8)-C(7)	119.1(2)
C(1)-Zr(1)-B(1)	34.42(7)	C(8)-C(7)-C(6)	120.9(3)
C(2)-Zr(1)-B(1)	59.42(7)	C(11)-C(6)-C(7)	120.5(2)
C(5)-Zr(1)-B(1)	59.72(7)	N(2)-C(15)-C(16)	112.59(19)
C(3)-Zr(1)-B(1)	88.54(7)	N(2)-C(15)-C(17)	112.37(19)
C(4)-Zr(1)-B(1)	88.34(7)	C(16)-C(15)-C(17)	111.8(2)
C(21)-Zr(1)-B(1)	114.88(8)	N(2)-C(12)-C(14)	111.84(18)
C(11)-N(1)-B(1)	131.99(18)	N(2)-C(12)-C(13)	113.0(2)
C(11)-N(1)-Zr(1)	123.15(13)	C(14)-C(12)-C(13)	111.0(2)
B(1)-N(1)-Zr(1)	103.37(13)	N(4)-C(21)-Zr(1)	43.44(10)

Table 58. Crystal data and structure refinement for **121**.

Empirical formula	$C_{21}H_{35}BHfN_4$
Formula weight	532.83
Temperature	173(2) K
Wavelength	0.71073 Å
Crystal system	Triclinic
Space group	P-1
Unit cell dimensions	a = 9.4684(11) Å
	b = 9.8068(13) Å
	c = 13.8449(19) Å
	α = 101.509(2)°
	β = 103.455(2)°
	γ = 102.932(3)°
Volume	1174.9(3) Å^3
Z	2
Density (calculated)	1.506 Mg/m^3
Absorption coefficient	4.451 mm^{-1}
F(000)	532
Crystal size	0.34 x 0.24 x 0.21 mm
q range for data collection	1.57 to 26.06°
Index ranges	-11<=h<=11, -12<=k<=12, -17<=l<=17
Reflections collected	13292
Independent reflections	4628 [R_{int} = 0.0200]
Completeness to q = 26.06°	99.6 %
Absorption correction	Semi-empirical from equivalents
Max. and min. transmission	0.39 and 0.2651
Refinement method	Full-matrix least-squares on F^2
Data / restraints / parameters	4628 / 0 / 252
Goodness-of-fit on F^2	S = 1.065
R indices [for 4491 reflections with I>2s(I)]	R_1 = 0.0153, wR_2 = 0.0390
R indices (for all 4628 data)	R_1 = 0.0159, wR_2 = 0.0393
Largest diff. peak and hole	0.653 and -0.361 eÅ^{-3}
CCDC reference number	278304

Table 59. Atomic coordinates ($\times 10^4$) and equivalent isotropic displacement parameters ($Å^2 \times 10^3$) for **121**. U(eq) is defined as one third of the trace of the orthogonalised U_{ij} tensor.

	x	y	z	U(eq)
Hf(1)	5210(1)	6905(1)	7990(1)	25(1)
N(1)	2816(2)	6071(2)	7567(2)	28(1)
N(2)	1173(2)	3499(2)	6447(1)	28(1)
N(4)	5746(2)	8924(2)	7755(2)	35(1)
N(3)	6090(2)	7179(2)	9517(2)	33(1)
C(15)	1133(3)	2045(2)	5841(2)	33(1)
C(1)	4166(3)	4513(2)	6822(2)	30(1)
C(2)	5306(3)	4341(2)	7625(2)	33(1)
C(11)	1876(2)	6739(2)	8033(2)	28(1)
C(5)	4959(3)	5399(3)	6304(2)	36(1)
C(3)	6743(3)	5152(3)	7618(2)	38(1)
C(4)	6528(3)	5797(3)	6800(2)	40(1)
C(6)	1486(3)	6374(3)	8879(2)	39(1)
B(1)	2536(3)	4627(3)	6924(2)	28(1)
C(18)	5475(3)	8191(3)	10102(2)	46(1)
C(10)	1376(3)	7841(3)	7697(2)	40(1)
C(20)	6917(3)	10185(3)	8461(2)	46(1)
C(16)	2000(3)	1248(3)	6489(2)	48(1)
C(12)	-314(3)	3640(2)	6536(2)	32(1)
C(7)	615(3)	7075(3)	9362(2)	47(1)
C(14)	-967(3)	2653(3)	7142(2)	46(1)
C(13)	-1450(3)	3411(3)	5485(2)	47(1)
C(8)	108(3)	8148(3)	9010(2)	49(1)
C(19)	7020(4)	6568(4)	10200(2)	54(1)
C(17)	1622(3)	2120(3)	4872(2)	47(1)
C(9)	498(3)	8530(3)	8180(3)	53(1)
C(21)	5219(4)	9207(4)	6759(3)	62(1)

Table 60. Anisotropic displacement parameters ($Å^2 \times 10^3$) for **121**. The anisotropic displacement factor exponent takes the form: $-2\pi^2[h^2 a^{*2} U_{11} + ... + 2 h k a^* b^* U_{12}]$.

	U_{11}	U_{22}	U_{33}	U_{23}	U_{13}	U_{12}
Hf(1)	22(1)	23(1)	28(1)	4(1)	7(1)	5(1)
N(1)	24(1)	24(1)	34(1)	4(1)	9(1)	6(1)
N(2)	26(1)	23(1)	34(1)	3(1)	9(1)	6(1)
N(4)	31(1)	29(1)	44(1)	14(1)	9(1)	6(1)
N(3)	33(1)	41(1)	28(1)	10(1)	9(1)	16(1)
C(15)	30(1)	23(1)	38(1)	-1(1)	9(1)	3(1)
C(1)	28(1)	24(1)	33(1)	-2(1)	10(1)	5(1)
C(2)	32(1)	28(1)	42(1)	5(1)	15(1)	13(1)
C(11)	21(1)	23(1)	33(1)	0(1)	4(1)	3(1)
C(5)	36(1)	39(1)	30(1)	2(1)	13(1)	7(1)
C(3)	25(1)	40(1)	45(1)	-1(1)	9(1)	13(1)
C(4)	33(1)	41(1)	44(1)	1(1)	23(1)	4(1)
C(6)	35(1)	46(1)	39(1)	13(1)	10(1)	15(1)
B(1)	27(1)	27(1)	29(1)	6(1)	8(1)	7(1)
C(18)	51(2)	52(2)	39(1)	6(1)	14(1)	23(1)
C(10)	39(1)	36(1)	51(2)	14(1)	17(1)	16(1)
C(20)	45(2)	31(1)	57(2)	7(1)	18(1)	1(1)
C(16)	49(2)	27(1)	60(2)	5(1)	8(1)	11(1)
C(12)	25(1)	28(1)	39(1)	2(1)	9(1)	5(1)
C(7)	34(1)	64(2)	37(1)	1(1)	13(1)	10(1)
C(14)	39(1)	44(2)	58(2)	12(1)	24(1)	7(1)
C(13)	35(1)	49(2)	49(2)	5(1)	0(1)	13(1)
C(8)	30(1)	47(2)	60(2)	-13(1)	14(1)	12(1)
C(19)	53(2)	86(2)	42(2)	31(2)	21(1)	39(2)
C(17)	47(2)	41(1)	40(2)	-7(1)	17(1)	2(1)
C(9)	45(2)	39(2)	78(2)	10(1)	18(2)	22(1)
C(21)	59(2)	56(2)	64(2)	30(2)	0(2)	11(2)

Table 61. Bond lengths [Å] for **121**.

Hf(1)-N(3)	2.0225(19)	N(3)-C(18)	1.462(3)
Hf(1)-N(4)	2.0415(19)	C(15)-C(16)	1.522(4)
Hf(1)-N(1)	2.1236(18)	C(15)-C(17)	1.527(4)
Hf(1)-C(1)	2.408(2)	C(1)-C(2)	1.424(3)
Hf(1)-C(5)	2.429(2)	C(1)-C(5)	1.428(3)
Hf(1)-C(2)	2.490(2)	C(1)-B(1)	1.608(3)
Hf(1)-C(4)	2.510(2)	C(2)-C(3)	1.417(3)
Hf(1)-C(3)	2.537(2)	C(11)-C(10)	1.391(3)
Hf(1)-B(1)	2.826(3)	C(11)-C(6)	1.395(3)
N(1)-C(11)	1.414(3)	C(5)-C(4)	1.410(4)
N(1)-B(1)	1.444(3)	C(3)-C(4)	1.400(4)
N(2)-B(1)	1.414(3)	C(6)-C(7)	1.389(4)
N(2)-C(12)	1.475(3)	C(10)-C(9)	1.387(4)
N(2)-C(15)	1.491(3)	C(12)-C(14)	1.523(4)
N(4)-C(20)	1.454(3)	C(12)-C(13)	1.535(3)
N(4)-C(21)	1.457(4)	C(7)-C(8)	1.377(4)
N(3)-C(19)	1.450(3)	C(8)-C(9)	1.381(5)

Table 62. Bond angles [°] for **121**.

N(3)-Hf(1)-N(4)	105.96(8)	C(20)-N(4)-Hf(1)	125.53(17)
N(3)-Hf(1)-N(1)	109.79(8)	C(21)-N(4)-Hf(1)	123.06(18)
N(4)-Hf(1)-N(1)	108.92(7)	C(19)-N(3)-C(18)	110.6(2)
N(3)-Hf(1)-C(1)	120.91(8)	C(19)-N(3)-Hf(1)	139.06(18)
N(4)-Hf(1)-C(1)	132.37(8)	C(18)-N(3)-Hf(1)	109.97(16)
N(1)-Hf(1)-C(1)	64.40(7)	N(2)-C(15)-C(16)	112.8(2)
N(3)-Hf(1)-C(5)	143.02(9)	N(2)-C(15)-C(17)	112.2(2)
N(4)-Hf(1)-C(5)	100.80(9)	C(16)-C(15)-C(17)	112.2(2)
N(1)-Hf(1)-C(5)	84.40(8)	C(2)-C(1)-C(5)	105.6(2)
C(1)-Hf(1)-C(5)	34.35(8)	C(2)-C(1)-B(1)	123.6(2)
N(3)-Hf(1)-C(2)	90.73(8)	C(5)-C(1)-B(1)	120.7(2)
N(4)-Hf(1)-C(2)	150.38(8)	C(2)-C(1)-Hf(1)	76.30(13)
N(1)-Hf(1)-C(2)	87.22(7)	C(5)-C(1)-Hf(1)	73.63(13)
C(1)-Hf(1)-C(2)	33.75(8)	B(1)-C(1)-Hf(1)	87.08(13)
C(5)-Hf(1)-C(2)	54.99(9)	C(3)-C(2)-C(1)	109.0(2)
N(3)-Hf(1)-C(4)	117.64(8)	C(3)-C(2)-Hf(1)	75.48(14)
N(4)-Hf(1)-C(4)	96.07(9)	C(1)-C(2)-Hf(1)	69.95(12)
N(1)-Hf(1)-C(4)	116.66(8)	C(10)-C(11)-C(6)	117.7(2)
C(1)-Hf(1)-C(4)	56.20(8)	C(10)-C(11)-N(1)	120.9(2)
C(5)-Hf(1)-C(4)	33.13(8)	C(6)-C(11)-N(1)	121.2(2)
C(2)-Hf(1)-C(4)	54.31(8)	C(4)-C(5)-C(1)	109.5(2)
N(3)-Hf(1)-C(3)	89.66(8)	C(4)-C(5)-Hf(1)	76.61(14)
N(4)-Hf(1)-C(3)	121.22(8)	C(1)-C(5)-Hf(1)	72.01(13)
N(1)-Hf(1)-C(3)	118.21(8)	C(4)-C(3)-C(2)	108.2(2)
C(1)-Hf(1)-C(3)	55.69(8)	C(4)-C(3)-Hf(1)	72.82(14)
C(5)-Hf(1)-C(3)	54.33(9)	C(2)-C(3)-Hf(1)	71.80(13)
C(2)-Hf(1)-C(3)	32.72(8)	C(3)-C(4)-C(5)	107.7(2)
C(4)-Hf(1)-C(3)	32.21(9)	C(3)-C(4)-Hf(1)	74.97(14)
N(3)-Hf(1)-B(1)	118.28(8)	C(5)-C(4)-Hf(1)	70.26(13)
N(4)-Hf(1)-B(1)	126.49(8)	C(7)-C(6)-C(11)	121.1(2)
N(1)-Hf(1)-B(1)	29.84(7)	N(2)-B(1)-N(1)	130.6(2)
C(1)-Hf(1)-B(1)	34.63(7)	N(2)-B(1)-C(1)	124.2(2)
C(5)-Hf(1)-B(1)	59.77(8)	N(1)-B(1)-C(1)	105.19(18)
C(2)-Hf(1)-B(1)	60.00(7)	N(2)-B(1)-Hf(1)	176.53(17)
C(4)-Hf(1)-B(1)	89.11(8)	N(1)-B(1)-Hf(1)	47.03(10)
C(3)-Hf(1)-B(1)	88.91(8)	C(1)-B(1)-Hf(1)	58.29(11)
C(11)-N(1)-B(1)	131.59(19)	C(9)-C(10)-C(11)	120.8(3)
C(11)-N(1)-Hf(1)	123.89(14)	N(2)-C(12)-C(14)	112.16(19)
B(1)-N(1)-Hf(1)	103.13(14)	N(2)-C(12)-C(13)	112.5(2)
B(1)-N(2)-C(12)	123.16(18)	C(14)-C(12)-C(13)	111.2(2)
B(1)-N(2)-C(15)	122.35(19)	C(8)-C(7)-C(6)	120.5(3)
C(12)-N(2)-C(15)	114.45(17)	C(7)-C(8)-C(9)	119.0(2)
C(20)-N(4)-C(21)	110.2(2)	C(8)-C(9)-C(10)	120.9(3)

Table 63. Crystal data and structure refinement for **122**.

Empirical formula	$C_{25}H_{37}BN_4Zr$
Formula weight	495.62
Temperature	193(2) K
Wavelength	0.71073 Å
Crystal system	Triclinic
Space group	P-1
Unit cell dimensions	a = 9.735(2) Å
	b = 9.947(2) Å
	c = 13.809(3) Å
	α = 88.482(4)°
	β = 80.798(5)°
	γ = 75.240(4)°
Volume	1276.3(5) $Å^3$
Z	2
Density (calculated)	1.290 Mg/m^3
Absorption coefficient	0.449 mm^{-1}
F(000)	520
Crystal size	0.25 x 0.25 x 0.15 mm
q range for data collection	2.12 to 27.53°
Index ranges	-12<=h<=12, -12<=k<=12, -17<=l<=17
Reflections collected	12377
Independent reflections	5821 [R_{int} = 0.0182]
Completeness to q = 27.53°	98.9 %
Absorption correction	Semi-empirical from equivalents
Max. and min. transmission	0.94 and 0.758
Refinement method	Full-matrix least-squares on F^2
Data / restraints / parameters	5821 / 0 / 287
Goodness-of-fit on F^2	S = 1.045
R indices [for 5477 reflections with I>2s(I)]	R_1 = 0.0281, wR_2 = 0.0728
R indices (for all 5821 data)	R_1 = 0.0301, wR_2 = 0.0741
Largest diff. peak and hole	0.497 and -0.263 $eÅ^{-3}$
CCDC reference number	278301

Table 64. Atomic coordinates ($\times 10^4$) and equivalent isotropic displacement parameters ($Å^2 \times 10^3$) for **122**. U(eq) is defined as one third of the trace of the orthogonalised U_{ij} tensor.

	x	y	z	U(eq)
Zr	6880(1)	5802(1)	6889(1)	29(1)
B	8545(2)	3582(2)	7869(1)	31(1)
N(4)	7607(2)	6135(2)	5460(1)	37(1)
N(3)	4684(2)	6386(2)	7028(1)	38(1)
N(1)	7518(2)	3640(1)	7210(1)	33(1)
N(2)	9388(1)	2422(1)	8289(1)	33(1)
C(1)	8537(2)	5172(2)	8057(1)	32(1)
C(2)	9198(2)	5986(2)	7358(1)	36(1)
C(3)	8370(2)	7371(2)	7382(1)	39(1)
C(9)	6043(2)	8648(2)	8542(2)	47(1)
C(8)	5069(2)	8438(2)	9316(2)	55(1)
C(7)	5173(2)	7118(2)	9738(2)	51(1)
C(6)	6245(2)	5982(2)	9381(1)	41(1)
C(5)	7304(2)	6154(2)	8588(1)	33(1)
C(4)	7194(2)	7506(2)	8162(1)	37(1)
C(25)	7003(2)	5357(2)	4837(2)	53(1)
C(24)	8640(2)	6785(2)	4885(2)	53(1)
C(22)	3628(2)	6066(3)	7809(2)	57(1)
C(23)	3997(2)	7486(2)	6417(2)	53(1)
C(15)	7141(2)	2579(2)	6733(1)	33(1)
C(14)	8065(2)	1819(2)	5950(1)	47(1)
C(13)	7709(3)	761(2)	5492(2)	55(1)
C(12)	6417(3)	459(2)	5787(2)	59(1)
C(11)	5467(3)	1229(2)	6535(2)	62(1)
C(10)	5816(2)	2281(2)	7013(2)	47(1)
C(16)	9328(2)	990(2)	8103(1)	40(1)
C(17)	10780(3)	69(3)	7645(2)	72(1)
C(18)	8688(3)	352(2)	9012(2)	62(1)
C(19)	10368(2)	2537(2)	8987(1)	40(1)
C(20)	11590(2)	3165(3)	8526(2)	55(1)
C(21)	9570(2)	3277(2)	9938(1)	49(1)

Table 65. Anisotropic displacement parameters ($Å^2 \times 10^3$) for **122**. The anisotropic displacement factor exponent takes the form: $-2\pi^2[h^2 a^{*2} U_{11} + ... + 2 h k a^* b^* U_{12}]$.

	U_{11}	U_{22}	U_{33}	U_{23}	U_{13}	U_{12}
Zr	29(1)	26(1)	31(1)	-2(1)	-3(1)	-8(1)
B	30(1)	30(1)	32(1)	-4(1)	-2(1)	-9(1)
N(4)	40(1)	35(1)	36(1)	-1(1)	0(1)	-11(1)
N(3)	31(1)	37(1)	44(1)	-4(1)	-3(1)	-8(1)
N(1)	35(1)	27(1)	38(1)	-2(1)	-10(1)	-10(1)
N(2)	34(1)	29(1)	35(1)	-5(1)	-10(1)	-4(1)
C(1)	33(1)	32(1)	34(1)	-4(1)	-8(1)	-11(1)
C(2)	33(1)	38(1)	39(1)	-5(1)	-4(1)	-14(1)
C(3)	45(1)	34(1)	42(1)	-2(1)	-4(1)	-19(1)
C(9)	52(1)	29(1)	59(1)	-11(1)	-3(1)	-12(1)
C(8)	51(1)	40(1)	67(1)	-25(1)	7(1)	-10(1)
C(7)	54(1)	52(1)	46(1)	-17(1)	11(1)	-20(1)
C(6)	49(1)	41(1)	35(1)	-7(1)	0(1)	-19(1)
C(5)	39(1)	30(1)	33(1)	-6(1)	-6(1)	-12(1)
C(4)	44(1)	30(1)	40(1)	-7(1)	-6(1)	-14(1)
C(25)	59(1)	62(1)	43(1)	-7(1)	-4(1)	-24(1)
C(24)	64(1)	49(1)	43(1)	-2(1)	12(1)	-24(1)
C(22)	41(1)	71(1)	58(1)	1(1)	3(1)	-20(1)
C(23)	42(1)	44(1)	68(1)	4(1)	-9(1)	-2(1)
C(15)	40(1)	27(1)	36(1)	5(1)	-16(1)	-11(1)
C(14)	59(1)	43(1)	41(1)	-5(1)	-4(1)	-22(1)
C(13)	85(2)	43(1)	43(1)	-6(1)	-16(1)	-21(1)
C(12)	83(2)	37(1)	72(1)	2(1)	-43(1)	-25(1)
C(11)	53(1)	45(1)	100(2)	6(1)	-30(1)	-26(1)
C(10)	40(1)	38(1)	68(1)	0(1)	-12(1)	-13(1)
C(16)	42(1)	27(1)	50(1)	-6(1)	-18(1)	-1(1)
C(17)	60(1)	51(1)	93(2)	-30(1)	-7(1)	8(1)
C(18)	72(2)	48(1)	75(2)	8(1)	-19(1)	-30(1)
C(19)	40(1)	37(1)	45(1)	0(1)	-17(1)	-9(1)
C(20)	41(1)	66(1)	64(1)	4(1)	-16(1)	-21(1)
C(21)	65(1)	46(1)	41(1)	-4(1)	-17(1)	-17(1)

Table 66. Bond lengths [Å] for **122**.

Zr-N(4)	2.0356(15)	C(1)-C(2)	1.424(2)
Zr-N(3)	2.0469(15)	C(1)-C(5)	1.446(2)
Zr-N(1)	2.1361(14)	C(2)-C(3)	1.406(2)
Zr-C(1)	2.4201(16)	C(3)-C(4)	1.423(2)
Zr-C(5)	2.4945(17)	C(9)-C(8)	1.360(3)
Zr-C(2)	2.4953(17)	C(9)-C(4)	1.420(3)
Zr-C(3)	2.5547(17)	C(8)-C(7)	1.409(3)
Zr-C(4)	2.5791(17)	C(7)-C(6)	1.368(3)
Zr-B	2.8374(19)	C(6)-C(5)	1.418(2)
Zr-C(25)	2.858(2)	C(5)-C(4)	1.438(2)
B-N(2)	1.406(2)	C(15)-C(10)	1.389(2)
B-N(1)	1.446(2)	C(15)-C(14)	1.391(3)
B-C(1)	1.608(2)	C(14)-C(13)	1.386(3)
N(4)-C(24)	1.452(2)	C(13)-C(12)	1.364(3)
N(4)-C(25)	1.453(2)	C(12)-C(11)	1.372(4)
N(3)-C(22)	1.454(2)	C(11)-C(10)	1.391(3)
N(3)-C(23)	1.455(2)	C(16)-C(18)	1.509(3)
N(1)-C(15)	1.412(2)	C(16)-C(17)	1.524(3)
N(2)-C(16)	1.472(2)	C(19)-C(21)	1.518(3)
N(2)-C(19)	1.485(2)	C(19)-C(20)	1.525(3)

Table 67. Bond angles [°] for **122**.

N(4)-Zr-N(3)	105.42(6)	C(25)-N(4)-Zr	108.88(12)
N(4)-Zr-N(1)	110.36(6)	C(22)-N(3)-C(23)	110.53(16)
N(3)-Zr-N(1)	108.17(6)	C(22)-N(3)-Zr	128.63(13)
N(4)-Zr-C(1)	120.59(6)	C(23)-N(3)-Zr	119.52(12)
N(3)-Zr-C(1)	133.37(6)	C(15)-N(1)-B	131.51(13)
N(1)-Zr-C(1)	64.15(5)	C(15)-N(1)-Zr	124.69(10)
N(4)-Zr-C(5)	141.72(6)	B-N(1)-Zr	103.08(10)
N(3)-Zr-C(5)	102.54(6)	B-N(2)-C(16)	122.50(14)
N(1)-Zr-C(5)	84.59(5)	B-N(2)-C(19)	123.15(14)
C(1)-Zr-C(5)	34.17(5)	C(16)-N(2)-C(19)	114.30(13)
N(4)-Zr-C(2)	90.46(6)	C(2)-C(1)-C(5)	104.76(14)
N(3)-Zr-C(2)	151.78(6)	C(2)-C(1)-B	123.86(14)
N(1)-Zr-C(2)	87.05(5)	C(5)-C(1)-B	122.45(14)
C(1)-Zr-C(2)	33.63(5)	C(2)-C(1)-Zr	76.09(9)
C(5)-Zr-C(2)	54.19(6)	C(5)-C(1)-Zr	75.73(9)
N(4)-Zr-C(3)	88.37(6)	B-C(1)-Zr	87.13(9)
N(3)-Zr-C(3)	123.27(6)	C(3)-C(2)-C(1)	111.02(15)
N(1)-Zr-C(3)	117.91(6)	C(3)-C(2)-Zr	76.17(10)
C(1)-Zr-C(3)	55.85(6)	C(1)-C(2)-Zr	70.28(9)
C(5)-Zr-C(3)	54.21(5)	C(2)-C(3)-C(4)	107.66(15)
C(2)-Zr-C(3)	32.31(6)	C(2)-C(3)-Zr	71.52(9)
N(4)-Zr-C(4)	116.37(6)	C(4)-C(3)-Zr	74.86(9)
N(3)-Zr-C(4)	98.33(6)	C(8)-C(9)-C(4)	118.74(18)
N(1)-Zr-C(4)	116.52(6)	C(9)-C(8)-C(7)	121.52(18)
C(1)-Zr-C(4)	56.00(6)	C(6)-C(7)-C(8)	121.68(18)
C(5)-Zr-C(4)	32.88(5)	C(7)-C(6)-C(5)	118.90(18)
C(2)-Zr-C(4)	53.47(6)	C(6)-C(5)-C(4)	119.10(16)
C(3)-Zr-C(4)	32.18(6)	C(6)-C(5)-C(1)	131.63(16)
N(4)-Zr-B	118.41(6)	C(4)-C(5)-C(1)	109.23(14)
N(3)-Zr-B	126.42(6)	C(6)-C(5)-Zr	117.95(12)
N(1)-Zr-B	29.75(5)	C(4)-C(5)-Zr	76.80(9)
C(1)-Zr-B	34.46(5)	C(1)-C(5)-Zr	70.09(9)
C(5)-Zr-B	59.87(5)	C(9)-C(4)-C(3)	132.90(17)
C(2)-Zr-B	59.83(5)	C(9)-C(4)-C(5)	120.02(17)
C(3)-Zr-B	88.76(6)	C(3)-C(4)-C(5)	107.08(15)
C(4)-Zr-B	88.92(6)	C(9)-C(4)-Zr	121.18(13)
N(4)-Zr-C(25)	28.75(6)	C(3)-C(4)-Zr	72.97(9)
N(3)-Zr-C(25)	88.75(6)	C(5)-C(4)-Zr	70.32(9)
N(1)-Zr-C(25)	94.53(6)	C(10)-C(15)-C(14)	117.61(16)
C(1)-Zr-C(25)	135.97(6)	C(10)-C(15)-N(1)	121.10(16)
C(5)-Zr-C(25)	168.39(6)	C(14)-C(15)-N(1)	121.28(15)
C(2)-Zr-C(25)	114.22(6)	C(13)-C(14)-C(15)	121.38(19)
C(3)-Zr-C(25)	117.12(6)	C(12)-C(13)-C(14)	120.4(2)
C(4)-Zr-C(25)	143.56(6)	C(13)-C(12)-C(11)	119.13(18)
B-Zr-C(25)	115.35(6)	C(12)-C(11)-C(10)	121.2(2)
N(2)-B-N(1)	129.53(15)	C(15)-C(10)-C(11)	120.2(2)
N(2)-B-C(1)	125.03(15)	N(2)-C(16)-C(18)	111.78(16)
N(1)-B-C(1)	105.44(13)	N(2)-C(16)-C(17)	112.65(17)
N(2)-B-Zr	175.70(12)	C(18)-C(16)-C(17)	111.69(19)
N(1)-B-Zr	47.16(7)	N(2)-C(19)-C(21)	112.67(15)
C(1)-B-Zr	58.41(8)	N(2)-C(19)-C(20)	112.85(16)
C(24)-N(4)-C(25)	111.28(15)	C(21)-C(19)-C(20)	111.87(17)
C(24)-N(4)-Zr	139.45(13)		